

1. Report No. FHWA/TX-84/37+248-3		2. Government Accession No.		3. Recipient's Catalog No.	
4. Title and Subtitle EXPERIMENTAL VERIFICATION OF DESIGN PROCEDURES FOR SHEAR AND TORSION IN REINFORCED AND PRESTRESSED CONCRETE				5. Report Date November 1983	
				6. Performing Organization Code	
7. Author(s) J. A. Ramirez and J. E. Breen				8. Performing Organization Report No. Research Report 248-3	
9. Performing Organization Name and Address Center for Transportation Research The University of Texas at Austin Austin, Texas 78712-1075				10. Work Unit No.	
				11. Contract or Grant No. Research Study 3-5-80-248	
12. Sponsoring Agency Name and Address Texas State Department of Highways and Public Transportation; Transportation Planning Division P. O. Box 5051 Austin, Texas 78763				13. Type of Report and Period Covered Interim	
				14. Sponsoring Agency Code	
15. Supplementary Notes Study conducted in cooperation with the U. S. Department of Transportation, Federal Highway Administration. Research Study Title: "Reevaluation of AASHTO Shear and Torsion Provisions for Reinforced and Prestressed Concrete"					
16. Abstract The object of this study is to propose and evaluate a design procedure for shear and torsion in reinforced and prestressed concrete beams, with the aim of clarifying and simplifying current design requirements and AASHTO requirements. This report summarizes an extensive experimental verification of a powerful three-dimensional space truss model with variable angle of inclination of the diagonal elements. This conceptual model was developed by European and Canadian engineers over the past fifteen years. The model is shown to be a conservative method of predicting the strength of such members under combined loading. Detailed comparison with current ACI/AASHTO procedures indicate greatly reduced scatter when comparisons are made to test results. Detailed design procedures and specifications, and example applications are given in the final report in this series.					
17. Key Words beams, concrete, reinforced, prestressed, shear, torsion, design, reinforcement, verification, experimental			18. Distribution Statement No restrictions. This document is available to the public through the National Technical Information Service, Springfield, Virginia 22161.		
19. Security Classif. (of this report) Unclassified		20. Security Classif. (of this page) Unclassified		21. No. of Pages 322	22. Price

EXPERIMENTAL VERIFICATION OF DESIGN PROCEDURES FOR SHEAR AND TORSION
IN REINFORCED AND PRESTRESSED CONCRETE

by

J. A. Ramirez and J. E. Breen

Research Report No. 248-3

Research Project 3-5-80-248

"Reevaluation of AASHTO Shear and Torsion Provisions for
Reinforced and Prestressed Concrete"

Conducted for

Texas

State Department of Highways and Public Transportation

In Cooperation with the
U. S. Department of Transportation
Federal Highway Administration

by

CENTER FOR TRANSPORTATION RESEARCH
BUREAU OF ENGINEERING RESEARCH
THE UNIVERSITY OF TEXAS AT AUSTIN

November 1983

The contents of this report reflect the views of the authors who are responsible for the facts and accuracy of the data presented herein. The contents do not necessarily reflect the official views or policies of the Federal Highway Administration. This report does not constitute a standard, specification, or regulation.

P R E F A C E

This report is the third in a series which summarizes a detailed evaluation of AASHTO design procedures for shear and torsion in reinforced and prestressed concrete beams. The first report summarized an exploratory investigation of the shear transfer between joints using details commonly found in segmental box girder construction. The second report reviews the historical development of design procedures for shear and torsion in concrete members as found in American practice. Both the AASHTO Specifications and the ACI Building Code are examined, since they have been closely related. In addition, this report presents the background and equilibrium relationships for use of a space truss with variable inclination diagonals as a design model. This report summarizes special considerations required for the practical usage of the variable inclination truss model. It also compares the theoretical capacity as computed by the truss model to experimental results for a great variety of previously reported tests as well as the results of tests run in this program to investigate several variables. The fourth and final report in this series draws on the analytical and experimental results presented in the earlier reports. It uses these results to develop procedures and suggested AASHTO Specification procedures for girder shear and torsion. The final report also contains several examples to illustrate the application of the design criteria and procedures.

This work is part of Research Project 3-5-80-248, entitled "Reevaluation of AASHTO Shear and Torsion Provisions for Reinforced and Prestressed Concrete." The studies described were conducted at the Phil M. Ferguson Structural Engineering Laboratory as part of the overall research program of the Center for Transportation Research of The University of Texas at Austin. The work was sponsored jointly by the State Department of Highways and Public Transportation and the Federal Highway Administration under an agreement with The University of Texas at Austin and the Texas State Department of Highways and Public Transportation.

Liaison with the State Department of Highways and Public Transportation was maintained through the contact representatives Mr. Warren A. Grasso and Mr. Dean W. Van Landuyt; the Area IV Committee Chairman, Mr. Robert L. Reed; and the State Bridge Engineer, Mr. Wayne Henneberger. Mr. T. E. Strock was the contact representative for the Federal Highway Administration.

The overall study was directed by Dr. John E. Breen, who holds the Carol Cockrell Curran Chair in Engineering. The project was under the immediate supervision of Dr. Julio A. Ramirez, Research Engineer. He was assisted by Mr. Thomas C. Schaeffer and Mr. Reid W. Castrodale, Assistant Research Engineers.

S U M M A R Y

The object of this study is to propose and evaluate a design procedure for shear and torsion in reinforced and prestressed concrete beams, with the aim of clarifying and simplifying current design requirements and AASHTO requirements.

This report summarizes an extensive experimental verification of a powerful three-dimensional space truss model with variable angle of inclination of the diagonal elements. This conceptual model was developed by European and Canadian engineers over the past fifteen years. The model is shown to be a conservative method of predicting the strength of such members under combined loading. Detailed comparison with current ACI/AASHTO procedures indicate greatly reduced scatter when comparisons are made to test results. Detailed design procedures and specifications, and example applications are given in the final report in this series.

I M P L E M E N T A T I O N

This report is the third in a series which summarizes a major experimental and analytical project aimed directly at suggesting new design recommendations for treating shear and torsion in reinforced and prestressed concrete girders. The detailed recommendations are included in the fourth and concluding report of this series.

This report contains background information of interest to those responsible for deciding on specifications and codes. It contains detailed comparisons of the proposed model predictions with a wide range of test data and with current ACI/AASHTO requirements. The comparisons indicate that the procedure is conservative yet substantially more accurate than current ACI-AASHTO procedures. Examples of detailing failures suggest procedures for improving design.

C O N T E N T S

Part	Page
1 INTRODUCTION	1
2 SPECIAL CONSIDERATION REGARDING THE TRUSS MODEL	5
2.1 Introduction	5
2.2 Effects of Different Types of Loadings	7
2.2.1 Beams Subjected to Uniformly Distributed Load	7
2.2.2 Introduction of Concentrated Loads	10
2.2.3 Heavy Concentrated Loads Near the Supports	18
2.2.4 Hanging Loads	24
2.3 Compression Strength of the Diagonal Strut	25
2.4 Detailing of Reinforcement	42
2.4.1 Torsion	42
2.4.2 Shear	51
2.5 Uncracked, Transition and Full Truss States	63
2.6 Additional Effects	70
2.6.1 Effective Web Thickness	70
2.6.2 Effect of the Cross Section Shape in the Case of Torsion	74
2.6.3 Strand Draping	79
2.7 Summary	82
3 EXPERIMENTAL VERIFICATION OF THE SPACE TRUSS MODEL	83
3.1 Introduction	83
3.2 Torsion	84
3.3 Torsion-Bending	96
3.4 Torsion, Bending, and Shear	112
3.5 Bending and Shear	127
3.5.1 Comparison with Current Test Series	130
3.5.2 Comparisons with Tests Reported in Literature	160
3.6 Evaluation of the Compression Strength of the Diagonal Strut	175
3.7 Different Types of Failure	187
3.7.1 Torsion	187
3.7.2 Torsion-Bending	192
3.7.3 Torsion-Bending-Shear	193
3.7.4 Failures Due to Inadequate Detailing	195
3.8 Evaluation of the Additional Concrete Contribution in the Uncracked and Transition States	211

Part	Page
3.9 Comparison between ACI/AASHTO and Truss Model	
Predicted Values With Test Results	250
3.9.1 Torsion	251
3.9.2 Torsion-Bending	251
3.9.3 Torsion-Bending-Shear	263
3.9.4 Bending and Shear	267
4 CONCLUSIONS	281
4.1 Summary	281
4.2 Recommendations	283
REFERENCES	285

T A B L E S

Table		Page
3.1	Data for Reinforced Concrete Rectangular Beams	85
3.2	Data on Reinforced Concrete Rectangular Beams	86
3.3	Test Data of Reinforced Concrete L-Beams Subjected to Restrained Torsion	89
3.4	Data on Prestressed Concrete Beams of Various Sections	92
3.5	Data on Prestressed and Reinforced Concrete I-Beams With Restrained Warping	94
3.6	Data on Reinforced Concrete Rectangular Beams With $r = 0.7$	99
3.7	Data for Prestressed Concrete Box Beams With $r = 0.33$	103
3.8	Test Data on Reinforced and Prestressed Concrete Beams With $r = 1.0$	105
3.9	Data on Reinforced and Prestressed Members With an "r" of 0.50	108
3.10	Data from Tests Reported by Warwaruk and Taylor [161] on Prestressed	111
3.11	Test Data from Reinforced Concrete Members Subjected to Torsion-Bending-Shear	115
3.12	Test Data from Reinforced Concrete Members Subjected to Torsion-Bending-Shear	116
3.13	Test Data from Prestressed Concrete Members Subjected to Torsion-Bending-Shear	117
3.14	Test Data from Prestressed Concrete Members Subjected to Torsion-Bending-Shear	118
3.15	Data on Reinforced Concrete One-Way Members Failing in Shear	132
3.16	Data from Specimens 0.40A, 0.40B, and 0.45	145

Table		Page
3.17	Data for Prestressed Concrete I-Beams Failing in Shear	156
3.18	Data on Reinforced Concrete Rectangular Beams Failing in Shear	164
3.19	Data on Reinforced Concrete Rectangular Beams Failing in Shear	165
3.20	Data on Prestressed Concrete I-Beams Failing in Shear	166
3.21	Data on Prestressed Concrete T-Beams Failing in Shear	167
3.22	Data on Two-Span Continuous Reinforced Concrete Beams with Rectangular Cross Section	172
3.23	Data on Continuous Prestressed Concrete Members with I-Shape Cross Section Failing in Shear	173
3.24	Shear Tests on Reinforced Concrete Members Experiencing Web Crushing Failure	177
3.25	Shear Tests on Prestressed Concrete Members Experiencing Web Crushing	178
3.26	Torsion Tests on Reinforced and Prestressed Concrete Members Experiencing Web Crushing Failures	181
3.27	Combined Torsion and Shear Tests on Prestressed Concrete Members Experiencing Web Crushing	183
3.28	Data on Reinforced and Prestressed Concrete Beams Subjected to Pure Torsion Where Only the Longitudinal Reinforcement Yielded Prior to Failure	188
3.29	Data on Reinforced and Prestressed Concrete Beams Under Pure Torsion With Only Yielding of the Transverse Reinforcement Prior to Failure	189
3.30	Data on Reinforced and Prestressed Concrete Members Subjected to Torsion-Bending	192

Table		Page
3.31	Data on Prestressed Concrete Beams Under Combined Torsion-Bending-Shear Experiencing Only Yielding of the Transverse Reinforcement at Failure	194
3.32	Data on Prestressed Concrete Members Subjected to Torsion-Bending-Shear Where Only the Longitudinal Steel Yielded at Failure	196
3.33	Data on Prestressed Concrete Inverted T-Bent Caps Failing Prematurely Due to Improper Detailing	198
3.34	Data on Reinforced Concrete L-Beams Under Combined Torsion-Bending-Shear Failing Locally at the Diaphragm Region	204
3.35	Data on Prestressed Concrete I-Beam 0.50B	204
3.36	Test Data on Beams with No Web Reinforcement Failing in Shear	217
3.37	Test Data on Beams with No Web Reinforcement Failing in Shear	218
3.38	Data on Beams with No Web Reinforcement Failing in Shear	219
3.39	Test Data on Beams with No Web Reinforcement Failing in Shear	220
3.40	Test Data on Reinforced Concrete Beams with No or Very Light Web Reinforcement Failing in Shear	221
3.41	Data on Prestressed Concrete Beams with No Web Reinforcement Failing in Shear	229
3.42	Data on Prestressed Concrete Beams with No Web Reinforcement Failing in Shear	230
3.43	Data on Prestressed Concrete Beams with No Web Reinforcement Failing in Shear	231
3.44	Data on Reinforced Concrete Rectangular Beams with No Web Reinforcement under Pure Torsion	244

Table		Page
3.45	Data on Prestressed Concrete Rectangular, T, and I-Beams with No Web Reinforcement Subjected to Pure Torsion	246
3.46	Data on Reinforced Concrete Beams with Web Reinforcement Subjected to Pure Torsion	252
3.47	Data on Reinforced Concrete Beams with Web Reinforcement Subjected to Pure Torsion	253
3.48	Data on Reinforced Concrete Rectangular Beams with Web Reinforcement Subjected to Pure Torsion	254
3.49	Data on Reinforced Concrete L-Beams with Web Reinforcement Subjected to Pure Torsion	255
3.50	Data on Reinforced Concrete I-Beams with Web Reinforcement Subjected to Pure Torsion	256
3.51	Data on Reinforced Concrete Rectangular Beams with Web Reinforcement Subjected to Combined Bending-Torsion	259
3.52	Data on Reinforced Concrete Rectangular Beams with Web Reinforcement Subjected to Combined Bending-Torsion	261
3.53	Data on Reinforced Concrete Rectangular and L-Beams with Web Reinforcement Subjected to Combined Torsion-Bending-Shear	264
3.54	Data on Reinforced Concrete Rectangular and L-Beams with Web Reinforcement Subjected to Combined Torsion-Bending-Shear	265
3.55	Data on Simply Supported Reinforced Concrete Rectangular Beams Failing in Shear	268
3.56	Data on Simply Supported Reinforced Concrete Rectangular Beams Failing in Shear	269
3.57	Data on Simply Supported Reinforced Concrete Rectangular Beams	270
3.58	Data on Simply Supported Prestressed Concrete T and I Beams Failing in Shear	273

Table		Page
3.59	Data on Simply Supported Prestressed Concrete Beams Failing in Shear	274
3.60	Data on Prestressed Concrete I-Beams	276
3.61	Data on Two-Span Continuous Reinforced Concrete Beams Failing in Shear	278
3.62	Data on Semicontinuous Prestressed Concrete I-Beams Failing in Shear	279

F I G U R E S

Figure		Page
2.1	Shear and moment diagrams for a beam under uniformly distributed load	8
2.2	Internal truss forces in the case of uniformly distributed loading	9
2.3	Concentrated loads--compression fans	12
2.4	Compression fan at the support	13
2.5	Forces in the top and bottom chords of the truss model	15
2.6	Equilibrium system under the applied load	16
2.7	Forces in the top and bottom chords of the truss model	17
2.8	Typical support conditions where the maximum design shear force is that computed at a distance "d" from the face of the support	19
2.9	Cases where the critical section for shear is located at the face of the support	20
2.10	Definition of a/z ratio	21
2.11	Analogy of deep beams with a/z < 0.5 and brackets and corbels	22
2.12	Hanging loads	26
2.13	Compression stress f_d in the diagonal strut	28
2.14	Mean crack strain ϵ_r	30
2.15	Relationship between the mean crack strain and the strains in the reinforcement for different angle of inclination of the diagonal strut	32
2.16	Stress f_d as a function of the angle	33
2.17	Stress and strain conditions for diagonally cracked concrete neglecting principal tensile stress	35

Figure		Page
2.18	Thürlimann recommendation for effective concrete strength vs. concrete compressive strength	36
2.19	Distortional effect	38
2.20	Forces acting on edge members of parabolic arches	38
2.21	Sections of a hyperbolic paraboloid surface taken at 45 degrees to the coordinate axis	39
2.22	Web crushing limits	41
2.23	Torsion in statical systems	43
2.24	Pushing out failure of the corner longitudinal bars	46
2.25	Distribution of the longitudinal steel	47
2.26	Stirrup anchorage details	49
2.27	Detailing considerations for a beam subjected to shear	52
2.28	Anchorage of reinforcement at support	53
2.29	The effect of shear on flexural steel requirements	54
2.30	Detailing of transverse reinforcement	58
2.31	Effect of large web widths	60
2.32	Uncracked, transition, and full truss states	66
2.33	State of stresses in an uncracked prestressed section	67
2.34	Influence of the prestress force on the principal diagonal tension stress	68
2.35	Effective web thickness for solid cross sections	71
2.36	Restrained torsion	76
2.37	Sections not influenced by the restraining effect	77
2.38	Sections influenced by the restraining effect	77

Figure		Page
2.39	Strand draping effect	79
2.40	Prestressed beam with inclined tendons in the case of torsion	81
3.1	Reinforced concrete rectangular beams subjected to pure torsion	88
3.2	Evaluation of the truss model predictions using data from reinforced concrete L-sections	90
3.3	The truss model in the case of prestressed concrete members	93
3.4	Comparison between test values and truss model prediction in the case of pure torsion in I-beams where warping of the cross section is restrained . . .	95
3.5	Dispersion coefficient I measured along radial lines from the origin	100
3.6	Torque-bending interaction diagram for rectangular reinforced concrete beams with $r = 0.7$	101
3.7	Comparison of the truss with test results of prestressed concrete box members	104
3.8	Torsion-bending predicted interaction in the case of members with $r = 1.0$	106
3.9	Evaluation of the truss model predictions in the case of members of various cross sections	109
3.10	Evaluation of the truss model in the case of complex cross sections	110
3.11	Torsion-bending-shear interaction with $V_u/V_{u0} =$ 0.75 for reinforced and prestressed concrete specimens	121
3.12	Torsion-bending-shear interaction with $V_u/V_{u0} =$ 0.40 in the case of reinforced concrete members with L-shape cross sections	122
3.13	Torsion-bending-shear interaction for $r = 0.50$ and $V_u/V_{u0} = 0.45$	123

Figure		Page
3.14	Evaluation of the truss model using test results of reinforced and prestressed concrete members with $r = 0.27$ and $V_u/V_{u0} = 0.40$	124
3.15	Torsion-bending-shear interaction with $V_u/V_{u0} = 1.0$	125
3.16	Torsion-bending-shear interaction with $V_u/V_{u0} = 0.70$	126
3.17	Torsion-bending-shear interaction with $V_u/V_{u0} = 0.45$	128
3.18	Reinforcing details of members RL-0.50, RL-1.25, and RH-0.50	133
3.19	Crack patterns of beam RL-0.50 at load stage of 60 kips, 100 kips, and failure (top to bottom)	135
3.20	Crack patterns of beam RL-1.25 at load stages of 60 kips, 100 kips, and failure (top to bottom)	136
3.21	Crack patterns of beam RH-0.50 at load stages of 80 kips, 140 kips, and failure (top to bottom)	138
3.22	Load-deflection curves of beams RL-0.50 and RL-1.25	139
3.23	Load-deflection curve of beam RH-0.50	140
3.24	Predicted ultimate bending and shear interaction using the truss model	141
3.25	Details of the cross section	143
3.26	Details of the nonprestressed longitudinal and transverse reinforcements	144
3.27	Crack patterns of beam 0.40A at load stages of 4.2k/f, 6.7k/f, and failure (top to bottom)	147
3.27d	Strain in stirrups for north half of specimen 0.40A	148
3.28	Crack patterns of beam 0.40B at load stages of 6.7 k/f and failure (top to bottom)	149
3.28c	Strain in stirrups for south half of specimen 0.40B	150

Figure		Page
3.29	Crack patterns of beam 0.45 at load stages of 7.5 k/f and failure (top to bottom)	151
3.30	Load-deflection curves for beams 0.40A, 0.40B, 0.45	154
3.31	Comparison between the ultimate load interaction predicted by the truss model and the ultimate test values at different sections along the span length for beam 0.40A	157
3.32	Evaluation of the truss model using beam 0.40B	158
3.33	Comparison between the truss model predicted ultimate load interaction and the results from beam 0.45	159
3.34	Tests on reinforced concrete one-way members	161
3.35	Tests on prestressed concrete one-way members	162
3.36	Evaluation of the accuracy of the truss model predictions in the area of shear-bending by means of the dispersion index I	168
3.37	Shear stress at failure vs. specified compressive strength of the concrete f'_c for the case of reinforced and prestressed concrete beams failing due to web crushing	179
3.38	Shear stress due to torsion at failure vs. specified compressive strength of the concrete f'_c for the case of a reinforced and prestressed concrete beam failing due to web crushing	182
3.39	Shear stress due to shear and torsion vs. the maximum allowed shear stress for prestressed concrete members failing due to web crushing	184
3.40	Shear stress due to shear and/or torsion vs. concrete compression strength f'_c for reinforced and prestressed concrete members due to web crushing	186
3.41	Cross section, and types of premature failures due to improper detailing occurring in specimens TP43, TP54, and TP63	199

Figure		Page
3.42	Truss model and reinforcement details of the web-flange connection region of the inverted T-bent cap	201
3.43	Revision in reinforcement detailing at the end region due to premature failure of specimen 0.5B . . .	205
3.44	Premature failure due to inadequate detailment of the end region of specimen 0.5B	206
3.45	Distribution of the diagonal compression stresses at the end regions of simple supported beams where the reaction induces compression	208
3.46	Comparison between the ultimate load interaction predicted by the truss model and the ultimate test values at different sections along the span length for beam 0.50B	210
3.47	Concrete contributions for the case of reinforced concrete members	212
3.48	Effect of prestressing on the shear strength of an uncracked concrete member	214
3.49	Additional concrete contribution for the case of prestressed concrete members	215
3.50	Evaluation of the concrete contribution in the case of reinforced concrete beams	223
3.51	Evaluation of the concrete contributions in reinforced concrete beams failing in shear	224
3.52	Evaluation of the concrete contribution in reinforced concrete beams failing in shear	225
3.53	Evaluation of the concrete contribution in reinforced concrete members failing in shear	226
3.54	Evaluation of the concrete contribution in the case of members with no or very light web reinforcement failing in shear	228

Figure		Page
3.55	Evaluation of the concrete contribution in prestressed concrete members failing in shear with $K = 2.0$	232
3.56	Evaluation of the concrete contribution in prestressed concrete members failing in shear with $K = 1.3$	233
3.57	Evaluation of the concrete contribution in prestressed concrete beams failing in shear with values of $K = 2.0$ and $K = 1.7$	234
3.58	Evaluation of the concrete contribution in prestressed concrete beams failing in shear with values of $K = 1.3$ and $K = 1.0$	235
3.59	Evaluation of the concrete contribution in prestressed concrete beams failing in shear with values of $K = 2.0$ and $K = 1.7$	236
3.60	Evaluation of the concrete contribution in prestressed concrete beams failing in shear with $K = 1.3$ and $K = 1.0$	237
3.61	Evaluation of the concrete contribution in prestressed concrete beams failing in shear with values of K equal to 2.0, 1.88 and 1.7	238
3.62	Evaluation of the concrete contribution in prestressed concrete beams failing in shear with values of K equal to 1.3 and 1.0	239
3.63	Stiffness and strength factor for rectangular section subjected to torsion	241
3.64	Evaluation of the concrete contribution in reinforced concrete rectangular members under pure torsion	245
3.65	Evaluation of the concrete contribution in prestressed concrete rectangular members subjected to torsion with $K = 2.0$	247
3.66	Evaluation of the concrete contribution in prestressed concrete T-beams subjected to torsion with $K = 2.0$	248

Figure		Page
3.67	Evaluation of the concrete contribution in prestressed concrete I-beams subjected to torsion with $K = 2.0$	249
3.68	Comparison between the ACI/AASHTO and space truss model predictions with test results of reinforced concrete beams under pure torsion	257
3.69	Comparison between the ACI/AASHTO and space truss model predictions with test results of reinforced concrete beams under combined torsion-bending	262
3.70	Comparison between the space truss and the ACI/AASHTO prediction with test results of reinforced concrete beams under torsion-bending-shear	266
3.71	Comparison between the ACI/AASHTO and space truss model predictions with test results of reinforced concrete beams where shear failures were observed . .	271
3.72	Comparison between the space truss model and the ACI/AASHTO predictions with test results of prestressed concrete beams failing in shear	275
3.73	Comparison between the space truss model and the ACI/AASHTO predictions with test results of continuous reinforced and prestressed concrete beams failing in shear	280

C H A P T E R 1

INTRODUCTION

Design provisions for shear and torsion for reinforced and prestressed concrete members and structures in both the AASHTO Specifications (17) and the ACI Building Code (24) have evolved into complex procedures in recent revisions. The complexity of such procedures results from their highly empirical basis and the lack of a unified treatment of shear and torsion. Ironically, such design procedures seem better suited for analysis, since they become cumbersome and obscure when used for design.

Such deficiencies could be overcome if the design procedures in the shear and torsion areas were based on behavioral models rather than on detailed empirical equations. If the design procedures were based on a physical model, the designers would be able to envision the effects of the forces acting on the member, and then provide structural systems capable of resisting those forces. Furthermore, design provisions based on a conceptual model would become more simple and would not require as much test verification.

The present study attempts to answer the challenge posed by the ACI-ASCE Committee 426 (28):

During the next decade it is hoped that design regulations for shear strength can be integrated, simplified, and given a physical significance so that designers can approach unusual design problems in a rational manner.

An overall review of the current AASHTO Specifications and the ACI Building Code in the areas of shear and torsion was summarized in Report 248-2. That study showed that design procedures have become more and more complex with every revision. The highly empirical provisions are difficult to use in many design situations.

It is the nature of the empirical approach, and of its consequence, the lack of a conceptual model, which are the primary reasons for the complex and fragmented design approach to shear and torsion reflected in current codes and specifications.

The main objective of this study is to propose and evaluate a design procedure for shear and torsion in reinforced and prestressed concrete beams. The goal is to clarify and simplify current design recommendations and AASHTO requirements in such areas. The basic reevaluation of the current procedures and development of new procedures are to be carried out using a conceptual structural model rather than detailed empirical equations wherever practical.

Report 248-2 summarized the background and basic derivation of the space truss model with variable angle of inclination of the diagonal elements. This model was selected as the one which best represents the behavior of reinforced and prestressed concrete beams subjected to shear and torsion. This conceptual model was developed over the past 20 years. Principal contributions were made by Thürlimann, Lampert, Nielsen, Müller, Marti, Collins and Mitchell. Much of the European work has been based on highly complex proofs of the application of plasticity theorems in the fields of shear and torsion. The complete formulations

are generally not in English and are quite complex. The more limited reports, which are in English, have not had wide American readership. The apparent complexity of the proofs of the plasticity theorems as applied to shear and torsion can cause the more design-oriented reader to lose sight of the fact that the authors use these proofs only as a theoretical basis for proving the application of a refined truss model. The model was shown to be a lower bound solution giving the same result as the much more rigorous plasticity upper bound solution. Hence it is a valid solution which correctly represents the failure load.

This report extends the application of the space truss model to consider many special limits and approaches which must be incorporated in the design framework. The highlights of the refined truss model approach are the relatively simple design procedures that can be developed from the space truss model, and the extremely logical way the designer can envision providing and proportioning reinforcement for shear and torsion under special circumstances as in the case of box sections, concentrated loads on lower flanges, etc. Several of these are illustrated in Chapter 2.

However, it was felt that before the generalized refined truss model approach could be used as the basic design procedure in American practice, a complete evaluation of the accuracy of the model using a significant body of the available test data reported in the American literature was necessary. In Chapter 3, thorough comparisons of the space truss model with a wide range of test data and with predicted failure loads from other design procedures are presented.

In companion Report 248-4F, the general procedures derived from the space truss model are translated into design recommendations and draft AASHTO requirements are suggested. Design applications for typical highway structures using the proposed design recommendations as well as the current AASHTO approach are also presented for comparison in Report 248-4F.

C H A P T E R 2

SPECIAL CONSIDERATION REGARDING THE TRUSS MODEL

2.1 Introduction

Before design recommendations based on the space truss model can be proposed, several questions with regard to the behavior of the truss model under special conditions must be addressed.

In Report 248-2, the basic model was presented for the case of a thin-walled box section subjected to a constant shear flow produced by a shear force and/or a torsional moment and for a solid rectangular section subjected to bending and shear but not torsion. However, many questions still remain unanswered, such as the application for other cross sections or for the case when the shear force is not constant through the design region $z \cot \alpha$ such as in beams subjected to distributed loading.

In the space truss model, the ultimate strength of a given section is based on yielding of both the longitudinal and the transverse reinforcement. As a result, it is essential that premature failures caused by crushing of the concrete diagonal strut be avoided. This can be achieved by limiting the compression stresses in the diagonal strut to values equal or less than a certain specified allowable compression stress f_c . However, due to the special conditions existing in the diagonal compression strut, the value of f_c has to be substantially less than the specified compressive strength of the concrete f'_c .

In this chapter, the state of the diagonal compression strut when a beam is subjected to shear and/or torsional stresses, and the effect that the special conditions have on the compression strength of the strut, will be discussed.

In order that members subjected to shear and torsion perform adequately, not only must a correct amount of reinforcement be provided, but it is equally important that this reinforcement be correctly detailed. This situation becomes even more apparent when the truss model is used to illustrate the behavior of those members. If the space truss model is to be applicable, several detailing requirements must be satisfied. A discussion of those requirements is given in this chapter.

The variable angle space truss approach applies to beams in which the shear stresses are of great enough magnitude so as to produce considerable cracking in the web. In such cases the ultimate load capacity of the beam may be solely determined from the space truss. In this chapter the question of how to determine if the beam is in this full truss zone will be addressed. In addition, since ordinarily beams are first designed for flexure and then usually checked to see that they satisfy shear and torsion requirements, frequently a beam at its factored design load might be diagonally uncracked or only in the transition zone between the uncracked and the full truss state. Thus, it is important to be able to evaluate if beams are in this transition zone and how that affects the ultimate load prediction of the space truss model.

In this chapter, the relationships derived in Report 248-2 for equilibrium in the space truss model are discussed to the extent necessary to draw conclusions which will permit the presentation of simple but safe and complete design recommendations based on the space truss model.

2.2 Effects of Different Types of Loading

The case of members subjected to a constant shear and/or torsion was illustrated in 248-2. In this section the effects of different loading conditions using the truss model are presented. First, the case of beams under uniformly distributed load is considered. Next, the special effects of concentrated loads is considered. The presence of a concentrated load induces a series of diagonal compression forces which "fan out" from the concentrated load. The effects of this disturbance on the assumed regular truss action are considered. Next, the case where heavy concentrated loads are applied near the supports is given. Finally, the case of loadings applied on/or near the bottom face causing the so called "hanger effect" is also included.

2.2.1 Beams Subjected to Uniformly Distributed Load. Consider the case of a simple beam subjected to a uniformly distributed load w as shown in Fig. 2.1. In this case the shear force varies linearly from a maximum at the support to zero at midspan. The analysis of this particular case with the truss model (see Fig. 2.2a) yields, from equilibrium of vertical forces on the free body shown in Fig. 2.2b, the value of the design shear force V_s in the zone $z \cot \alpha$:

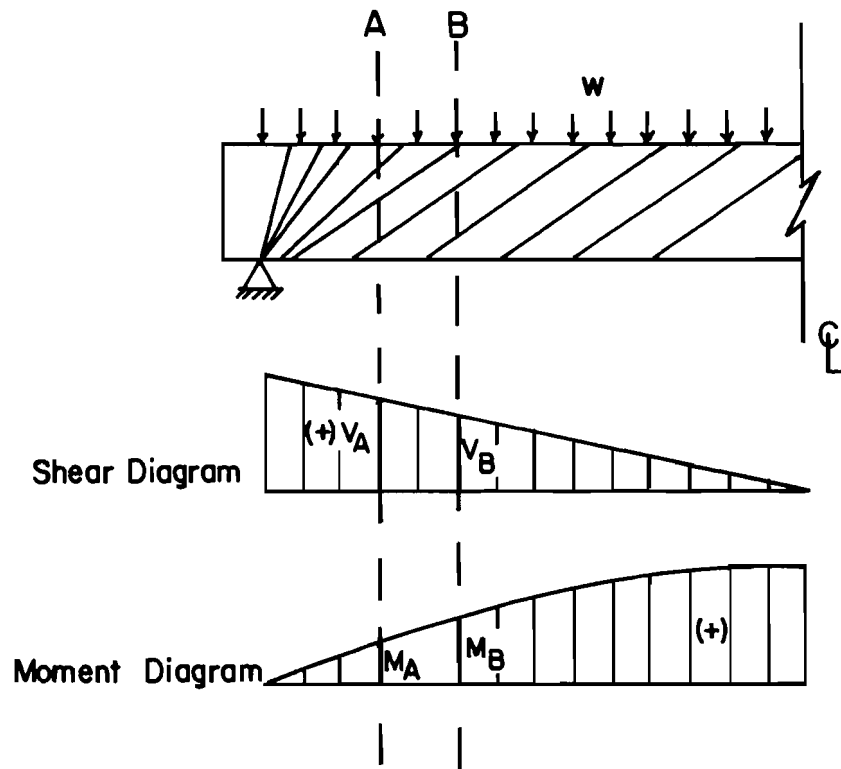


Fig. 2.1 Shear and moment diagrams for a beam under uniformly distributed load

$$V_s = V_A - w z \cot \alpha \quad (2.1)$$

This value is actually the shear force at section B and is based on the assumption that a uniform stirrup spacing "s" exists within the zone $z \cot \alpha$. Using the same free body the force in the moment tension chord F_1 can be found by summing moments about point B.

$$F_1 = \frac{M_A}{z} + V_A \cot \alpha - \frac{V_s}{2} \cot \alpha - \frac{w}{2} z (\cot \alpha)^2 \quad (2.2)$$

Substituting the value of V_s from Eq. 2.1 yields:

$$F_1 = \frac{M_A}{z} + \frac{V_A}{2} \cot \alpha \quad (2.3)$$

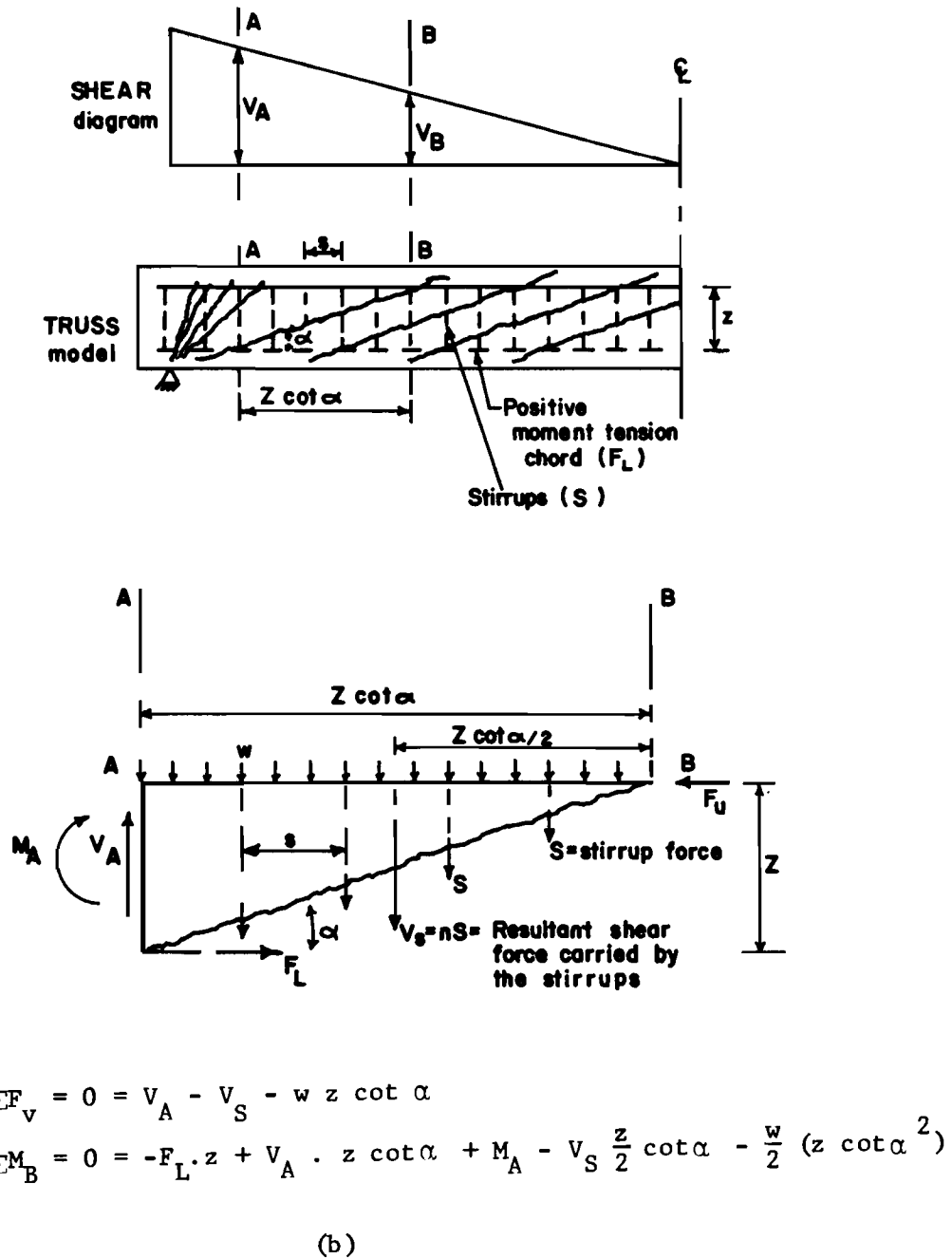


Fig. 2.2 Internal truss forces in the case of uniformly distributed loading

Using these sectional forces the design procedure can be carried out for the case of bending and shear in reinforced and prestressed concrete beams subjected to distributed loads.

2.2.2 Introduction of Concentrated Loads. In Report 248-2, the truss model with variable angle of the diagonal compression members was introduced as an idealized structural model which better describes the behavior of reinforced and prestressed concrete one-way members subjected to bending and shear. In the truss model approach it is usually assumed that the compression diagonals of the truss form a continuous uniform compression field with a constant angle of inclination throughout the span of the member. The development of such a regular truss action in beams is disturbed by the introduction of concentrated loads.

Consider the case of a simply supported beam subjected to a concentrated load. The presence of the concentrated load introduces a series of diagonal compressive forces which "fan out" from the concentrated load. In the idealized truss model each diagonal compression strut has to be anchored at the joint of the truss formed by the longitudinal steel and the vertical stirrup reinforcement.

At the end regions of simply supported members or at the point of application of concentrated loads, the absence of well-distributed longitudinal steel over the entire depth of the member or the lack of end distribution plates causes these diagonal compression forces to concentrate at the last truss joint where they can be anchored producing a fanning out of the diagonal compression forces. Hence, for the beam

shown in Fig. 2.3, compression fans will form both at the support and under the applied concentrated load.

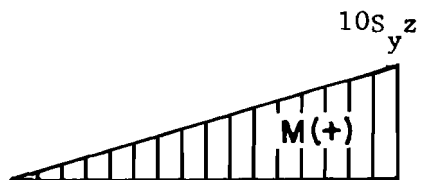
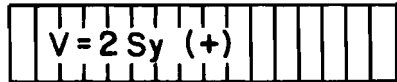
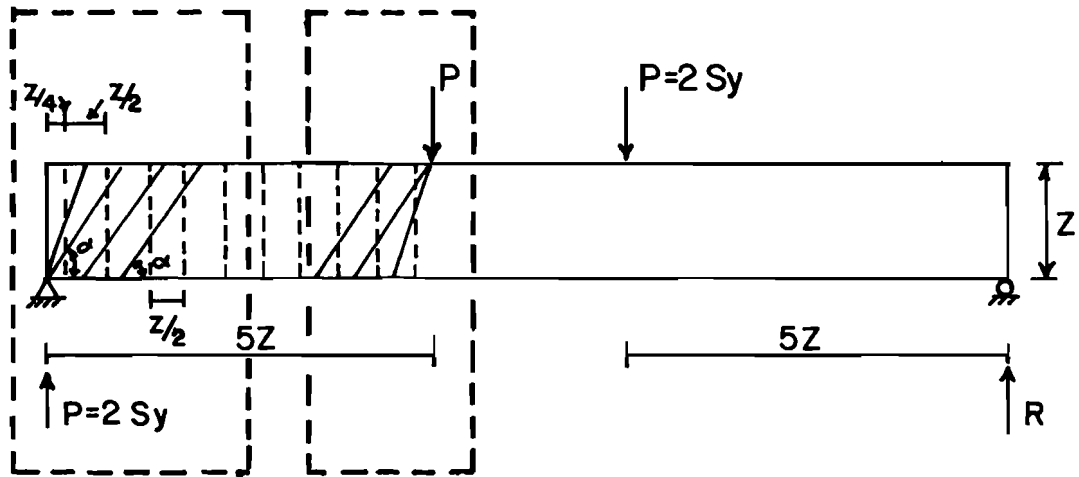
The geometry of the compression fans depends upon the stirrup spacing and the selected angle α . Figure 2.4a shows the equilibrium system at the support for the case of $\tan\alpha = 1.0$ and $s = z/2$.

In Fig. 2.4a the horizontal force $\Delta F(v)$ is shown as a tension force in the truss model. However, the minus sign attached to the value of this force in the table shown in Fig. 2.4a indicates that in reality it acts in the opposite direction, thus becoming a compression force. The presence of this horizontal compression force due to the "fanning" effect eliminates the need for longitudinal tension steel near the ends of simply supported beams where the end reaction induces compression (71).

As can be seen from Fig. 2.4a, as soon as the inclination of the diagonal compression force, "D", in the strut reaches the inclination of the chosen angle α , the effects of the compression fan vanishes.

Since each of the diagonal compression forces acting at an inclination equal to chosen angle α can be anchored at a joint of the truss, a diagonal compression field with uniform inclination becomes feasible, thus eliminating the need of a compression fan to satisfy equilibrium.

Figure 2.4b illustrates the effect of the compression fan on the required anchorage force for the bottom (tension) chord at the support. For the case shown in Fig. 2.4b, the bottom chord of the truss model

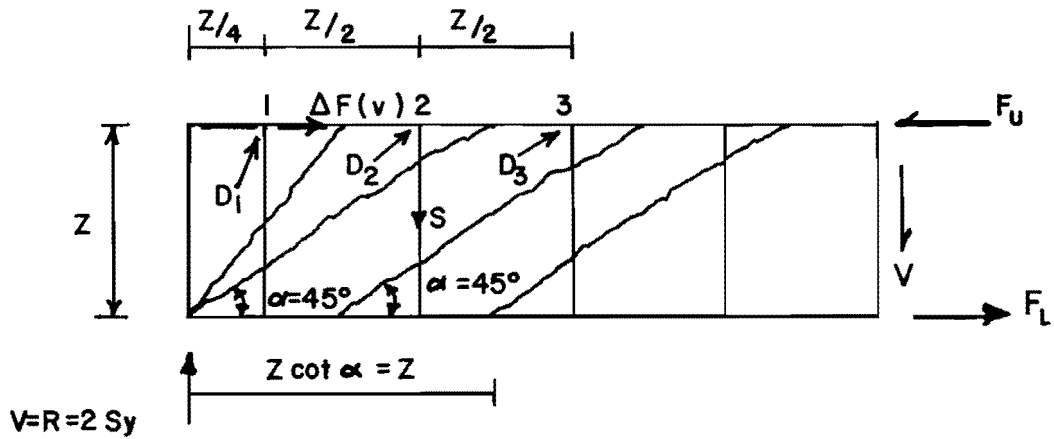


Assumptions:

- $\tan \alpha = 1.0$
- stirrup spacing $s = \frac{z}{2}$

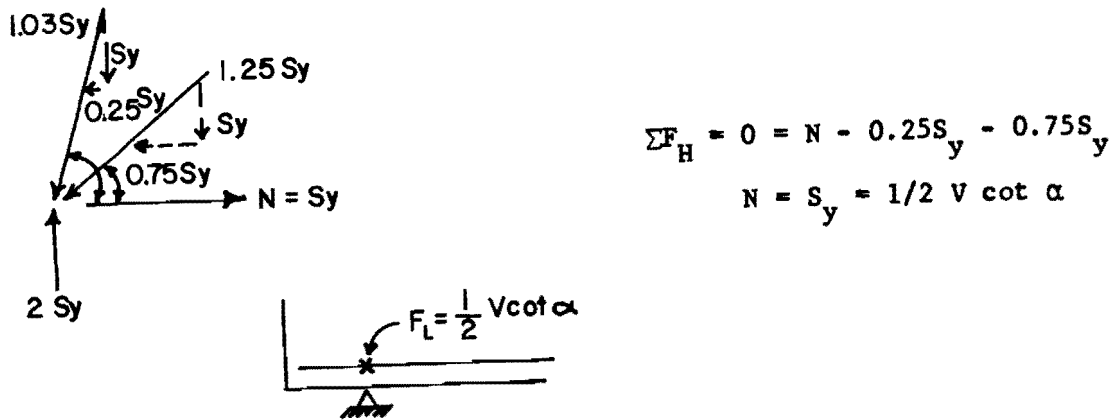
$$V = nS_y = \frac{z \cot \alpha}{\frac{z}{2}} S_y = 2S_y$$

Fig. 2.3 Concentrated loads--compression fans



Point (i)	α (i)	$\cos\alpha$ (i)	$\tan\alpha$ (i)	S (i)	$D_1 = S/\sin\alpha(i)$	$\Delta F(v) D(i)\cos\alpha(i)$
1	75.96°	0.24	4	S_y	$1.03S_y$	$-0.25S_y$
2	53.13°	0.60	4/3	S_y	$1.25S_y$	$-0.75S_y$
						$\Sigma\Delta F(v) = -S_y$
3	45	0.71	1	S_y	$1.41S_y$	$-S_y$

(a) Equilibrium system at support



(b) Anchorage force at the support

Fig. 2.4 Compression fan at the support

requires an anchorage length such that a force equal to $V \cot\alpha/2$, or as in this particular case a force of S_y is adequately developed. Figure 2.4a also shows that the forces acting in the stirrups are the same in the fans as in the regular truss. However, the chord forces F_u and F_1 are influenced by the fan. This effect is shown in Fig. 2.5.

In Report 248-2, it was shown that for the case of bending and shear the force in the compression chord was given by

$$F_u = -M/z + V \cot \alpha / 2 \quad (2.4)$$

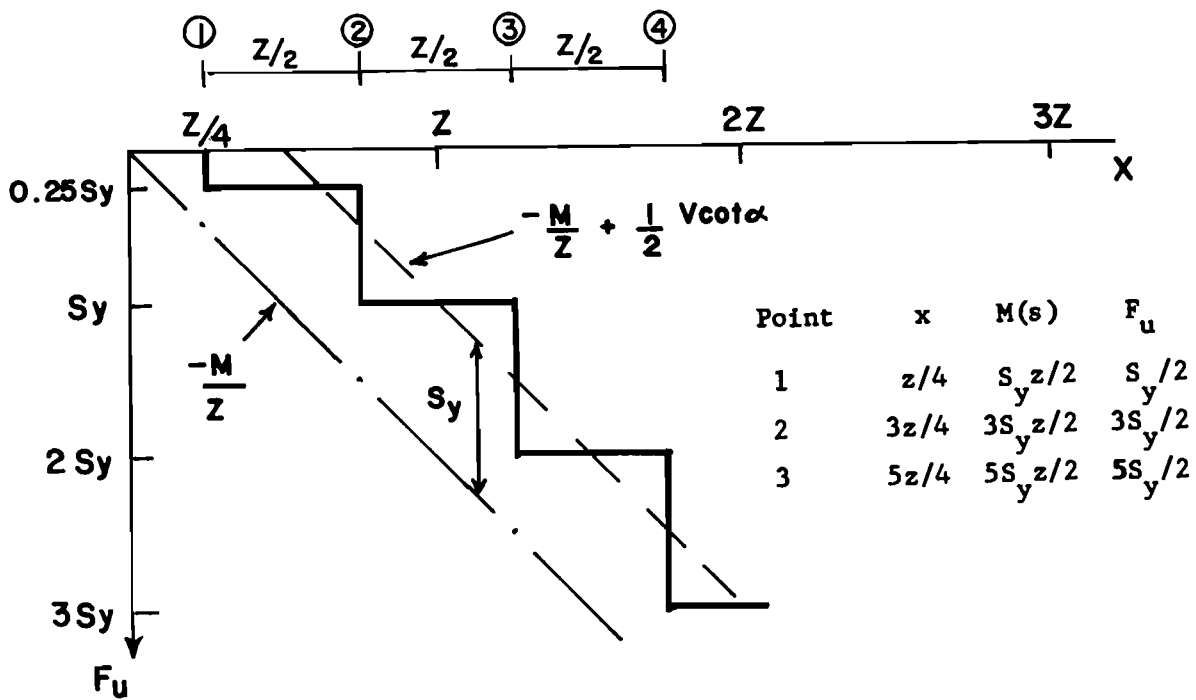
and the force in the tension chord was computed as:

$$F_1 = M/z + V \cot \alpha / 2 \quad (2.5)$$

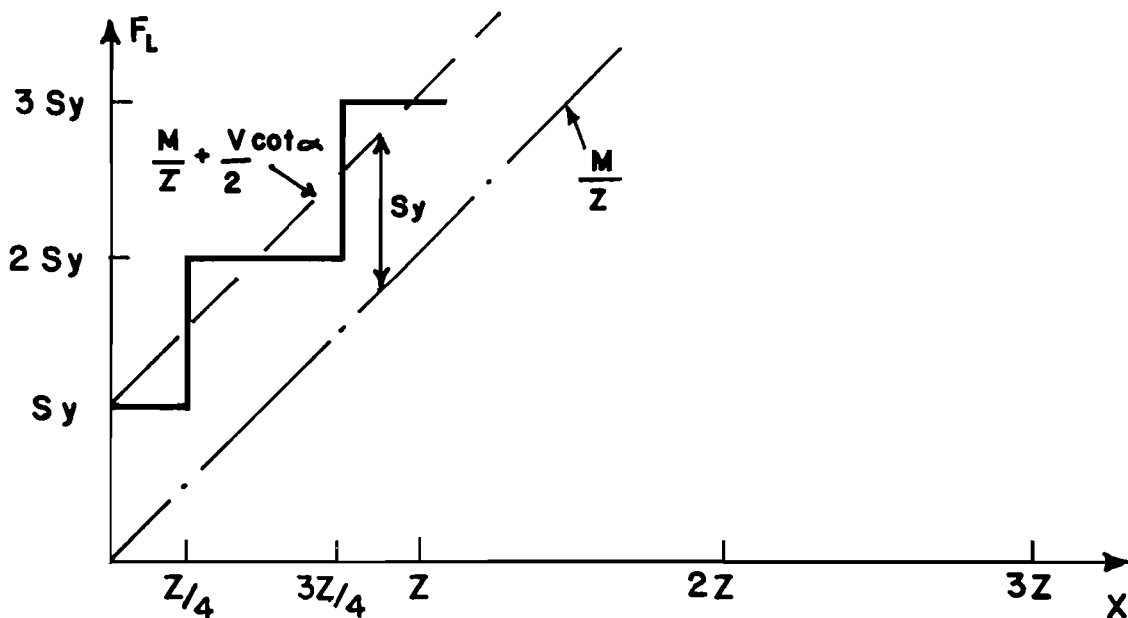
It should be noted that in the discrete truss model the increase in the force in the upper and lower chords takes place in steps while in the actual beam it is more continuous. From Fig. 2.5a it can be seen that no horizontal tensile reinforcement is required due to the effects of shear in the top (compression) face of the member within a distance $z \cot\alpha / 2$ (in this case $z/2$) from the centerline of the support.

Figure 2.6 shows the equilibrium system for the zone of the compression fan under the applied concentrated load. Similar to the case of the compression fan at the support, the forces in the stirrups are the same in the compression fan zone as well as in the regular truss. Figure 2.7 illustrates the effect of the compression fan on the chord forces F_u and F_1 .

From Fig. 2.7b a very interesting fact should be noted. Directly under the applied load the angle of inclination of the crack is equal to 90 degrees, hence the shear will not cause any increase in the

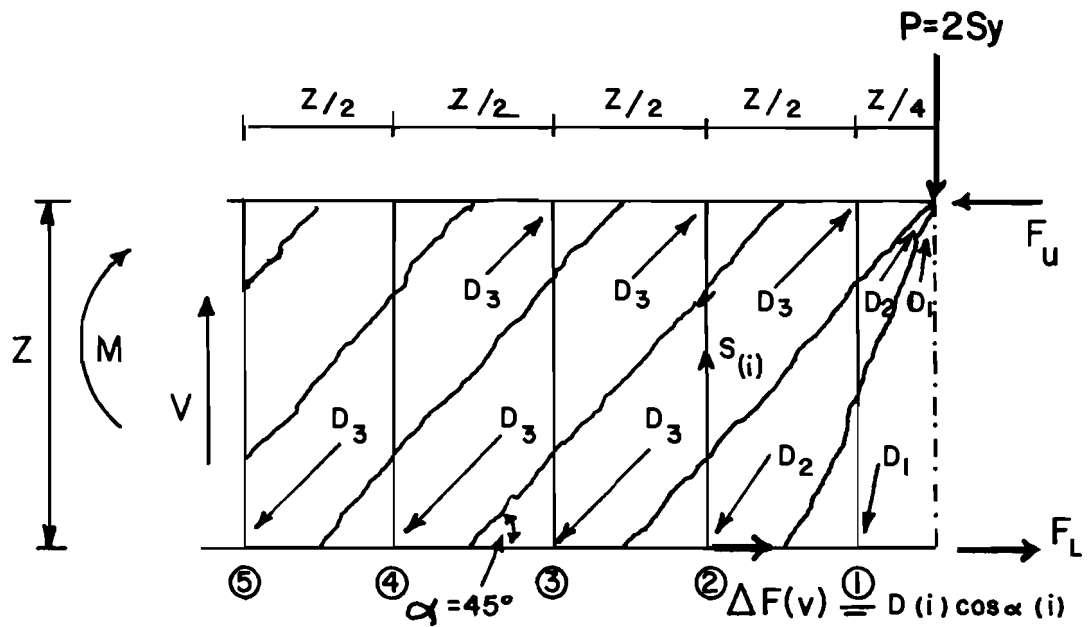


(a) Force in the upper chord



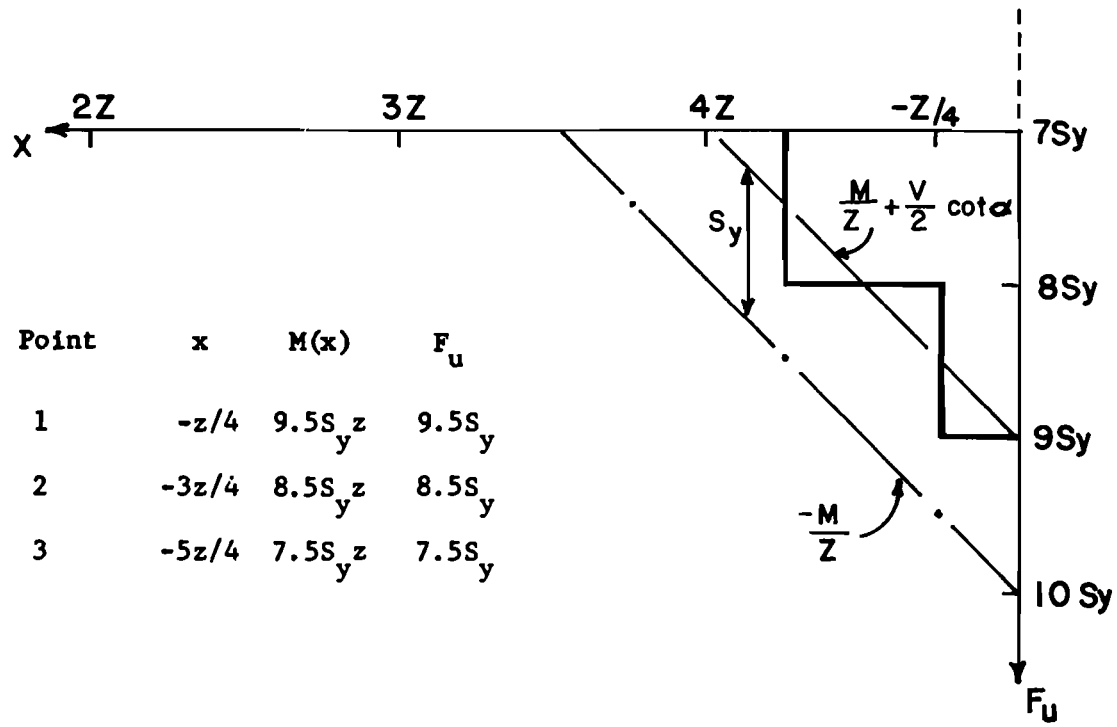
(b) Force in the lower chord

Fig. 2.5 Forces in the top and bottom chords of the truss model

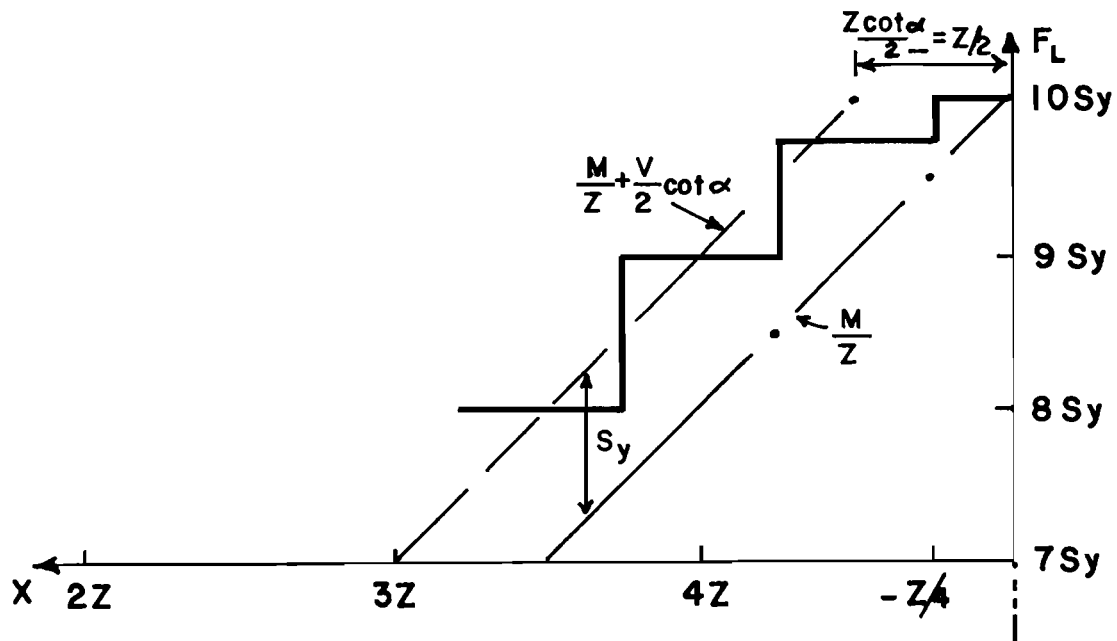


Point (i)	$\alpha (i)$	$\cos \alpha (i)$	$\tan \alpha (i)$	$S (i)$	$D(i) / \sin \alpha (i)$	$\Delta F (v)$
1	75.96°	0.24	4	S_y	$1.03S_y$	$-0.25S_y$
2	53.13°	0.60	$4/3$	S_y	$1.25S_y$	$-0.75S_y$
3	45°	0.71	1.0	S_y	$1.41S_y$	$-S_y$

Fig. 2.6 Equilibrium system under the applied load



(a) Force in the upper chord (compression)



(b) Force in the lower chord (tension)

Fig. 2.7 Forces in the top and bottom chords of the truss model

tensile force of the longitudinal stringer. As a consequence, the area of longitudinal tension steel in this region need not exceed the area required for the maximum flexure. However, because of the presence of the compression fan under the applied load, when dimensioning the tension chord reinforcement using Eq. 2.5, the calculations should be made at a distance $z \cot \alpha / 2$ from the concentrated load.

2.2.3 Heavy Concentrated Loads Near the Supports. In the case of beams where the support reaction introduces compression into the ends of the member, current design procedures (17,24) state that the calculation of the maximum shear force shall be as follows:

1. For nonprestressed members, sections located less than a distance "d" from face of support may be designed for the same shear V_u as that computed at a distance "d".
2. For nonprestressed members, sections located less than a distance $h/2$ from face of support may be designed for the same shear V_u as that computed at a distance $h/2$.

Typical support conditions where the shear force at a distance "d" from the support may be used, include: (1) members supported by bearing at the bottom of the member, such as shown in Fig. 2.8a and, (2) beams framing monolithically into a supporting column as shown in Fig. 2.8b.

In such cases a local state of compression is induced, which delays the appearance of diagonal tension cracks. Thus, an increase in the shear strength of the beam results. Therefore, the closer the point of application of the load is to the reaction producing local compression in the member, the more difficult it will be for diagonal cracking to occur.

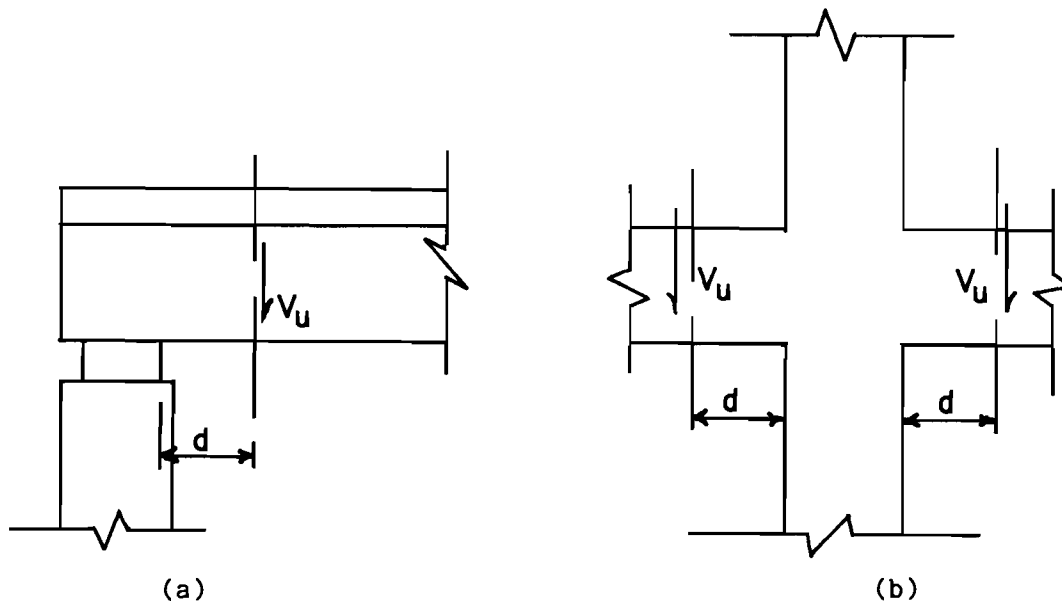


Fig. 2.8 Typical support conditions where the maximum design shear force is that computed at a distance "d" from the face of the support

However, this provision is not always valid. These are two major exceptions. The first one is the case when the support reaction does not induce a state of compression in the end region of the beam. Such is the case of members framing into a supporting member in tension, as seen in Fig. 2.9a. In that case the critical section for shear is taken at the face of the support.

The second major exception is in the case of members where the shear at section between the support and a distance "d" differs radically from the shear at a distance "d". This occurs in brackets, and in beams where a heavy concentrated load is located close to the support such as in bridge bent caps (see Fig. 2.9b). In these cases current shear design provisions recommend (17,24) that the actual shear at the face of the support should be used.

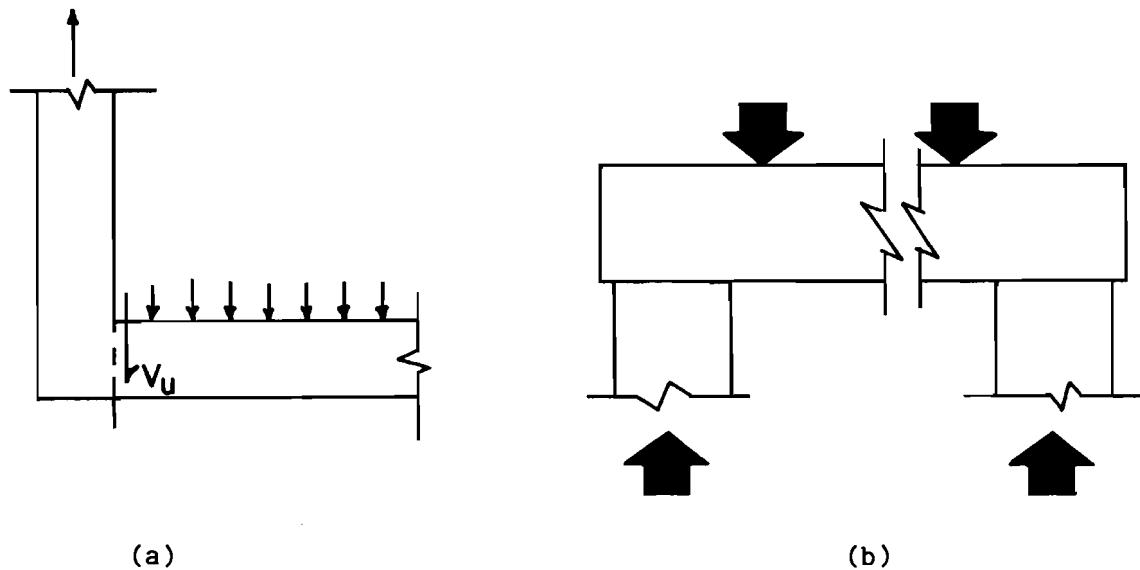


Fig. 2.9 Cases where the critical section for shear is located at the face of the support

Bridge bent caps often are clear examples of members subjected to heavy concentrated loads near the supports. The bent caps support the main longitudinal girders in the bridge. These girders transmit heavy concentrated loads to the bent caps. Usually high capacity piers provide the support for the bent caps. In the case of a two pier cap the bent cap often becomes a "deep beam".

The case of most deep beams can be analyzed using the truss model described in Report 248-2, since the upper limit of the angle α ($\tan \alpha = 2.0$) would produce a design region $z \cot \alpha$ equal to $z/2$. This makes possible design of beams with a shear span-to-depth ratio (a/z) as low as $1/2$ (see Fig. 2.10) which would cover most of the deep beam range.

For any members which may be deeper than this or where the heavy concentrated load is located within the distance $z/2$ from the centerline

of the support it is recommended that the basic truss model be applied consistently as recommended by Marti (183,184) as a more general check than the usual shear friction theory.

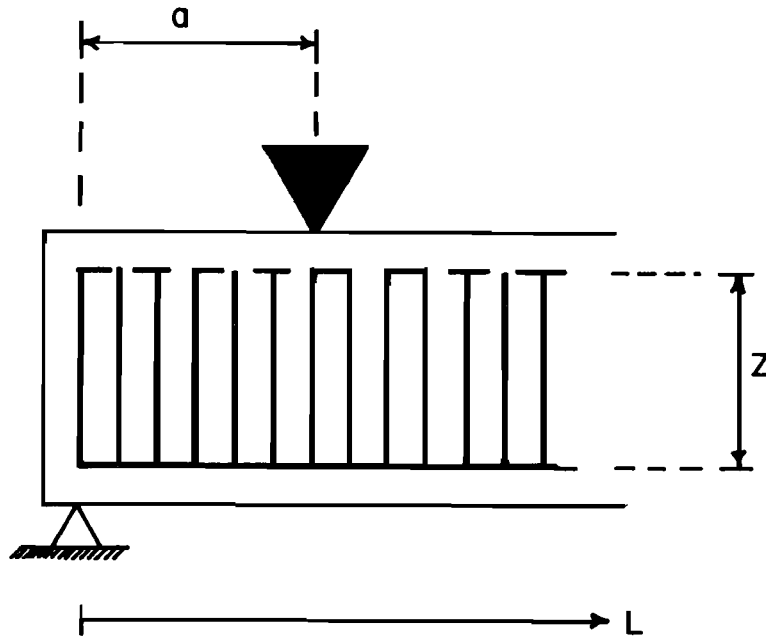
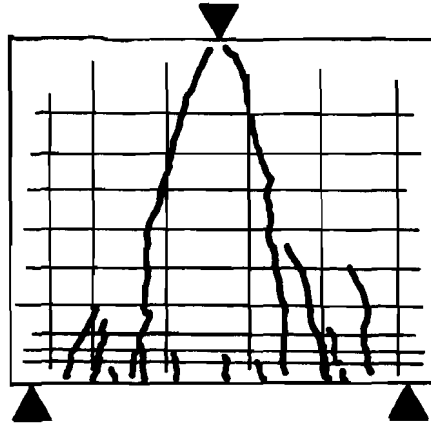
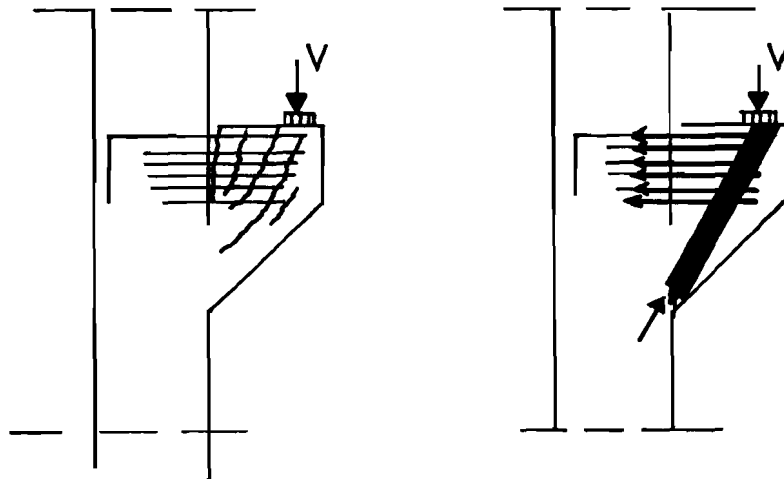


Fig. 2.10 Definition of a/z ratio

In general, tests of beams with a/z ratios less than 0.5 have shown crack patterns at failure similar, to that shown in Fig. 2.11a. The pattern of cracks at failure in Fig. 2.11a shows an inclination which is very close to 90 degrees from the horizontal. Normally, therefore, vertical stirrups will not be effective. However, in the case of brackets and corbels (see Fig. 2.11b), shear would act along the vertical plane of the crack. Vertical slip of one crack face occurs with respect to the other. If the crack faces are rough and irregular, this slip will be accompanied by a horizontal separation of the crack faces. Thus it is obvious that horizontal web reinforcement should be



(a) Failure of simply supported deep beam
($a/z < 0.5$)



(b) Typical crack pattern and assumed internal force distribution of a bracket near failure

Fig. 2.11 Analogy of deep beams with $a/z < 0.5$ and brackets and corbels

provided (shear friction reinforcement). At ultimate, the horizontal crack separation will be sufficient to stress this reinforcement to its yield point.

Consequently, applying the previous discussion to Fig. 2.11a, it is reasonable to assume that the design of this type of member can be based on a simple truss analogy consisting of the main reinforcement acting as horizontal tension ties and concrete struts acting as inclined compression members. In this strut and tie system shear failure as such is not considered as a primary failure mode. The basic assumptions followed in the construction of this truss model are:

1. Equilibrium must be satisfied.
2. The concrete transmits only compression forces. The strength of the concrete in tension is neglected.
3. The reinforcement acts only as linear members, i.e. dowel effect is neglected.
4. Yielding of the reinforcement will take place at failure.
5. Well-distributed horizontal reinforcement should be placed across the potential length of the vertical cracks to control cracking at service load levels and to ensure the assumed redistribution of internal forces in the cracked state.

In the strut and tie system, provided the anchorage of the tie is adequate, eventual failure is caused either by yielding of the main steel, or by crushing of the concrete in the flexural compression zone or in the diagonal strut. Since brittle failures due to crushing of the concrete must be avoided, the stress in the flexural compression zone and in the diagonal strut should be kept below specified limits. In

this case the ultimate load capacity should be governed by yielding of the longitudinal steel acting as a tension ties. Based on this strut and tie system derived using the truss model, the design of members where heavy concentrated loads are applied within the distance $zcot\alpha/2$ can be carried out. The concentrated load located within $zcot\alpha/2$ from the centerline of the support can be assumed to be carried by a single diagonal compressive strut from the load to the support.

In this system special attention has to be paid to the detailing and in particular to the adequate anchorage into the support of the longitudinal steel used as tension ties. This may require embedment hooks, or welding of special devices. Service load level control of the vertical cracking in the web regions will require distributed horizontal reinforcement. Another important aspect in the design of these members is the large diagonal compression stresses near the support after the onset of cracking. It is recommended that a reduced concrete compressive strength, f_c , be used to determine the strength of the diagonal compression strut, since this would be crossed by the horizontal tension ties, which would put the concrete in a biaxial state of stresses (tension and compression). The diagonal strength of this compression strut and specific guidelines on the reduced concrete compressive strength will be discussed in subsequent sections.

2.2.4 Hanging Loads. The case of a simple beam loaded at the bottom face is greatly clarified by the use of the truss model. This is shown by considering the case of a truss loaded first on the top chord and then for contrast loaded on the bottom chord.

In Fig. 2.12a, the case of a truss loaded on the top chord is analyzed and the force in the vertical tension member C is found to be $1.5P$ (tension). In Fig. 2.12b, the same truss is analyzed but the load is placed on the bottom chord. The tension force in the same member C becomes $2.5P$ (tension).

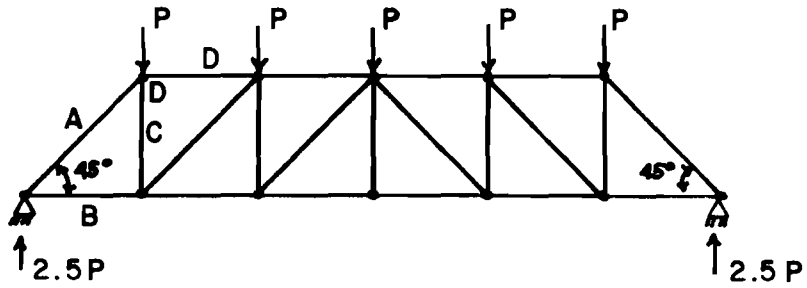
The increase in the tension force in the member C when the load is applied at the bottom chord reflects the so called "hanger effect".

The additional area of steel required in the vertical is that necessary to "hang up" the load P by transmitting it from the bottom face to the top of an effective compression strut in the member. For the case of members subjected to an uniformly distributed load w , the additional tension force in the vertical elements when the member is loaded at the bottom chord would be $w*s$, where "s" represents the spacing between the vertical elements in the truss model.

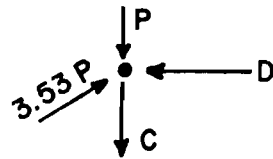
2.3 Compression Strength of the Diagonal Strut

The use of the truss model with variable angle of inclination of the diagonal struts in the design of reinforced and prestressed concrete members requires that the steel reinforcement yield prior to failure of the concrete in compression. Concrete failure can be due to crushing of the bending compression zone or the concrete compression diagonals.

The stresses in the bending compression zone can be determined using the well-known bending theory (135). They are limited by restricting the tensile reinforcement to a fraction of the amount which produces a balanced failure. In the case where torsion exists together with bending the situation is even less critical. Since a torsional



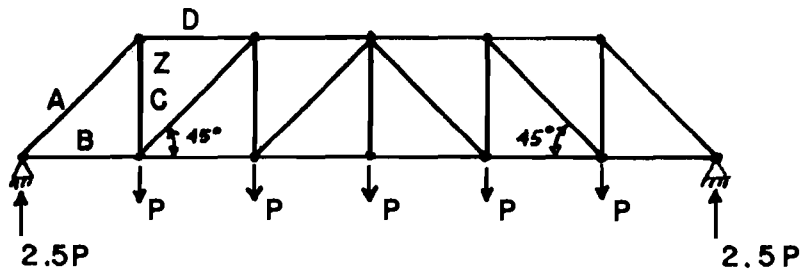
Equilibrium at joint 2



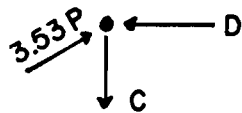
$$+ \sum F_v = 0 = P - 3.53P (\sin 45) + C$$

$$C = 1.5P \text{ (tension)}$$

(a) Truss loaded at the top chord



Equilibrium at joint 2



$$+ \sum F_v = 0 = -3.53P (\sin 45) + C$$

$$C = 2.5P \text{ (tension)}$$

(b) Truss loaded at the bottom chord

Fig. 2.12 Hanging loads

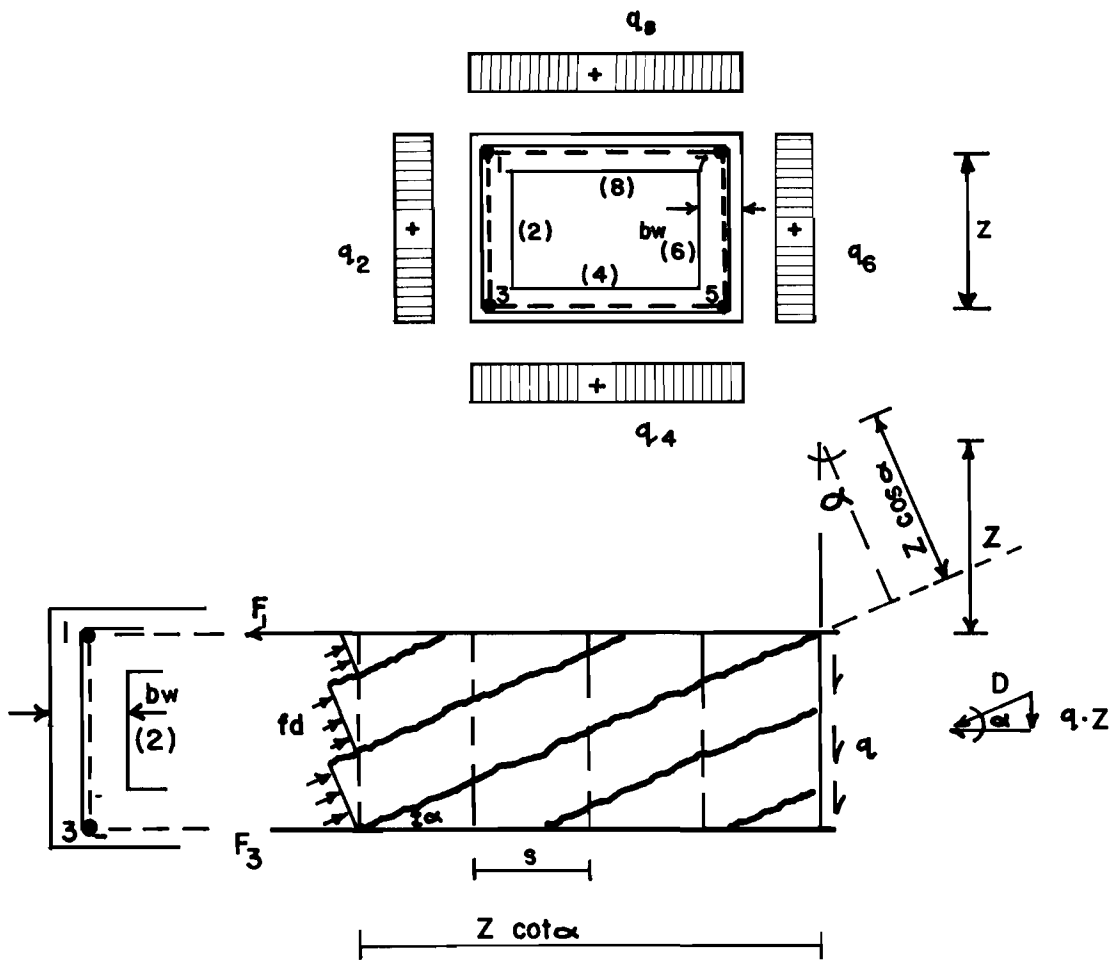
moment introduces longitudinal tension on all faces of the member, it will raise the neutral axis in the case of positive bending moment (tension at the bottom of the member), therefore reducing the compression stresses in the bending compression zone. The same holds true for the case of a negative bending moment (tension at the top) since now the torque will lower the neutral axis, hence reducing the stress in the bending compression zone. Thus, the restrictions on longitudinal reinforcement as a fraction of balanced reinforcement based on simultaneous yielding of the longitudinal steel and crushing of the concrete in the case of pure bending constitutes a safe lower bound for the case of combined torsion and bending.

The concrete compression diagonal struts carry the diagonal forces necessary for truss equilibrium. The stresses f_d in the diagonal compression strut are caused by the diagonal force D . Consider the case of a shear field element subjected to a constant shear flow as shown in Fig. 2.13. From geometric considerations the stress in the diagonal strut caused by the diagonal force D is given by the relation:

$$f_d = \frac{q}{b_w \sin\alpha \cos\alpha} \quad (2.6)$$

where "q" is the shear flow due to shear or shear and torsion. Assuming a constant shear flow over the entire height of the section the term q/b_w becomes the average shear stress "v". Rearranging Eq. 2.6 yields

$$\frac{f_d}{v} = \frac{1}{\sin\alpha \cos\alpha} \quad (2.7)$$



$$f_d = \frac{D}{A}$$

Geometry: $D = \frac{q \cdot z}{\sin \alpha}$

$$A = b_w \cdot z \cos \alpha$$

Thus: $f_d = \frac{q}{b_w \cos \alpha \sin \alpha}$

Fig. 2.13 Compression stress f_d in the diagonal strut

This relation represents the normalized compression stress in the diagonal strut as a function of the angle of inclination α of the strut.

It has been suggested (28,57,58,65) that the limiting value of the average principal compressive stress in the diagonal concrete strut is governed not so much by the compression strength of the uncracked portions of the strut but by the capacity of the interface shear transfer mechanisms, such as aggregate interlock, to transmit the require shear stress across previously existing cracks. When a crack is developed in a concrete mass the surfaces are usually rough and irregular. Movement is then restricted by the bearing and friction of the aggregate particles on the crack surface. Provided that restraint is available to prevent large increases in the crack width, substantial shear forces can be transmitted across the crack interface through the mechanism of aggregate interlock. The principal factors affecting the aggregate interlock are:

1. Quality of the concrete. Usually the top part of a member, because of the particle sedimentation and water gain under the coarse aggregate will contain weaker concrete.
2. The size of the crack width. Smaller crack widths lead to larger shear stresses, but also to more sudden failures.

Tests by T. Paulay and P. J. Loeber (32), in which the crack width increased proportionally with the applied load, verified that the stiffness of the aggregate interlock mechanism gradually decreased as the shear stress across the interface increased. In order for the aggregate interlock mechanism to remain effective, the crack width should be limited. For larger crack widths only limited transfer of shear forces across the crack interfaces is possible and, thus, no

further redistribution of forces in the member is possible. The available contact area reduces with increasing crack widths. Hence, the smaller the contact area, the smaller the force to be transmitted for the same shear displacement.

In Report 248-2, the relation between the mean crack strain ϵ_r (see Fig. 2.14) and the strains in the transverse [ϵ_s] and the longitudinal [ϵ_1] reinforcement were developed

$$\epsilon_r = \epsilon_s + \epsilon_1 \quad (2.8)$$

$$\epsilon_s = \epsilon_1 \cot^2 \alpha \quad (2.9)$$

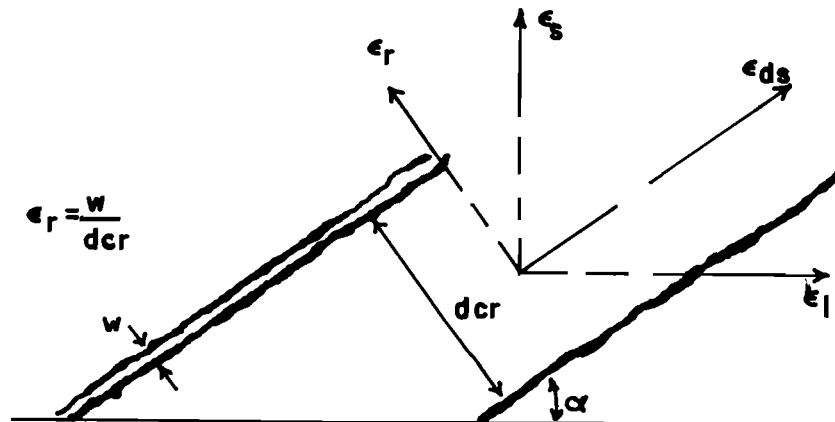


Fig. 2.14 Mean crack strain ϵ_r

These relationships can be discussed by rearranging Eqs. 2.8 and 2.9 into

$$\epsilon_r = \epsilon_s (1 + \tan^2 \alpha) \quad (2.10)$$

$$\epsilon_r = \epsilon_1 (1 + \cot^2 \alpha) \quad (2.11)$$

Equations 2.10, for the case of yielding of the transverse reinforcement [$\epsilon_s = \epsilon_y$], and 2.11, when the longitudinal reinforcement yields [$\epsilon_l = \epsilon_y$], are shown in Fig. 2.15.

From Fig. 2.15 it can be seen that, for an inclination of the compression diagonals of $\alpha = 45$ degrees, the crack parameter ϵ_r and hence, the crack width becomes a minimum for yielding of both the longitudinal and stirrup reinforcement. A smaller angle α requires asymptotically increasing crack opening and stirrup strains to obtain yielding of the longitudinal reinforcement. An angle larger than 45 degrees will demand larger crack openings and longitudinal strains to obtain yielding of the transverse reinforcement. Therefore, the mean crack strain is largely dependent upon the angle of inclination of the diagonal compression strut. Since the aggregate interlock disintegrates with large crack widths, and the mechanism of shear transfer in the diagonally cracked concrete is largely dependent on the aggregate interlock, it is apparent that the maximum compressive stress that the diagonal strut can take will be a function of the angle α .

Equation 2.7, which relates the stress in the diagonal compression strut and the angle of inclination α of this element, is plotted in Fig. 2.16.

From Fig. 2.16 it can be seen that the compression stress f_d in the diagonal strut does not vary significantly within the limits of the angle α proposed in Report 248-2. The maximum difference from the minimum value at 45 degrees is only 25%. Thus, within the limits for the angle of inclination of the diagonal compression strut,

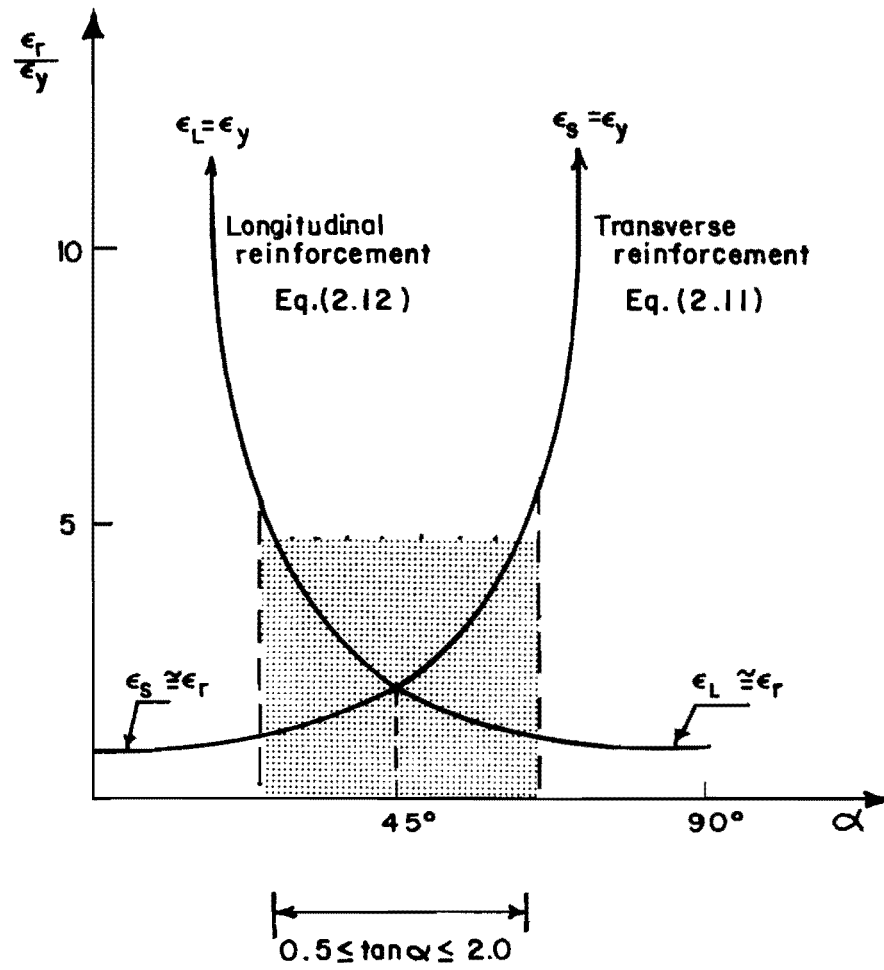


Fig. 2.15 Relationship between the mean crack strain and the strains in the reinforcement for different angles of inclination of the diagonal strut

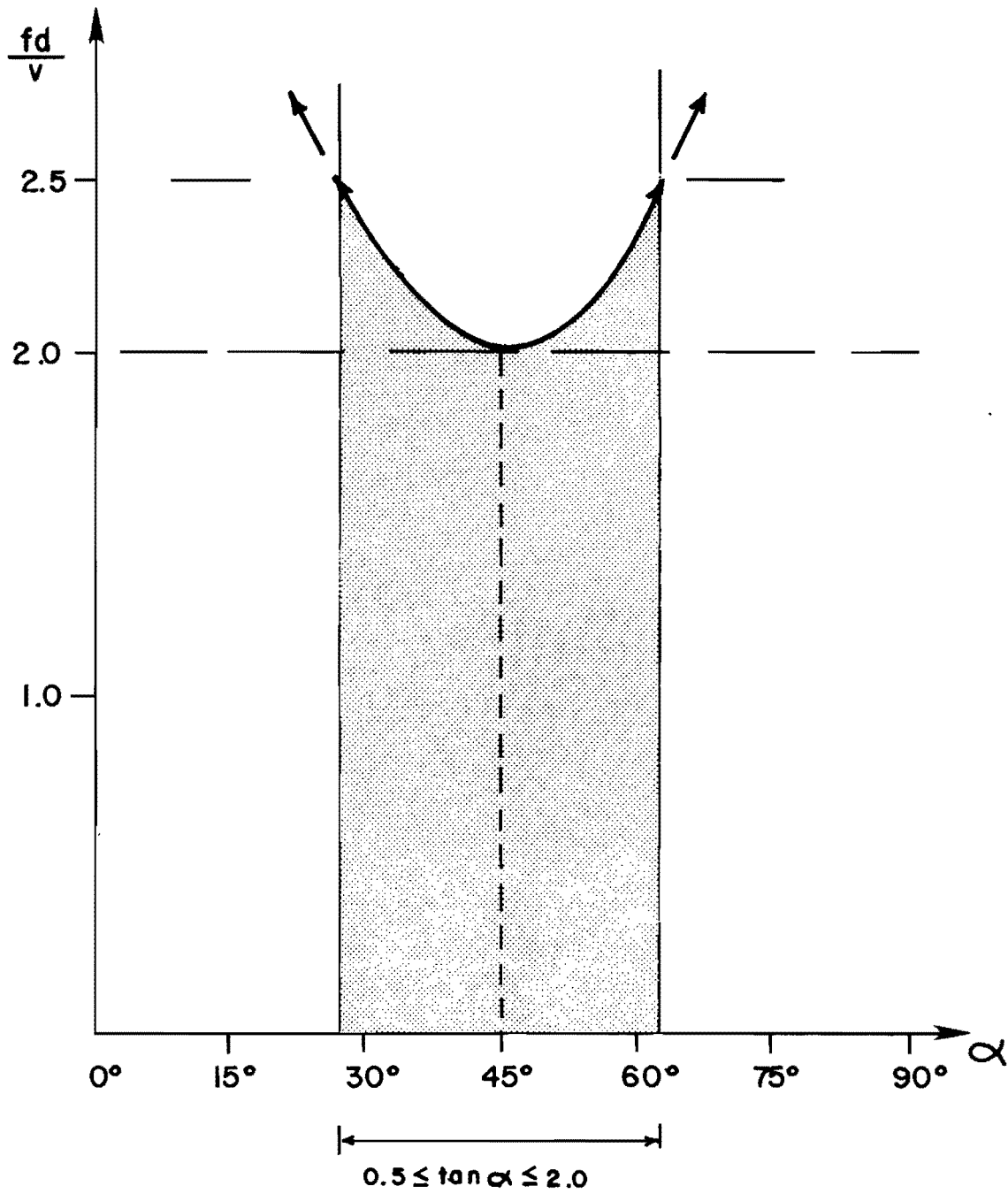


Fig. 2.16 Stress f_d as a function of the angle

$$0.5 \leq \tan \alpha \leq 2.0$$

$$26^\circ < \alpha < 63^\circ$$

the average diagonal compression stress f_d can be controlled by limiting the nominal shear stress independently of the inclination α of the compression diagonals.

As shown in Fig. 2.15, the shear stress v that can be transferred is at a maximum for an angle α of 45 degrees. Thus, the maximum shear stress v_{\max} is obtained from Eq. 2.6 with an angle α equal to 45 degrees.

$$v_{\max} = \frac{q}{b_w} = \frac{f_d}{2} \quad (2.12)$$

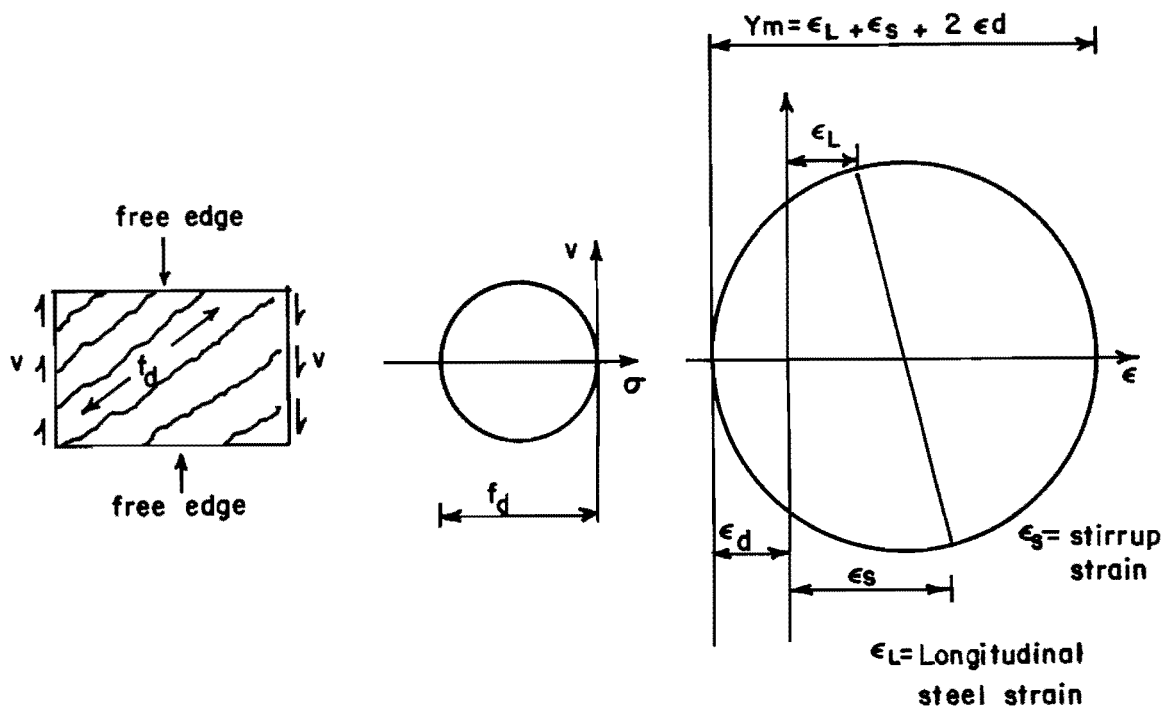
where q is the vertical shear flow due to shear or shear and torsion, and b_w is the effective web width of the section resisting the vertical shear flow. Hence, compression stress in the diagonal strut associated with the maximum shear is

$$f_d = \frac{2q}{b_w} \quad (2.13)$$

By limiting the compression stress in the diagonal strut f_d to a maximum allowable value f_c failure due to crushing of the concrete would be avoided.

Several relations to evaluate the maximum allowable compression stress f_c in the diagonal strut have been proposed. In all of them a reduced value of the 28-day concrete compression strength f'_c is recommended. Collins (58) suggested that the maximum allowable

compression stress in the diagonal strut should be a function of the average principal compressive strain in the strut ϵ_d , the ratio of the maximum shear strain γ_m (i.e. the diameter of the strain circle), and the 28 day concrete compression strength f'_c (see Fig. 2.17).



(a) Diagonally cracked concrete (b) Stress circle (c) Strain circle

Fig. 2.17 Stress and strain conditions for diagonally cracked concrete neglecting principal tensile stress

The proposed equation is:

$$f_c = f_{dmax} = \frac{5.5f'_c}{4 + \frac{\gamma_m}{\epsilon_d}} \quad (2.14)$$

Thürlimann (162) on the basis of test evidence and practical experience proposed that the allowable compression stress f_c be:

$$f_c = f_{dmax} = 0.36f'_c + 696 \leq 2400 \text{ psi} \quad (2.15)$$

where f_c and f'_c are in terms of psi (see Fig. 2.18).

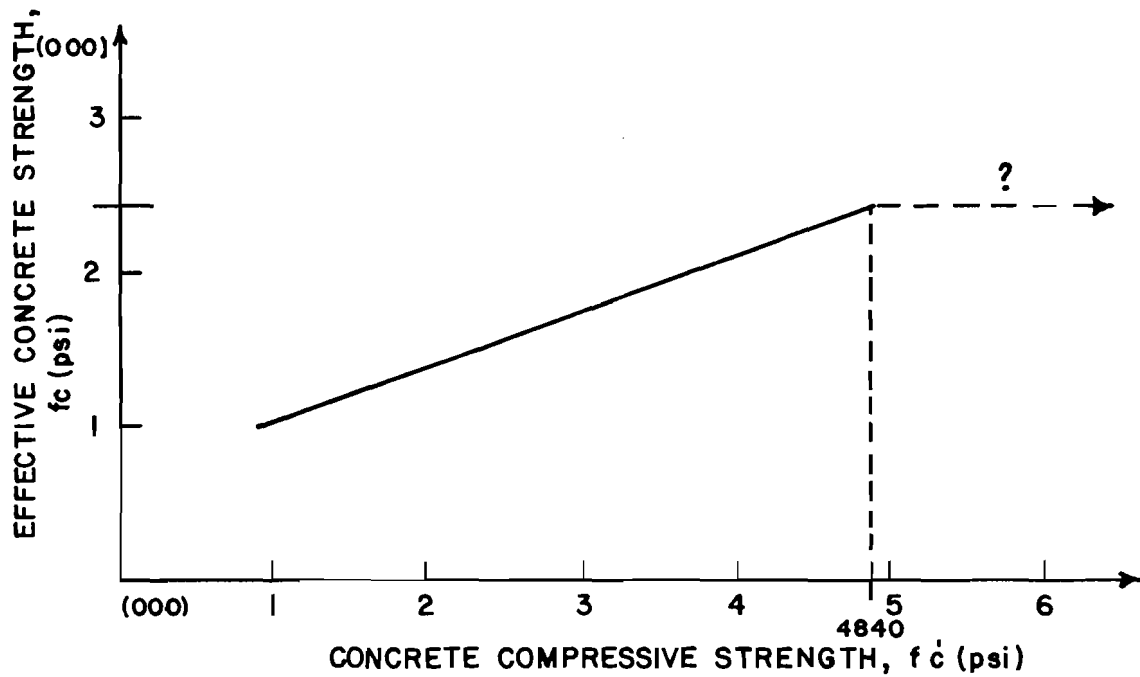


Fig. 2.18 Thürlimann recommendation for effective concrete strength vs. concrete compressive strength

Thürlimann cites several factors which influence the value of f_c . Due to the fact that the stirrups across the diagonal tension cracked concrete are in tension, the diagonal concrete strut is then in a biaxial state of stress which reduces its compressive strength. Another factor is the redistribution of forces in the member due to the different ratios of longitudinal to transverse reinforcement which may cause the failure crack to be at an inclination other than the 45 degree angle corresponding to initial diagonal tension cracking of the concrete. Another important factor is the undesirability of a failure due to crushing of the concrete in the web because of its brittle nature.

Another factor considered was the fact that in the case of torsion the twisting of the beam induces an additional compression stress into the diagonal. Thürlimann and Lampert (95) stated that the increase in the diagonal compression stress was due to a distortional effect in the walls of the cross section. Through twisting, the originally plane walls of the section are distorted to hyperbolic paraboloids (Fig. 2.19) limited by four straight edges.

The distorted wall constitutes then a hyperbolic paraboloid shell subjected to a uniform shear flow "q". The entire shell when loaded in this fashion is subjected solely to pure shear stresses of constant intensity (see Fig. 2.20).

This state of pure shear, which actually resolves into principal stresses of equal and opposite magnitude (tension and compression) acting on sections at 45 degrees to the shear plane, can be deduced from

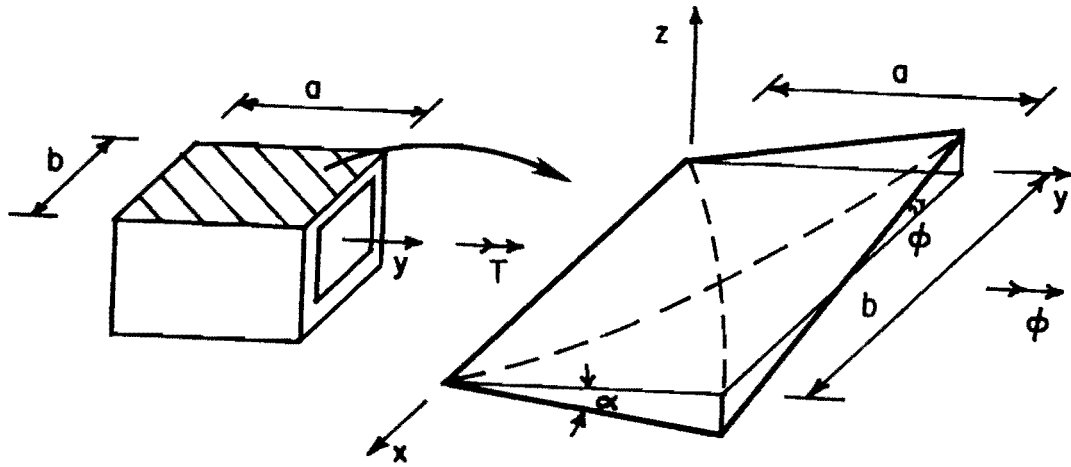


Fig. 2.19 Distortional effect

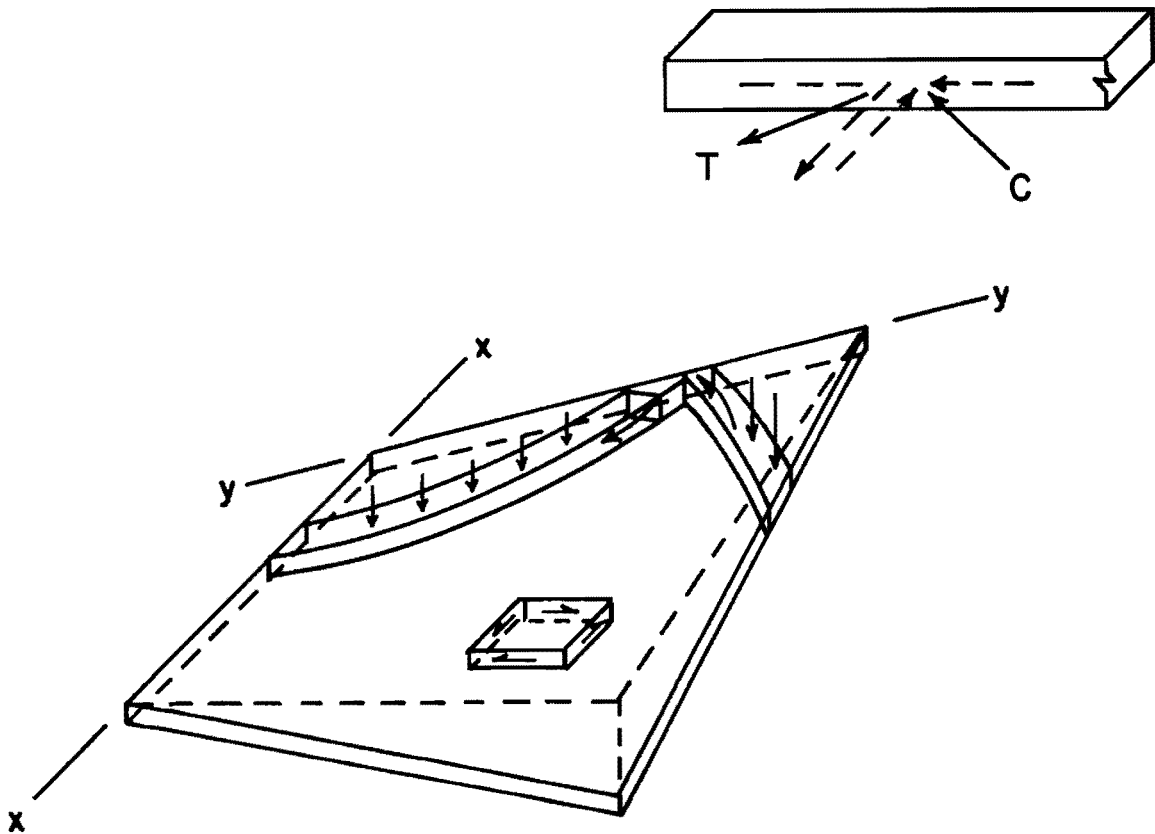


Fig. 2.20 Forces acting on edge members of parabolic arches

purely physical considerations without recourse to differential equations.

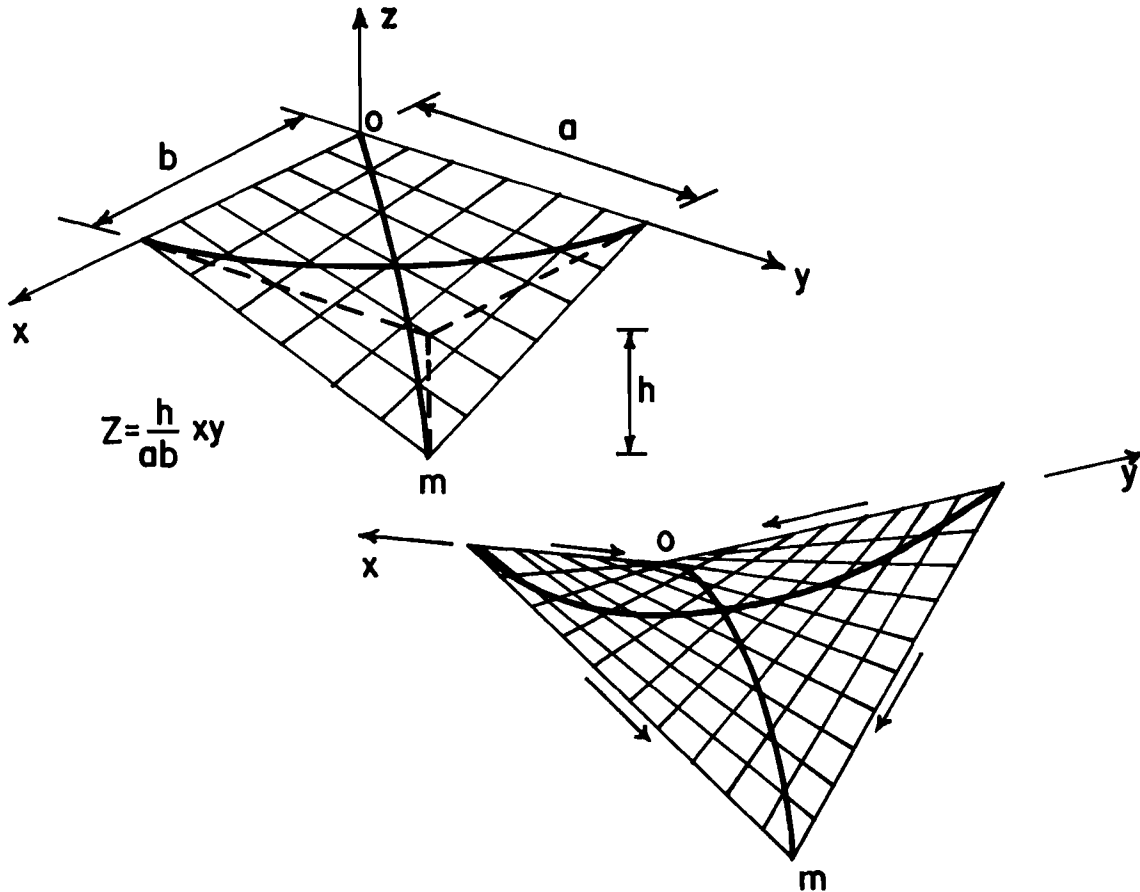


Fig. 2.21 Sections of a hyperbolic paraboloid surface taken at 45 degrees to the coordinate axis

As shown in Fig. 2.21, sections of a hyperbolic paraboloid surface taken at 45 degrees to the coordinate axis form identical parabolic arches. In other words, the surface shown in Fig. 2.21 can be obtained by moving a parabolic curve along curve $o-m$. The parabolas parallel to the curve $o-m$ curve downward, whereas those at right angles to these parabolas curve in the opposite direction. Assuming that the

load is equally divided between the two sets of perpendicular parabolas, it is evident that at the edge the parabolas parallel to the curve o-m exert an outward thrust, whereas those perpendicular to curve o-m exert an inward pull. Although opposite in character, the magnitude of these forces intersecting at any point on the boundary of the surface is equal because the intersecting parabolas are identical. The net effect, as shown in Fig. 2.20, is that the outward force acting on the edge is cancelled and only pure shear acts along the edge.

These edge shears require edge members. In the case of the truss model these edge members are provided by the longitudinal chords which are thereby loaded axially. The additional compressive stresses on the outer surface of the diagonal due to wall distortion must be added to those obtained from the actual shear flow q .

As a result Thürlimann suggests that the maximum value of f_c used, be approximately 2400 psi, which corresponds to f'_c of about 4800 psi. It is important to note that Thürlimann states that this limit is somewhat arbitrary as shown in Fig. 2.18. The current ACI Building Code (24) and AASHTO Standard Specifications (12) require an upper limit for the maximum shear stress, v , of $10\sqrt{f'_c}$. As previously explained in Report 248-2, the ACI and AASHTO (24.12) assume a truss model with a constant angle of inclination of the diagonal compression struts equal to 45 degrees. Substituting in Eq. 2.7, the value of $10\sqrt{f'_c}$ for the shear stress " v ", " d " for $0.9z$, and setting α equal to 45 degrees yields a maximum allowable compression stress, f_c of $22\sqrt{f'_c}$. In Fig. 2.22, the Thürlimann (Eq. 2.15) and Collins (Eq. 2.14) proposed limits (f_c) and

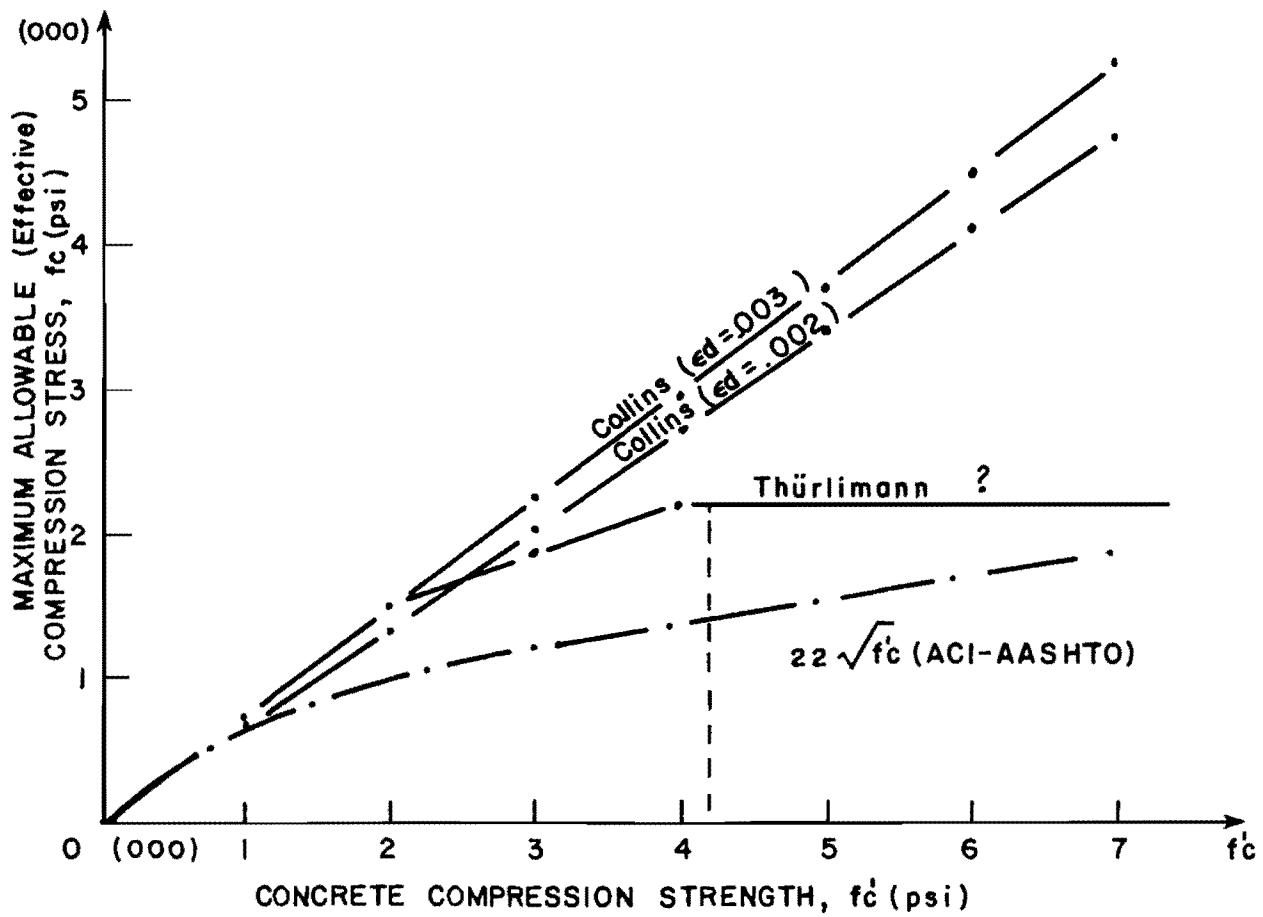


Fig. 2.22 Web crushing limits

the current ACI and AASHTO limit of $22\sqrt{f'_c}$ for the compression stress that the section can carry to avoid crushing of the compression diagonal are plotted for comparison. In Chapter 3, in the section dealing with web crushing, an extensive evaluation of these limits using test data is conducted.

2.4 Detailing of Reinforcement

The space truss model is based on the assumption that all the load has to be carried through yielding of the web and flexural tension reinforcement. Thus, reinforced and prestressed concrete members not only have to be designed as underreinforced sections but, in addition, premature failures due to improper detailing of the reinforcement must be avoided.

In designing reinforced and prestressed concrete beams with the aid of the space truss model, it becomes clear to the designer that not only an adequate amount of reinforcement has to be provided but its distribution and detailing are also of great importance.

2.4.1 Torsion. When designing members to resist torsional moments, it is necessary to establish the difference between equilibrium and compatibility torsion. As previously discussed in Report 248-2, torsion may arise as a result of primary (equilibrium torsion) or secondary (compatibility torsion) actions (see Fig. 2.23). The case of primary torsion occurs when the external load has no alternate path except to be resisted by torsional resistance. In such situations the torsional resistance required can be uniquely determined from static

equilibrium. It is primarily a strength problem because the structure, or its component, will collapse if the torsional resistance cannot be supplied.

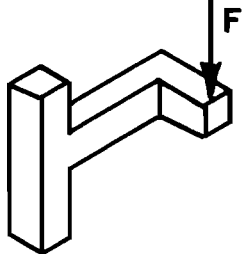
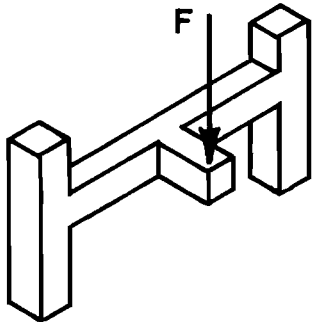
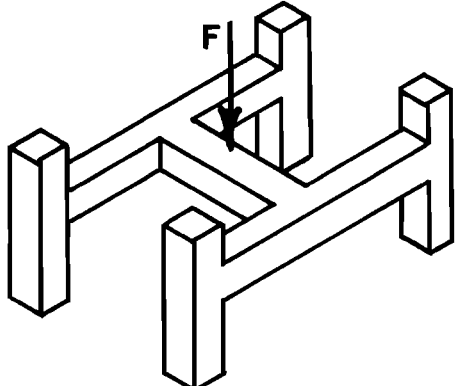
	Equilibrium torsion	Compatibility torsion
Statically determinate structures		Impossible
Statically indeterminate structures		

Fig. 2.23 Torsion in statical systems

As shown in Fig. 2.23, in statically determinate structures only equilibrium torsion exists, while in indeterminate structures both types are possible. If equilibrium is possible in a system even if the torsional stiffness is neglected in the service load state or even if the torsional resistance is neglected in the ultimate state, then one is dealing with compatibility torsion. In this case torsional moments are developed by resistance to rotation and may be relieved when local

cracking occurs. Tests in torsion showed (100) that the torsional stiffness of cracked sections compared with uncracked sections decreased 4 to 8 times as much as the bending stiffness. These tests showed that even before cracks were visible a decrease in stiffness of up to 30% could be noted with increasing load.

Because of this considerable reduction in the stiffness, torsional moments decrease very much and even become negligible, if they are due to a restraint of twist. The spandrel beams of frames which support slabs or secondary beams are typical of this situation.

Disregard for the effects of such restraint in design may lead to excessive torsional crack widths but need not result in collapse if the cracked structure has alternate load paths which can resist the loading from an equilibrium stand-point. In these cases, stronger torsional reinforcement only slightly influences the twist, so that at service load level the behavior of a beam with weak torsional reinforcement corresponds to that of a beam with strong torsional reinforcement. However, in the case of compatibility torsion it is recommended that a minimum amount of reinforcement be provided for two reasons:

1. Minimum reinforcement (both transverse and longitudinal) helps at service load level to maintain adequate crack control.
2. Minimum amount of torsional reinforcement might raise the ultimate load of the entire structure since after the onset of yield in the flexural reinforcement of the adjacent members, further redistribution of forces can take place.

Specific guidelines to compute the minimum amount of torsional reinforcement that should be provided in the case of compatibility torsion are given in Report 248-4F.

This differentiation between equilibrium torsion and compatibility torsion is also required when properly detailing the reinforcement. In the case of compatibility torsion, the function of the reinforcement consists for the most part in providing crack control. Hence, the distribution is more important than the amount. The case of equilibrium torsion is different. Here the amount of reinforcement becomes equally as important as its distribution. When dealing with equilibrium torsion it is necessary to both provide enough reinforcement to resist the torsion required by statics and to properly detail of reinforcement to ensure that such strength can be fully developed.

In designing a member subjected to torsion, it is necessary in order to provide adequate crack control that the longitudinal steel be uniformly distributed around the perimeter of the cross section. The trusslike behavior of the member shows that the longitudinal steel in each corner of the section is anchoring the diagonal compression struts. If the reinforcement at the corners is too weak, a brittle premature failure will result from the bulging out of the corner bars (see Fig. 2.24). For this reason, ductility and strength requirements would be better served by concentrating a considerable amount of the required longitudinal steel for torsion at the corners of the cross section. However, a torsional moment causes a general lengthening of the member. Hence, longitudinal steel anywhere in the cross section can be effective

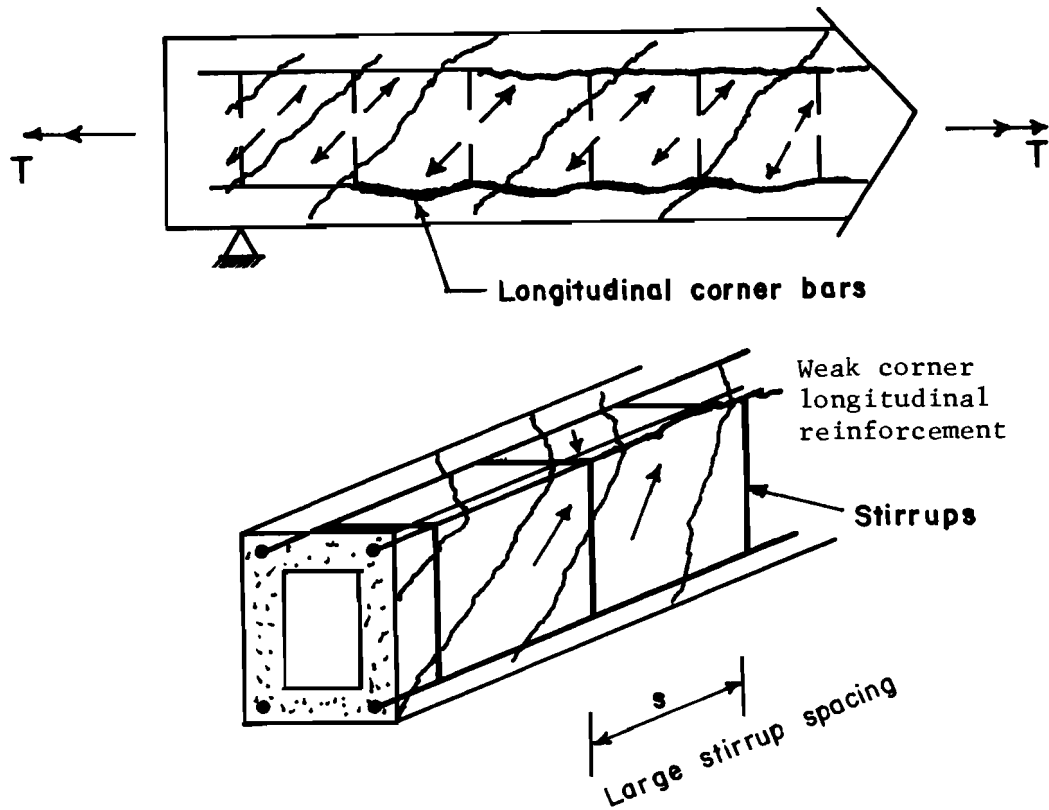
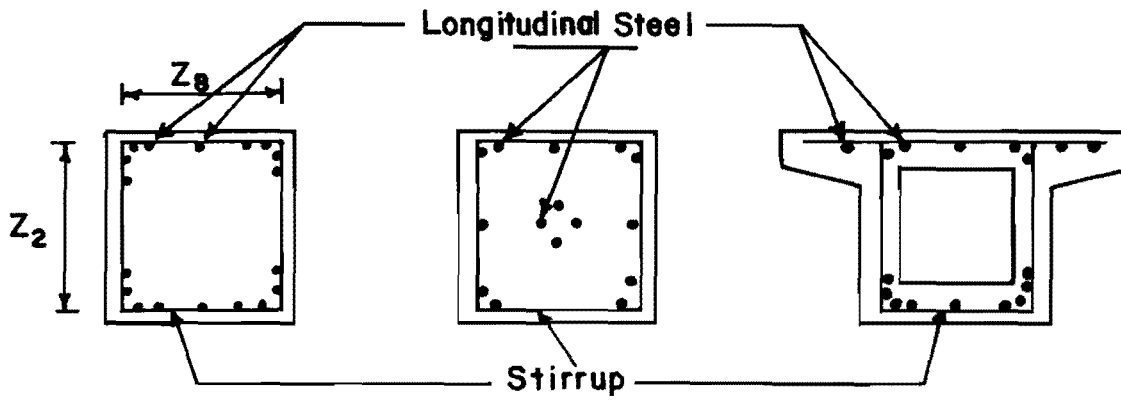
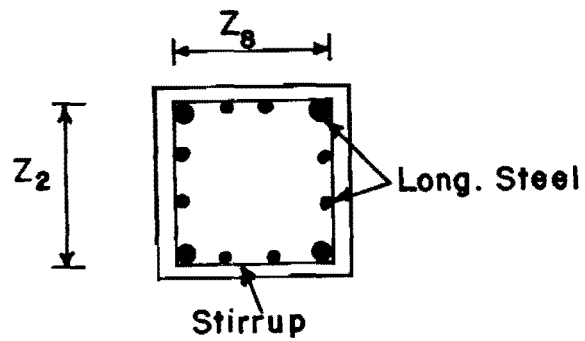


Fig. 2.24 Pushing out failure of the corner longitudinal bars

as torsional longitudinal reinforcement, since it will resist the lengthening of the member in spite of its position in the cross section (93). Consequently, provided that the longitudinal steel at the corners is adequate to anchor the compression diagonals, the three sections shown on Fig. 2.25a, will have the same ultimate torque when subjected to a constant torsional moment. However, the distribution of longitudinal steel shown in Fig. 2.25b is recommended as the best practice, since it would satisfy both ductility by concentrating some longitudinal steel in the corners of the member and crack control at service load because of the uniform distribution of the longitudinal



(a) Sections with same ultimate torque

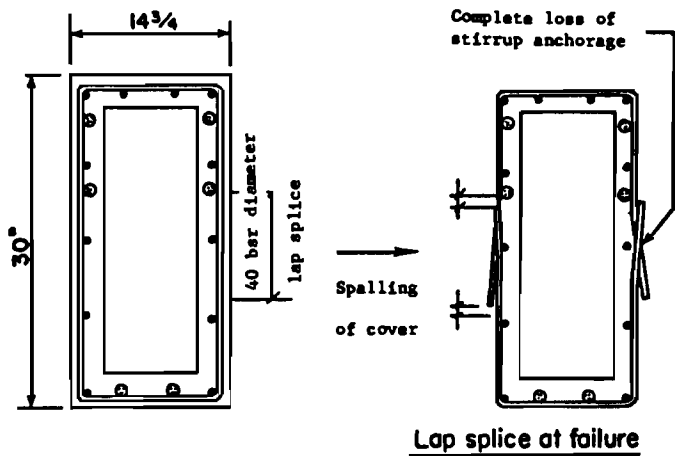


(b) Optimal distribution of longitudinal steel

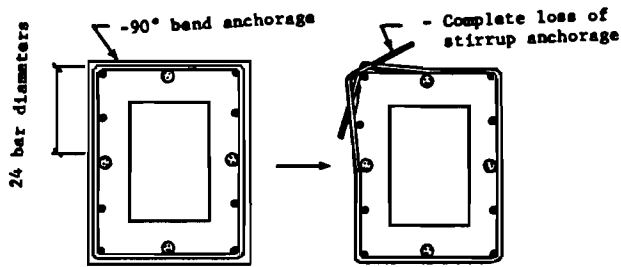
Fig. 2.25 Distribution of the longitudinal steel

steel around the perimeter of the cross section. Due to this lengthening effect in the member, the longitudinal steel in the case of torsion is acting as a tension tie between the ends of the member and it is necessary to provide it with adequate end anchorage to allow the longitudinal reinforcement to develop its full yield strength everywhere within the section subjected to a torsional moment.

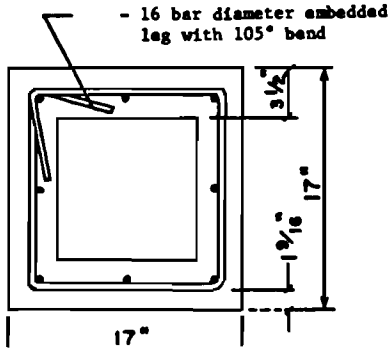
Since torsion produces cracking on all sides of the beam, the transverse reinforcement must be provided in the form of closed hoops. The function of the stirrups in the space truss model is to resist the vertical component of the diagonal compression strut; therefore, they must act as tension ties between the corner longitudinal stringers (see Fig. 2.24). Because of the torsionally induced tensile stresses acting on the outer shell of the section, it is expected that at high torsional stresses the outer shell of concrete will spall off. This leads to special considerations in regard to the proper end anchorage of the stirrups. For example, lapped splice stirrups as well as stirrups ending with 90 degree hooks, constitute inadequate details (see Fig. 2.26a and 2.26b). In order for the stirrup to be properly detailed it is recommended that the free ends must be bent into the concrete contained within the stirrups (see Fig. 2.26c). Furthermore, so that trusslike behavior exists and to prevent the compression diagonals from breaking out between the stirrups, it is necessary that every crack be crossed by at least one stirrup. Thürlimann and Lampert proposed a minimum stirrup spacing of $s \leq h_2/2$, but no more than 8", where h_2 is the shortest dimension of the cross section.



(a) Lap splice inadequate detail for torsion



(b) 90 degree hook inadequate detail for torsion



(c) Properly detailed transverse reinforcement

Fig. 2.26 Stirrup anchorage details [from Ref. 118]

However, this recommendation seemed conservative in the case of shallow rectangular sections common in buildings, and where the spacing requirement $s = (x_1 + y_1)/4$, where x_1 is the shorter center-to-center dimension of closed rectangular stirrup and y_1 is the longer center-to-center dimension of closed rectangular stirrup, proposed in the ACI Code (24) seems more appropriate. Collins and Mitchell (56) proposed spacing of transverse reinforcement in the case of torsion is given by the relation $S \leq (2x_1 + 2y_1)/(8 \tan \alpha)$, where α is the design angle of inclination of the diagonal compression strut at ultimate. The limitation on the maximum stirrup spacing is due to the fact that the stirrups acting together with the longitudinal reinforcement in the corners must prevent the compression diagonals from prematurely breaking out between two stirrups. A comprehensive treatment of this limit should then include the force in the diagonal strut as well as the flexural strength of the chord. Since these two quantities are a function of the inclination of the diagonal strut at failure, it initially seems reasonable to include the value of $\tan \alpha$ in the computation of the maximum stirrup spacing. Hence, the maximum stirrup spacing could be evaluated as $s_{\max} \leq h_2/(2 \tan \alpha)$, where h_2 is the shortest dimension of the cross section. This requirement would ensure that at least one stirrup on each face would cross any failure crack. However, first diagonal cracking in reinforced concrete members takes place at 45 degrees or $\tan \alpha = 1$, and if the member had been designed using the lower limit of $\tan \alpha = 0.5$ there could be the possibility that the initial diagonal crack would not be crossed by a single stirrup.

Thus, it is suggested that when setting the maximum stirrup spacing the value of $\tan\alpha = 1.0$ be used regardless of the assumed angle of inclination at failure.

As a result, the maximum stirrup spacing for torsion is then $s_{\max} \leq h_2/2$, which is similar to the limit proposed by Thürlimann of $h_2/2$ but less than 8". Therefore, it is felt that the use of Thürlimann's proposal is more practical and reasonable.

2.4.2 Shear. Detailing for shear strength requires that just as in the case of torsion, both the longitudinal and the transverse reinforcement must be properly anchored so as to allow the development of their full tensile strength. Required anchorage can be provided by means of adequate straight embedment length, standard hooks or even mechanical anchorage.

The function of all of the reinforcement has been nicely explained by Collins and Mitchell (56), and is fully illustrated in Fig. 2.27. From Fig. 2.27, it is apparent that the function of the longitudinal steel is to act as a tension chord as required for flexure and to balance the horizontal components of the diagonal compression struts. In addition, it must provide adequate end support for the stirrup reinforcement. In the truss model the longitudinal tension chords must tie the beam together along its longitudinal axis and be properly anchored at the ends.

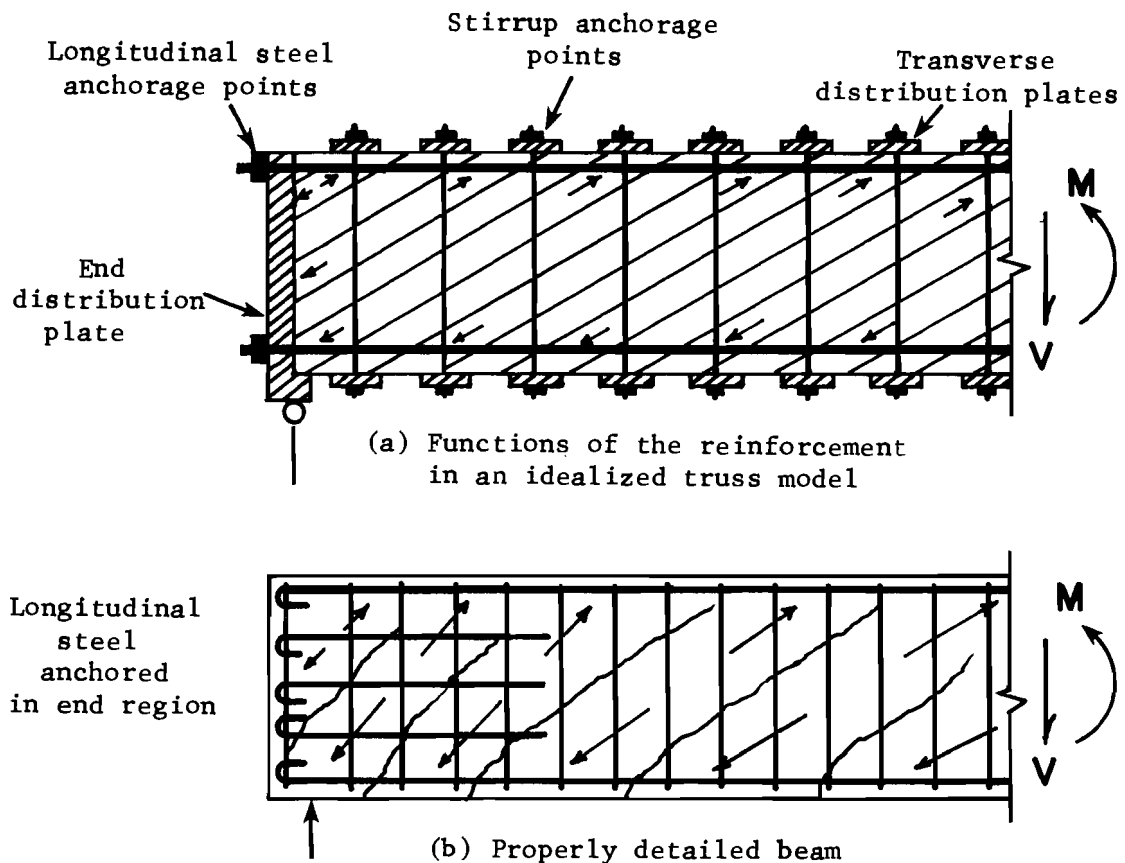


Fig. 2.27 Detailing considerations for a beam subjected to shear [from Ref. 56]

I) Longitudinal Reinforcement

It is of importance in properly detailing the longitudinal reinforcement to consider its proper anchorage at the support regions, as well as its correct curtailment.

(a) Support region

Consider a simply supported beam such as that of Fig. 2.28. As illustrated in Section 2.2.2 (Introduction of Concentrated Loads), a compression fan forms at the support of beams where the reaction induces compression. From the study of the compression fan it was shown that

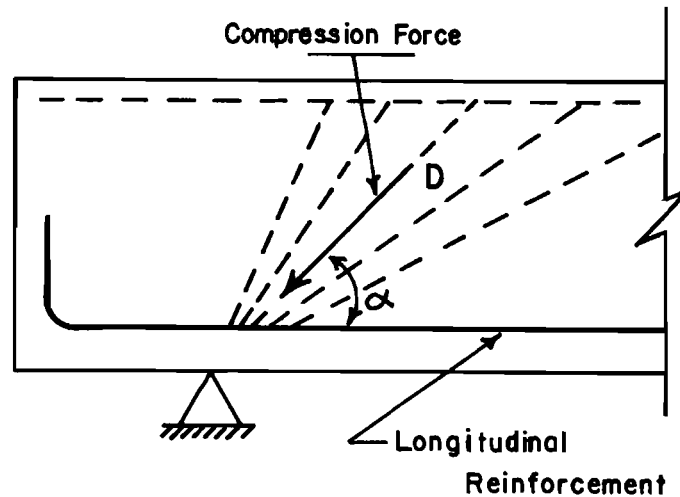


Fig. 2.28 Anchorage of reinforcement at support

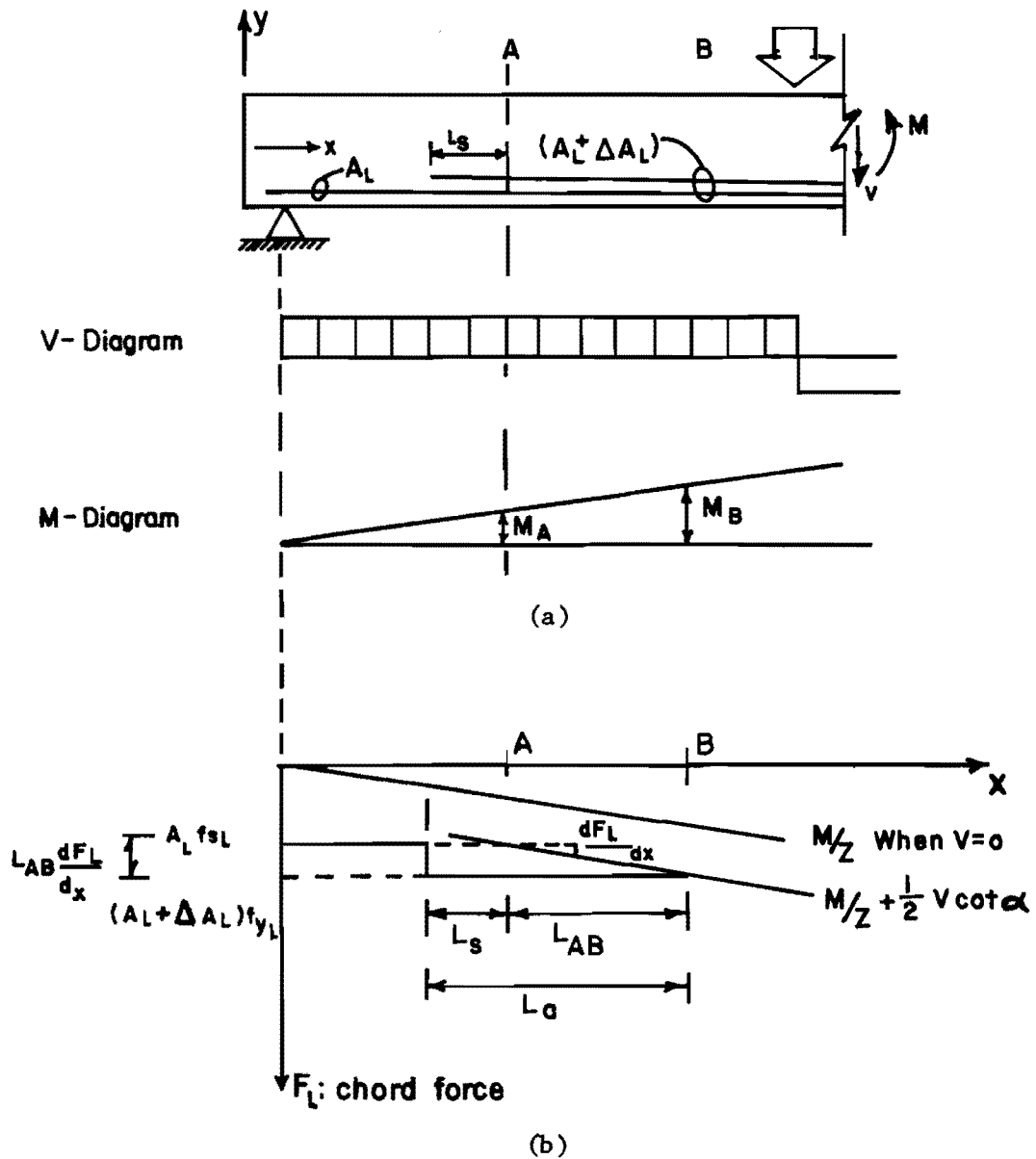
the bottom (tension of flexure) chord requires an anchorage length such that a force equal to $V \cot \alpha / 2$ is adequately developed (see Fig. 2.4b).

In a more physical sense, the concrete compression strut is "pushing" on the end of the beam, and the smaller the angle of inclination, the more anchorage force that would be required at the support.

(b) Curtailement of the longitudinal steel

Consider the case of curtailment of the longitudinal reinforcement (see Fig. 2.29a). The question is how far should the longitudinal steel extend, distance l_s beyond the point at which it is no longer required for flexure. In Report 248-2 it was shown that the force in the lower tension chord is found as:

$$F_1 = (M/z) + [(V \cot \alpha) / 2] \quad (2.16)$$



L_a = anchorage length required to develop yielding of the bar
 L_s = supplemental length beyond theoretical cutoff point
 $= L_a - L_{AB}$

Fig. 2.29 The effect of shear on flexural steel requirements

From Fig. 2.29b the step in the diagram due to the change in steel is given by:

$$L_{AB} \left(\frac{dF_L}{dx} \right) = \Delta A_L f_{yL} \quad (2.17)$$

and

$$\frac{dF_L}{dx} = \frac{d}{dx} \left(\frac{M}{z} + \frac{1}{2} V \cot \alpha \right) \quad (2.18)$$

Since the shear force V is constant and the angle of inclination of the diagonal compression strut is assumed constant in the design process Eq. 2.18 yields:

$$\frac{dF_L}{dx} = \frac{1}{z} \frac{dM}{dx} = \frac{V}{z} \quad (2.19)$$

Substituting in Eq. 2.17 yields:

$$L_{AB} = \Delta A_L f_{yL} z/V \quad (2.20)$$

thus, from Fig. 2.29b

$$L_s = L_a - L_{AB} = L_a - \frac{\Delta A_L * f_{yL} * z}{V} \quad (2.21)$$

This equation is also applicable when detailing positive moment tension reinforcement at points of inflection and simple supports. In the current ACI Code (24) a similar requirement is established for the adequate development of the positive moment tension reinforcement at simple supports and points of inflection. This reinforcement is limited to a diameter such that the development length, l_d , required to develop

the yield strength of this reinforcement meets the following requirements:

$$l_d < [M_n/V_u] + l_s \quad (2.22)$$

where M_n is the nominal moment strength assuming all reinforcement at the section to be stressed to its full f_y , V_u is the factored shear force at the section, and l_s at a support is the sum of the embedment length beyond the center of the support and the equivalent embedment length of any hook or mechanical anchorage provided; l_s at points of inflection is limited to "d" or $12 d_b$ where " d_b " is the longitudinal bar diameter, whichever is greater.

Rearranging Eq. 2.22 yields

$$l_s = l_d - M_n/V_n \quad (2.23)$$

which at points of inflection or simple supports is the same as Eq. 2.21. Since at these points A_1 is the total tension reinforcement present, this would produce M_n .

For the case of distributed loading, w , in Sec. 2.2.1 it was shown that the force in the longitudinal tension chord is also evaluated using Eq. 2.16. Hence,

$$\frac{dF_L}{dx} = \frac{1}{z} \frac{dM}{dx} + \left(\frac{1}{2} \cot\alpha\right) \frac{dV}{dx} \quad (2.24)$$

since $dM/dx = V$, and $dV/dx = w$, Eq. 2.24 yields

$$dF_1/d_x = (V/z) + w \cot\alpha/2 \quad (2.25)$$

Substituting in Eq. 2.17 yields

$$L_{AB} = \frac{\Delta A_L f_{yL}}{\frac{V}{z} + \frac{w}{2} \cot \alpha} \quad (2.26)$$

Thus from Fig. 2.29b

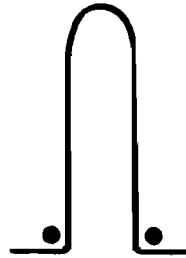
$$L_s = L_a - L_{AB} = L_a - \frac{\Delta A_L f_{yL}}{\frac{V}{z} + \frac{w}{2} \cot \alpha} \quad (2.27)$$

where l_s represents the supplemental length required beyond the theoretical cut-off point.

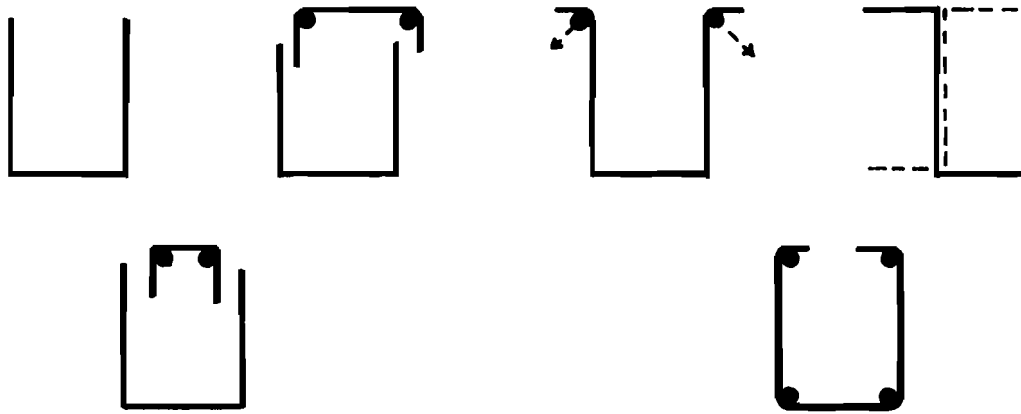
II) Transverse Reinforcement

The transverse reinforcement in the truss model provides, as shown in Fig. 2.27, the vertical tension ties to resist the vertical component of the diagonal compression struts. All stirrups must be properly anchored in the compression and tension zones of the member. The cracking of the concrete in the tension zone demands that the stirrup be continuous throughout this zone. No splicing of stirrups should be permitted.

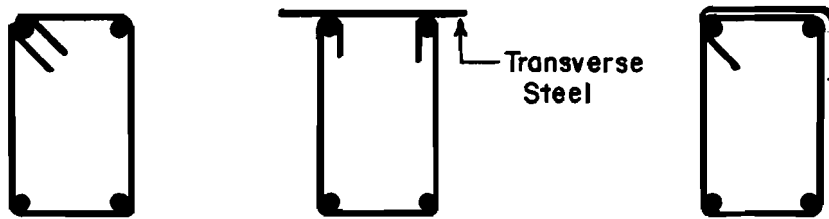
Typical prestressed beam stirrup detailing as shown in Fig. 2.30a is not unadmissible. Such details are often used to simplify plant fabrication. The reason it should not be used is that the cracking of the concrete in the tension zone would destroy the bond between the concrete and the stirrups. This means that stirrup tension force could not be developed. Also, as shown in Fig. 2.27, the stirrups must provide effective reactions for the diagonal compression struts to bear against, both in the tension and compression zones. This detail



(a) Typical inadequate detail often used in prestressed T-beams



(b) Incorrect or insufficient detailing



(c) Adequate detailing

Fig. 2.30 Detailing of transverse reinforcement

fails in both respects. A clear example of the type of failure this improper detailing can lead to is illustrated in Chapter 3 of this study in the section dealing with failures due to inadequate detailing.

For the same general reasons, detailing of stirrups such as the ones shown in Fig. 2.30b, is also undesirable. Figure 2.30c shows some examples of adequate detailing. From the study of members subjected to bending and shear using the truss analogy it is clear that the diagonal compression struts can only be anchored at the joints of the truss, i.e. intersection points between the transverse and the longitudinal reinforcement. The loads can only be transmitted at the joints of the truss because the members of a truss can only resist axial forces and their resistance to direct bending (i.e. loads applied to the member between the joints), or direct shear (dowel action) is almost negligible. For this reason, the stirrup which is the vertical tension member, must be able to develop its full strength over the entire height between the top and bottom joints of the truss. Hooks of the stirrups should be anchored around large longitudinal bars in order to distribute the concentrated force from the stirrups. A highly recommended practice would be to always bend stirrups around longitudinal bars, and terminate them only in the compression zone with at least a 135 degree hook at the ends.

In the detailing of transverse reinforcement it is also important to point out the width effect. This is important in the case of members having large web widths, and where more than two bars are used to resist flexure (see Fig. 2.31). In this case it is important to

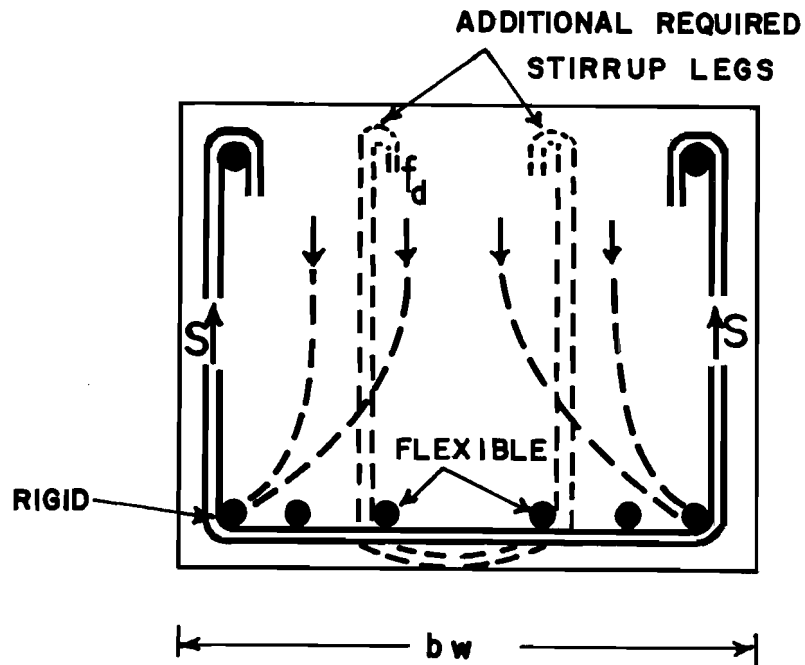


Fig. 2.31 Effect of large web widths

form a truss joint at a high porportion of the longitudinal bars. Therefore, multiple leg stirrups should be used. The lack of sufficient vertical stirrups around a high percentage of the interior bars would make the interior bars flexible and incapable of resisting vertical forces. Thus, the inclined compressive strut would not be properly anchored, and this would create a concentration of diagonal compression stresses at the corner bars which might cause a premature failure.

Leonhardt and Walther (101,102) based on test results suggested that, as can be seen from Fig. 2.31, in substantially wider webs the diagonal compression struts are supported only laterally at the edges where the stirrup forces are acting. The strut in this case is somewhat

like a deep beam, and its load-carrying capacity will be exhausted when the concrete fails near the bearing due to the concentration of the diagonal compression stresses. Based on this assumption and test results Leonhardt and Walther suggested that when large shear stresses exist in the member, the transverse spacing of stirrup legs should not exceed 7.5 in.. In the case of members with small nominal shear stresses it was suggested that the transverse spacing of stirrup legs can be made 15 in. or more but not exceed the effective depth, "d" of the member.

An upper limit on the maximum longitudinal stirrup spacing must be imposed to avoid the concentration of large compression forces at the joints between the stirrups and longitudinal chords and to ensure that all compression struts have effective reactions to bear against. The space truss model assumes a uniform distribution of the diagonal compression struts over the length of the beam. With large stirrup spacings these inclined struts react most effectively at the stirrup locations. These local concentrations may induce premature failures due to crushing of the diagonal strut or bulging out of the corner longitudinal bars.

The current ACI Building Code (24) and AASHTO Standard Specifications (12) require a maximum stirrup spacing for reinforced concrete beams of no more than $d/2$ or $d/4$ depending on the level of shear stress but in any case no more than 24 in. (d being the distance between the extreme compression fiber and the centroid of the tension reinforcement). In the case of prestressed concrete beams the stirrup

spacing is limited to $3/4 h$, where h is the overall depth of the section, but not more than 24 in.

Collins and Mitchell (56) proposed that the spacing of shear reinforcement placed perpendicular to the axis of the member shall not exceed $z/(3 \tan \alpha)$ where z can be taken as the flexural lever arm, but need not be more than the vertical distance between centers of the bars or prestressing tendons in the corners of the stirrups.

The Swiss Code (156) proposes that the spacing be limited to $z/2$ but less than 12" if the nominal shear stress is less than $15\sqrt{f'_c}$ when $f'_c > 3500$ psi, or $z/3$ but less than 8" if the nominal shear stress is more than $15\sqrt{f'_c}$ but less than $18\sqrt{f'_c}$ when $f'_c > 3500$ psi.

In all these proposals the basic idea is that every crack must be crossed by at least one stirrup to allow trusslike behavior and to prevent the diagonal compression struts from crushing or breaking out between the stirrups, and to provide uniform closely spaced anchors for the diagonal compression struts so as to produce a uniform compression field.

Since the horizontal projection of the failure crack is given by the distance $z \cot \alpha$ in order to ensure that every crack is crossed by at least one stirrup, the maximum stirrup spacing would have to be limited to $z \cot \alpha / 2$. Similar to the case of torsion, first diagonal cracking due to shear in reinforced concrete members takes place at 45 degrees or $\tan \alpha = 1.0$, and if the member had been designed using the lower limit $\tan \alpha = 0.5$ there could be the possibility that the initial diagonal crack would not be crossed by a single stirrup. Thus, a value of $\tan \alpha =$

1.0 should be used when setting the maximum stirrup spacing. This yields a maximum stirrup spacing of $z/2$ which is similar to the one proposed in the Swiss Code (156). Since the maximum shear stress is limited to $15\sqrt{f'_c}$ in order to prevent diagonal crushing it seems reasonable to suggest a maximum stirrup spacing of $S_{\max} \leq z/2$ but no more than 12 in.

2.5 Uncracked, Transition, and Full Truss States

In the behavior of reinforced and prestressed concrete beams subjected to shear or shear and torsion, as in the case of flexure, three well-defined failure states can be distinguished. The first is the uncracked state. This state is terminated in the case of shear by a shear failure when first inclined cracking of the web occurs. Then, there is a transition state for the section at which failure might be in between the uncracked state and its ultimate full truss state. While the member is in the transition state more cracking takes place and there is a redistribution of internal forces in the member. This redistribution of forces is possible due to the aggregate interlock forces and the concrete tensile strength. Failure occurs with the aggregate interlock and similar mechanisms supplementating the truss behavior. Lastly, a member may fail in the full truss state.

In the truss model, the inclination of the inclined compression strut is the inclination at ultimate and not first inclined cracking. The inclination at ultimate may coincide with the inclination at first inclined cracking but this does not necessarily have to be the case.

The change in the angle of inclination or redistribution of forces in the member is possible if contact forces act between the crack surfaces. These contact forces will induce tensile stresses between the compression struts, which must be taken by the concrete. Thus, in the transition state the concrete in the web provides an additional continuously diminishing resistance. As the member marches through its transition state more cracking takes place and/or the previously existing cracks continue growing and become wider. As the crack width increases the mechanisms of aggregate interlock diminish. Thus, the contact forces become smaller and no further redistribution of forces in the member is possible. At this point, it is said that the member has reached the full truss state.

Since only underreinforced sections are being considered (that is, failures due concrete crushing either in the bending compression zone or the diagonal strut are not allowed) and premature failure due to poor detailing are excluded, in the ultimate load state or full truss condition the strength of the member is entirely provided by the truss mechanism.

The ratio q/q_{\max} (applied shear flow due to shear or shear and torsion to the value of the maximum shear flow q_{\max} that the section can withstand before failure due to crushing of the web occurs) can be used as a gauge to determine what state of behavior the member will exhibit. The maximum shear flow may be found from Eq. 2.13.

$$q_{\max} = f_d \max b_w/2 \quad (2.28)$$

In terms of nominal shear stress v , which may be expressed as

$$v = q/b_w \quad (2.29)$$

Hence, Eq. 2.28 becomes

$$v_{\max} = f_d \max/2 \quad (2.30)$$

The nominal shear stress in the case of shear since $q(V) = V/z$ results in:

$$v = V/[z b_w] \quad (2.31)$$

for the case of torsion since $q(T) = T/(2A_o)$ yields:

$$v = T/[2A_o b_w] \quad (2.32)$$

From tests (48,95,96,101) and experience Thürlimann (162) suggests that for values of v/v_{\max} of less than approximately 1/6, a reinforced concrete section will remain uncracked. For a ratio greater than 1/6 and less than approximately 1/2, the section is in the transition state between uncracked and the full truss state. In this transition state the concrete tensile strength will provide a continuously diminishing additional shear strength (see Fig. 2.32).

For the values of v/v_{\max} between 1/2 and 1, the section is in the full truss state, where the total ultimate strength of the section is provided by the truss system.

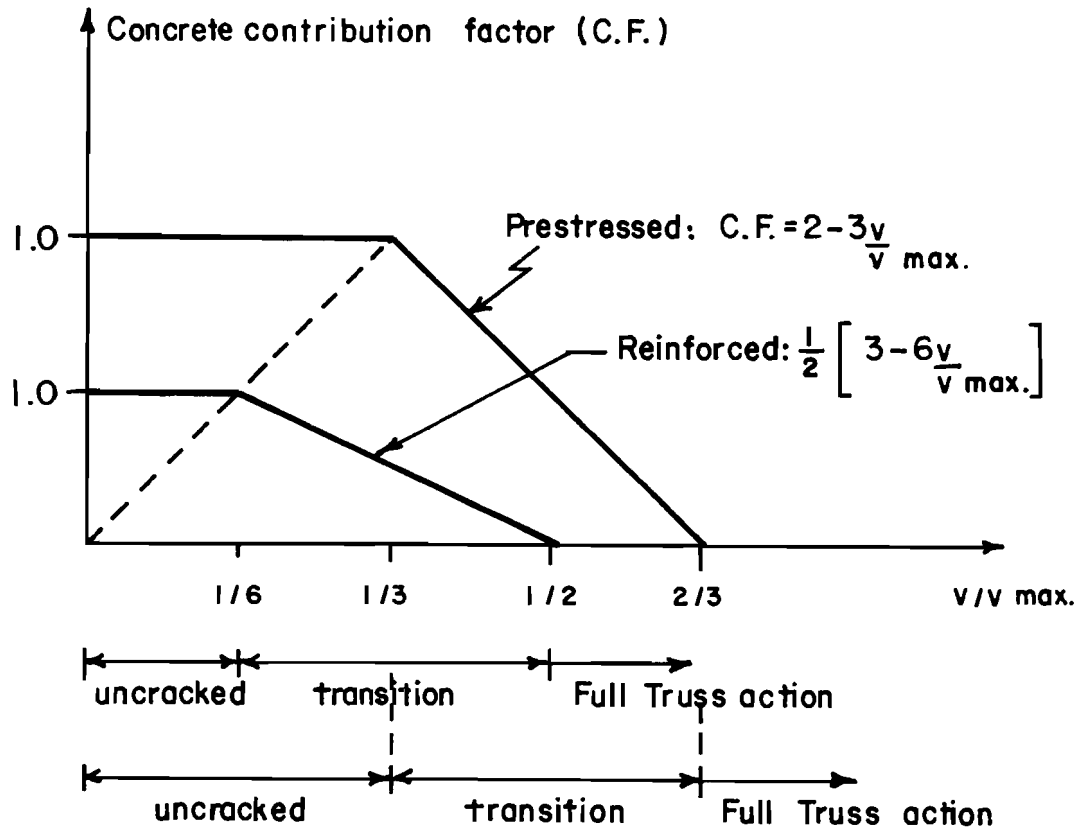


Fig. 2.32 Uncracked, transition, and full truss states

Since only underreinforced sections are being considered and premature failures due to either crushing of the concrete or poor detailing are avoided, the presence of prestress will only influence the cracking load and will not influence the ultimate load of prestressed concrete members (162,165,166). Consider the case of a prestressed concrete beam prior to cracking subjected to a bending moment and a shear force. The state of stress in the member will correspond to that shown in Fig. 2.33.

The Mohr circle for the case of a reinforced concrete beam, that is the case when $\sigma(P) = 0$ is shown in Fig. 2.34a. In this case the

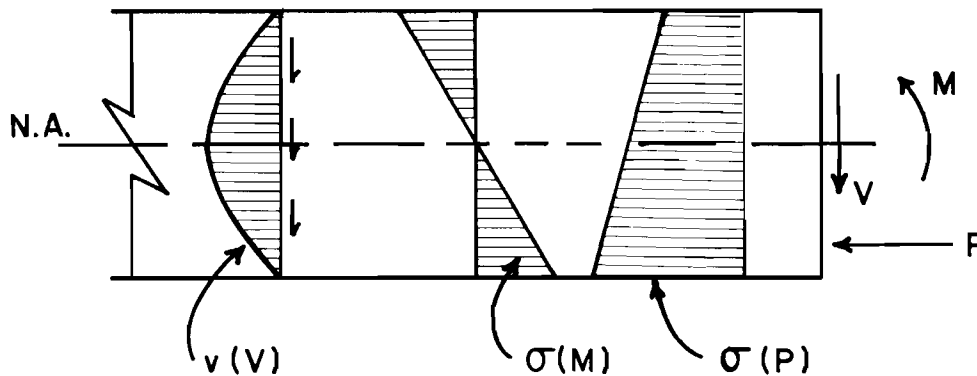
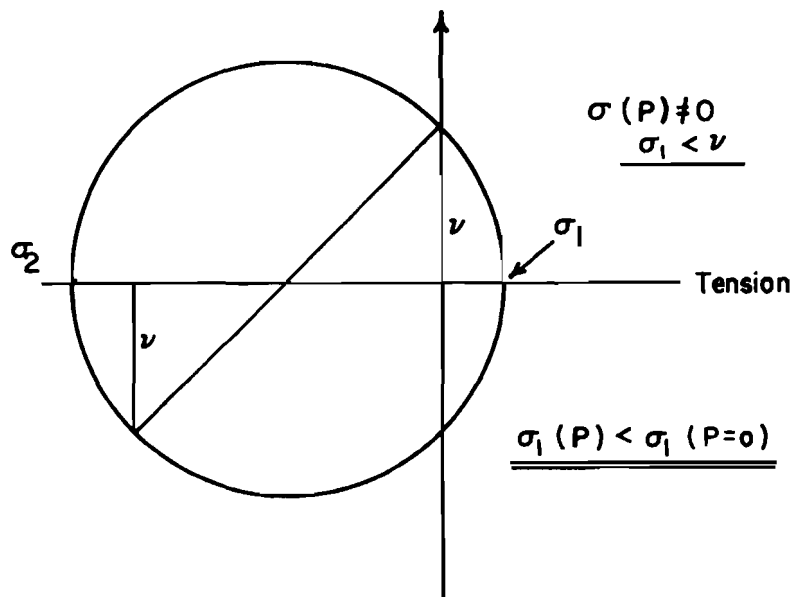
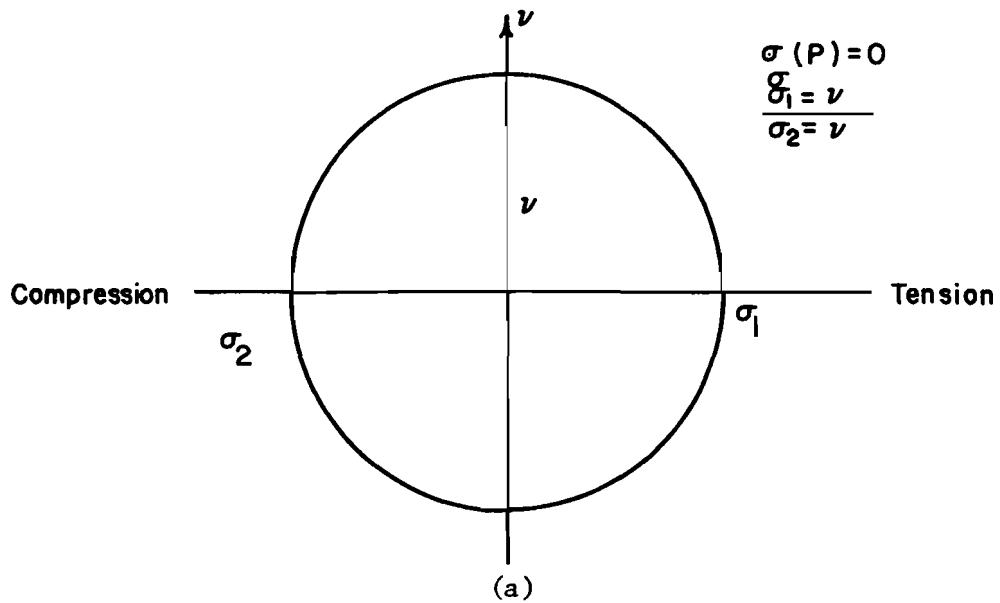


Fig. 2.33 State of stresses in an uncracked prestressed section

maximum tensile stress σ_1 equals the maximum applied shear stress v being the radius of the Mohr circle. In Fig. 2.34b, the Mohr circle corresponding to the state of stress shown in Fig. 2.33 for an element at the neutral axis is shown. The principal tensile stress resulting in the section is smaller than the actual applied shear stress. Thus, the load required to produce diagonal tension cracking in the member increases. The resulting effect is that the uncracked state of the member is increased. For this reason Thürlimann (162) suggests that an increase in the upper limit of the uncracked state from a value of v/v_{\max} of $1/6$ to $1/3$ should be considered for prestressed concrete.

The higher limit is also based on the observation of actual test beams and practical experience.

Therefore, the concrete contribution factor in the transition zone in the case of prestressed concrete members can be derived by



Being: $\sigma_1 = f_{ct}$ = concrete diagonal tension strength

Then $\nu [\sigma(P); \sigma_1 = f_{ct}] > \nu [0; \sigma_1 = f_{ct}]$

(b)

Fig. 2.34 Influence of the prestress force on the principal diagonal tension stress

moving the limit of the uncracked state up to $v = 1/3 v_{\max}$. This results in a concrete contribution factor C.F. equal to (see Fig. 2.32):

$$\text{C.F.} = 2 - 3 v/v_{\max} \geq 0 \quad (2.33)$$

Many times because of the design process followed, loading conditions, clear span length, or even architectural constraints, flexure will control the design of a given member. In such case the shear stress on the cross section, defined as $v_u = V_u/[b_w z]$ for shear, and $v_u = T_u/[2A_o b_e]$ for torsion, might be of such low magnitude that the member at failure as far as shear stresses are concerned would be in a transition state between its uncracked condition and the behavioral state where the truss action would provide the entire resistance of the member. Moreover, the limits previously proposed for the inclination of the diagonal strut, and in particular the lower limit of 26 degrees, which is established in order to prevent extensive web cracking under service load conditions, might sometimes force a member into this transition state.

For members in the transition state, components of the shear failure mechanism, such as aggregate interlock, and the concrete tensile strength, become of importance. The contribution of these mechanisms to the ultimate strength of the member is reflected in the additional concrete contribution to the shear and/or torsional capacity of the member in this transition state, and as such should be considered in the actual design process.

Other regulatory provisions such as requirements for minimum web reinforcement interact with and complicate the transition zone contribution to the truss model resistance. This will be further discussed in Report 248-4F.

2.6 Additional Effects

In this section a number of special effects such as the effects of the web thickness and cross-sectional shape on the use of the truss model for the design of members subjected to shear and torsion are considered. In addition, the effect of strand draping in the truss model is considered.

2.6.1 Effective Web Thickness. When using the truss model as a design approach it is required that failures due to crushing of the diagonal strut be avoided. In this situation the web width of the cross section plays an important part in the compression strength of the diagonal strut. In the case of members subjected to a shear force and a bending moment the effective web thickness is the minimum web width of the cross section resisting the applied shear. However, in the case of torsion the effective width resisting the compression stresses in the diagonal strut is not always the actual web width of the section. This is especially true in the case of members with solid cross sections.

The concrete compression diagonals carry the diagonal forces necessary for the truss equilibrium. Beams with solid cross sections have shown essentially the same failure mode as the corresponding hollow sections (82,95,96,120).

Since the core offers no contribution to the torsional strength, and, in the cracked state the outer concrete shell may eventually spall off, it is reasonable to consider an effective web thickness " b_e " to determine the concrete stresses in the diagonal strut. Based on experimental evidence Thurlimann and Lampert (93) proposed that the thickness of this effective web should be taken as the smaller of the two values:

$$b_e = d/6 \quad \text{or} \quad b_e = d_o/5 \quad (2.34)$$

where " d " is the diameter of the largest inscribed circle in the cross section and d_o is the diameter of the circle inscribed in the largest area enclosed by the centroids of the longitudinal chords in the cross section (see Fig. 2.35). More recent studies provide detailed information of b_e (56,180).

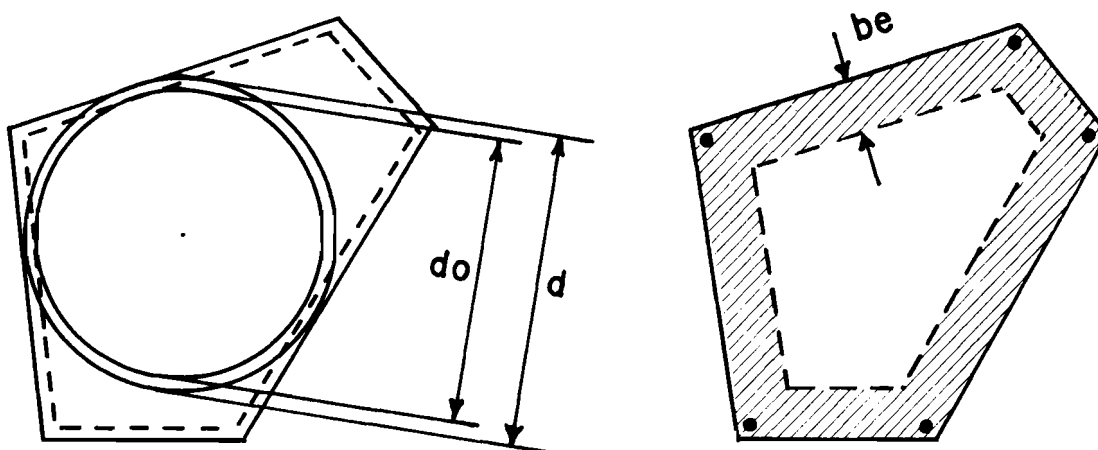


Fig. 2.35 Effective web thickness for solid cross sections

In box sections b_e will be equal to the actual web thickness as long as this is smaller than the effective web thickness obtained using Eq. 2.34.

In the case of combined actions, the addition of the effects of shear and torsion may be safely approximated if shear induced stresses are computed using b_w and torsion induced stresses are computed using an effective width " b_e " as given by Eq. 2.34 (62,156).

One more factor that has to be considered in regard to the effective web width and, particularly in the case of shear, is the presence of openings in the web girder caused by prestressing ducts. Developments in prestressed concrete have led to the increasing use of thin-webbed prestressed concrete sections, especially in highway bridges and elevated guideways for transit systems. Such girders are susceptible to a web crushing mode of shear failure due to the high diagonal compressive stress induced in the thin web by the applied shear force. When such a girder is post-tensioned by cables located in the web, a significant width of web concrete may be replaced by the prestressing ducts.

It has been recognized that the presence of a prestressing duct reduces the diagonal compressive strength of the web (100). This factor can be accounted for in design by the use of an effective or reduced web width " b_e ".

Campbell and Batchelor (45), reviewed several of the expressions that have been proposed whereby the effective web width " b_e " may be related to the actual web width and the diameter of the duct. In this

review, Campbell and Batchelor, based on tests of I-beams with thin webs conducted by Chitnuyanondh (47), proposed that when the truss model with variable angle of inclination is used in the design, the effective web width of the members may be computed using the following relations:

$$b_e = b_w - 0.75d_d \quad (2.35)$$

for an ungrouted duct, and

$$b_e = b_w - 0.33d_d \quad (2.36)$$

for a grouted tendon. In Eqs. 2.35 and 2.36, d_d represents the diameter of the duct. These equations were derived from tests on beams containing a single duct in the web and with a d_d/b_w ratio of 0.46.

Leonhardt (100) suggested that if multiple ducts having a diameter d_d greater than 1/10 of the web width are located in the web, then the effective web width " b_e " should be taken as:

$$b_e = b_w - \sum d_d \quad (2.37)$$

for ungrouted ducts, and

$$b_e = b_w - 0.67 \sum d_d \quad (2.38)$$

for the case of grouted ducts. These equations may be applied when more than one duct is located at the same level in a web as indicated by the summation sign. Smaller values for the web width are obtained when these relations are used instead of Eqs. 2.35 and 2.36 as should be

expected when several ducts exist, thus providing a more conservative value in the design of these members.

Mitchell and Collins (56) proposed that in the case of both shear and torsion, the unrestrained cover down to the centerline of the outer transverse reinforcing bar shall be assumed to have spalled off when evaluating the effective web width resisting the shear force, but this so-called effective web width need not be taken less than one-half of the minimum unspalled web width, b_w . This proposition seems more logical in the case of torsion where the high tension stresses induced in the outer shell of the member would induce the unrestrained cover to spall off. However, in the case of shear, even at high shear stresses, this assumption seems too conservative. It would unduly penalize thin web members not subjected to torsion.

2.6.2 Effect of the Cross Section Shape in the Case of Torsion.

In 1853, St. Venant (154), in his memoir on the torsion of prismatic bars (non-circular cross sections), showed that if a bar whose transverse cross section is not circular is twisted by applying moments at its ends, a plane transverse section before twisting does not remain a plane section after twisting. It becomes a warped surface. This warping is accompanied by an increase of shearing stress in some parts of the cross section and a decrease in others. For example, in a member with rectangular cross section, the maximum shearing stresses occur at the center of the long side, that, is at a point on the surface nearest to the axis of the bar. The shearing stress at each corner is zero.

If all the cross sections in a member subjected to twisting are free to warp (unrestrained torsion), the longitudinal elements (lines) of the surface of the twisted member remain practically straight lines with negligible change in their lengths, unless the angle of twist per unit length is very large and the cross sections are unusually extended. Hence, longitudinal stresses may usually be neglected. As a consequence, it is reasonable to assume that a torsional moment in this case produces pure shearing stresses distributed over the ends as well as all other cross sections of the member. In the use of the truss model as a design procedure, this type of torsion is referred to as circulatory torsion. When this type of torsion exists, the cross section of the member can be replaced by corresponding hollow sections using the truss model. The resultant shear stresses will then generate a uniform shear flow around the perimeter of the cross section.

If, however, any cross section of the member subjected to a torsional moment is held rigidly (see Fig. 2.36) and, as a consequence, the warpage is restrained (restrained torsion), then the longitudinal elements of the surface become curved with marked changes in their lengths. The resulting longitudinal stresses in the outer elements of the flanges are not negligible. The torsional moment T is transmitted along the member near the free end mainly by torsional shearing stresses (see Fig. 2.36c). However, near the fixed end the torsional moment is transmitted mainly by the lateral shearing forces V (see Fig. 2.36a) which accompany the lateral bending of the flanges. At intermediate sections (see Fig. 2.36b), the torsional moment will be transmitted by a

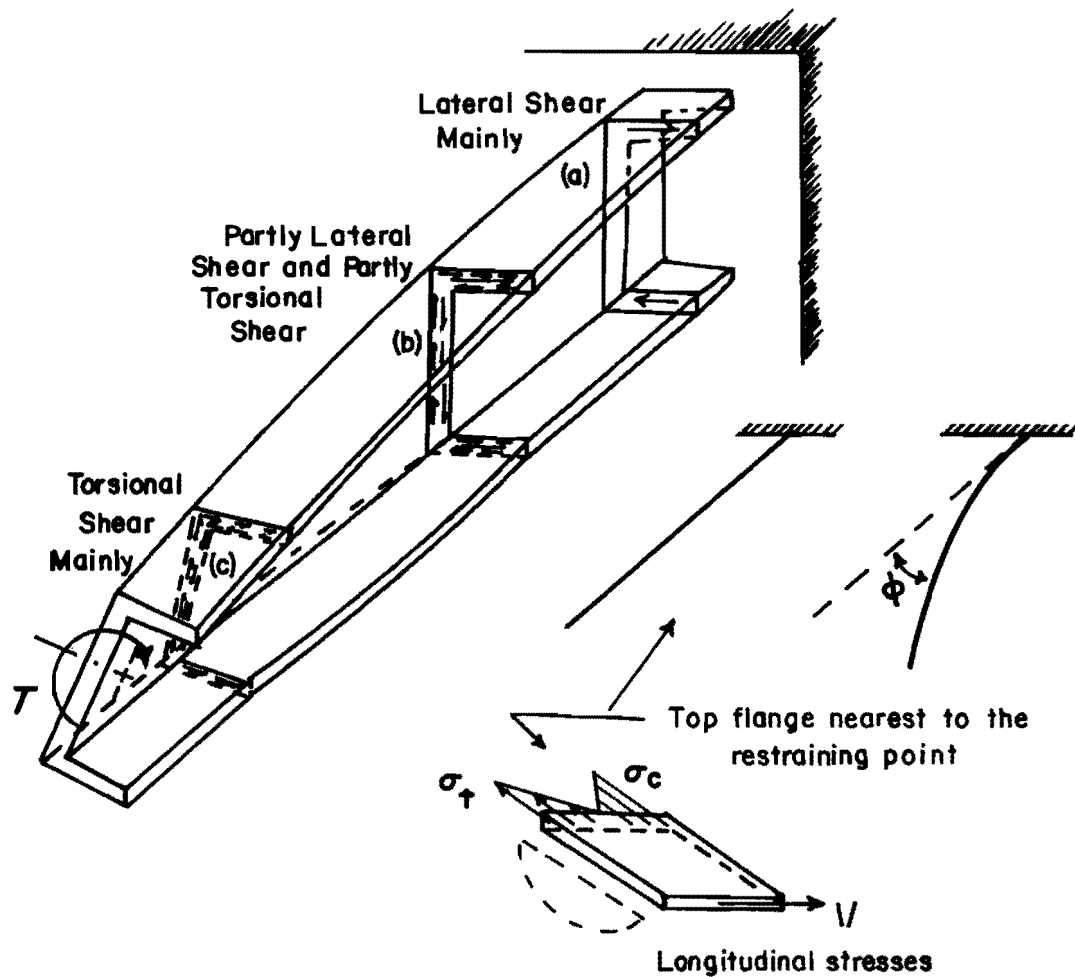
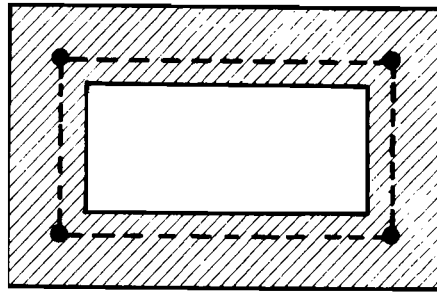


Fig. 2.36 Restrained torsion

combination of torsional shear stresses and lateral shear forces in the flanges.

While the restraining effect has little influence in the closed sections, and the so called non-warping sections (see Fig. 2.37), it is important when dealing with open thin-walled sections such as channels or I-beams (see Fig. 2.38).

For the sections shown in Fig. 2.38, solutions have been worked out in the case of members made out of homogenous materials or for the



(a) Closed box section



(b) Nonwarping sections

Fig. 2.37 Sections not influenced by the restraining effect

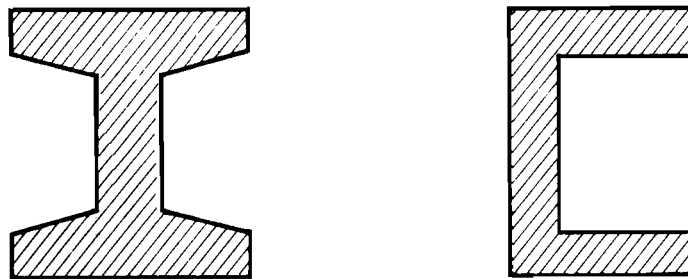


Fig. 2.38 Sections influenced by the restraining effect

uncracked elastic state of members made out of non-homogenous materials such as reinforced concrete (154). Grob (71) and Krpan and Collins (91,92) have worked out solutions for the case of pure torsion in open walled reinforced concrete sections in both the uncracked and cracked states. It is particularly interesting in the cracked state, how the authors combine the effects of circulatory torsion evaluated using the truss model and the effect of warping torsion which can be obtained from conventional flexural theory, provided the adequate section properties are used (91).

Although it is possible to predict the ultimate load of members where warping effects are considered (92), it is very difficult to study the interaction between the circulatory and the warping torsion (92), as well as the respective contributions of the transverse and the longitudinal reinforcement to the ultimate strength of the member. However, the applicability of the basic truss model without inclusion of deformation predictions has been shown on an empirical basis by comparison with test results.

Mitchell and Collins (119) extended the truss analogy by developing the general Compression Field Theory. In this theory an expression for the angle of inclination of the diagonal compression members of the truss is presented based on Mohr's circle geometry:

$$\tan^2 \alpha = \frac{\epsilon_L + \epsilon_d}{\epsilon_s + \epsilon_d} \quad (2.39)$$

where ϵ_L = longitudinal tensile strain, ϵ_s = transverse tensile strain,

and ϵ_d = diagonal compressive strain. This geometric relation is presented as the compatibility equation assuming coinciding principal stress and strain axes in the cracked concrete. It relates the strains in the concrete diagonals, the longitudinal steel, the transverse steel, and the angle of inclination of the diagonal compression strut. However, this equation is not valid in the case of combined actions.

In Chapter 3 the ultimate load predictions based on the truss model are also evaluated using test results of beams where the warping torsion effects are of significance.

2.6.3 Strand Draping. In general, it is considered that draping of the prestressing tendons will produce an upward vertical component which will counteract the downward shear force acting on a section (see Fig. 2.39).

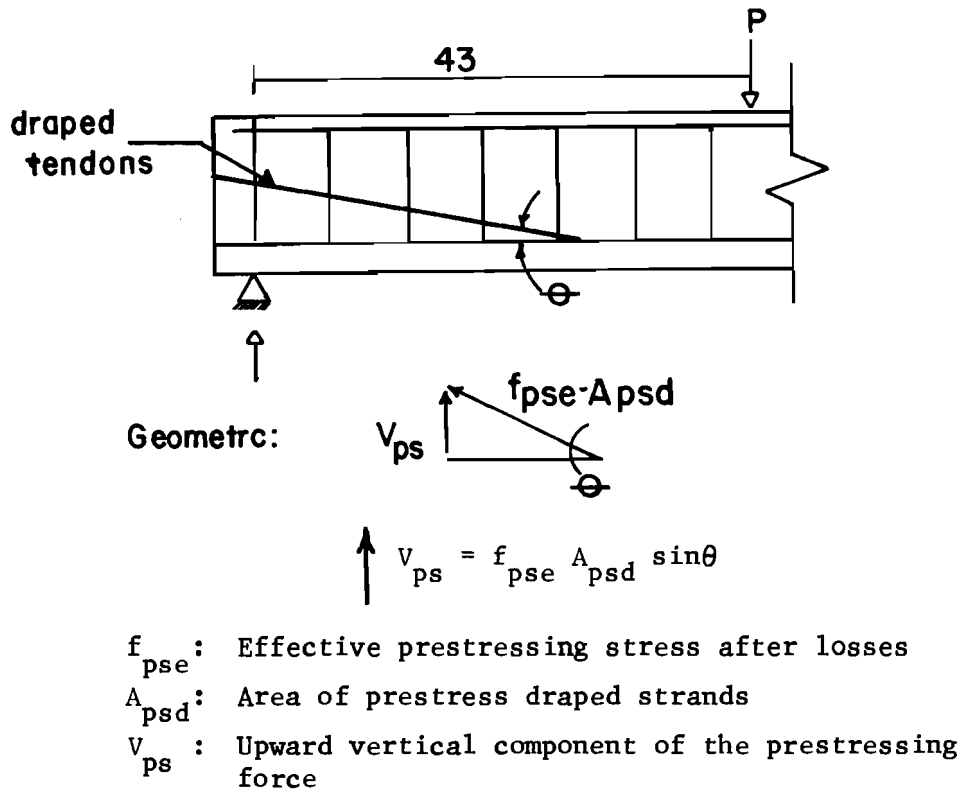


Fig. 2.39 Strand draping effect

For the case shown in Fig. 2.39, the value of the vertical component of the prestressing force obtained from geometric consideration results in:

$$V_{ps} = A_{psd} f_{pse} * \sin\theta \quad (2.40)$$

As a conservative estimate, it is assumed that the tension force in the strand will never exceed the value of the effective prestress force $F_{pse} = A_{psd} * f_{pse}$ after all losses.

In the design of prestressed concrete members using the truss model, the beneficial effect on the shear capacity of members with draped strands can be included by subtracting the vertical component of the prestressing force from the total applied shear force. However, enough longitudinal tendons should be continued straight and anchored at the support to provide the additional tension force required by the presence of shear as computed using the truss model at the section where draping takes place. Then, the effective depth of the truss z is given by the distance between this straight tension reinforcement and the top compression chord.

There are not enough data to provide conclusive information in regard to the effect of strand draping in the case of torsion. Collins and Mitchell (120) tested one beam in which the prestressing reinforcement consisted of four inclined tendons, as shown in Fig. 2.40. The authors reached the conclusion from this single test that, for members in which the torsional moment primarily acts in one direction, it may be advantageous to provide prestressing in the form shown in

Fig. 2.40. Due to the inclination of the tendons, the section shown in Fig. 2.40 undergoes a twist. The tangential components of the forces in the tendons then help to resist the applied torque.

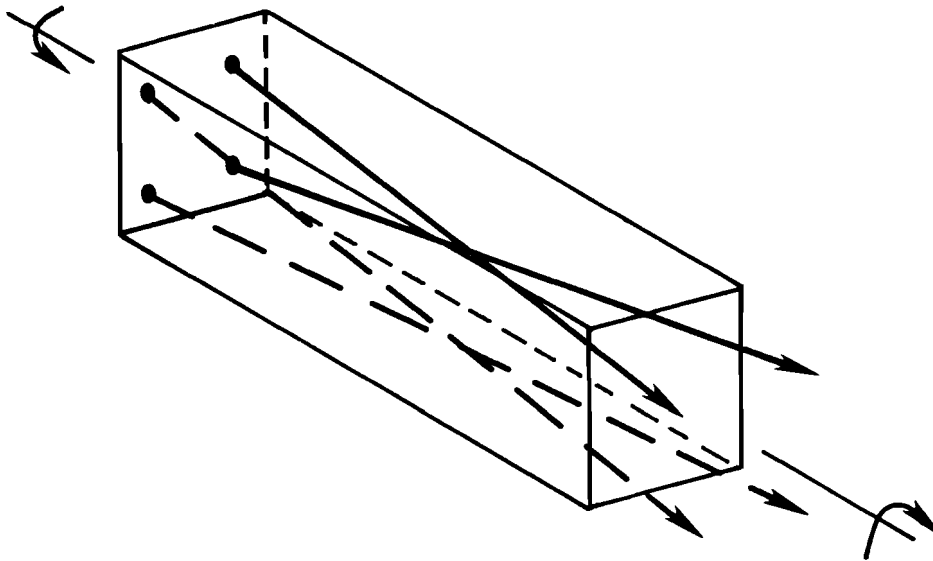


Fig. 2.40 Prestressed beam with inclined tendons in the case of torsion

However, in view of the lack of test data in this area, it is recommended that at least the area of longitudinal steel required from equilibrium consideration in the truss model to take care of the torsional and shear stresses, as derived in Report 248-2, should remain straight throughout the entire length of the member to provide effective truss action and prevent premature failures.

2.7 Summary

In Chapter 2, the effects of special conditions on the truss model have been studied. These considerations were necessary before a careful evaluation of the truss model using test data could be conducted. With these considerations in mind, an evaluation of the truss model, using test results in the cases of torsion, torsion-bending-shear, and bending-shear for both reinforced and prestressed concrete members, is carried out in Chapter 3.

C H A P T E R 3

EXPERIMENTAL VERIFICATION OF THE SPACE TRUSS MODEL

3.1 Introduction

Before the generalized variable inclination truss model approach is adopted as the basis of a design procedure in American practice, a complete evaluation of the accuracy of the model is necessary. Such an evaluation should check the accuracy of this model using a significant body of the available test data reported in the American literature which has formed the basis for current procedures. This model should be shown accurate and safe in comparison with such data. This chapter details the results of such an evaluation.

Using both tests reported in the literature and test results from beams tested in this program, truss model predicted ultimate values are compared with test results.

Since the truss model is to be proposed only for the design of underreinforced sections, a differentiation is made in the analysis of the test results. The specimens in which the reinforcement yielded at failure are differentiated from those in which yielding of the reinforcement was not reached or where failure was due to poor detailing. In the section dealing with the strength of the diagonal compression strut the results of beams where web crushing was observed at failure are used to propose web crushing limits.

3.2 Torsion

Test results of reinforced and prestressed concrete members containing web reinforcement in the form of closed ties are compared with the ultimate load predictions of the truss model in the case of pure torsion.

The ultimate strength of the members subjected to torsion is evaluated by means of Eq. 3.1. (See Eq. 3.33 of Report 248-2.)

$$T_u = 2 A_0 \left[\frac{R_{ymin} S_y}{u \cdot s} \right]^{0.5} \quad (3.1)$$

The angle of the diagonal compression struts at ultimate is evaluated by means of Eq. 3.2. (See Eq. 3.32 of Report 248-2.)

$$\tan \alpha = \left[\frac{S_y \cdot u}{R_{ymn} s} \right]^{0.5} \quad (3.2)$$

Equations 3.1 and 3.2 were derived in Report 248-2 from equilibrium conditions in the truss model. Equation 3.1 predicts the ultimate strength of both reinforced and prestressed concrete members subjected to pure torsion. Since ultimate load conditions are being considered, only the cases of equilibrium torsion are studied. Members in which failure was due to web crushing are examined in Section 3.5.

Test data for reinforced concrete rectangular beams subjected to pure torsion from Refs. 82, 114, 104, and 173 are presented in Tables 3.1 and 3.2.

Tests reported by Hsu (82) on reinforced concrete rectangular beams.

(1) Member ID	(2) r	(3) Tu(Eq. 3.1) (K-in)	(4) Ttest (K-in)	(5) α (Eq. 3.2) (degrees)	(6) Level of Prestress $\frac{\sigma}{f'_c}$	(7) Ttest (4) Tu(theory)(3)
B1	1.0	174.0	197	45	0	1.13
B2	1.0	250.0	259.0	44	0	1.04
B3	1.0	354.0	332.0	43	0	0.94
B4	1.0	473.0	419.0	43	0	0.89
B9	1.0	250.0	264.0	34	0	1.06
M1	1.0	222.0	269.0	39	0	1.21
M2	1.0	313.0	359.0	39	0	1.15
I2	1.0	272.0	319.0	45	0	1.17
I3	1.0	370.0	404.0	43	0	1.09
I4	1.0	471.0	514.0	44	0	1.09
I5	1.0	602.0	626.0	44	0	1.04
J2	1.0	266.0	258.0	45	0	0.97
G2	1.0	299.0	357.0	44	0	1.19
G4	1.0	537.0	574.0	43	0	1.07
G6	1.0	317.0	346.0	45	0	1.09
G7	1.0	441.0	406.0	44	0	1.06
G8	1.0	602.0	650.0	44	0	1.08
N1	1.0	86.0	81.0	49	0	0.94
N2	1.0	137.0	128.0	49	0	0.93
N3	1.0	129.0	108.0	49	0	0.84
K1	1.0	101.0	136.0	44	0	1.35
K2	1.0	168.0	210.0	44	0	1.25
K3	1.0	219.0	252.0	43	0	1.15

*Note: Specimens B5, B6, B7, B8, B10, D1, D2, D3
D4, M3, M4, M5, M6, I6, J1, J3, J4, G1, G3,
G5, N1a, N2a, N4, K4, C1, C2, C3, C4, C5,
and C6 are reported in Secs. 3.6 and
3.7

$\bar{X} =$ 1.07
 $S =$ 0.12

Table 3.1 Data for reinforced concrete rectangular beams

Tests reported by McMullen and Rangan (114)

(1) Member ID	(2) r	(3) Tu(Eq.3.1) (in.-kip)	(4) Ttest (in-KIP)	(5) α (Eq.3.2) (degrees)	(6) Level of Prestress	$\frac{\sigma}{f'_c}$	(7) $\frac{Ttest}{Ttheory}$ (4) (3)
A1	1.0	90.0	116.0	44	0		1.29
A2	1.0	165.0	200.0	44	0		1.21
A3	1.0	227.0	246.0	43	0		1.08
A4	1.0	312.0	305.0	43	0		0.98
B1R	1.0	81.0	109.0	44	0		1.35
B2	1.0	148.0	184.0	44	0		1.24
B3	1.0	200.0	224.0	44	0		1.12
* Specimens A1R and B4 are reported in Section 3.7					X =		1.18
					S =		0.13

Tests reported by Liao and Ferguson (104)

PT4	1.0	10.7	9.7	9	0		0.91
PT5	1.0	17.8	14.7	16	0		0.83
					X =		0.87
					S =		0.06

Tests reported by Wyss, Garland and Mattock (173)

D2	1.0	106	85	42	0		0.80
D3	1.0	178	154	45	0		0.87
D4	1.0	231	221	43	0		0.96
* Specimens D5,D6 are reported in Sec. 3.6					X =		0.88
					S =		0.08
Overall mean (X) and sample standard deviation (s) from Tables 3.1 and 3.2					X =		1.07
					S =		0.15

Table 3.2 Data on reinforced concrete rectangular beams

The value of "r" represents the ratio of the yield force of the top chord to the yield force of the bottom chord. The level of prestress is defined as the ratio between the average effective prestress in the cross section $[f_{se} * A_{pse}] / [A_{gross} * f'_c]$, where f_{se} is the effective prestress force in the strand or wire, A_{pse} is the total area of prestressing steel, A_{gross} represents the total cross-sectional area of the member, and f'_c is the concrete compressive strength.

In Fig. 3.1, a comparison between the test observed values and the predicted truss values for the data in Tables 3.1 and 3.2 is shown. As can be seen from this figure the truss model adequately predicts the ultimate strength in the case of pure torsion, provided that failures due to poor detailing or crushing of the concrete are prevented. The mean for all test prediction values is 1.07 with a standard deviation of 0.15.

In Sec. 2.6.2, the effect of the cross-sectional shape on the torsional ultimate strength was discussed. As long as the cross section is free to warp or the cross-sectional shape is nonwarpable such as in the case of rectangular, T, or L sections, the restraining effect will be of no significance.

Table 3.3 and Fig. 3.2 give a comparison between the ultimate test values for reinforced concrete L-sections. Again, there is a substantial agreement between test and theory, although the mean for all test/prediction values is 1.14 with a standard deviation of 0.17. These values are higher than those for rectangular sections as might be expected.

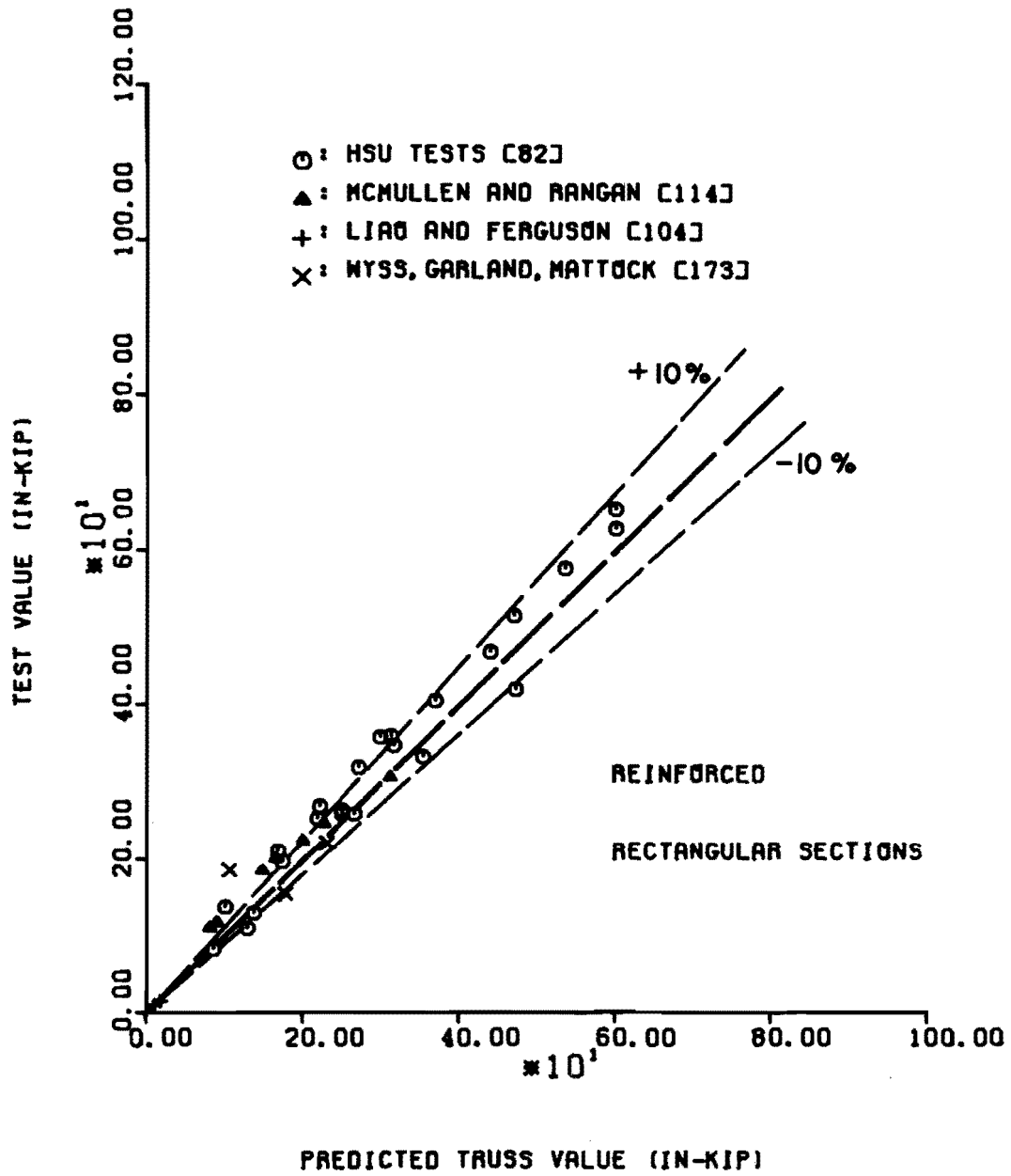


Fig. 3.1 Reinforced concrete rectangular beams subjected to pure torsion

Tests reported by Liao and Ferguson (104) on reinforced concrete L-beams

(1) Member ID	(2) r	(3) Tu(Eq. 3.1) (in.-kip)	(4) Ttest (in-KIP)	(5) α (Eq. 3.2) (degrees)	(6) Level of Prestress $\frac{\sigma}{f'c}$	(7) $\frac{Ttest}{T(theory)}$ (4)
PT-1	1.0	10.7	9.8	9	0	0.92
PT-2	1.0	17.8	17.1	16	0	0.96
PT-7	1.0	10.7	11.9	31	0	1.11
PT-8	1.0	17.9	18.4	16	0	1.03

Tests reported by Rajagopalan and Ferguson (140) on reinforced concrete L-beams

(1) Member ID	(2) r	(3) Tu(Eq. 3.1) (in-KIP)	(4) Ttest (in-KIP)	(5) α (Eq. 3.2) (degrees)	(6) Level of Prestress $\frac{\sigma}{f'c}$	(7) $\frac{Ttest}{T(theory)}$ (4)
R-7	1.0	11.2	13.5	18	0	1.21
R-8	1.0	8.1	11.2	12	0	1.38
R-17	1.0	23.5	27.7	24	0	1.18
R-19	1.0	16.7	22.5	17	0	1.35
					X =	1.14
					S =	0.17

Table 3.3 Test data of reinforced concrete L-beams subjected to restrained torsion

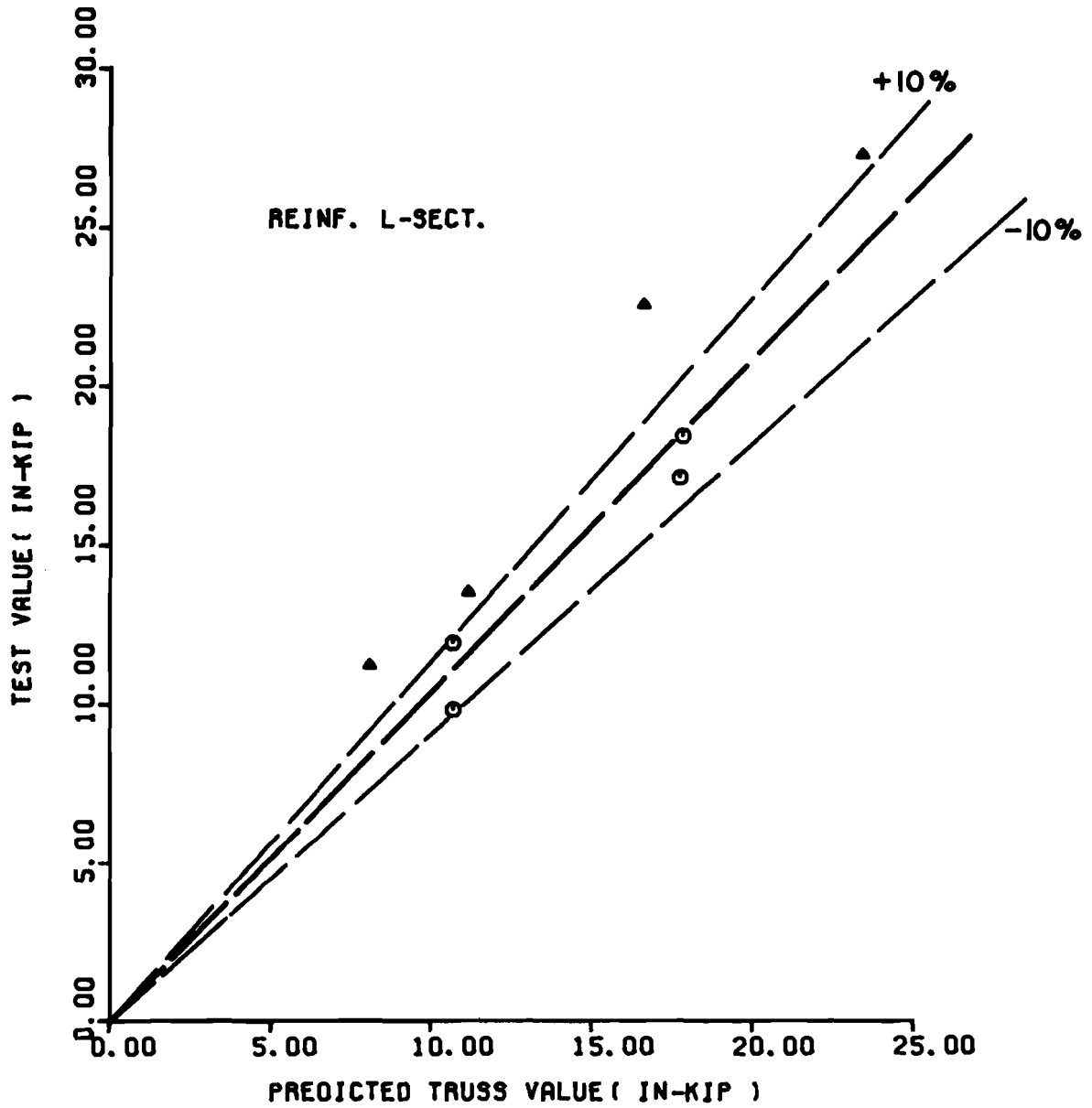


Fig. 3.2 Evaluation of the truss model predictions using data from reinforced concrete L-sections

Table 3.4 and Fig. 3.3 give a comparison between the ultimate test values and the truss model predictions for prestressed concrete beams subjected to pure torsion. The data presented include tests performed on both hollow and solid rectangular sections in addition to inverted T-beam bent caps.

From Table 3.4 and Fig. 3.3, it is apparent that the truss model adequately predicts the ultimate strength of both solid and hollow prestressed concrete members as long as yielding of the transverse and the longitudinal reinforcement at ultimate is ensured by designing underreinforced sections and avoiding premature failures due to poor detailing. The mean for all test predicted values is 1.01 with a standard deviation of 0.16.

The consequences of restraining the torsional warping of the cross section in the case of sections influenced by the restraining effect such as I-beams, is illustrated in Table 3.5 and Fig. 3.4. The results of tests on reinforced and prestressed concrete I-beams subjected to pure torsion presented in Table 3.5, are compared with the ultimate value predicted by the truss model. In this case, the mean for all test predicted values is 1.5 with a standard deviation of 0.68. From Fig. 3.4, it is apparent that the truss model tends to give more conservative estimates of the actual ultimate capacity of these members than for unrestrained warping cases. However, for the case of low values of the angle α (15 degrees to 30 degrees), and provided yielding of the stirrups and the longitudinal steel takes place at failure, it shows good agreement with the actual test values.

Tests reported by Mitchell and Collins (120), (56) on solid (S) and hollow (H) rectangular sections

(1) Member ID	(2) r	(3) T _u (Eq.3.1) (in.-kip)	(4) T _{test} (in-KIP)	(5) α (Eq.3.2) (degrees)	(6) Type of Section	(7) Level of Prestress	(8) $\frac{\sigma}{f'c} \frac{T_{test}(4)}{T(theory)(3)}$
P1	1.0	793.0	725.0	32	S	0.11	0.91
P2	1.0	793.0	715.0	32	H	0.15	0.90
P3	1.0	474.0	470.0	46	S	0.025	0.99
P4	1.0	793.0	805.0	32	H	0.15	1.02
TB4	1.0	643.0	176.0	22	H	0.214	0.9
* Specimen P5 is reported in Sec. 3.7						X =	0.94
						S =	0.06

Tests reported by Johnston and Zia (86) on box sections (H)

H-0-3-1	0.5	268.0	210.0	24	H	0.132	0.78
H-0-6-1	0.5	190.0	176.0	17	H	0.132	0.93
						X =	0.86
						S =	0.11

Tests reported by Mirza (116) on inverted T-bent caps

TP32	0.1	920.0	1085.0	32	T	0.17	1.18
TP33	0.1	920.0	1088.0	32	T	0.17	1.18
TP64	3.9	812.0	1096.0	39	T	0.12	1.35
TP65	3.9	938.0	938.0	44	T	0.12	1.00
* Specimens TP55, TP43, TP54, TP63 are reported on Section 3.7						X =	1.18
						S =	0.14

Overall X = 1.01
S = 0.16

Table 3.4 Data on prestressed concrete beams of various sections

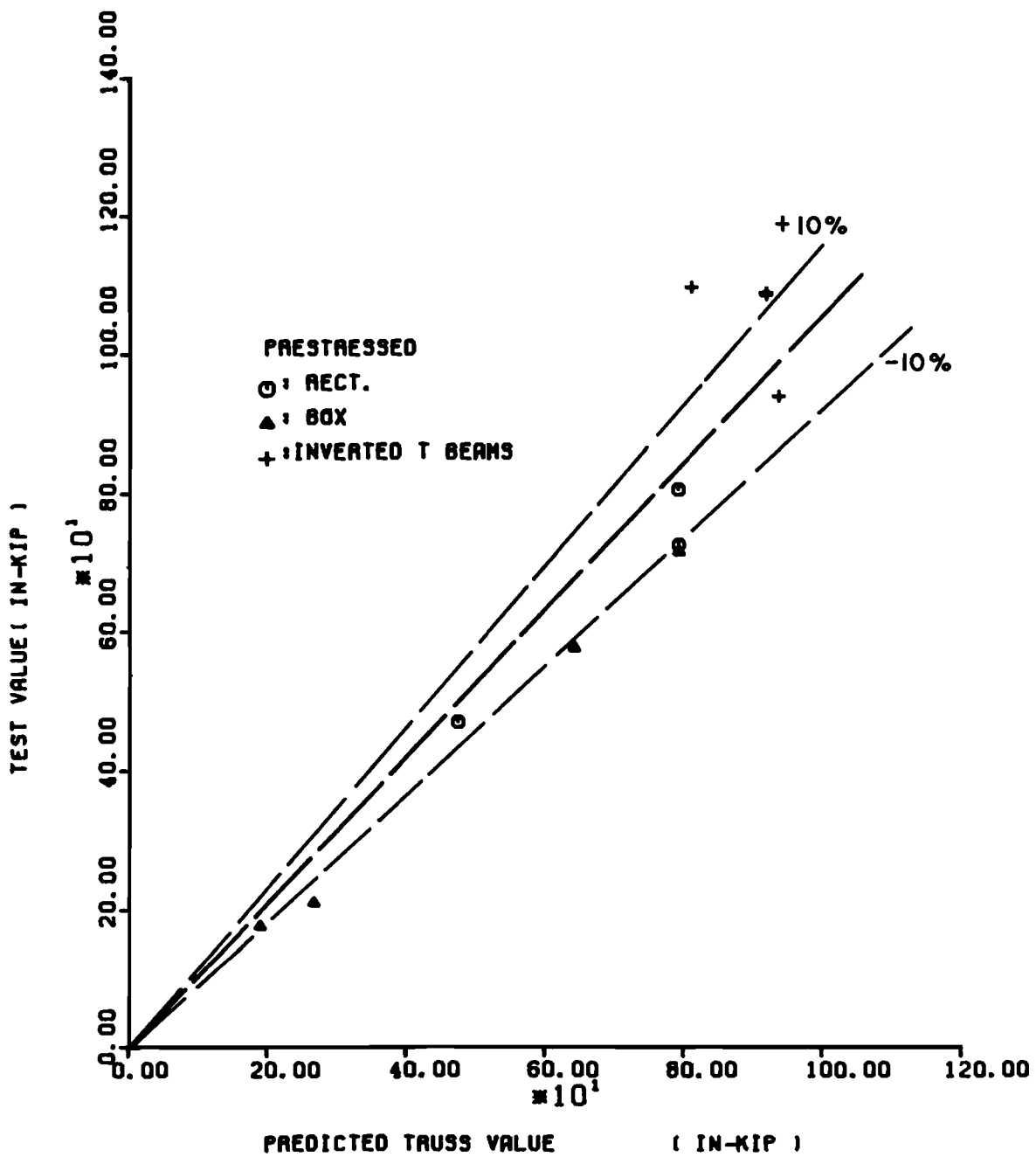


Fig. 3.3 The truss model in the case of prestressed concrete members

Tests reported By Wyss, Garland and Mattock (173) on reinforced concrete I-beams

(1) Member ID	(2) r	(3) Tu(Eq. 3.1) (in.-kip)	(4) Ttest (in-KIP)	(5) α (Eq. 3.2) (degrees)	(6) Level of Prestress $\frac{\sigma}{f'c}$	(7) Ttest Tu(Theory) (3)
C2	1.0	106.0	179.0	42	0.0	1.69
C3	1.0	178.0	254.0	45	0.0	1.43
C4	1.0	290.0	367.0	44	0.0	1.27
C5	1.0	472.0	450.0	45	0.0	0.95

* Specimen C6 is reported in
Sec. 3.6

X =	1.31
S =	0.31

Tests reported by Wyss, Garland and Mattock (173) on prestressed concrete I-beams

A2	0.29	321.0	318.0	16	0.19	0.99
A3	0.29	438.0	391.0	22	0.19	0.89
B2	0.33	218.0	219.0	23	0.10	1.00
B3	0.33	299.0	296.0	31	0.10	0.99
B4	0.33	378.0	320.0	37	0.10	0.85

* Specimens A5 and B6 are reported
in Sec. 3.6, A4 and B5 are
reported in Sec. 3.7

X =	0.94
S =	0.07

Tests reported by Rangan and Hall (143) on prestressed concrete I-beams

A1	0.77	34.0	66.5	40	0.10	1.96
AF1	0.80	39.0	101.7	35	0.10	2.61
B1	0.90	32.0	66.5	41	0.06	2.08
CF1	0.70	38.0	108.0	41	0.06	2.84
					X =	2.37
					S =	0.42
			Overall		X =	1.50
					S =	0.68

Table 3.5 Data on prestressed and reinforced concrete I-beams with restrained warping

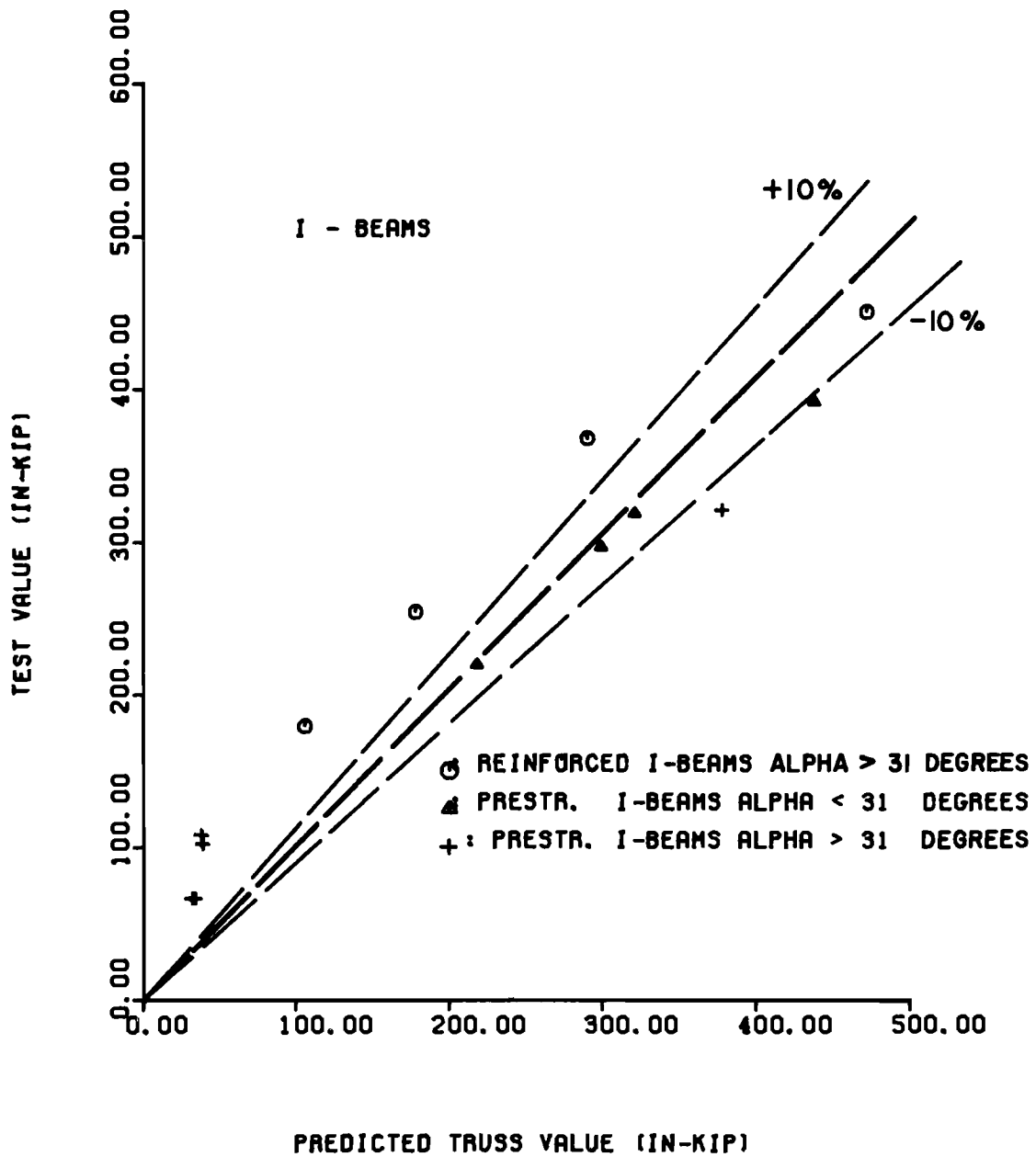


Fig. 3.4 Comparison between test values and truss model prediction in the case of pure torsion in I-beams where warping of the cross section is restrained

From the evaluation carried out in this section on members subjected to pure torsion it is apparent that the truss model adequately predicts the ultimate strength of both reinforced and prestressed concrete members where restraining effects are of no significance, such as box, solid rectangular, T, and L beams, as long as yielding of the transverse and longitudinal reinforcement is ensured by designing underreinforced sections and premature failures due to poor detailing are avoided.

3.3 Torsion-Bending

Tests results of reinforced and prestressed concrete members of various cross sections subjected to combinations of torsion and bending, are used to evaluate the truss model for this case. In order to examine the truss model ultimate load predictions, the interaction equations for the case of torsion and bending derived in Report 248-2 from equilibrium considerations of the truss model are used. These equations represent the interaction between torsion and bending at ultimate for the case of underreinforced members, provided premature failures due to poor detailing are avoided.

Equation 3.3 (see Eq. 3.53 of Report 248-2) predicts the interaction between torsion and bending at ultimate, for the case where yielding of the longitudinal reinforcement occurs on the side of the member where the applied bending moment induces tension.

$$1 = \left(\frac{T_u}{T_{uo}} \right)^2 r + \frac{M_u}{M_{uo}} \quad (3.3)$$

T_u and M_u are the ultimate load combinations of torsional and bending moments, "r" is the ratio of the longitudinal reinforcement F_{yu}/F_{yl} , where F_{yu} represents the total tension force $A_{yu} * f_y$ provided by the longitudinal reinforcement at the side of the member where the applied bending moment induces compression, and F_{yl} is the total tension force $A_{yl} * f_y$ provided by the longitudinal reinforcement at the side of the member where the applied bending moment induces tension. T_{u0} represents the ultimate torsional capacity of the section, when the applied bending moment M_u is zero. (See Eq. 3.33 of Report 248-2.)

$$T_{u0} = 2 A_0 \left[\frac{R_{ymin} S_y}{u s} \right]^{0.5} \quad (3.4)$$

M_{u0} is the ultimate bending strength of the section, when the applied torsional moment T_u is zero.

$$M_{u0} = F_{yL} * z \quad (3.5)$$

The derivation and the terms in Eqs. 3.4 and 3.5 have been fully explained in Report 248-2. (See Eqs. 3.33 and 3.48 of Report 248-2.)

Equation 3.6 (see Eq. 3.56 of Report 248-2) represents the interaction between bending and torsion at ultimate, when yielding of the longitudinal reinforcement takes place at the side of the member where the applied bending moment induces compression.

$$1 = \left(\frac{T_u}{T_{u0}} \right)^2 - \left(\frac{M_u}{M_{u0}} \right) \frac{1}{r} \quad (3.6)$$

Equations 3.3 and 3.6 together represent the total interaction between bending and torsion for underreinforced sections in both prestressed and reinforced concrete.

It is apparent, from Eqs. 3.3 and 3.6, that the interaction between bending and torsion for a given member is dependent on the ratio of longitudinal reinforcement "r". Test data from reinforced and prestressed concrete specimens with different ratios of longitudinal reinforcement are used to evaluate the truss model.

Test results reported by Gesund, Schuette, Buchanan and Gray (70), for reinforced concrete rectangular beams with a ratio of longitudinal reinforcement r of 0.7, are shown in Table 3.6. A comparison between these test observed values and the predicted interaction between torsion and bending at ultimate, obtained with the interaction equations 3.3 and 3.6 derived from the truss model, is shown in Fig. 3.6. It is more difficult to evaluate the accuracy of the truss model for combined actions than for a single action such as pure torsion. A reasonable way to judge the accuracy is to evaluate the dispersion between data points and interaction curves along radial lines from the origin. Data points inside the curves would be unconservative predictions, whereas points falling outside the interaction curves represent those cases where the truss model predictions yielded conservative results. Column (6) of Table 3.6 contains the dispersion coefficient I . This coefficient quantifies the dispersion between data points and interaction curves along radial lines from the origin (see Fig. 3.5). If I is equal to 1.0, then the truss model predicted values

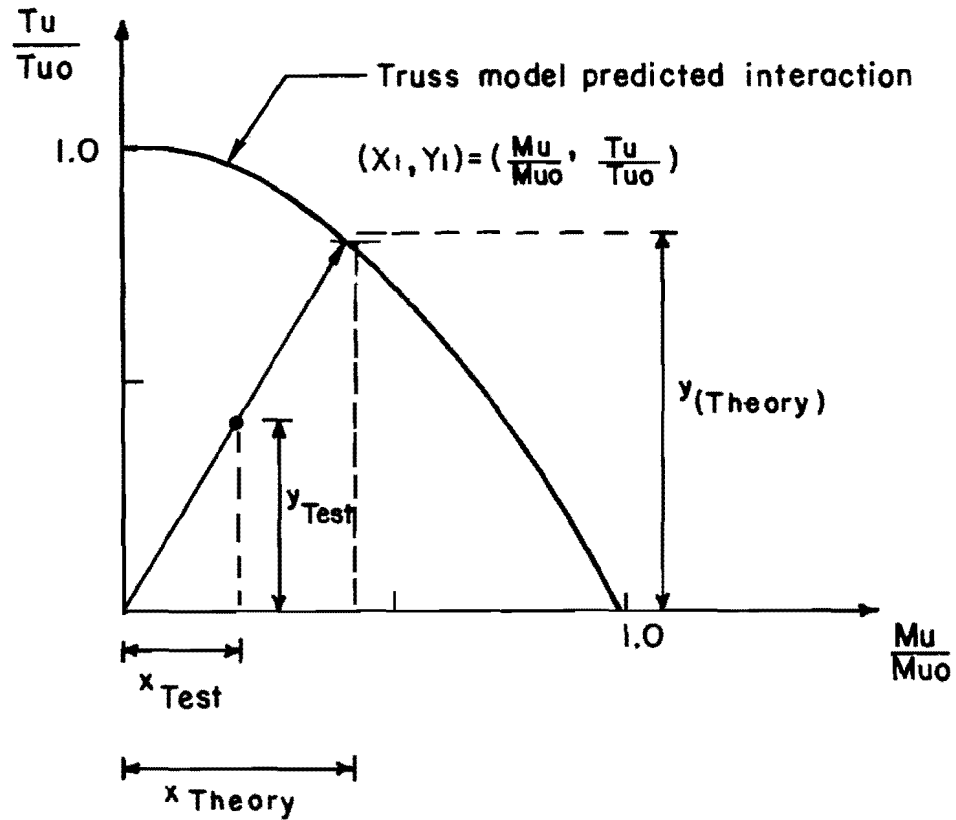
Tests reported by Gesund, Schuette, Buchanan and Gray (70)

(1) Member ID	(2) r	(3) $\frac{M_{test}}{M_{uo}}$	(4) $\frac{T_{test}}{T_{uo}}$	(5) Level of Prestress σ / f'	(6) I	(7) Failure mode
2	0.7	0.50	0.77	0	0.94	Yielding of longitudinal and transverse reinforcement
3	0.7	0.60	0.50	0	0.81	
4	0.7	0.70	0.50	0	0.90	
5	0.7	0.80	0.60	0	1.04	
6	0.7	0.90	0.40	0	1.01	
7	0.7	0.90	0.20	0	0.93	
8	0.7	0.92	0.30	0	0.98	
9	0.7	0.40	1.15	0	1.18	
10	0.7	0.60	0.80	0	1.03	
11	0.7	0.40	0.90	0	0.98	
12	0.7	0.70	0.70	0	1.03	

* Specimen 1 is reported
in Sec. 3.7

X = 0.98
S = 0.09

Table 3.6 Data on reinforced concrete rectangular
beams with $r = 0.7$



$$z_{\text{Test}} = [(y_{\text{Test}})^2 + (x_{\text{Test}})^2]^{0.5}$$

$$z_{\text{Theory}} = [(y_{\text{Theory}})^2 + (x_{\text{Theory}})^2]^{0.5}$$

$$\text{Dispersion Index} = I = \frac{z_{\text{Test}}}{z_{\text{Theory}}}$$

$I > 1.0$ Conservative Predictions

$I = 1.0$ Test = Theory

$I < 1.0$ Unconservative predictions

Fig. 3.5 Dispersion coefficient I measured along radial lines from the origin

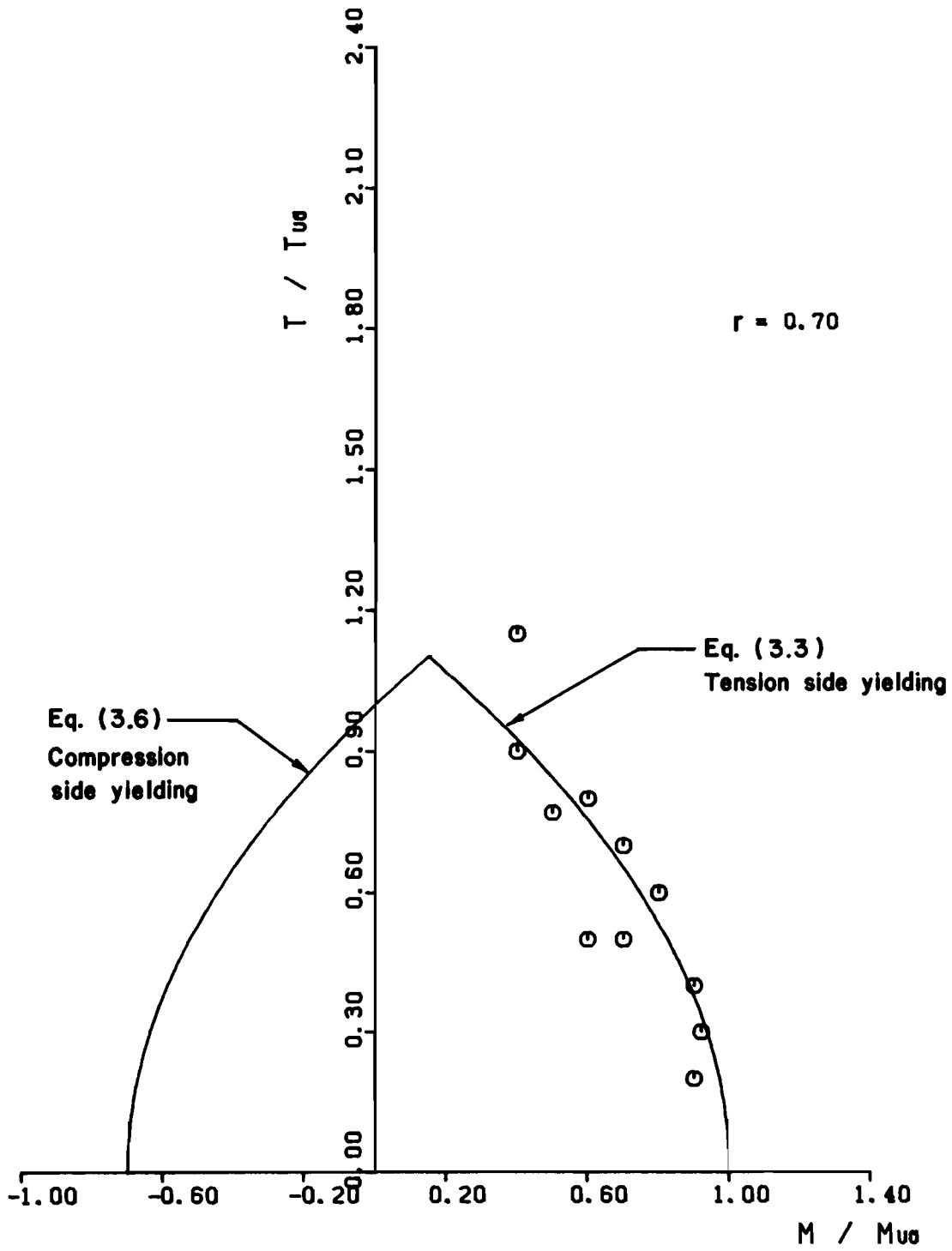


Fig. 3.6 Torque-bending interaction diagram for rectangular reinforced concrete beams with $r = 0.7$

are exactly the same as the observed test values. On the other hand, $I < 1.0$ indicates unconservative predictions.

For the specimens reported in Table 3.6 the mean of the dispersion index I is 0.98 and the standard deviation 0.09, indicating good agreement between observed test results and predicted values.

For the case of prestressed concrete members with a ratio of longitudinal reinforcement " r " of 0.33, the truss model is evaluated using the data shown in Table 3.7, obtained from tests reported by Rangan and Hall (144) on prestressed concrete box beams. For these specimens the mean of the dispersion index (I) is 1.13 and the standard deviation 0.12 indicating a reasonable agreement between the observed test values and the predicted results. In Fig. 3.7 the ultimate test values from Table 3.7 are shown to be in reasonable agreement with the ultimate load predicted by the generally conservative interaction equations derived from the truss model.

Data for members with symmetrical longitudinal reinforcement ($r = 1.0$) is presented for both reinforced concrete members of solid rectangular cross section and prestressed concrete box beams in Table 3.8. Figure 3.8 shows a comparison between the test values and the truss model predictions for the tests given in Table 3.8. For the test data reported in Table 3.8 the mean of the dispersion index is 1.28 and the standard deviation 0.11. Again, a reasonable but very conservative agreement can be observed.

The truss model is also evaluated using test results of members having different cross-sectional shapes. Table 3.9 gives data from

Tests reported by Rangan and Hall (144) on Prestressed concrete box beams

(1) Member ID	(2) r	(3) $\frac{M_{test}}{M_{uo}}$	(4) $\frac{T_{test}}{T_{uo}}$	(5) Level of Prestress σ/f'_c	(6) I	(7) Failure Mode
A1	0.33	1.16	0.92	0.03	1.36	Yielding of the bottom
A2	0.33	0.88	0.94	0.04	1.14	
A3	0.33	0.82	1.08	0.04	1.15	
A4	0.33	0.74	1.18	0.04	1.14	
A5	0.33	0.60	1.29	0.03	1.10	
B1	0.33	1.14	0.90	0.04	1.34	longitudinal and stirrup
B2	0.33	0.86	0.90	0.04	1.10	
B3	0.33	0.74	1.00	0.04	1.05	
B4	0.33	0.70	1.10	0.04	1.07	
B5	0.33	0.55	1.18	0.05	1.01	
C1	0.33	1.11	0.88	0.05	1.31	reinforcement
C2	0.33	0.84	0.89	0.05	1.08	
C3	0.33	0.72	1.15	0.05	1.11	
C4	0.33	0.67	1.06	0.05	1.03	
C5	0.33	0.52	1.10	0.05	0.94	
					X = 1.13	
					S = 0.12	

Table 3.7 Data for prestressed concrete box beams
with $r = 0.33$

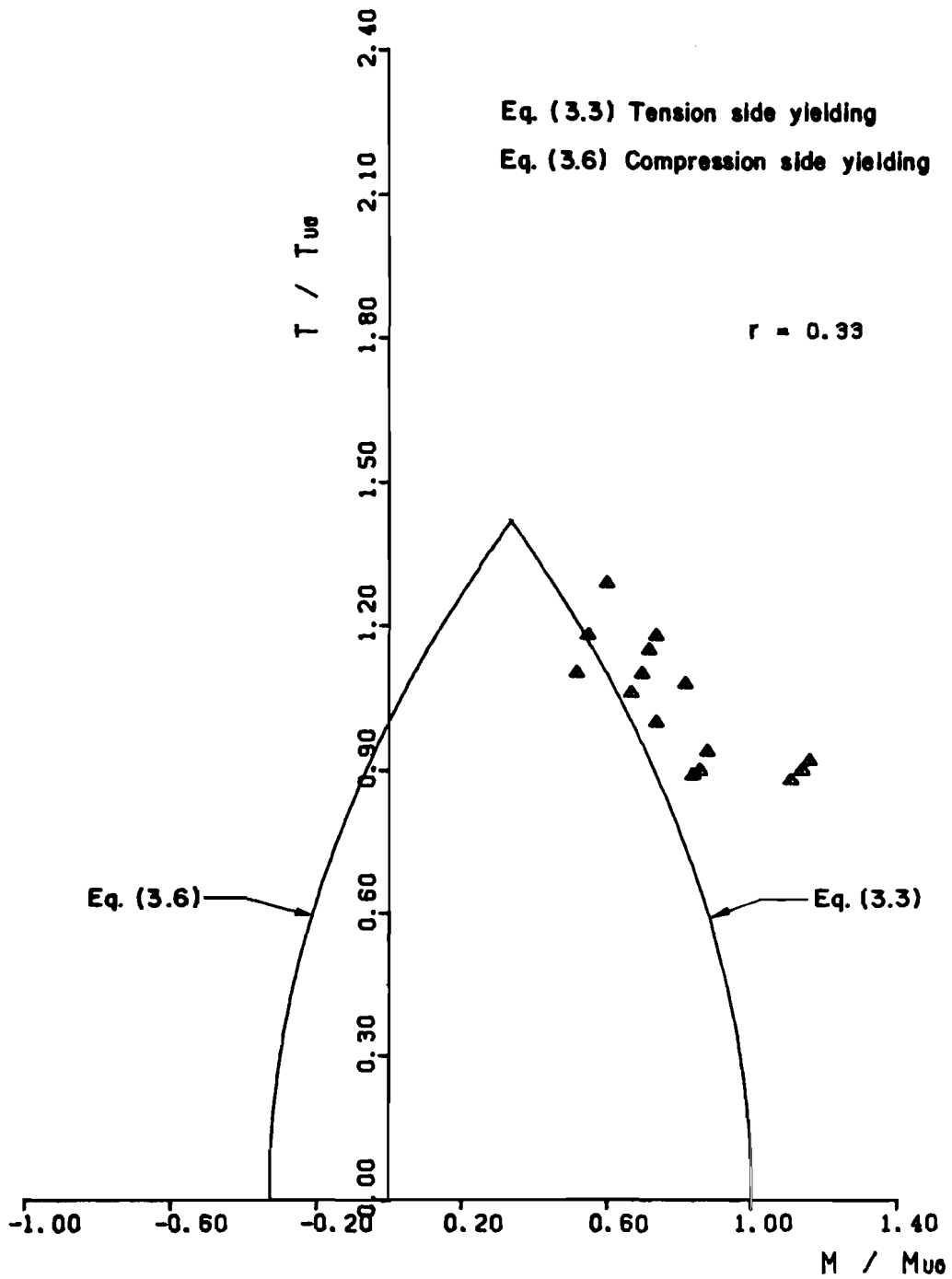


Fig. 3.7 Comparison of the truss with test results of prestressed concrete box members (144)

Tests reported by Pandit and Warwaruk (33) on reinforced concrete beams of rectangular cross section

(1) Member ID	(2) r	(3) $\frac{M_{test}}{M_{uo}}$	(4) $\frac{T_{test}}{T_{uo}}$	(5) Level of Prestress $\sigma / f'c$	(6) I	(7) Type of failure
E1	1.0	0.86	0.67	0	1.23	Yielding of the bottom longitudinal and stirrup reinforcement
E2	1.0	0.48	0.89	0	1.16	

* Specimens B2, B3, C1 and C2 are reported in Table 3.9; D1, D2, D3 are reported in Sec. 3.7

X = 1.20
S = 0.05

Tests reported by Mitchell and Collins (56) on prestressed concrete box beams

TB1	1.0	0.40	1.16	0.19	1.38	Yielding of the bottom longitudinal and stirrups
TB2	1.0	0.70	1.01	0.17	1.42	
TB3	1.0	0.98	0.55	0.23	1.23	
					X = 1.34	
					S = 0.10	
Overall					X = 1.28	
					S = 0.11	

Table 3.8 Test data on reinforced and prestressed concrete beams with $r = 1.0$

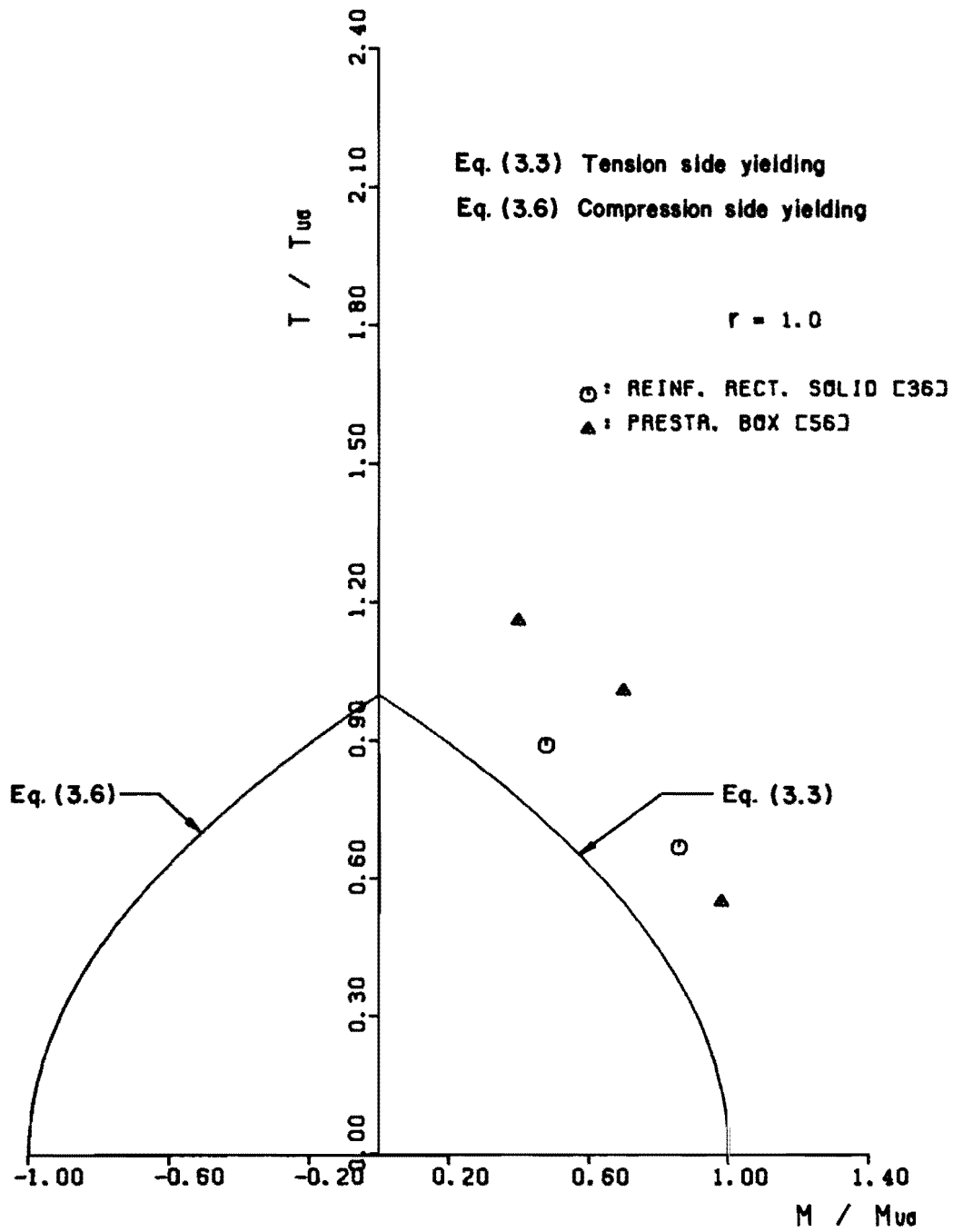


Fig. 3.8 Torsion-bending predicted interaction in the case of members with $r = 1.0$

tests on reinforced concrete beams of solid rectangular cross section, and prestressed concrete box beams, all with ratio of longitudinal steel "r" of 0.50.

In Fig. 3.9 the test data shown in Table 3.9 are compared with the truss model ultimate load interaction between torsion and bending. In this case the mean of the dispersion index is 1.06 and the standard deviation 0.09. Again, the truss model predictions seem to be in reasonable and generally conservative agreement with observed test values.

The versatility of the truss model allows the analysis of the interaction between torsion and bending in members with complex cross sections. Figure 3.10 shows the results presented in Table 3.10 for a series of tests conducted by Taylor and Warwaruk (161) on prestressed concrete double celled box beams with a longitudinal ratio "r" of 0.25. For these specimens, the mean of the dispersion index is 1.32 and the standard deviation 0.16.

As shown in Fig. 3.10, the truss model ultimate load interaction equations conservatively and adequately predict the ultimate load capacity in combined torsion and bending of such members.

The evaluation of the truss model in the case of reinforced and prestressed concrete members subjected to combined torsion and bending shows that the model can safely predict the ultimate load capacity of such members, as long as yielding of the longitudinal and transverse reinforcement is insured by designing underreinforced sections, and premature failures due to poor detailing are avoided.

Tests reported by Johnston and Zia (86) on Prestressed concrete box beams

(1) Member ID	(2) r	(3) Mtest Mu0	(4) Ttest Tu0	(5) Level of Prestress σ/f'_c	(6) I	(7) Type of failure
H-0-3-5	0.5	0.68	0.77	0.13	0.98	
H-0-3-6	0.5	0.48	0.88	0.13	0.91	Yielding of the
H-0-6-3	0.5	0.84	0.79	0.13	1.12	stirrups and
H-0-6-5	0.5	0.50	0.96	0.10	0.97	bottom longitudinal
H-0-6-6	0.5	1.08	0.52	0.10	1.19	steel

* Specimens H-0-3-2, H-0-3-3, H-0-3-4, H-0-6-2 and H-0-6-4 are reported in Sec. 3.7

X = 1.03
S = 0.12

Tests reported by Pandit and Warwaruk (33) on reinforced concrete rectangular beams

B2	0.5	0.35	0.80	0.0	1.13	
B3	0.5	0.48	1.06	0.0	1.03	Yielding of the
C1	0.5	0.94	0.67	0.0	1.14	stirrups and bottom
C2	0.5	0.65	0.90	0.0	1.04	steel

X = 1.09
S = 0.06

Overall X = 1.06
S = 0.09

Table 3.9 Data on reinforced and prestressed members with an "r" of 0.50

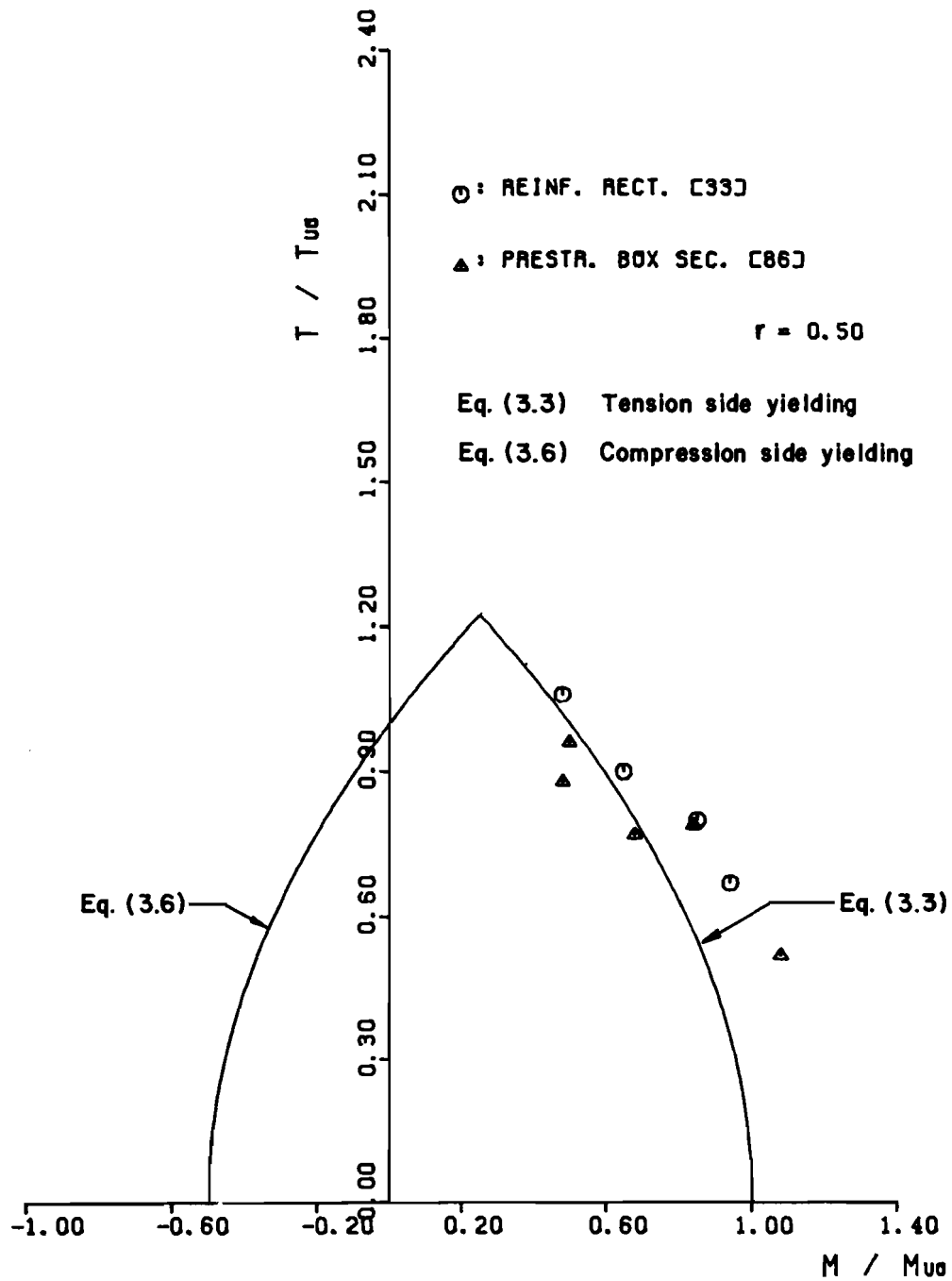


Fig. 3.9 Evaluation of the truss model predictions in the case of members of various cross sections

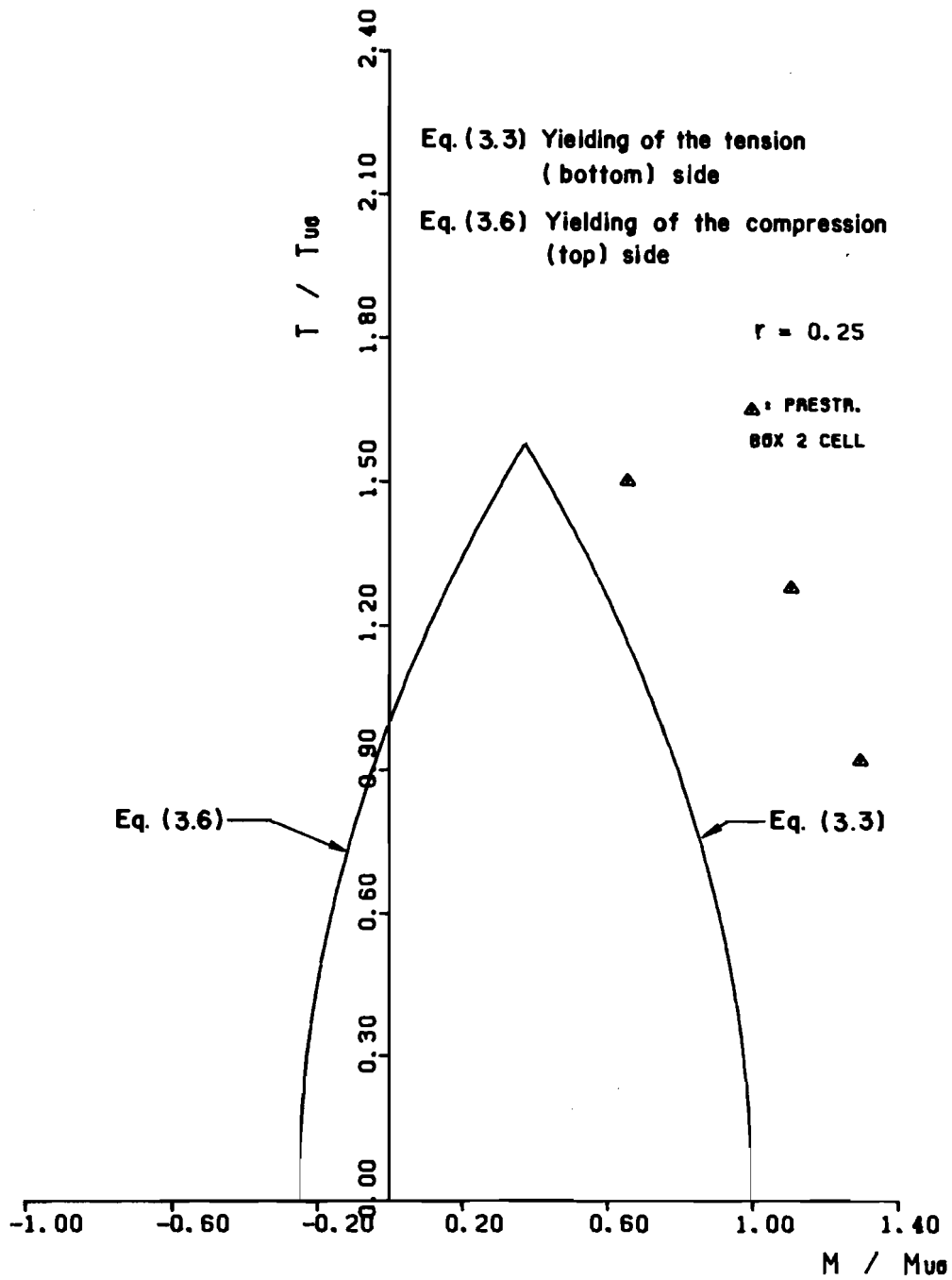


Fig. 3.10 Evaluation of the truss model in the case of complex cross sections

Tests reported by Warwaruk and Taylor (161) on Prestressed concrete
2 cell box beams

Member ID	r	$\frac{M_{test}}{M_{uo}}$ (in-Kip)	$\frac{T_{test}}{T_{uo}}$ (in-kip)	Level of prestress σ/f'_c	I	Type of failure
R1	0.24	1.11	1.28	0.07	1.39	Yielding of the stirrups and bottom longitudinal steel
R2	0.24	1.13	0.92	0.07	1.44	
R5	0.24	0.66	1.50	0.07	1.14	

* Specimens T1, T2 are reported in Sec. 3.7 X = 1.32
S = 0.16

Table 3.10 Data from tests reported by Warwaruk and Taylor (161) on prestressed

3.4 Torsion, Bending, and Shear

The truss model has also been evaluated using test data available in the literature for the case of reinforced and prestressed concrete members subjected to torsion-bending-shear.

The ultimate load behavior of members subjected to torsion-bending-shear can be studied by means of the interaction equations (3.80 and 3.83) developed in Report 248-2. These interaction equations were developed from equilibrium considerations in the truss model.

As in the problem of combined torsion-bending, two modes of failure are considered in the case of torsion-bending-shear. First, if at failure there is yielding of the longitudinal reinforcement in the side of the member where the applied moment induces tension (as well as yielding of the stirrups) then the interaction Eq. (3.7) (see Eq. 3.80 of Report 248-2) predicts the ultimate load interaction.

$$r \left[\left(\frac{T_u}{T_{uo}} \right)^2 + \left(\frac{V_u}{V_{uo}} \right)^2 \right] + \frac{M_u}{M_{uo}} = 1 \quad (3.7)$$

For simplicity, Eq. 3.7 is rearranged in the form shown in Eq.

3.8:

$$r \left[\frac{T_u}{T_{uo}} \right]^2 + \frac{M_u}{M_{uo}} = 1 - \left[\frac{V_u}{V_{uo}} \right]^2 r \quad (3.8)$$

T_u , M_u , and V_u represent the possible ultimate load combinations of torsional moment, bending moment, and shear force, respectively. The term "r" is defined to represent the ratio of longitudinal reinforcement, F_{yu}/F_{y1} . T_{uo} is the pure torsional capacity of the

section when both T_u and M_u are zero, as given by Eq. 3.4. M_u represents the pure moment capacity of the member when V_u and T_u are zero. The value of T_{u0} is given by Eq. 3.5. V_{u0} is the reference value in the case of pure shear as defined by Eq. 3.72 of Report 248-2. For sections with positive bending type reinforcement [$F_{y1} > F_{yu}$] V_{u0} is given by

$$V_{u0} = n*[2F_{yu}S_y z/s]^{0.5} \quad (3.9)$$

where F_{yu} is the tensile force capacity per web element in the truss model chord where the applied moment induces compression and "n" is the number of webs resisting the applied shear force. This derivation assumes the use of doubly reinforced sections in the design of members subjected to a combination of torsion, bending and shear. Since the resultant horizontal force due to shear always produces tension components in the lower and upper chords, the feasible maximum capacity is dictated by the weaker of the two longitudinal chords [$F_{y1} > F_{yu}$] in terms of tensile capacity.

The alternate case studied considers yielding of the stirrups at failure along with yielding in tension of the longitudinal reinforcement in the truss model chord in which the applied moment would induce compression [F_{yu}]. For this case, the ultimate load interaction of the member is evaluated using Eq. 3.10 (see Eq. 3.83 of Report 248-2).

$$\left(\frac{T_u}{T_{u0}}\right)^2 + \left(\frac{V_u}{V_{u0}}\right)^2 - \frac{1}{r} \frac{M_u}{M_{u0}} = 1 \quad (3.10)$$

To facilitate the comparison with test results, Eq. 3.10 is rearranged in the form shown in Eq. 3.11.

$$\left(\frac{T_u}{T_{uo}}\right)^2 - \frac{1}{r} \frac{M_u}{M_{uo}} = 1 - \left(\frac{V_u}{V_{uo}}\right)^2 \quad (3.11)$$

Equations 3.8 and 3.11 together represent the ultimate load interaction between torsion-bending-shear for underreinforced prestressed and reinforced concrete members, where premature failures due to poor detailing are prevented. The same criteria followed in the evaluation of the truss model for the case of bending and torsion are used in the case of combined torsion-bending-shear. The accuracy of the model is evaluated on the basis of the dispersion between data points and interaction curves (in this case given by Eq. 3.8 and 3.11) along radial lines from the origin (see Fig. 3.5).

Tables 3.11, 3.12, 3.13 and 3.14 show the test data used in the evaluation of the truss model. The test data include reinforced and prestressed concrete members of various cross-sectional shapes including rectangular, L beams, box sections and two cell box sections. The test data have been arranged taking into consideration the ratio of longitudinal reinforcement "r", and the ratio of ultimate applied shear to maximum pure shear capacity of the member [V_u/V_{uo}].

The dispersion index I, tabulated in column (7) of Tables 3.11, 3.12, 3.13, and 3.14, is again used as a measure of the dispersion between data points and the truss model predicted values, as given by Eqs. 3.8 and 3.11, measured along radial lines from the origin. A value of $I > 1$ indicates that the truss model predicted values are smaller

Tests reported by Collins, Walsh, Archer and Hall (33) on Rectangular Solid sections (R)

(1) Member ID and Section Type	(2) r	(3) $\frac{M_{test}}{M_{uo}}$	(4) $\frac{T_{test}}{T_{uo}}$	(5) $\frac{V_{test}}{V_{uo}}$	(6) Level of Prestress σ/f'_c	(7) I	(8) Type of failure
RE2 (R)	1.0	0.26	0.91	0.03	0.0	1.05	
RE3 (R)	1.0	0.37	0.89	0.05	0.0	1.09	Stirrups and
RE4 (R)	1.0	0.70	0.81	0.08	0.0	1.24	bottom steel
RE5 (R)	1.0	0.89	0.72	0.10	0.0	1.30	yielded
RE4*(R)	1.0	1.10	0.41	0.12	0.0	1.25	
RB1 (R)	0.26	0.02	0.75	0.01	0.0	0.80	
RB3*(R)	0.26	0.02	0.77	0.01	0.0	0.81	Stirrups and top steel yielded
RB5 (R)	0.26	0.94	0.77	0.34	0.0	1.11	Stirrups and
RB5A(R)	0.26	1.00	0.70	0.39	0.0	1.16	bottom longitudinal
RB6 (R)	0.26	1.06	0.60	0.41	0.0	1.19	steel yielded

$$X = 1.09$$

$$S = 0.20$$

Tests reported by Liao and Ferguson (104) on L-sections (L)

3LS-6(L)	1.0	0.29	0.99	0.29	0.0	1.20	Torsion + shear
3LS-8(L)	1.0	0.27	0.88	0.27	0.0	1.07	
3LS-3(L)	1.0	0.68	0.62	0.38	0.0	1.18	shear
1.5LS-1(L)	1.0	0.40	0.73	0.44	0.0	1.10	torsion + shear
3LS-2(L)	1.0	0.51	0.77	0.57	0.0	1.30	shear
1.5LS-2(L)	1.0	0.29	0.89	0.59	0.0	1.20	torsion + shear

* Specimens 3LS-4 and 3LS-7 are reported in Sec. 3.7

$$X = 1.18$$

$$S = 0.08$$

Table 3.11 Test data from reinforced concrete members subjected to torsion-bending-shear

Tests reported by Osburn, Magoglou and Mattock (133) on rectangular (R) and L-beams (L)

(1) Member (ID) Sec.Type()	(2) r	(3) $\frac{M_{test}}{M_{uo}}$	(4) $\frac{T_{test}}{T_{uo}}$	(5) $\frac{V_{test}}{V_{uo}}$	(6) Level of Prestress σ / f'_c	(7) I	(8) Type of failure
A1 (R)	0.15	1.04	0.62	1.08	0.0	1.31	
A2 (R)	0.15	1.01	0.56	1.08	0.0	1.27	
A3 (R)	0.15	0.93	0.57	1.10	0.0	1.19	
A4 (R)	0.15	0.90	0.62	0.69	0.0	1.03	
A5 (R)	0.15	0.80	0.47	0.73	0.0	0.91	
B1 (R)	0.15	1.04	0.95	0.71	0.0	1.24	Yielding of
B2 (R)	0.15	0.97	0.88	0.69	0.0	1.15	the
B3 (R)	0.15	0.99	0.88	0.60	0.0	1.15	stirrups and
B4 (R)	0.15	0.95	0.78	0.45	0.0	1.07	the bottom
B5 (R)	0.15	0.93	0.74	0.46	0.0	1.04	longitudinal
C1 (R)	0.10	1.03	0.61	0.84	0.0	1.14	steel (tension
C2 (R)	0.12	0.87	0.54	0.63	0.0	0.94	side in flexure)
C3 (R)	0.13	0.96	0.59	0.64	0.0	1.03	
C4 (R)	0.10	0.86	0.58	0.70	0.0	0.94	
D1 (L)	0.10	1.12	0.63	0.91	0.0	1.26	
D2 (L)	0.12	1.02	0.64	0.74	0.0	1.12	
D3 (L)	0.13	0.96	0.57	0.64	0.0	0.92	
D4 (L)	0.10	0.85	0.56	0.69	0.0	0.93	
E1 (L)	0.10	1.11	0.62	0.90	0.0	1.24	
E2 (L)	0.12	0.94	0.59	0.68	0.0	1.02	
E3 (L)	0.13	0.93	0.55	0.62	0.0	1.00	
E4 (L)	0.10	0.74	0.49	0.60	0.0	0.80	
					X =	1.08	
					S =	0.14	
					Overall for	X =	1.10
					Tables 3.11 and 3.12	S =	0.15

Table 3.12 Test data from reinforced concrete members subjected to torsion-bending-shear

Tests reported by Mukherjee and Warwaruk (123) on Prestressed concrete rectangular sections

(1) Member ID Section Ty. ()	(2) r	(3) $\frac{M_{test}}{\mu_{uo}}$	(4) $\frac{T_{test}}{\tau_{uo}}$	(5) $\frac{V_{test}}{\nu_{uo}}$	(6) Level of Prestress σ/f'_c	(7) I	(8) Type of failure
V102 (R)	1.0	0.99	0.61	0.21	0.11	1.33	
V104 (R)	1.0	0.34	1.03	0.09	0.11	1.22	
V105 (R)	1.0	0.08	1.03	0.04	0.11	1.07	Yielding of the stirrups and bottom longitudinal steel
V123 (R)	1.0	0.54	1.09	0.16	0.11	1.42	
V124 (R)	1.0	0.32	1.18	0.10	0.11	1.36	
V125 (R)	1.0	0.09	1.18	0.04	0.11	1.23	
S1 (R)	1.0	0.89	0.87	0.19	0.11	1.46	
S2 (R)	1.0	0.84	0.66	0.16	0.11	1.23	
* Specimens V107, V122, V127, V202, V203, V204, V205, V207, V223, V224, V225, and V227 are reported in Sec. 3.7					X =	1.29	
					S =	0.13	

Tests reported by Johnston and Zia (86) on Prestressed concrete box sections

H-4-3-5 (R)	0.5	0.45	0.75	0.41	0.09	0.85	
H-6-3-3 (R)	0.5	0.69	0.70	0.38	0.09	1.02	
H-6-3-4 (R)	0.5	1.12	0.58	0.42	0.09	1.36	Yielding of
H-6-3-5 (R)	0.5	1.07	0.40	0.42	0.09	1.24	stirrups and
H-6-6-3 (R)	0.5	0.50	0.79	0.44	0.10	0.92	bottom steel
H-4-3-3 (R)	0.5	0.49	0.50	0.55	0.10	0.79	
H-4-6-3 (R)	0.5	0.53	0.55	0.60	0.09	0.86	
H-6-6-4 (R)	0.5	1.10	0.28	0.62	0.10	1.38	
H-6-6-5 (R)	0.5	1.05	0.54	0.59	0.10	1.41	
H-4-6-2 (R)	0.5	0.45	0.37	0.81	0.09	0.80	
H-4-6-4 (R)	0.5	0.86	0.41	0.88	0.10	1.37	
* Specimens H-4-3-1, H-4-3-2, H-4-6-1, H-4-6-3, H-4-6-5, H-6-3-1 H-6-3-2, H-6-6-1, H-6-6-2 are reported in Sec. 3.7					X =	1.09	
					S =	0.26	

Table 3.13 Test data from prestressed concrete members subjected to torsion-bending-shear

Tests reported by Taylor and Warwaruk (161) on Prestressed concrete Double Celled Box-sections

(1) Member ID Sec.Type()	(2) r	(3) $\frac{M_{test}}{M_{uo}}$	(4) $\frac{T_{test}}{T_{uo}}$	(5) $\frac{V_{test}}{V_{uo}}$	(6) Level of Prestress σ / f'_c	(7) I	(8) Type of failure
R3(2-Cells)	.24	1.20	1.30	0.34	0.32	1.51	Yielding of the stirrups and bottom long. steel
R4(2-cells)	.24	1.30	0.80	0.55	0.33	1.51	
				X =	1.51		
				S =	0.00		
Overall from Tables 3.13 and 3.14				X =	1.21		
				S =	0.24		

Table 3.14 Test data from prestressed concrete members subjected to torsion-bending-shear

than the test values. Hence, the truss model is conservative in such cases. $I = 1$ indicates that the obtained test results and the predicted values are exactly the same. Finally, $I < 1$ indicates that the predicted values were larger than the actual test results and thus the theory would be unconservative for such specimens. The values of the mean (\bar{X}) and standard deviation (S) are provided at the bottom of each group of tests. In addition, the values of the mean and the standard deviation of all the reinforced and prestressed concrete members studied are provided at the bottom of Tables 3.12 and 3.14, respectively.

For the case of reinforced concrete members the mean of the dispersion coefficient is 1.10 and the standard deviation 0.15. This indicates that the truss model predictions were very good and in general conservative.

For the case of all the prestressed concrete members shown in Table 3.13 and 3.14 the mean of the dispersion coefficient is 1.14 and the standard deviation 0.24. This indicates a reasonable agreement between test results and truss model predictions. The truss model is more conservative for prestressed concrete members than for reinforced concrete members, and a larger scatter is observed as shown by the standard deviation value of 0.24. However, in spite of the large standard deviation, no test result was less than 80% of the predicted value.

To illustrate the predicted truss model ultimate load interaction evaluated by means of Eqs. 3.8 and 3.11 some of the test

data presented in Tables 3.11, 3.12, 3.13 and 3.14 are plotted in Figs. 3.11 thru 3.16.

Figure 3.11 shows the predicted truss model ultimate load interaction evaluated by means of Eqs. 3.8 and 3.11, for a section with $r = 1.0$ and subjected to a shear ratio V_u/V_{u0} equal to 0.75. Also shown, in Fig. 3.11 are the ultimate test values of reinforced concrete specimens RE2, RE3, RE4, RE5, and RE4* from Table 3.11 and prestressed concrete specimens V104 and V105 from Table 3.13. Test values falling outside the interaction curve indicate conservative truss model predictions. Good agreement is shown in this case.

The effect of increasing the applied shear while keeping the ratio of longitudinal steel constant, is illustrated in Fig. 3.12. The test data of reinforced concrete L-beams 3LS-3 and 1.5LS-1, from Table 3.11, are plotted in Fig. 3.12. The value of "r" remains equal to 1.0 while the value of V_u/V_{u0} has been increased to 0.40. Again, good agreement is shown.

The torsion-bending-shear ultimate load interaction of prestressed concrete box sections (86), having a ratio of longitudinal steel of 0.5, is illustrated in Fig. 3.13 which shows the ultimate test values of specimens H-4-3-5, H-6-3-3, H-6-3-4, H-6-3-5, and H-6-6-3 from Table 3.13. Generally good agreement exists with no test value less than 85% of the truss model prediction.

The ultimate test values of reinforced concrete rectangular specimens RU5, RU5A, RU6 from Ref. 33 in Table 3.11, prestressed concrete rectangular specimen V122 from Ref. 123 in Table 3.13, and the

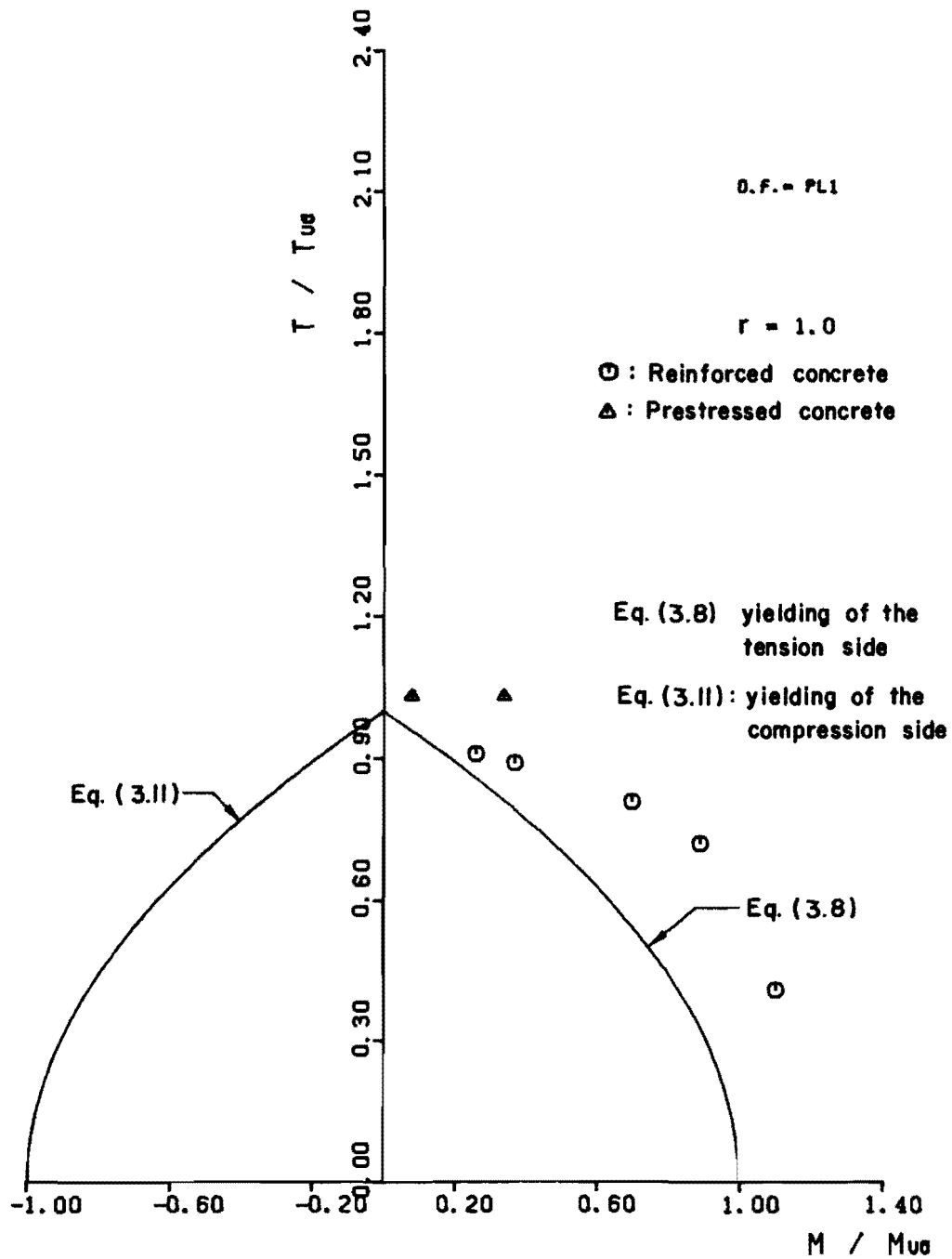


Fig. 3.11 Torsion-bending-shear interaction with $v/v_{u0} = 0.75$ for reinforced and prestressed concrete specimens

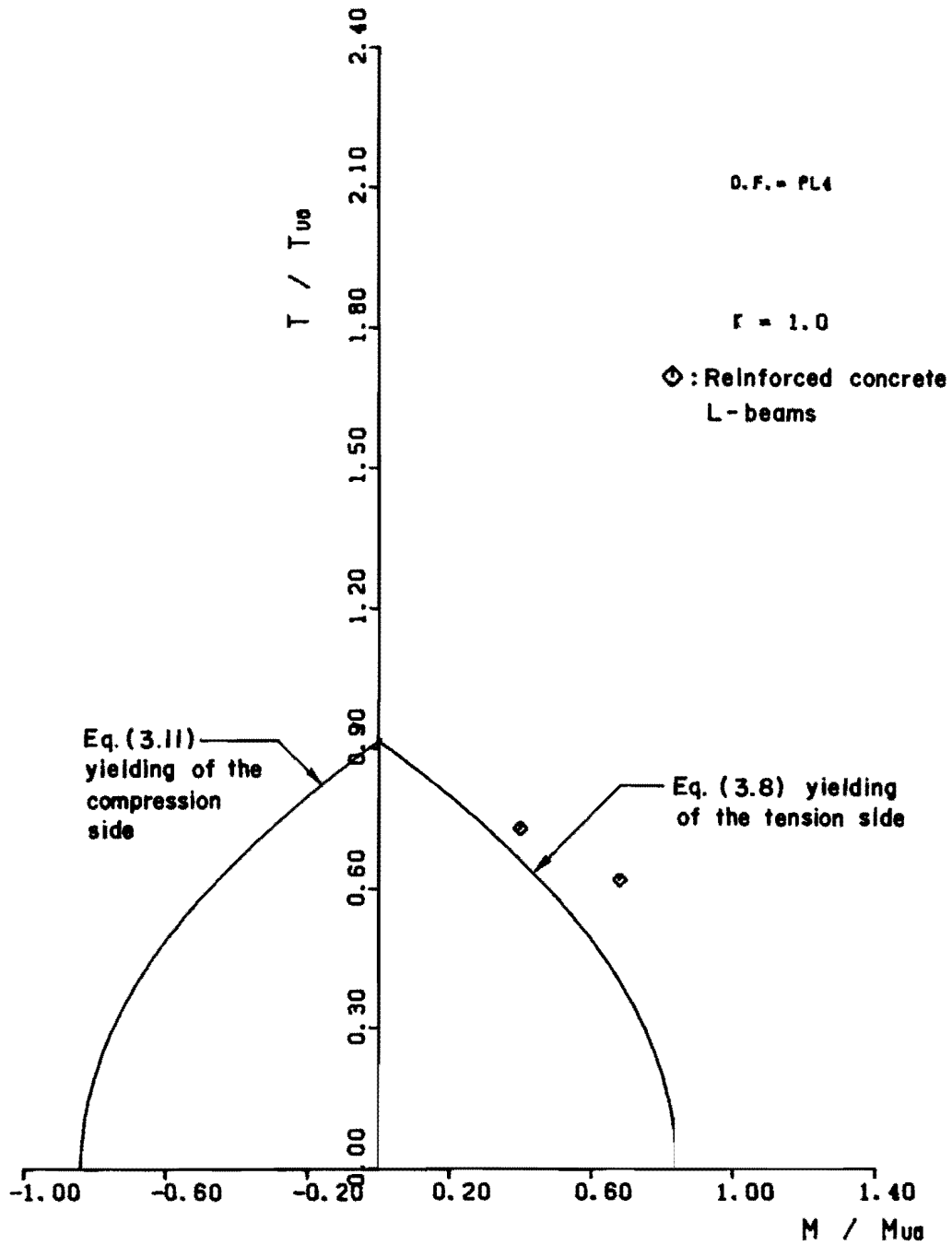


Fig. 3.12 Torsion-bending-shear interaction with $v_u/v_{u0} = 0.40$ in the case of reinforced concrete members with L-shape cross sections

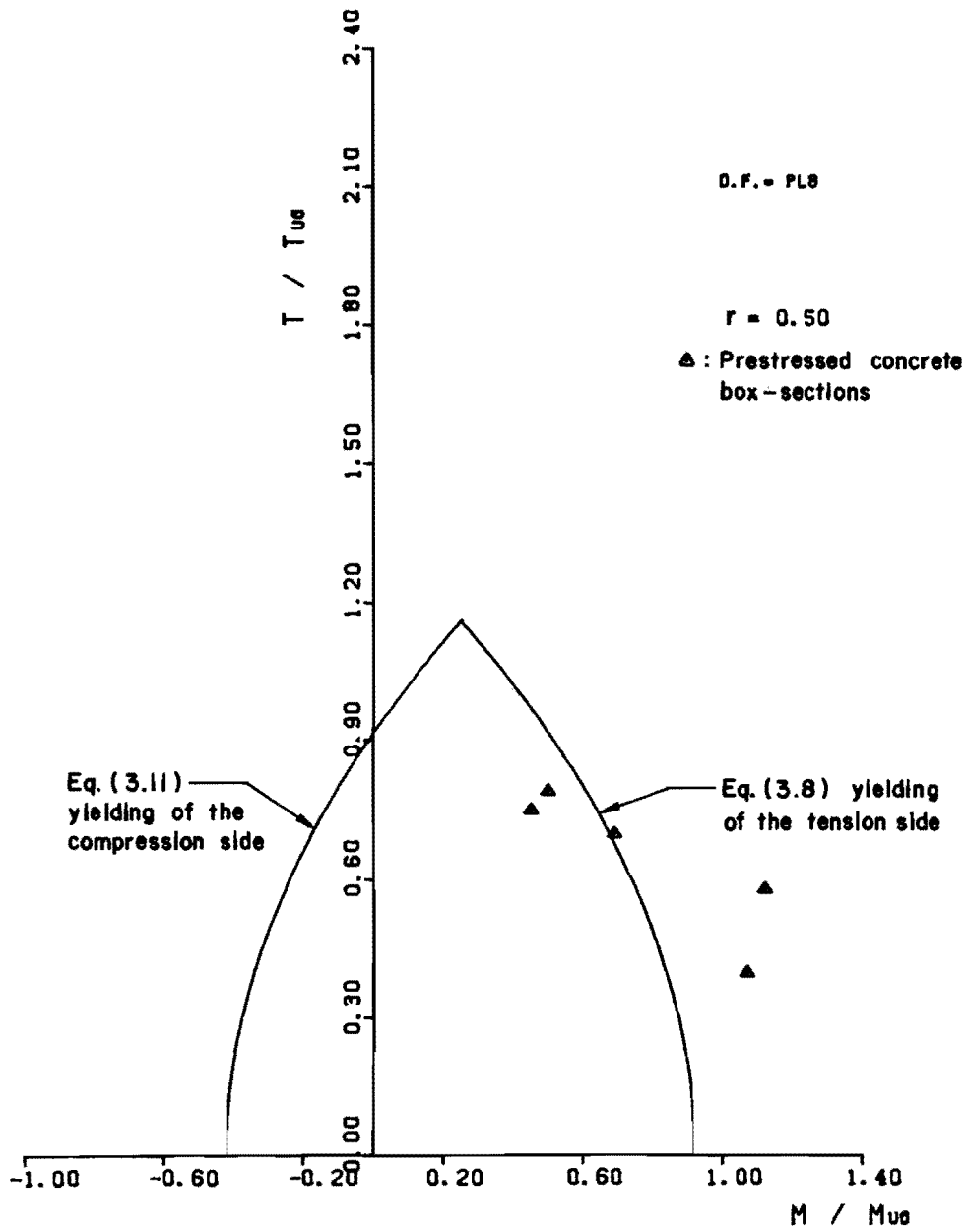


Fig. 3.13 Torsion-bending-shear interaction for $r = 0.50$ and $V_u / V_{u0} = 0.45$

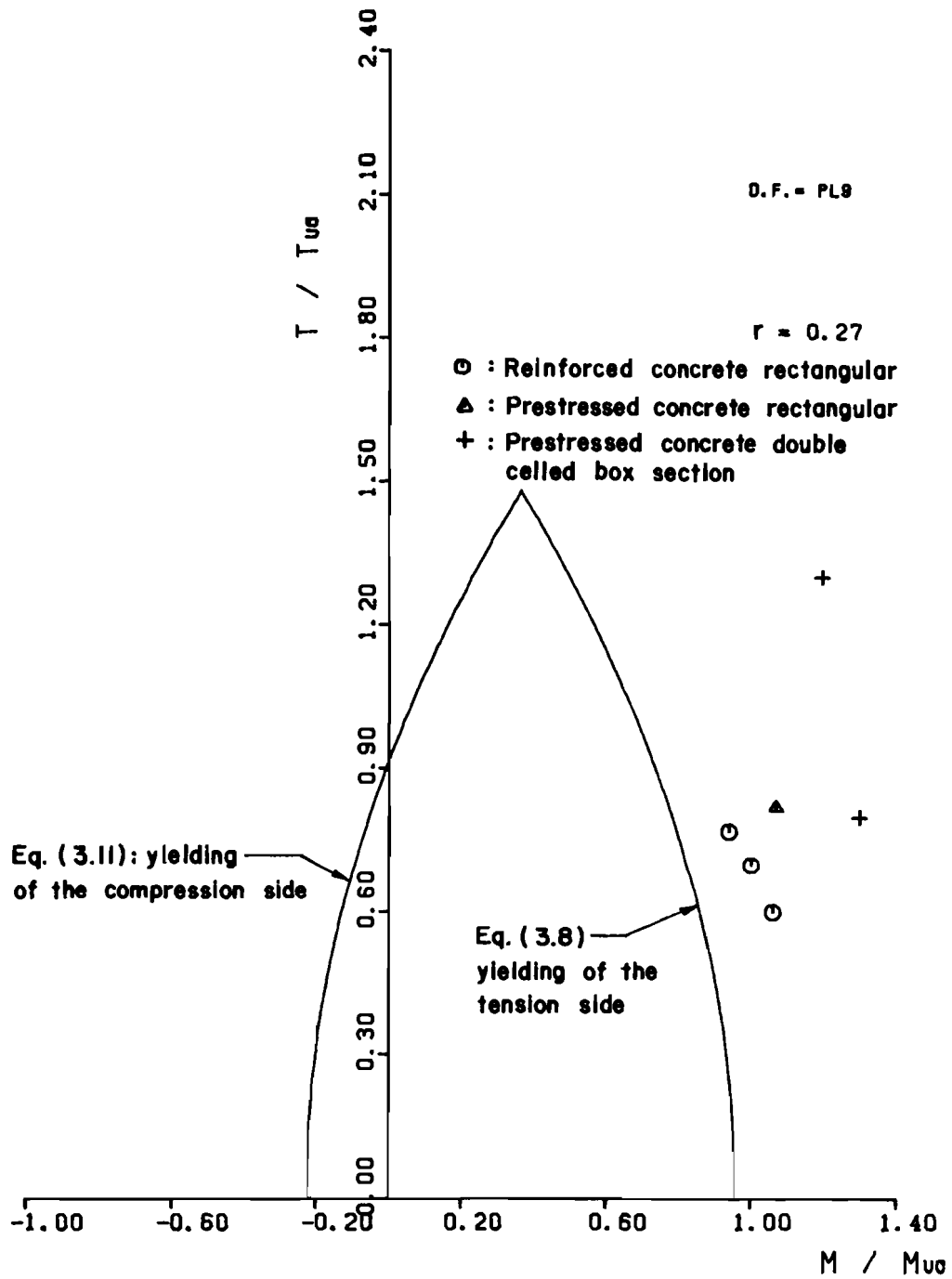


Fig. 3.14 Evaluation of the truss model using test results of reinforced and prestressed concrete members with $r = 0.27$ and $V_u / V_{u0} = 0.40$

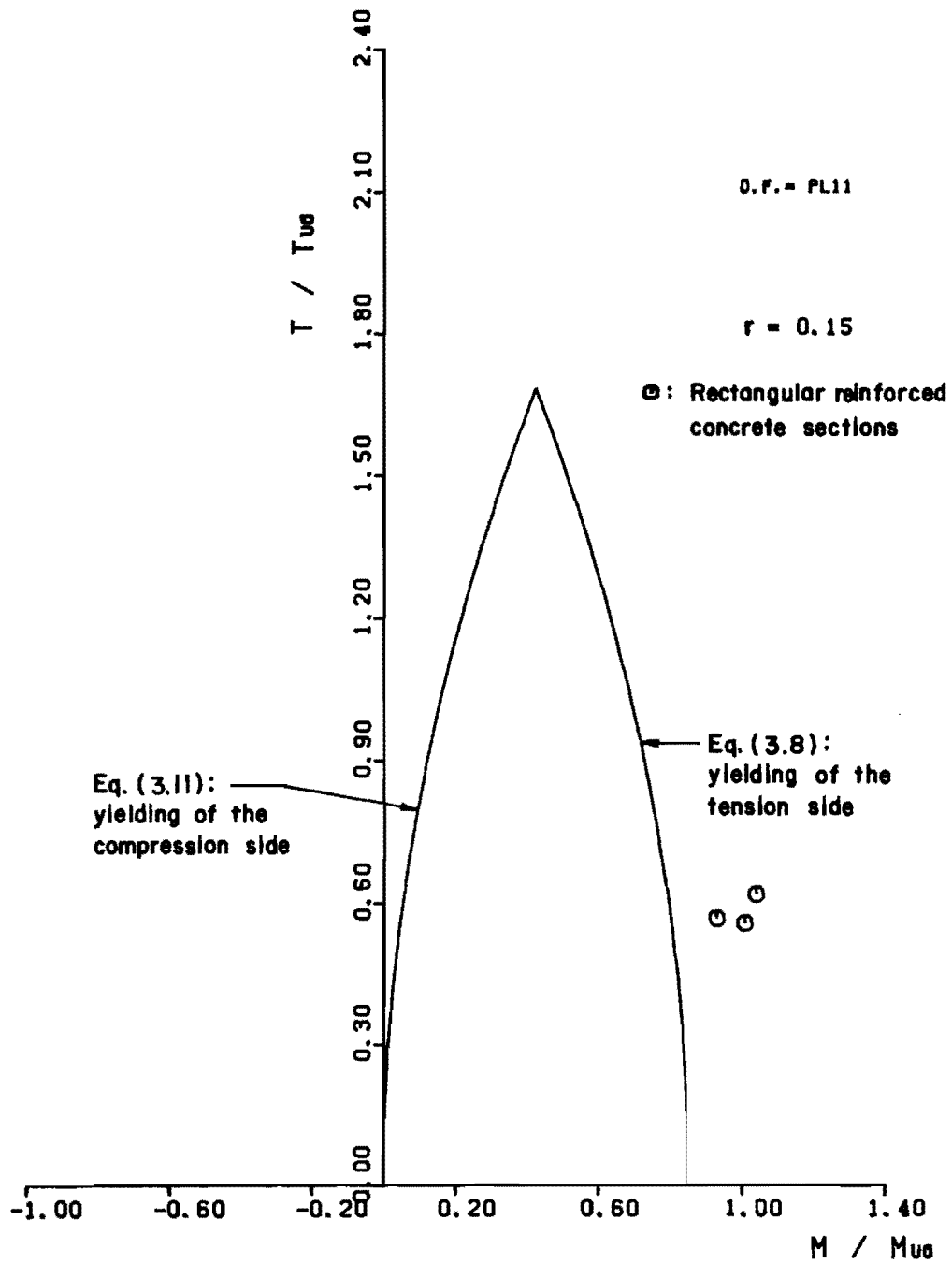


Fig. 3.15 Torsion-bending-shear interaction with $V_u / V_{u0} = 1.0$

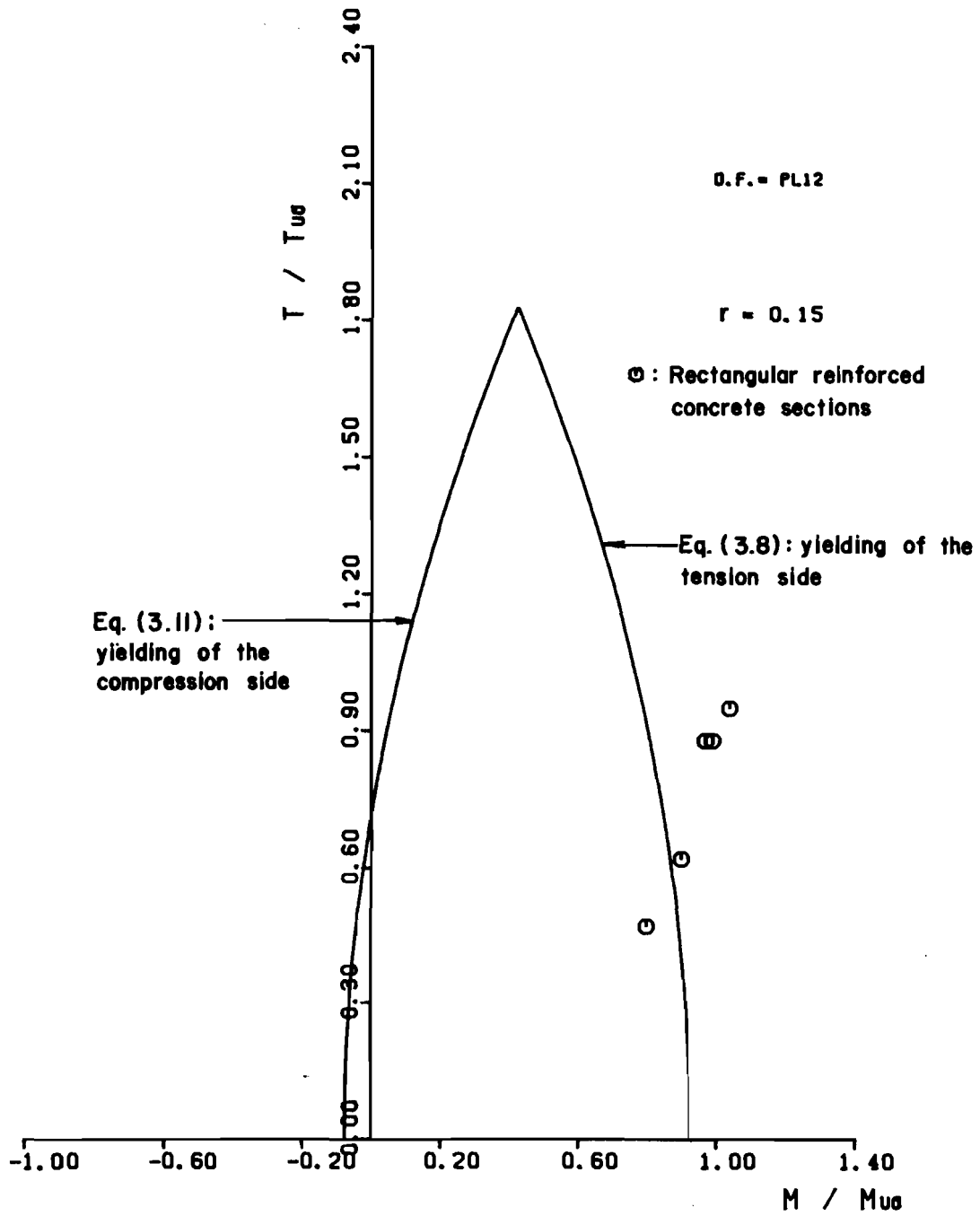


Fig. 3.16 Torsion-bending-shear interaction with
 $V_u / V_{u0} = 0.70$

double celled prestressed concrete box sections R3 and R4 from Ref. 161 in Table 3.14 are plotted in Fig. 3.14, together with the interaction Eqs. 3.8 and 3.11 for values of "r" of 0.27 and V_u/V_{u0} of 0.40. Again, there is generally good agreement, although in the case of the double celled prestressed concrete box sections assuming the shear distributed equally on each web, very conservative ($I = 1.5$) predictions are obtained.

In Figs. 3.15, 3.16, and 3.17, the effect of varying the applied shear ratio is studied using the ultimate test results of the rectangular reinforced concrete specimens A1, A2, A3, A4, A5, B1, B2, B3, B4, and B5 reported in Ref. 133 shown in Table 3.12. All the specimens were of rectangular cross section, had a value of "r" equal to 0.15, and the ratio V_u/V_{u0} varied from 1.0 to 0.45. The results show generally good and conservative agreement with only one specimen slightly inside the interaction curve ($I = 0.95$).

As a result of the comparison with actual test results carried out in this section, it can be concluded that the truss model can adequately and conservatively represent the ultimate load interaction of both prestressed and reinforced concrete members of various cross sections, provided that the section is underreinforced, and that premature failures due to poor detailing are prevented.

3.5 Bending and Shear

In this section the very important case of the ultimate load behavior of reinforced and prestressed concrete members subjected to

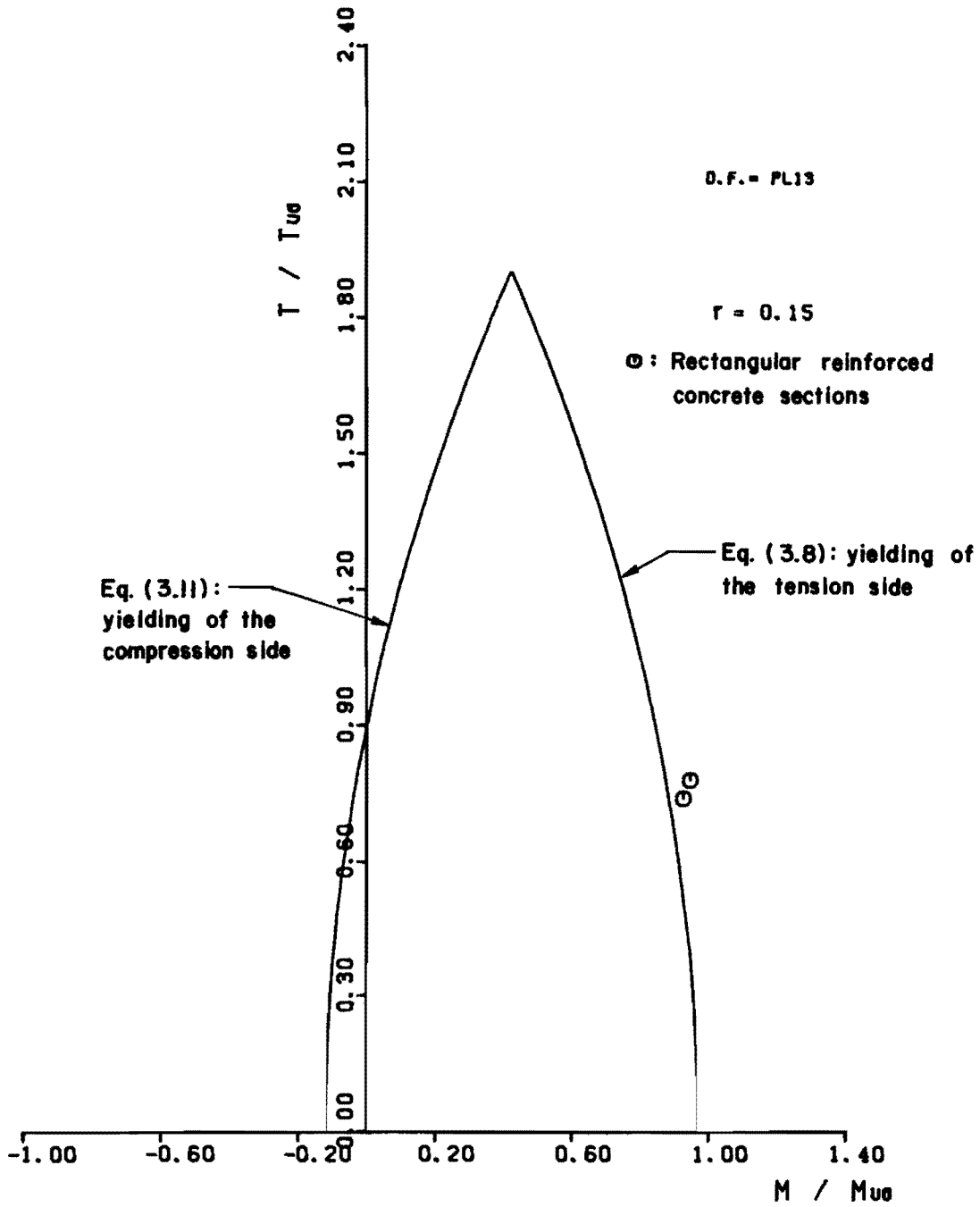


Fig. 3.17 Torsion-bending-shear interaction with $v_u / v_{u0} = 0.45$

shear and flexure as predicted by the truss model is evaluated using test data available in the American literature together with results of recent tests conducted at the Ferguson Laboratory during this research project.

The interaction equation (Eq. 3.68 of Report 248-2), which describes the ultimate load behavior of one-way flexural members subjected to bending and shear was derived as:

$$[M_u/M_{u0}] + [V_u/M_{u0}]^2 = 1 \quad (3.12)$$

Equation 3.12 was obtained from equilibrium conditions of the truss model. M_u and V_u are the ultimate load combination of bending moment and shear force. M_{u0} represents the pure bending capacity of the section.

$$M_{u0} = F_{y1} * z \quad (3.13)$$

where F_{y1} is the yield capacity in tension of the truss chord at the face of the member where the applied moment produces tension; "z" is the distance between the tension and compression chords of the truss model. V_{u0} is the shear capacity of the section, when yielding of the tension chord takes place, if the applied moment M_u is zero.

$$V_{u0} = [2F_{y1} S_y z/s]^{0.5} \quad (3.14)$$

The terms F_{y1} and "z" are those previously defined. S_y represents the stirrup force [$A_s * f_{ys}$], "s" is the center-to-center stirrup spacing.

Equation 3.12 was derived under the assumption that yielding of the truss chords where the applied moment induces tension together with yielding of the stirrups would take place at failure.

The evaluation of the truss model in the area of shear is conducted in two stages. First, it is compared with data from tests performed during this research project at the Ferguson Laboratory. Then it is compared with data from a wide group of references.

3.5.1 Comparison with Current Test Series. As has been previously discussed, the interaction equation (3.12) was derived under the assumption that both yielding of the truss chord where the applied moment induces tension and yielding of the stirrups takes place at failure. Thürlimann and Grob (72) suggested that this type of failure would take place if the section was designed assuming an angle of inclination of the diagonal strut at failure within the limits $0.5 \leq \tan \alpha \leq 2.0$.

After an extensive literature survey on tests of beams subjected to bending and shear where shear failures were reported it was found that unlike the cases of torsion, torsion-bending, or torsion-bending-shear, shear failures where yielding of both the longitudinal and transverse reinforcement were reported at failure were almost non-existent in American literature.

This situation was due to several reasons

1. A conscious decision by the researcher to design the specimen to have excessive longitudinal reinforcement to force failure in shear prior to flexural yielding.
2. Lack of adequate instrumentation to determine the strains in the longitudinal reinforcement at failure.

3. Poorly detailed specimens.

Therefore, it was decided that a series of tests on reinforced and prestressed concrete members designed using the truss model approach would be very useful to correctly evaluate the truss model in the area of bending and shear, as well as to illustrate the design procedure based on the truss model.

Schaeffer (153) conducted tests on a series of rectangular reinforced concrete beams specifically designed to illustrate the effect of assuming varied α angles on beam web reinforcement patterns using the truss model. The results of the three specimens failing in shear from that series are shown in Table 3.15.

The term $\rho_v f_y$ tabulated in column (6) represents a measure of the amount of web reinforcement in the member and is given by the web reinforcement ratio $\rho_v = A_v/b_w s$ (where A_v/s is the total area of vertical web reinforcement per inch of stirrup spacing, s , and b_w is the web width) times the yield strength, f_y of the stirrup reinforcement.

Again, as in Secs. 3.3 and 3.4, the dispersion coefficient I , tabulated in column (7) is used as an indicator to measure the accuracy of the truss model ultimate predicted values as given in the case of shear and bending by Eq. 3.12. For the three specimens shown in Table 3.15, the test obtained values are in excellent agreement with the truss predictions. The mean of the dispersion coefficient I is 1.05 and the standard deviation 0.10.

The detailing of the steel reinforcement provided in these members (RL-0.50, RL-1.25, and RH-0.50) is shown in Fig. 3.18. Note the

Tests reported by Schaeffer (153) on reinforced concrete rectangular beams

(1) Member ID	(2) V _{uo} (Eq. 3.14) (kips)	(3) V _{test} (kips)	(4) M _{uo} (Eq. 3.13) (in-kips)	(5) M _{test} (in-kips)	(6) ρ _v f _y (psi)	(7) I	(8) Level of Prestress σ/f' _c
RL-0.50	136	76	3835	2736	310	1.02	0.0
RL-1.25	205	78	3483	2808	400	0.96	0.0
RH-0.50	170	105	4535	3780	400	1.16	0.0
				X =		1.05	
				S =		0.10	

Table 3.15 Data on reinforced concrete one-way members failing in shear

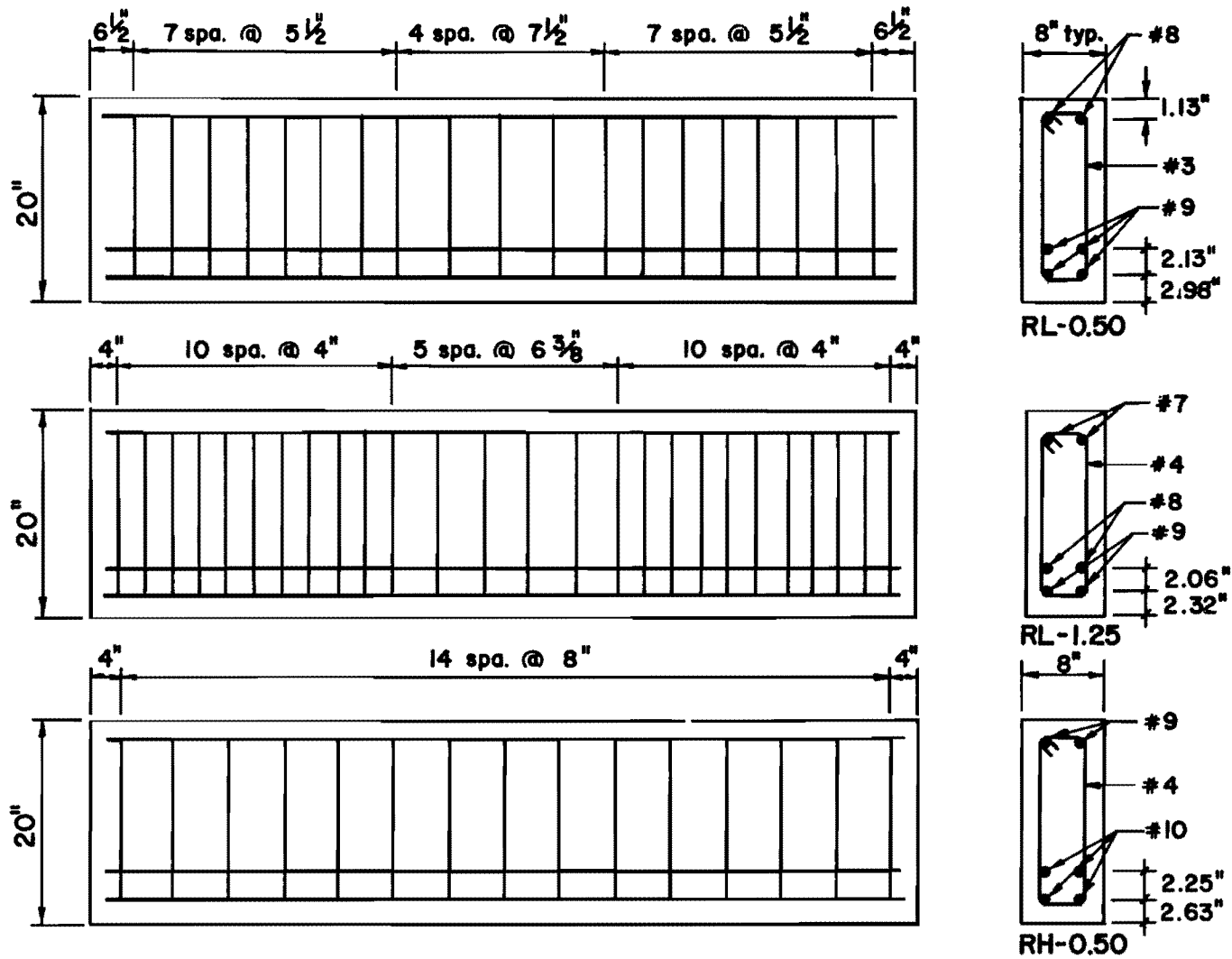


Fig. 3.18 Reinforcing details of members RL-0.50, RL-1.25, and RH-0.50

wide variation in stirrup reinforcement and in longitudinal tension reinforcement in these specimens which were originally designed for identical loads.

The specimens RL-0.50 and RL-1.25 were tested with equally applied concentrated loads at the third points. The specimen labeled RH-0.50 was subjected to a center point loading.

The member RL-0.50 was designed assuming $\tan\alpha$ equal to 0.50. In this specimen yielding of the stirrups in the failure zone was reached at about 95% of the ultimate load. The maximum average strain in the longitudinal reinforcement in the constant moment region corresponded to a stress of 52 ksi, which was about 77% of the yield stress of this reinforcement. Photographs of the crack patterns appear in Fig. 3.19.

The specimen RL-1.25 was designed assuming a value of $\tan\alpha$ of 1.25. In specimen RL-1.25, although the longitudinal reinforcement apparently did not yield, the strain measurements indicated an average stress on the bars in the constant moment region of 60 ksi which corresponded to about 90% of its yield strength. Strain measurements in the stirrups at the failure region indicated that this reinforcement was stressed up to 46 ksi on the average, which represented 73% of the yield stress. Photographs of the crack patterns are shown in Fig. 3.20.

The specimen RH-0.50 was designed assuming a $\tan\alpha$ of 0.50. This specimen failed due to shear, with the transverse reinforcement yielding, and the longitudinal reinforcement below yielding. The stirrups yielded at 93% of the ultimate load. Strain measurement in the longitudinal reinforcement indicated a stress of 28 ksi equivalent to

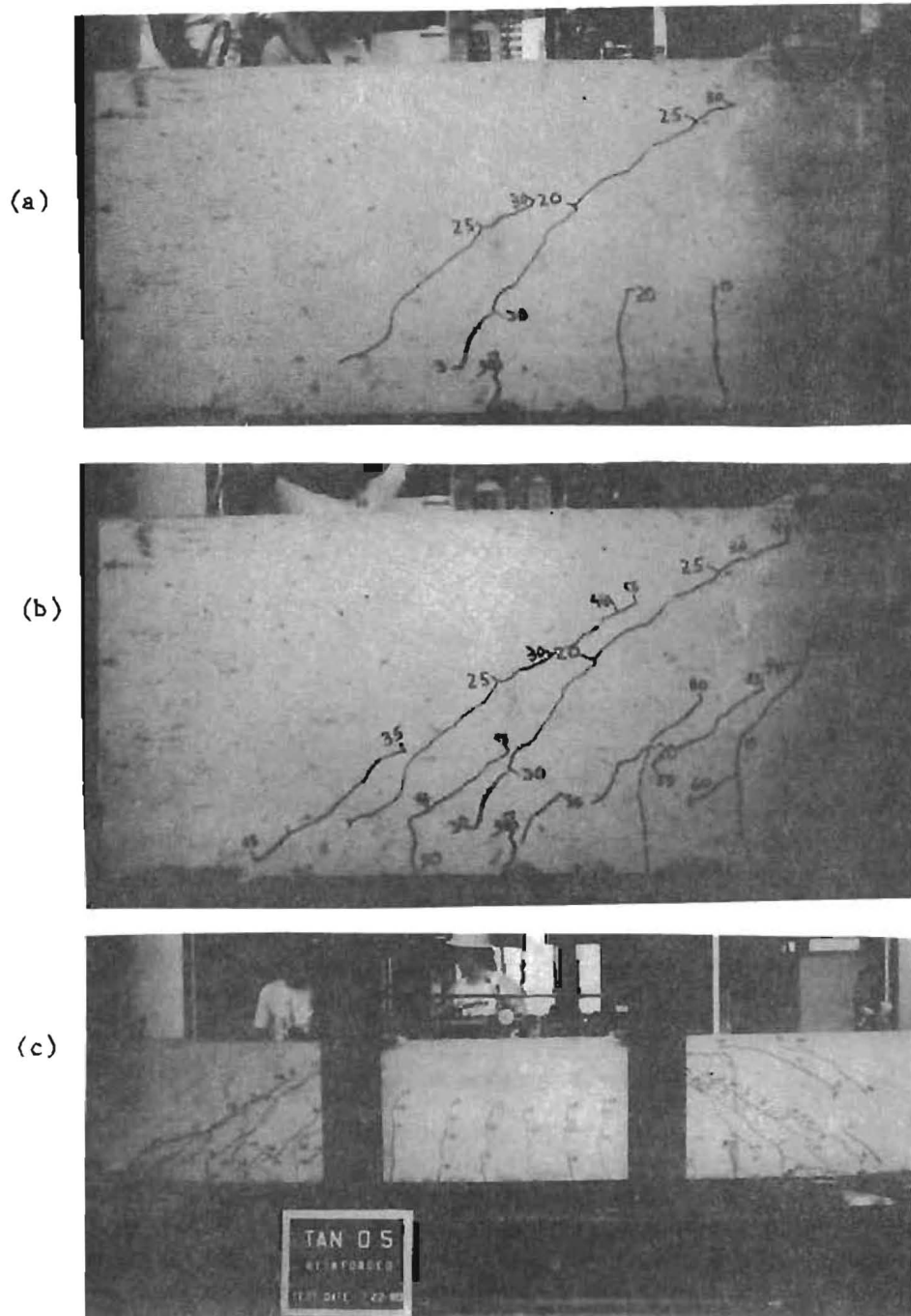


Fig. 3.19 Crack patterns of beam RL-0.50 at load stage of 60 kips, 100 kips, and failure (top to bottom)

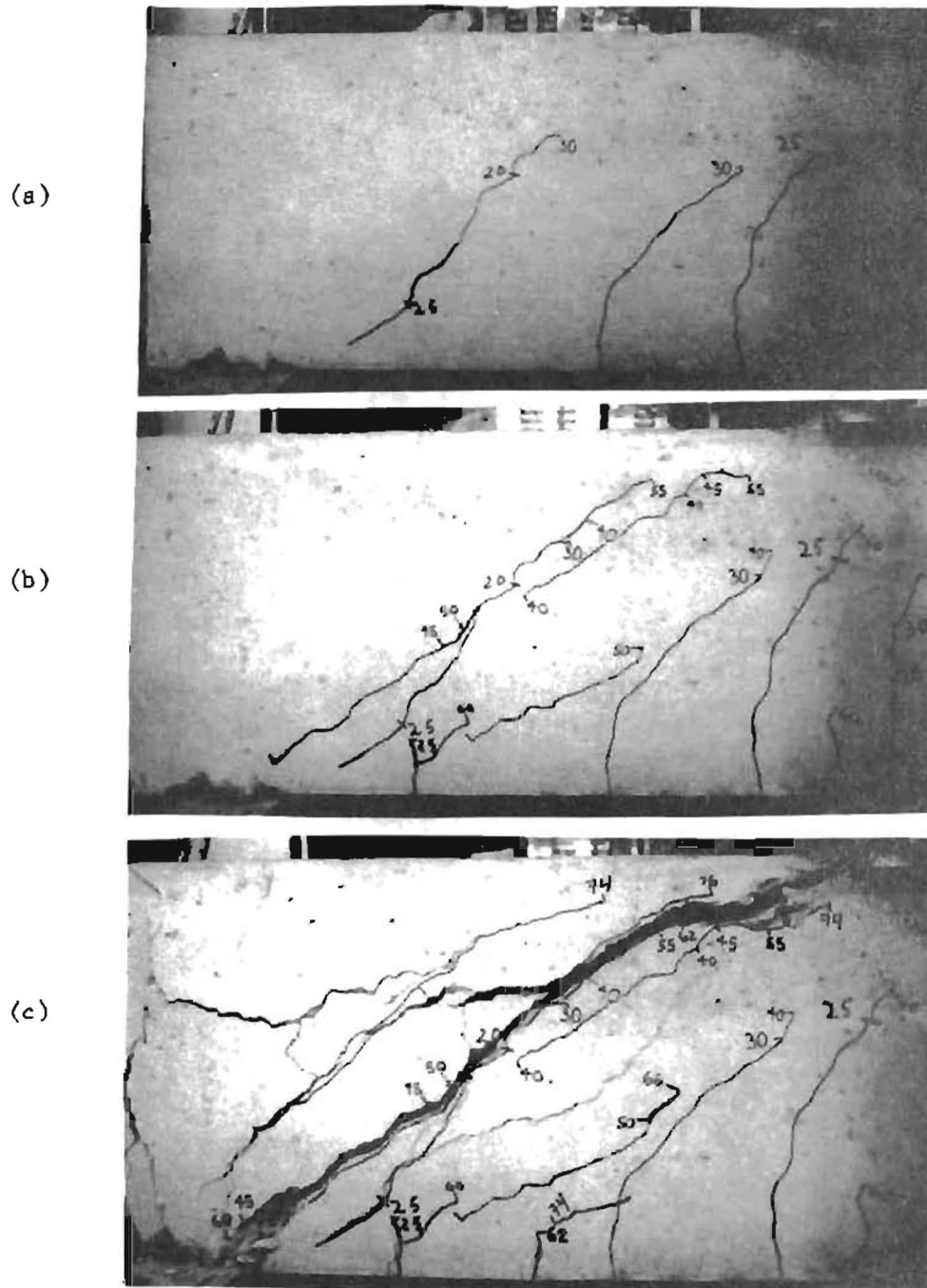


Fig. 3.20 Crack patterns of beam RL-1.25 at load stages of 60 kips, 100 kips, and failure (top to bottom)

43% of its yield point. Photographs of the crack patterns are shown in Fig. 3.21.

The load-deflection curves for RL-0.50 and RL-1.25 are shown in Fig. 3.22. The load-deflection curve for RH-0.50 is shown in Fig. 3.23.

In Fig. 3.24, a comparison is shown between the predicted ultimate load behavior obtained using the interaction Eq. 3.12 and the ultimate test values of the specimens RL-0.50, RL-1.25 and RH-0.50 given in Table 3.15.

Very good agreement was obtained between the test values and the truss model predictions as shown by the values of the dispersion index I in Table 3.15 and by Fig. 3.24. This good correlation was achieved in spite of the fact that yielding of the longitudinal reinforcement did not occur in two of the members at failure. This suggests that in these cases, provided the member is properly designed such as the ones presented in Table 3.15 and provided either stirrups or longitudinal reinforcement yielded prior to failure the truss model would adequately predict the ultimate load capacity.

A properly designed member should meet the following general requirements:

1. The section must be underreinforced for flexure, i.e. yielding of the longitudinal reinforcement must take place prior to crushing of the concrete in the compression zone.
2. Failures due to web crushing should be avoided by adequately checking the compression stresses in the diagonal strut of the truss model.
3. The angle of inclination of the diagonal strut at failure must be chosen within the prescribed limits $0.5 < \tan\alpha < 2.0$.

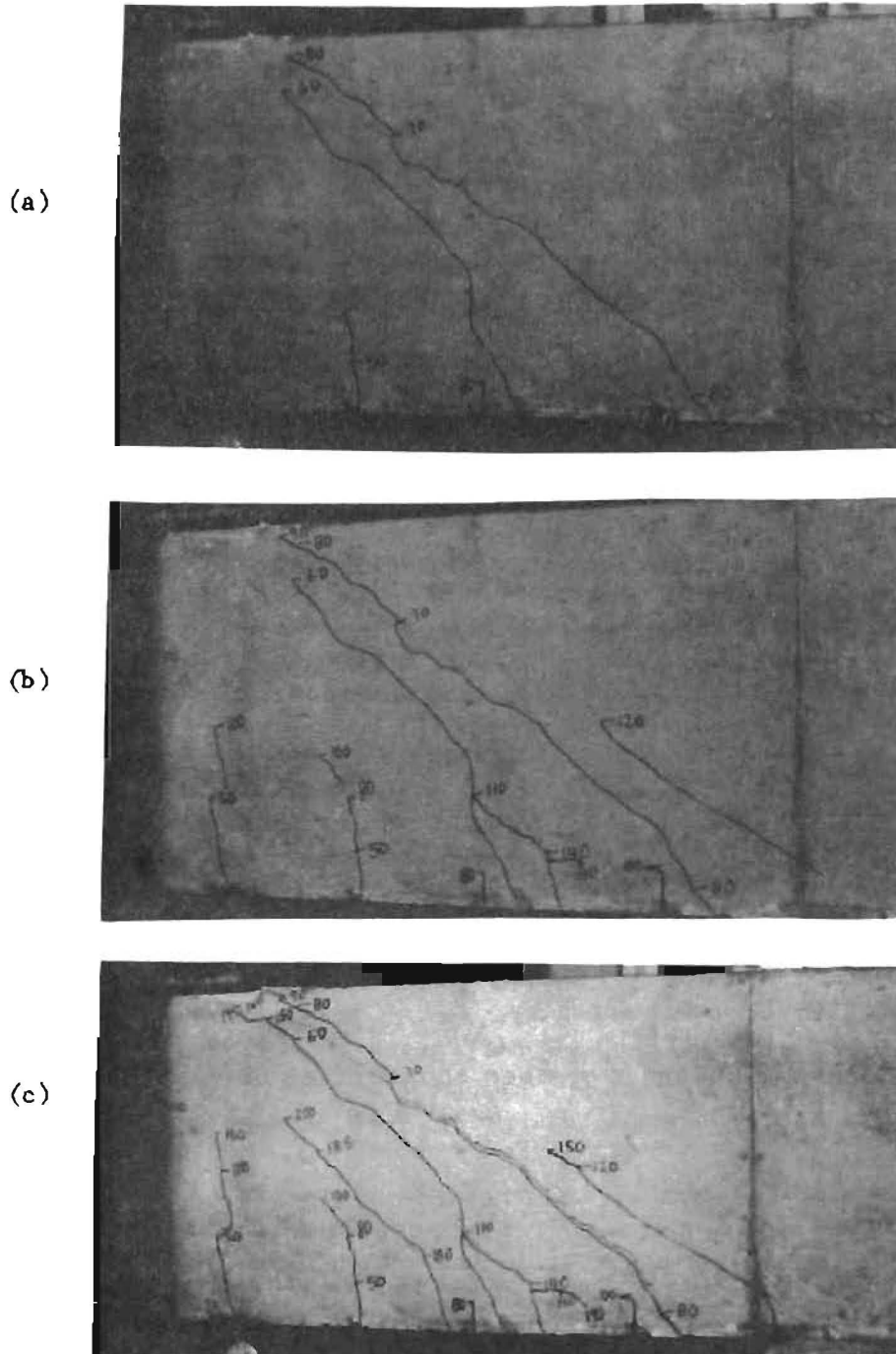


Fig. 3.21 Crack patterns of beam RH-0.50 at load stages of 80 kips, 140 kips, and failure (top to bottom)

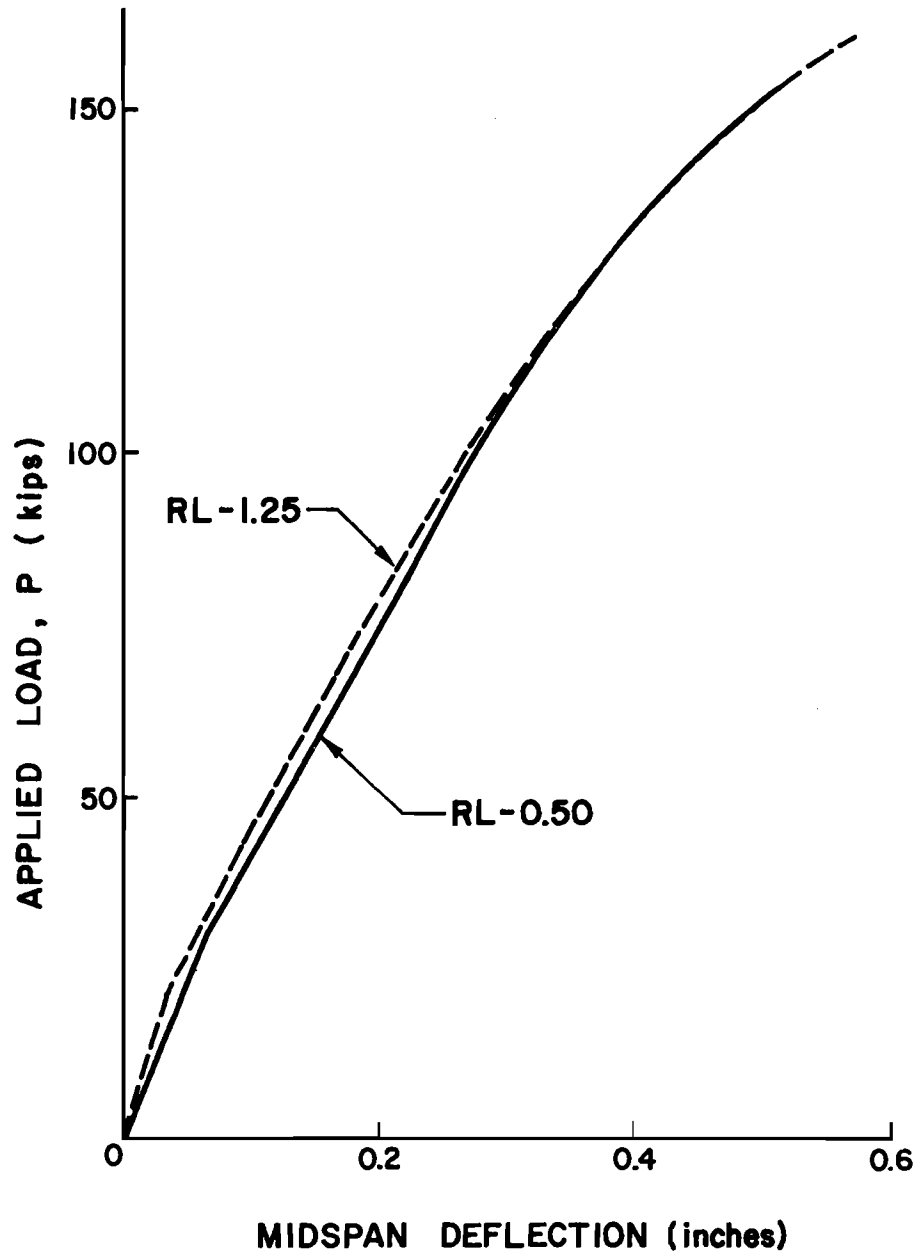


Fig. 3.22 Load-deflection curves of beams RL-0.50 and RL-1.25

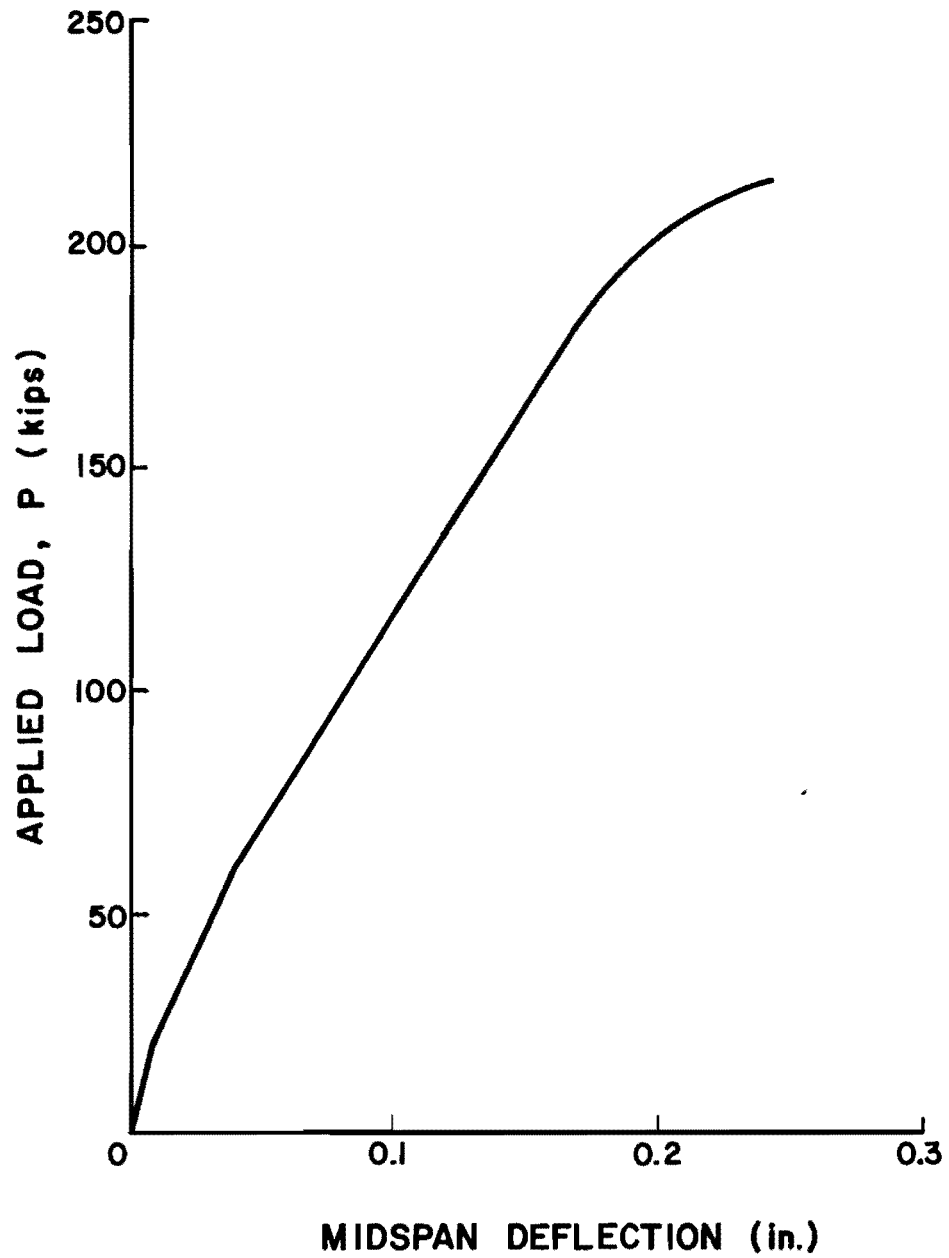


Fig. 3.23 Load-deflection curve of beam RH-0.50

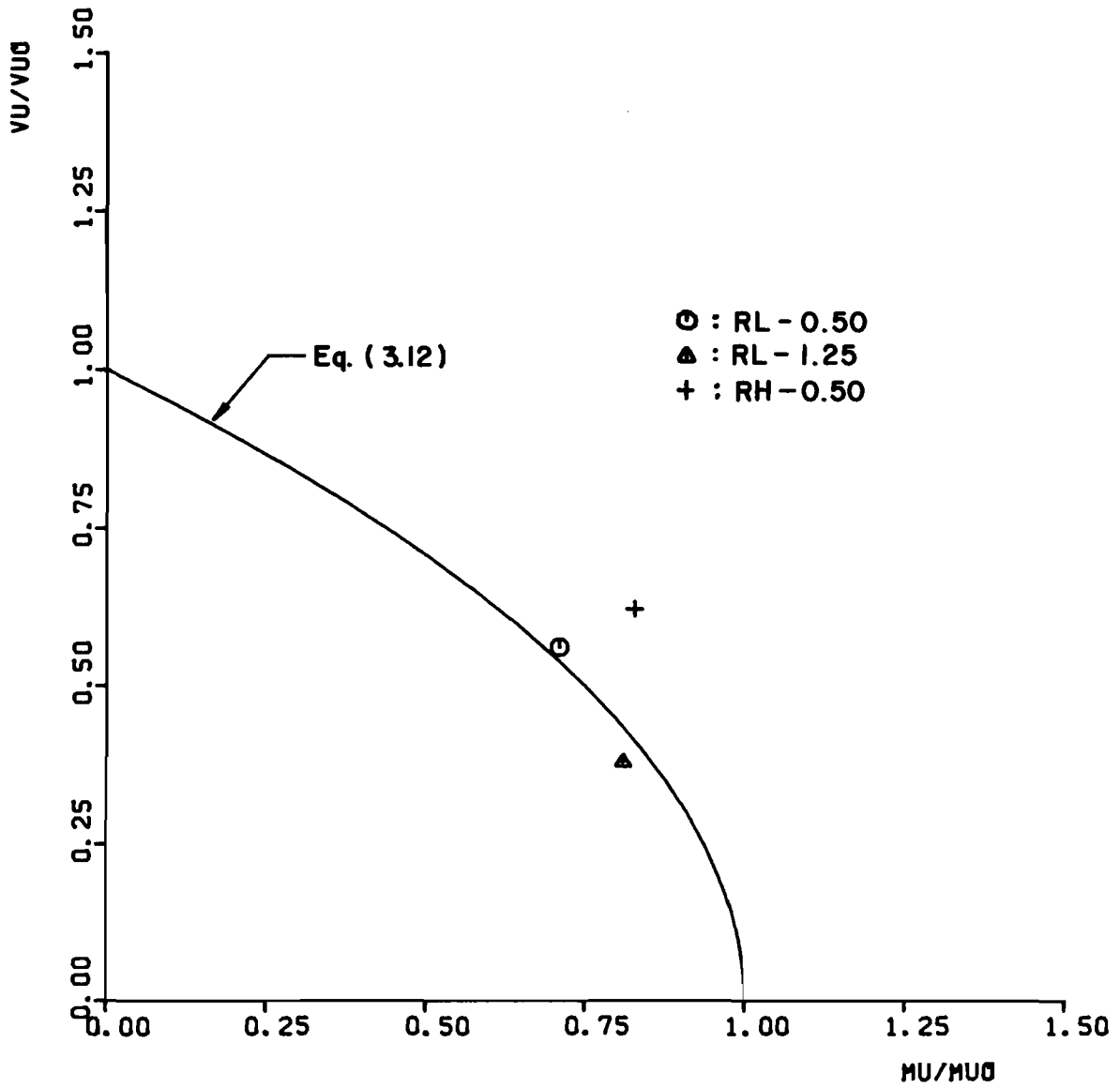


Fig. 3.24 Predicted ultimate bending and shear interaction using the truss model

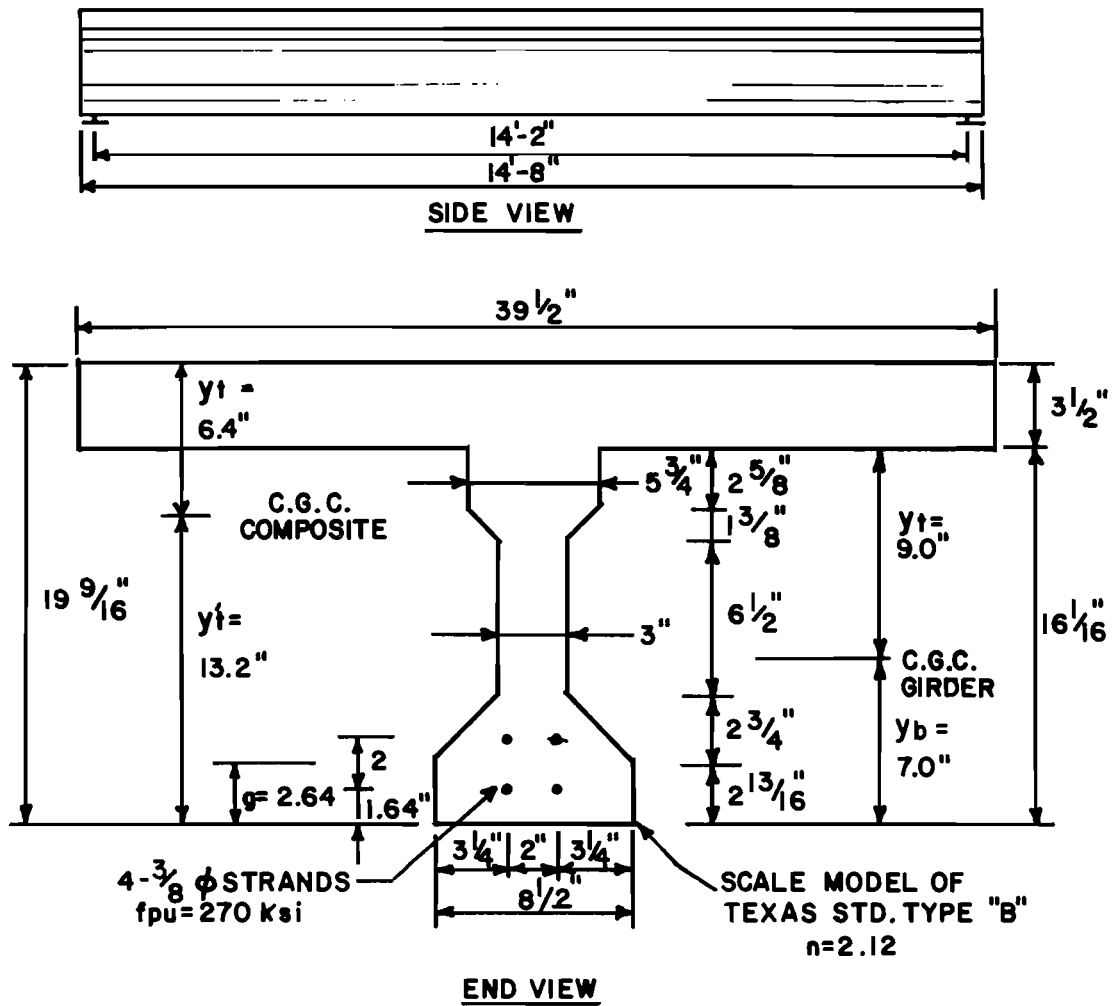
4. Premature failures due to inadequate detailing must be prevented.

In a different phase of this research project, a series of tests on prestressed concrete I-beams with web reinforcement and a composite slab were conducted. The specimens were about half-scale models of the Texas Standard Type B girder. These members were subjected to a uniformly distributed load. Details of all the specimens as well as the loading scheme are reported by Castrodale (50). In this evaluation of the truss model ultimate load predictions, only the results of those specimens labeled 0.40A, 0.40B and 0.45, which failed in shear, are considered.

In all the specimens of this series the prestressed reinforcement consisted of 4-3/8 in. diameter seven-wire strands of Grade 270. In addition, nonprestressed longitudinal tension and compression reinforcement was provided. The reinforcement details of the specimens 0.40A, 0.40B and 0.45 are shown in Figs. 3.25 and 3.26.

The test results of the specimens 0.40A, 0.40B and 0.45 are presented in Table 3.16. In Table 3.16, the values of the shear force and the flexural moment at ultimate, together with V_{UO} and M_{UO} , are shown for different sections along the uniformly loaded span length of the member.

Specimen 0.40A was designed assuming a $\tan\alpha$ of 0.40. In this member, yielding of the stirrup reinforcement was reached at about 75% of the ultimate load. The maximum average strain in the longitudinal nonprestressed tension reinforcement indicated that in the failure zone this reinforcement reached its yield strength. In the prestressed



MEMBER PROPERTIES

	Girder	Slab	Composite	
			Total	Transformed
Area =	80.3 in ²	138.2 in ²	218.5 in ²	186.7 in ²
I =	2144 in ⁴	141 in ⁴	-----	7620 in ⁴
Wt. =	84 plf	149 plf	233 plf	-----
f' _c =	5000 psi	3000 psi	-----	5000 psi

Fig. 3.25 Details of the cross section

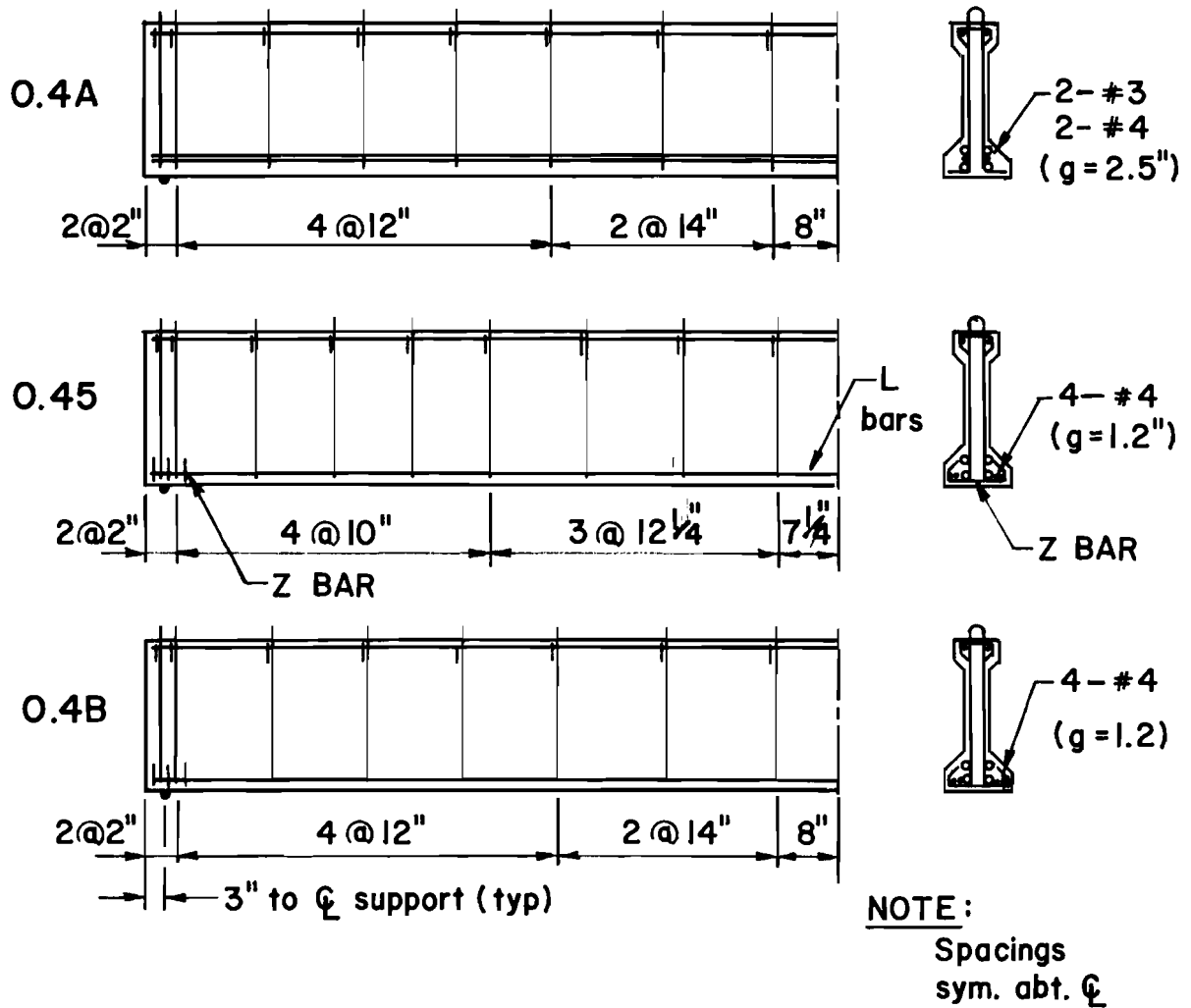


Fig. 3.26 Details of the nonprestressed longitudinal and transverse reinforcements

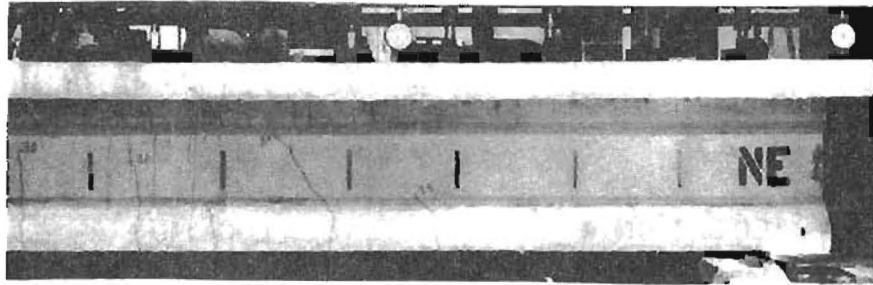
(1) Author Reference	(2) Member ID	(3) Section from support (ft)	(4) Vuo (Eq. 3.14) (kips)	(5) Vtest (Kips)	(6) Huo (Eq. 3.13) (in-kip)	(7) Mtest (in-kips)	(8) ρ_{vfy} (ksi)	(9) Level of Prestress $\sigma/f'c$
Castrodale (50)	0.40A	support	49.40	51.60	2232	0.0	0.18	0.10
		1.70	49.40	39.30		926.0	0.18	
		3.40	49.40	26.90		1600.0	0.18	
		5.10	45.70	14.50		2021.0	0.16	
		45.70	0.0			2194.0	0.16	
	0.40B	support	52.50	54.80	2522	0.0	0.18	0.13
		1.75	52.50	41.20		1008.0	0.18	
		3.50	52.50	27.70		1731.0	0.18	
		5.25	48.60	14.20		2171.0	0.16	
		48.60	0.0			2327.0	0.16	
	0.45	support	57.70	60.0	2537	0.0	0.22	0.12
		1.56	57.70	46.80		1003.0	3.22	
		3.13	57.70	33.50		1757.0	0.22	
		4.70	52.00	20.30		2263.0	0.18	
		6.26	48.60	7.00		2518.0	0.16	
		48.60	0.0		1553.0	0.16		

Table 3.16 Data from specimens 0.40A, 0.40B, and 0.45

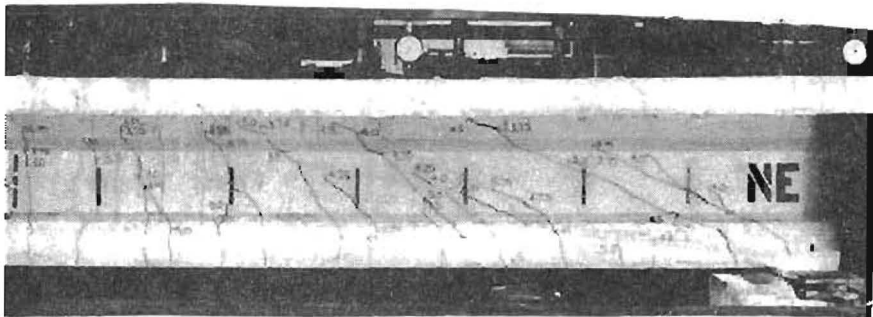
reinforcement the maximum average strain corresponded to a stress of 220 ksi, which was 85% of its yield strength. Photographs of the crack patterns appear in Fig. 3.27. The markings shown in the photographs in Fig. 3.27a,b,c correspond to load levels in kips/ram. In this specimen 16 rams were used, distributed over the 14.2 ft. clear span of the member. Thus, the load levels shown in Fig. 3.27a,b,c would have to be multiplied by 1.127 in order to obtain loads in kips/foot. The crack patterns shown in Figs. 3.28 and 3.29 correspond directly to loads in kip/foot.

As can be seen from Fig. 3.27c, at failure there was extensive damage over the north end region of the member. This suggested an anchorage type failure. Yielding of the transverse and longitudinal nonprestressed tension reinforcement was reached prior to failure. The transverse reinforcement yielded at about 75% of the ultimate load, fully developing the shear capacity of the member. Thus, it was concluded that member 0.40A had suffered a shear type failure in which the high shear stresses and the associated large cracking and shear deformations at the end region of the member had caused the concrete to spall off, but not before the member had reached its ultimate shear capacity.

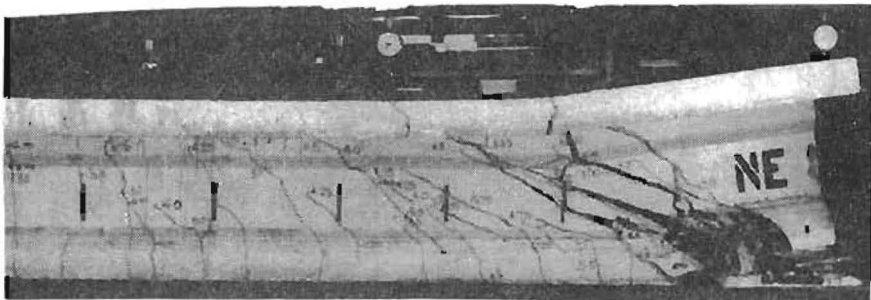
In specimen 0.40B the transverse reinforcement was designed assuming a $\tan\alpha$ of 0.40. However, an excess amount of longitudinal nonprestressed tension reinforcement was provided (see Fig. 3.26). This change was introduced to study the effects of the presence of excess longitudinal reinforcement on the high shear region of the member by



(a)

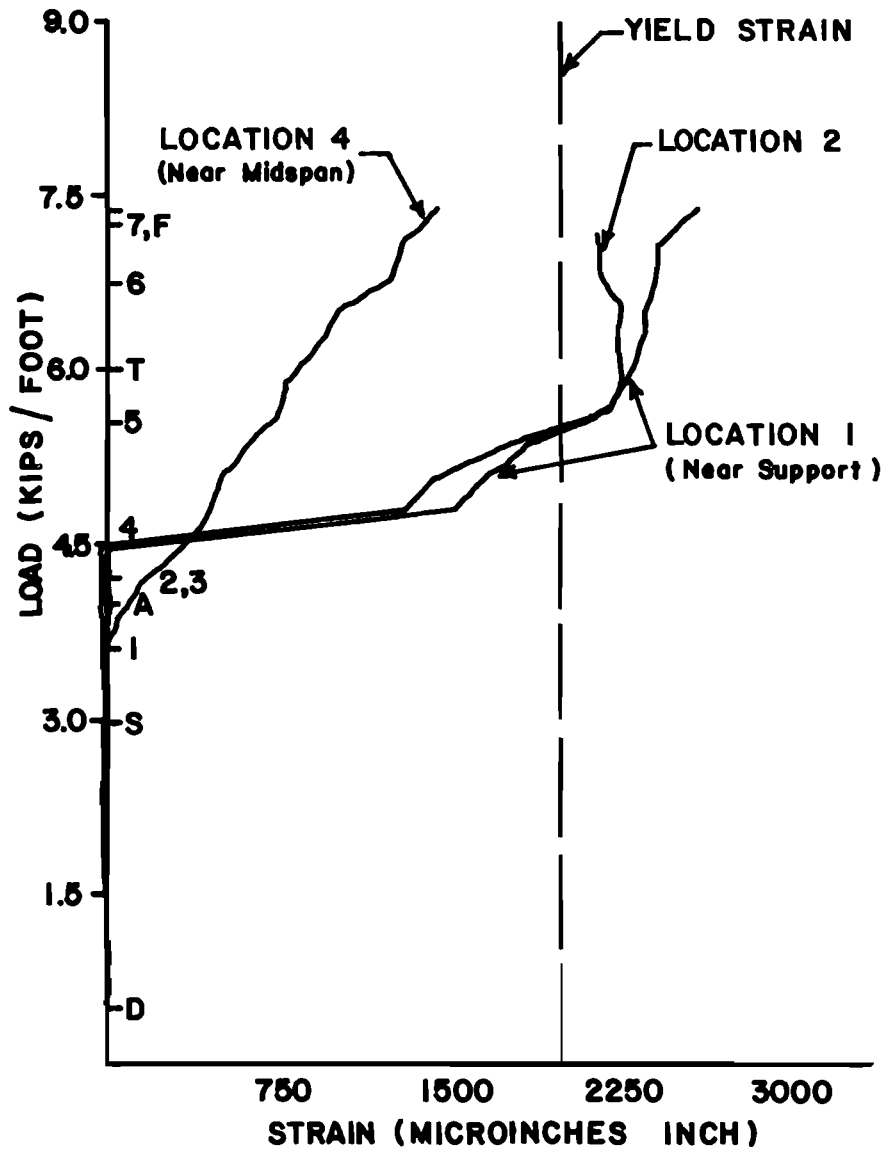


(b)



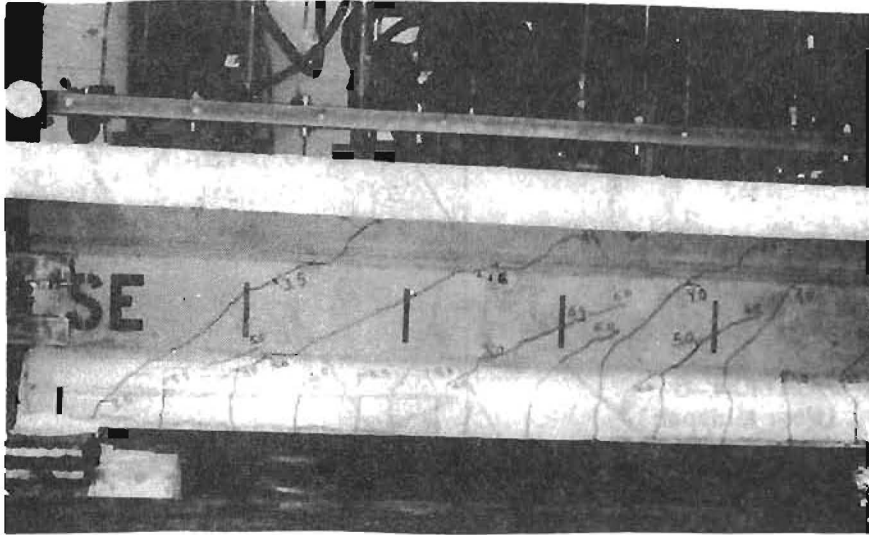
(c)

Fig. 3.27 Crack patterns of beam 0.40A at load stages of 4.2 k/f, 6.7 k/f, and failure (top to bottom)

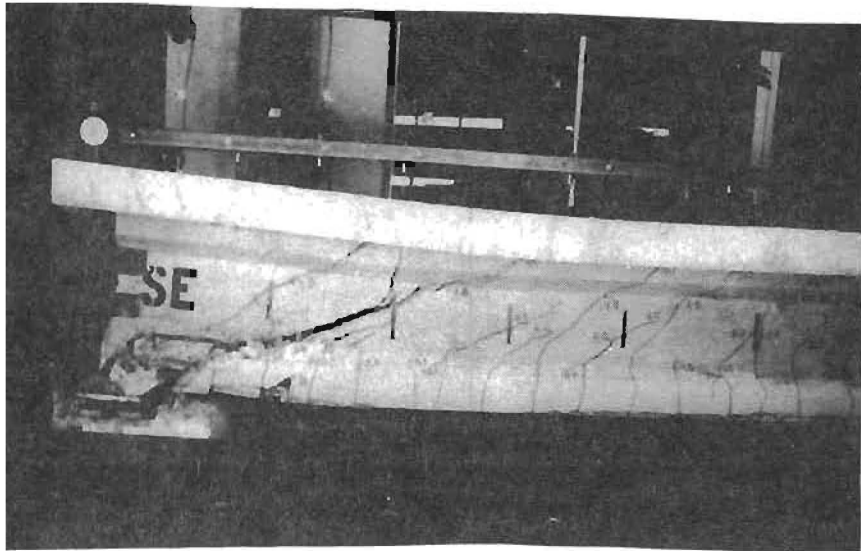


(d) Strain in stirrups for north half of specimen 0.40A

Fig. 3.27 (Continued)

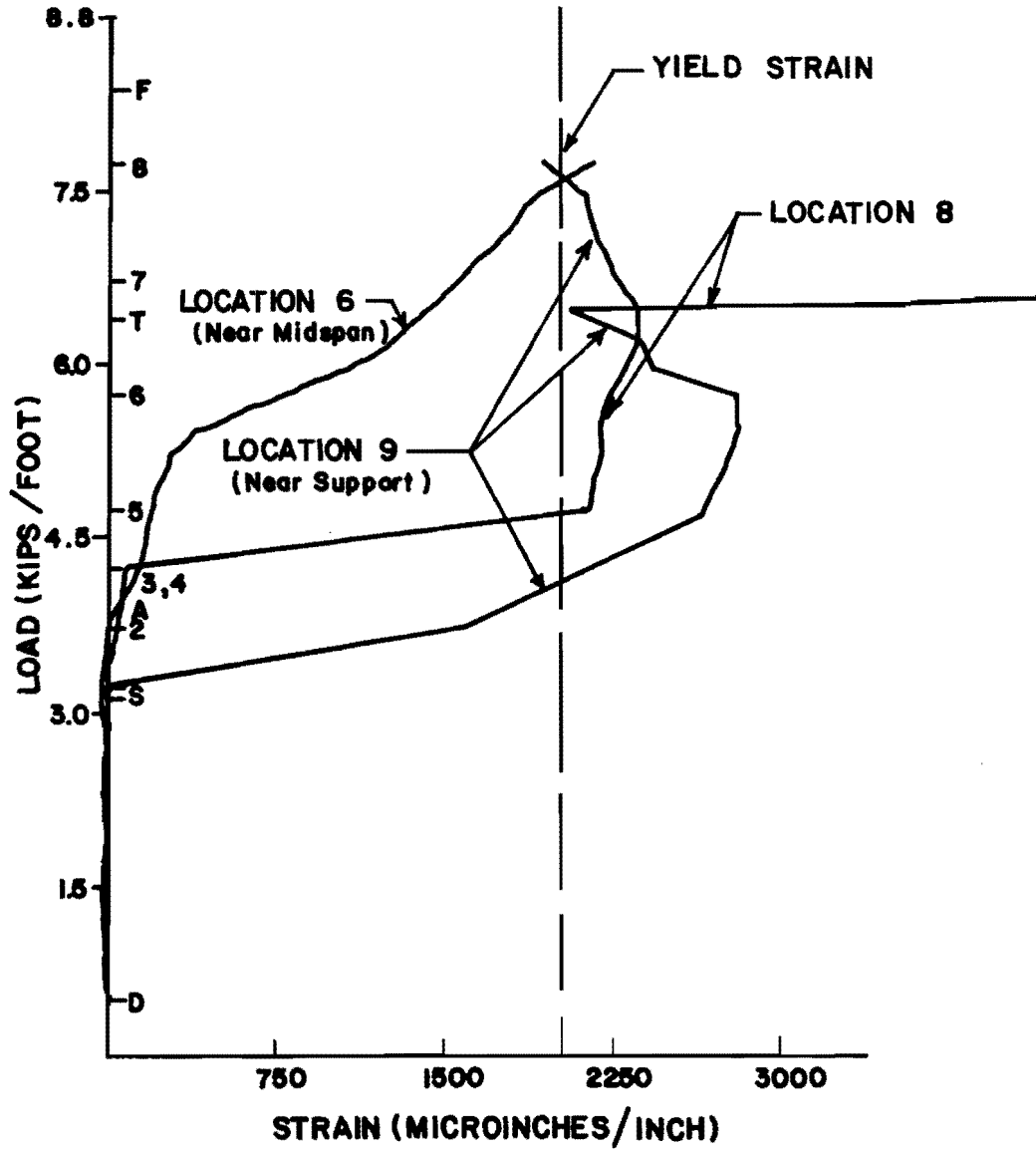


(a)



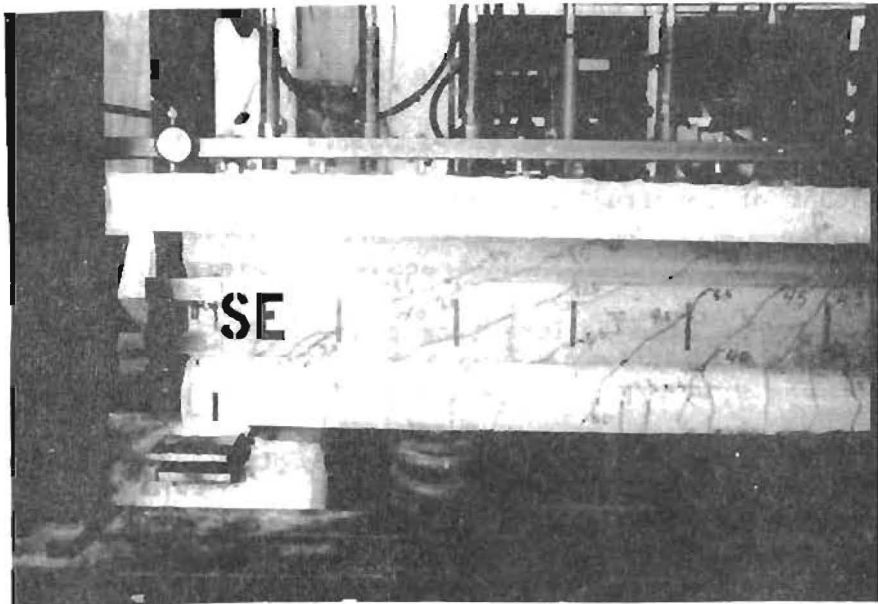
(b)

Fig. 3.28 Crack patterns of beam 0.40B at load stages of 6.7 k/f and failure (top to bottom)

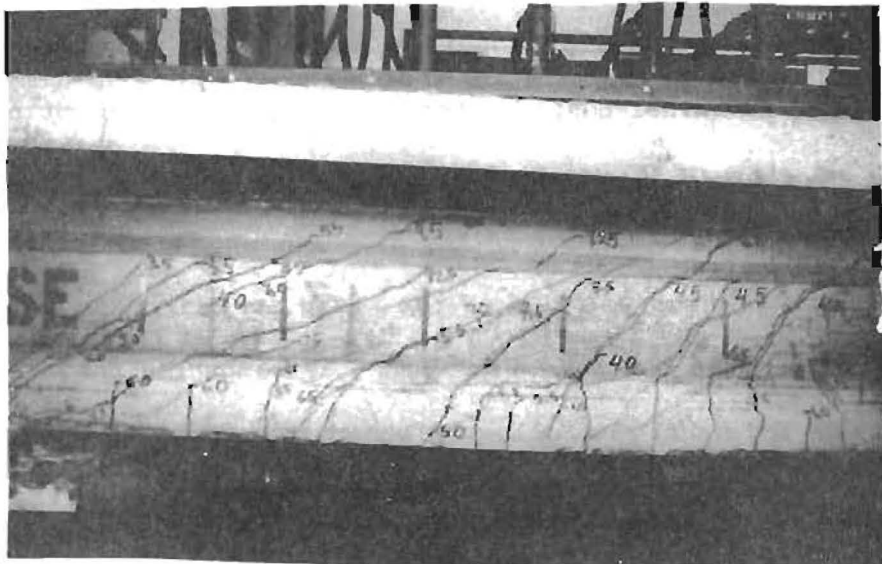


(c) Strain in stirrups for south half of specimen 0.40B

Fig. 3.28 (Continued)



(a)



(b)

Fig. 3.29 Crack patterns of beam 0.45 at load stages of 7.5 k/f and failure (top to bottom)

comparing the results of this test with those obtained from specimen 0.40A. In this specimen, first yielding of the stirrup reinforcement in the failure zone was reached at about 55% of the ultimate test load. The extra amount of longitudinal nonprestressed steel in 0.40B caused a general yielding at failure of the transverse reinforcement at the SE region of the member where failure took place (see Fig. 3.28a,b,c). The failure load was 7.73 k/F in specimen 0.40B. On the other hand, in specimen 0.40A, which had a smaller amount of longitudinal nonprestressed steel than 0.40B, the stirrup reinforcement in the failure zone did not achieve the same general yielding at failure (see Fig. 3.27a,b,c,d). Member 0.40A failed at a load of 7.29 k/F which was less than the failure load of specimen 0.40B. The maximum average strain in the longitudinal nonprestressed tension reinforcement produced a stress at ultimate of 37 ksi or 47% of its actual yield strength. The maximum average strain recorded in the prestressing strands indicated a stress of 182 ksi, which was 70 % of the yield stress. Photographs of the crack patterns are shown in Fig. 3.28. By comparing the results of specimens 0.40A and 0.40B the following observations can be made:

1. The increase in longitudinal steel while maintaining the amount of web reinforcement constant increased the ultimate load capacity and stiffness of specimen 0.40B (see Fig. 3.30).
2. The excess longitudinal nonprestressed steel prevented this reinforcement from reaching its yield strength.

As can be seen in Fig. 3.28b, although failure took place at the south end of the member, the same extensive damage of the end region was observed. However, since yielding of the transverse reinforcement took

place prior to failure, the same comments made in the case of specimen 0.40A apply in this case.

The specimen labeled 0.45 was designed assuming a $\tan \alpha$ of 0.45. The maximum average strain in the transverse reinforcement indicated that first yielding of the stirrup reinforcement in the failure zone was reached at about 88% of the ultimate test load. In the longitudinal nonprestressed tension steel, the maximum average strain recorded in the failure zone indicated yielding of this reinforcement at failure. The stress in the prestressing strands reached 216 ksi, which was 84% of its yield strength. Photographs of the crack patterns are shown in Fig. 3.29.

In specimen 0.45 several significant changes were made. Increasing the design angle of inclination of the diagonal compression strut to a value of $\tan \alpha$ of 0.45 produced a closer stirrup spacing while the longitudinal reinforcement did not have to be increased as compared to specimen 0.40B (see Fig. 3.26). This undoubtedly caused a redistribution of forces in the member. The closer stirrup spacing near the support region forced the critical region away from the support and at the same time caused a more uniform distribution of the diagonal cracks as can be seen in Fig. 3.29b. Furthermore, the increase of transverse reinforcement did not prevent yielding of the stirrups yet at the same time controlled the cracking at the support thus preventing the spalling of concrete at the end support regions of the member.

The load-deflection curves for these three specimens are shown in Fig. 3.30.

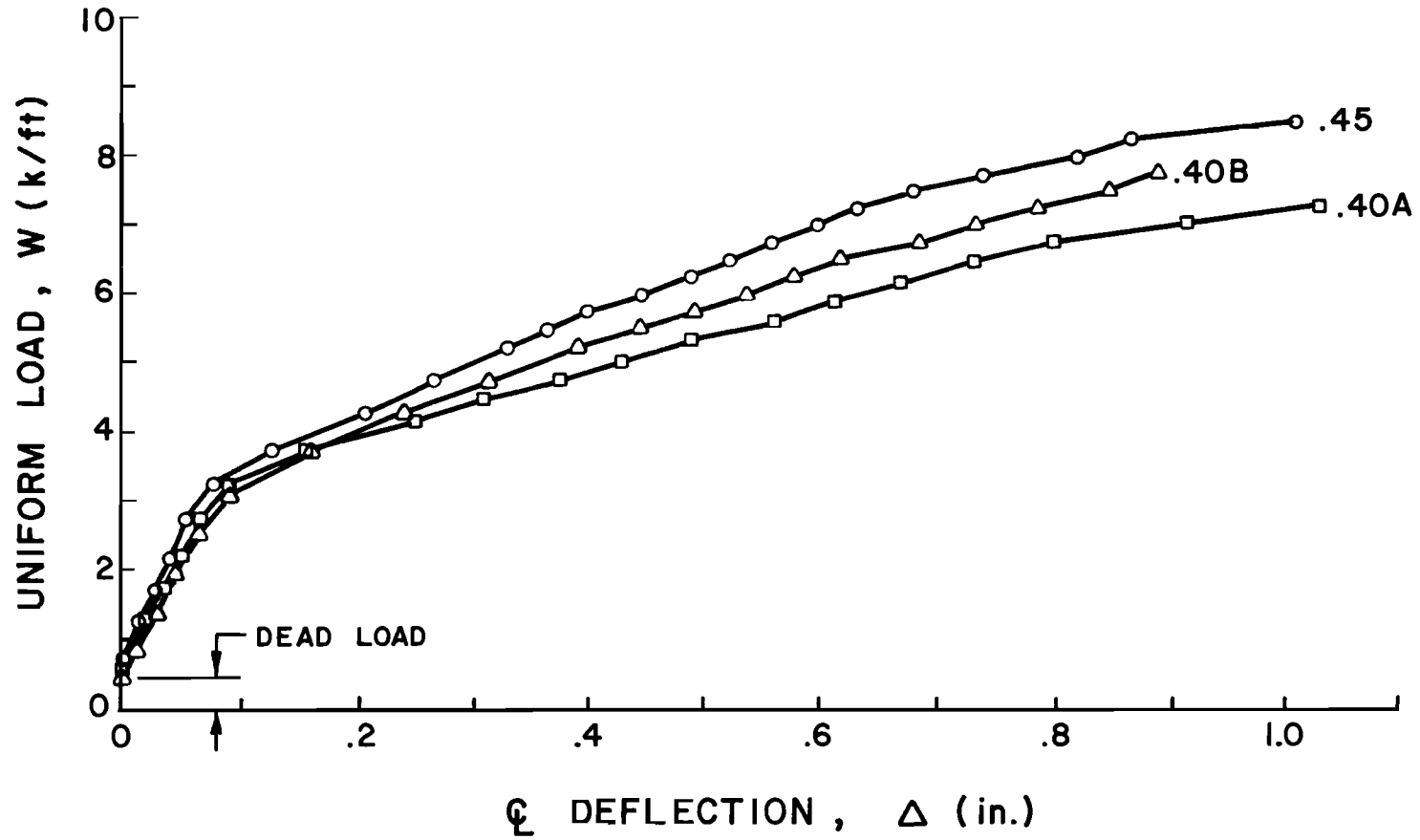


Fig. 3.30 Load-deflection curves for beams 0.40A, 0.40B, 0.45

In column (6) of Table 3.17 are shown the values of the dispersion index I . The mean of the dispersion coefficient for the three specimens at several different sections was 1.01 and the standard deviation 0.03. This indicates excellent agreement between the predicted ultimate values and the test results.

In Figs. 3.31, 3.32 and 3.33, the ultimate test values shown in Table 3.17 evaluated at different sections using the ultimate test load are compared with the ultimate load interaction predicted by the truss model as obtained from Eq. 3.12.

Figures 3.31, 3.32 and 3.33 confirm the good agreement observed between the test results and the truss model predictions. This agreement was achieved in spite of the fact that the yielding of the longitudinal reinforcement did not occur at failure. Furthermore, the data presented in Table 3.17 in column (4) show that in regions of maximum shear (at the supports $M_u = 0$) the maximum shear capacity in the absence of moment as given by Eq. 3.14 coincide with the value of the shear at failure. Therefore, the results of this series also supports the statement that for sections designed in accordance with the procedures suggested in the truss model would correctly predict their ultimate shear capacity as long as yielding of the stirrups is reached at failure and premature failure due to crushing of the concrete or poor detailing are prevented.

The specimens analyzed in this section were specifically designed to evaluate the truss model analogy and the design procedures suggested for the case of members failing in shear. As suggested, low

Tests reported by Castrodale (50) on prestressed concrete I-beams under distributed loading

(1) Member (ID)	(2) Section from support (ft)	(3) $\frac{M_{test}}{M_{uo}}$	(4) $\frac{V_{test}}{V_{uo}}$	(5) $\rho_v f_y$ (psi)	(6) I	(7) Level of Prestress σ/f'_c
0.40A	0.00	0.0	1.04	180	1.04	0.10
	1.70	0.41	0.80	180	1.03	
	3.40	0.72	0.54	180	1.01	
	5.10	0.91	0.32	160	1.01	
		0.98	0.00	160	0.98	
0.40B	0.00	0.0	1.04	180	1.04	0.13
	1.75	0.43	0.78	180	1.02	
	3.50	0.69	0.53	180	0.98	
	5.25	0.86	0.29	160	0.95	
		0.92	0.00	160	0.92	
0.45	0.00	0.00	1.04	220	1.04	0.12
	1.56	0.40	0.81	220	1.03	
	3.13	0.69	0.58	220	1.02	
	4.70	0.89	0.35	180	1.01	
	6.26	6.99	0.14	160	1.01	
		1.01	0.0	160	1.01	
				X = 1.01		
				S = 0.03		

Table 3.17 Data for prestressed concrete I-beams failing in shear (from Ref. 50)

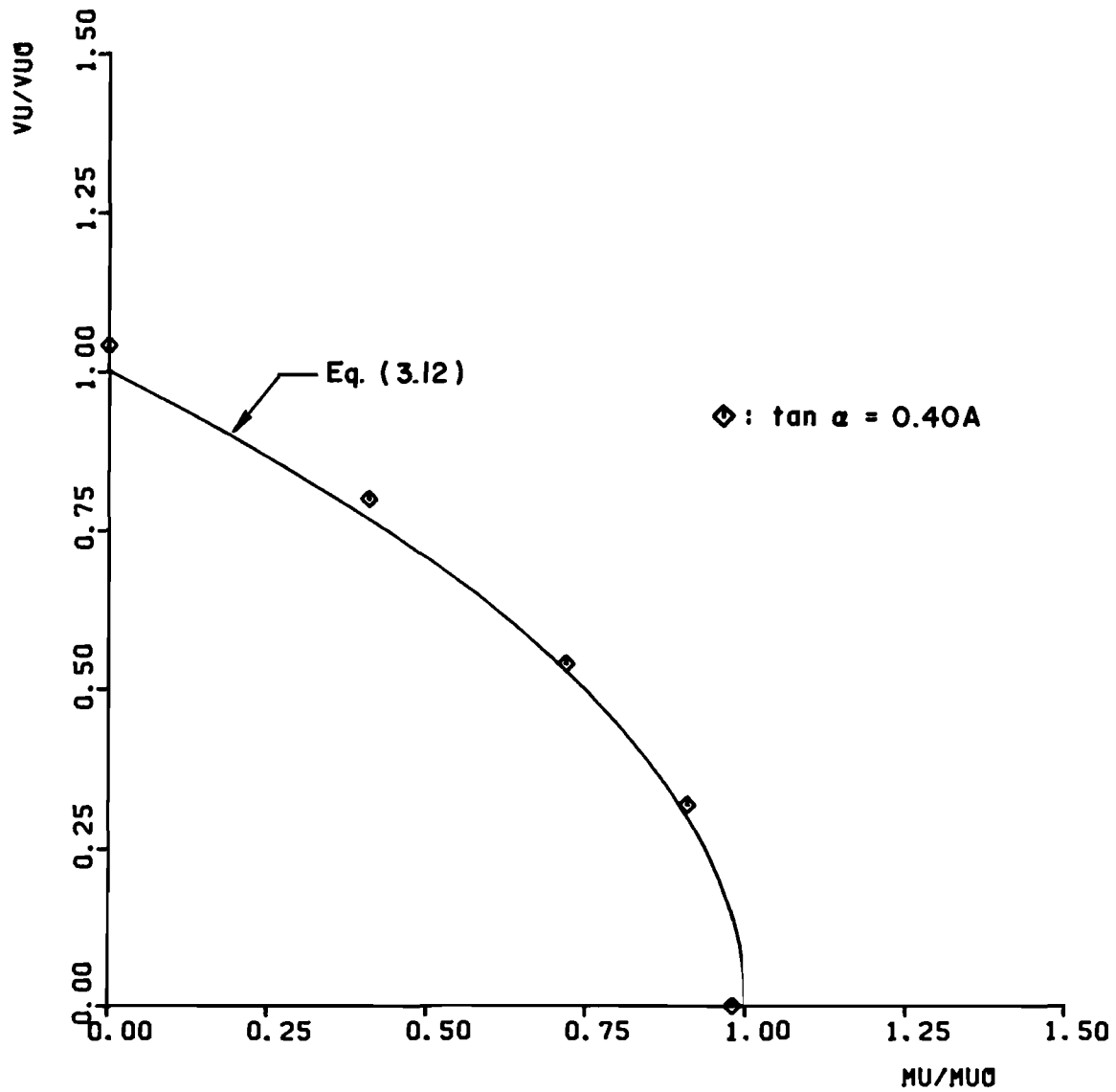


Fig. 3.31 Comparison between the ultimate load interaction predicted by the truss model and the ultimate test values at different sections along the span length for beam 0.40A

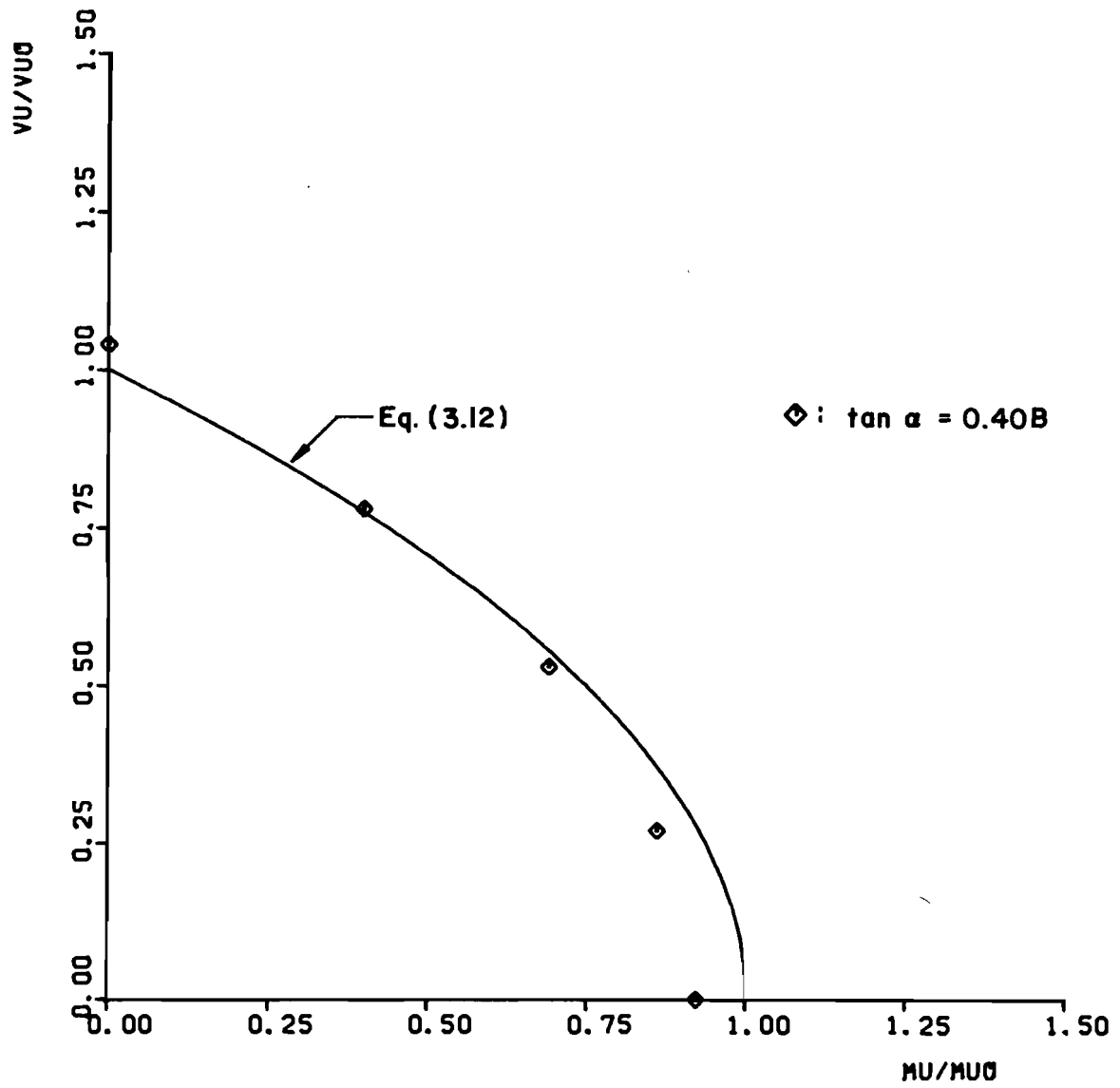


Fig. 3.32 Evaluation of the truss model using beam 0.40B

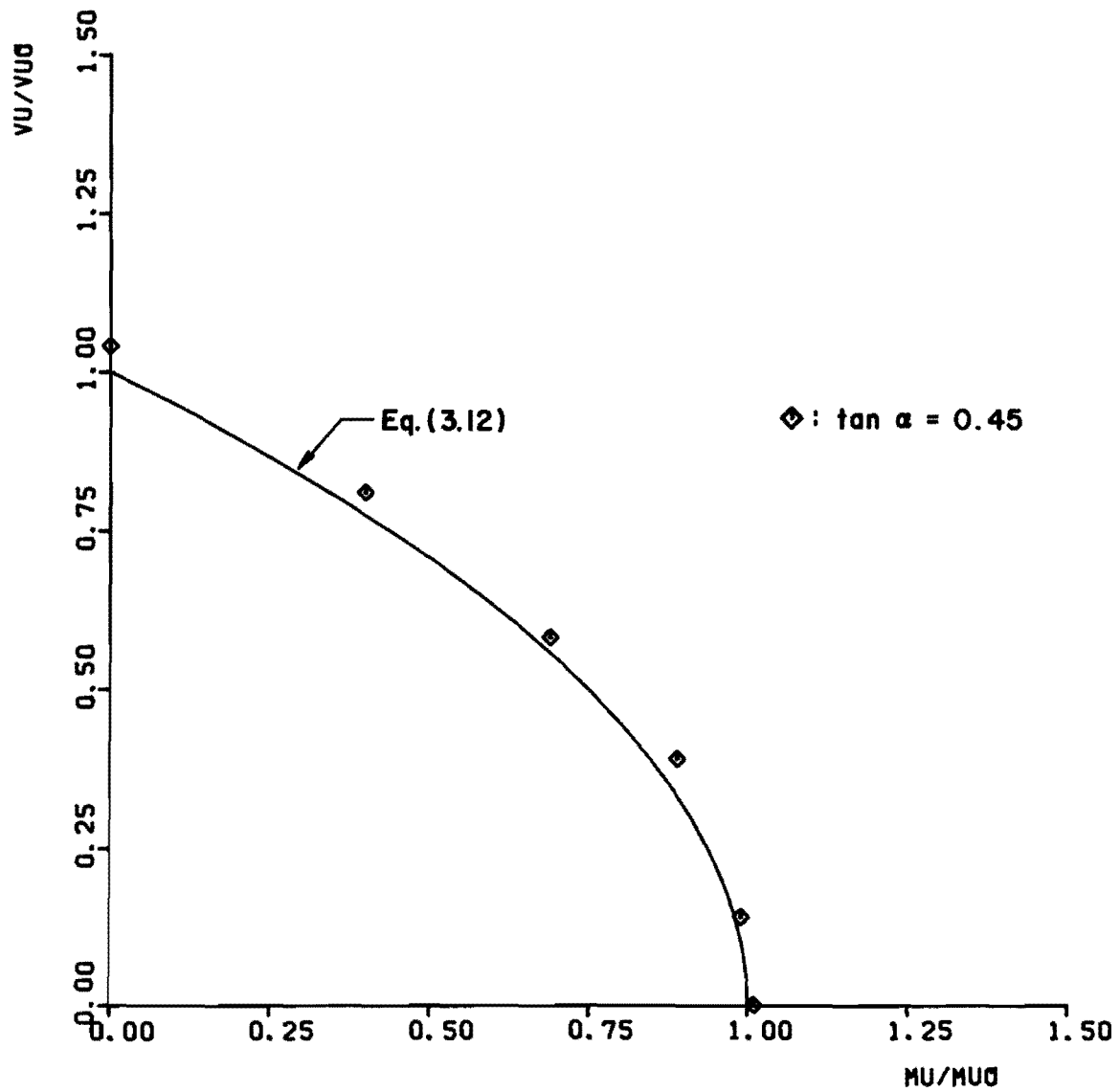


Fig. 3.33 Comparison between the truss model predicted ultimate load interaction and the results from beam 0.45

values of $\tan \alpha$ such as the ones used in the design of the specimens summarized in this section lead towards large stirrup spacings and increased amounts of longitudinal reinforcement and produce shear type failures. The test results also show that the truss model adequately predicts the ultimate shear capacity of both reinforced and prestressed concrete members even if yielding of the longitudinal reinforcement is not reached at failure, provided that the members are underreinforced for flexure and that premature failures due to diagonal crushing of the concrete in the web and/or poor detailing are avoided.

3.5.2 Comparisons with Tests Reported in Literature. An extensive review of test data available in the American literature in the area of shear in reinforced and prestressed concrete was conducted. This review revealed that a substantial amount of the tests where shear failures were reported had been performed on members containing no web reinforcement or very minimum values ($\rho_v f_y < 100$ psi) (see Figs. 3.34 and 3.35).

Shear tests with minimal web reinforcement provide mainly an evaluation of the diagonal tensile strength of the concrete (so-called concrete contribution at ultimate in the case of shear). The absence of tests with significant amounts of web reinforcement results in a lack of significant information on the behavior at ultimate of major shear carrying members.

In the evaluation of the truss model in this section only tests performed on members with a percentage of web reinforcement $\rho_v f_y$ greater or equal to 100 psi and failing in shear are considered. The

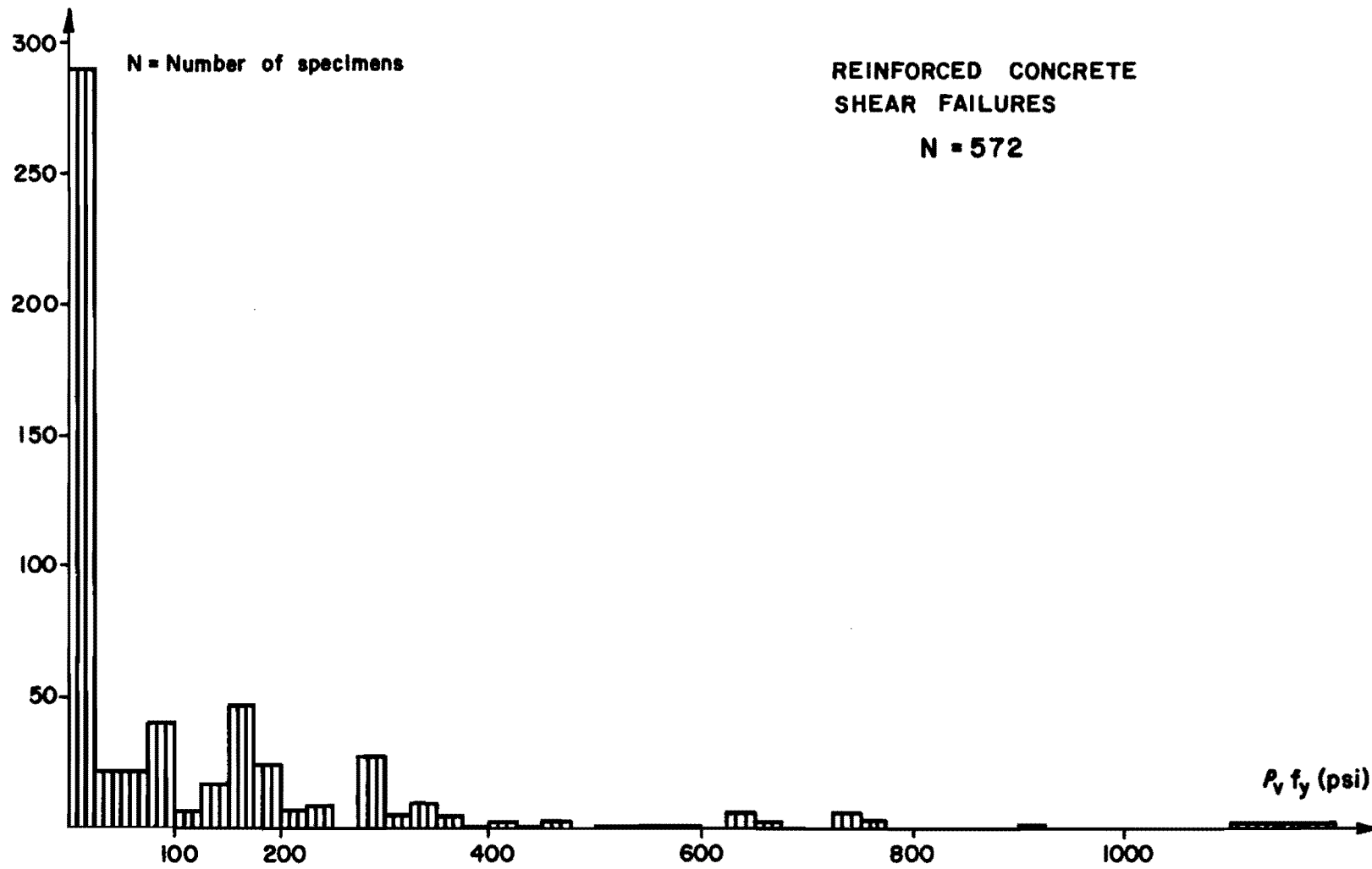


Fig. 3.34 Tests on reinforced concrete one-way members

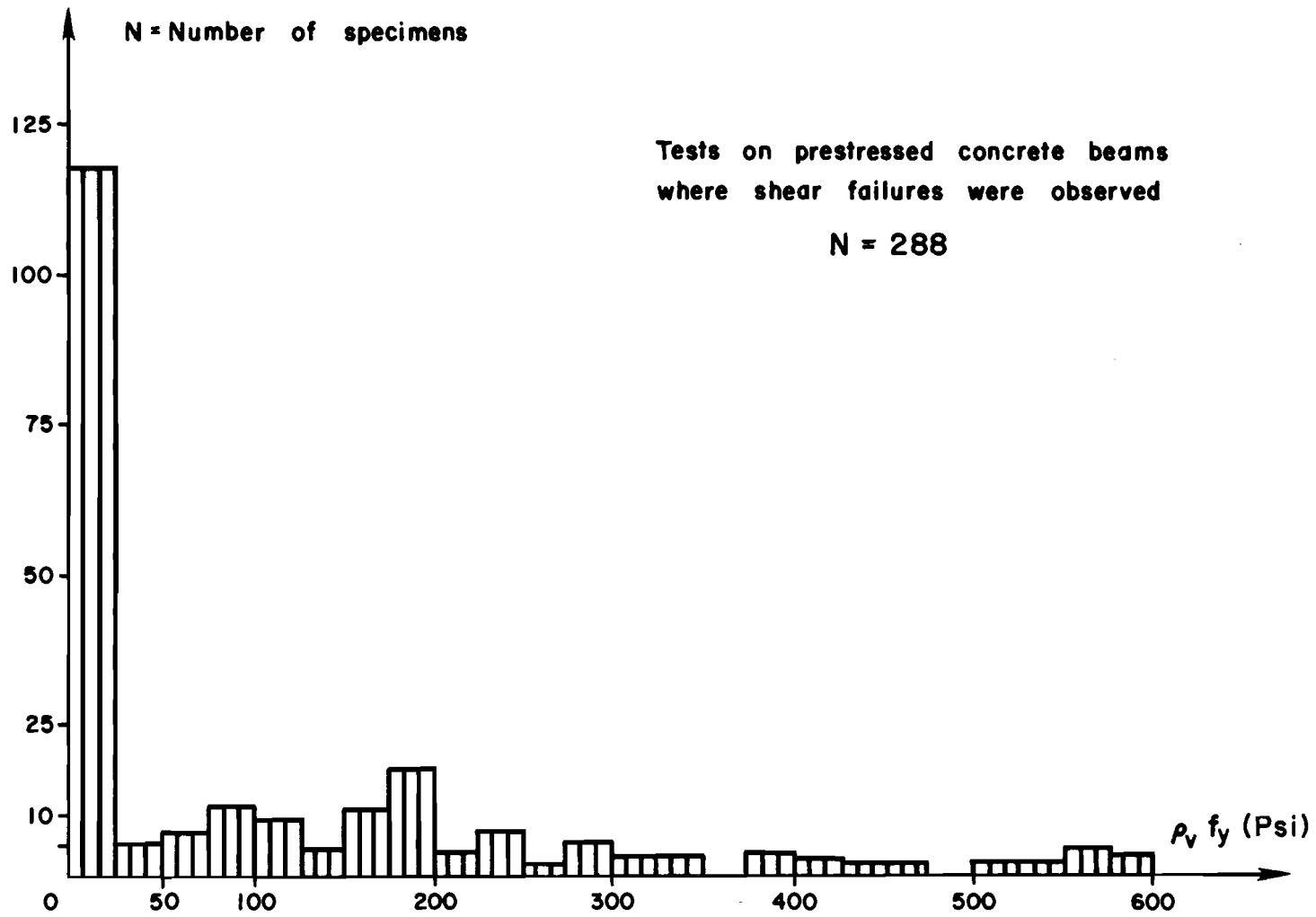


Fig. 3.35 Tests on prestressed concrete one-way members

web reinforcement percentage $\rho_v f_y$ is defined as

$$\rho_v f_y = [A_v f_y] / [b_w s] \quad (3.15)$$

In a later section, members with minimal shear reinforcement (defined as $\rho_v f_y < 100$ psi) will be discussed. The ultimate load as predicted by the truss model for members subjected to bending and shear and containing web reinforcement is presented by the interaction Eqs. 3.12.

In the comparison of the truss model with test results reported in the literature in the area of combined bending and shear, a similar procedure to the one followed in the areas of combined torsion-bending and torsion-bending-shear is used. The index I shown in column (7) of Tables 3.18 thru 3.21 is again used as a measure of the dispersion between data points and the truss model predictions measured along radial lines from the origin (see Fig. 3.36).

The truss model predicted ultimate values are given by the interaction Eq. 3.12. Values $I > 1$ indicate conservative predictions. Values of $I < 1$ represent unconservative predictions. The values of the mean (X) and standard deviation (S) of the dispersion index I are also given for both reinforced and prestressed concrete members.

As previously explained, the interaction Eq. 3.12 is derived under the assumption that yielding of the transverse and longitudinal reinforcement is achieved at failure. This situation is almost nonexistent in the case of test data where shear failures were observed. In Sec. 3.5.1 it was shown, however, that as long as the members were

Tests reported by A.P. Clark (53) on reinforced concrete rectangular beams. (Point load tests)

(1) Member ID	(2) \underline{M}_{test} μ_{uo} (Eq. 3.13)	(3) \underline{V}_{test} ν_{uo} (Eq. 3.14)	(4) ρ_{vfy} (psi)	(5) a/d	(6) $\tan \alpha$ (Eq. 3.16)	(7) I	(8) Level of Prestress σ/f'_c
B1-1	0.77	0.76	180	1.95	0.30	1.23	0.0
B1-2	0.71	0.70	180	1.95	0.34	1.14	0.0
B1-3	0.78	0.77	180	1.95	0.30	1.25	0.0
B1-4	0.73	0.72	180	1.95	0.32	1.17	0.0
B1-5	0.66	0.65	180	1.95	0.36	1.06	0.0
B2-1	0.83	0.52	350	1.95	0.58	1.13	0.0
B2-2	0.88	0.61	350	1.95	0.54	1.19	0.0
B2-3	0.91	0.64	350	1.95	0.52	1.24	0.0
C1-1	0.91	0.94	170	1.57	0.29	1.50	0.0
C1-2	1.03	1.07	170	1.57	0.25	1.70	0.0
C1-3	0.81	0.84	170	1.57	0.33	1.34	0.0
C3-1	0.74	0.76	170	1.57	0.36	1.21	0.0
C3-2	0.66	0.69	170	1.57	0.40	1.09	0.0
C3-3	0.62	0.64	170	1.57	0.43	1.02	0.0
C2-1	0.96	0.70	330	1.57	0.56	1.33	0.0
C2-2	1.00	0.63	330	1.57	0.53	1.39	0.0
C2-4	0.96	0.70	330	1.57	0.56	1.33	0.0
C4-1	0.68	0.87	170	1.56	0.26	1.27	0.0
C6-2	0.93	1.18	170	1.56	0.19	1.73	0.0
C6-3	0.96	1.21	170	1.56	0.18	1.78	0.0
C6-4	0.94	1.19	170	1.56	0.19	1.75	0.0
D1-1	0.91	0.99	220	1.18	0.35	1.55	0.0
D1-3	0.78	0.84	220	1.18	0.41	1.32	0.0
D3-1	0.79	0.75	440	1.17	0.55	1.24	0.0
D2-1	0.87	0.82	290	1.18	0.49	1.37	0.0
D2-2	0.94	0.88	490	1.18	0.46	1.47	0.0
D4-1	0.94	0.62	590	1.18	0.92	1.25	0.0
D1-6	0.71	0.66	170	1.96	0.38	1.10	0.0

Table 3.18 Data on reinforced concrete rectangular beams failing in shear

Tests reported by A.P. Clark (53) on reinforced concrete rectangular beams (continuation)

(1) Member ID	(2) M_{test} Mu0 (Eq. 3.13)	(3) V_{test} Vu0 (Eq. 3.14)	(4) $\rho v f_y$ (psi)	(5) a/d	(6) tana (Eq. 3.16)	(7) I	(8) Level of Prestress σ/f'_c
D1-7	0.73	0.68	170	1.96	0.36	1.13	0.0
D1-8	0.76	0.71	170	1.96	0.35	1.19	0.0
E1-2	0.95	0.67	260	2.02	0.47	1.30	0.0
D2-6	0.86	0.56	220	2.42	0.51	1.14	0.0
D2-7	0.80	0.51	220	2.42	0.56	1.04	0.0
D2-8	0.86	0.56	220	2.42	0.51	1.13	0.0
D4-1	0.86	0.62	180	2.42	0.41	1.19	0.0
D4-2	0.80	0.57	180	2.42	0.45	1.09	0.0
D4-3	0.84	0.61	180	2.42	0.42	1.16	0.0
D5-1	0.75	0.63	130	2.42	0.36	1.10	0.0
D5-2	0.80	0.66	130	2.42	0.34	1.17	0.0
D5-3	0.80	0.66	130	2.42	0.34	1.17	0.0
A1-1	0.73	0.59	180	2.34	0.41	1.06	0.0
A1-2	0.69	0.55	180	2.34	0.43	0.99	0.0
A1-3	0.73	0.59	180	2.34	0.41	1.06	0.0
A1-4	1.73	0.59	180	2.34	0.41	1.06	0.0

Tests reported by O. Moretto (99) on reinforced concrete rectangular beams (Point load tests)

1V $\frac{1}{2}$ 1	0.59	0.79	150	1.75	0.24	1.14	0.0
1V $\frac{1}{2}$ 2	0.59	0.79	150	1.75	0.24	1.14	0.0
2V $\frac{1}{2}$ 1	0.69	0.93	150	1.75	0.20	1.33	0.0
2V $\frac{1}{2}$ 2	0.68	0.92	150	1.75	0.20	1.33	0.0
1V3/81	0.72	0.70	290	1.75	0.38	1.15	0.0
1V3/82	0.76	0.74	290	1.75	0.36	1.21	0.0
2V3/81	0.75	0.74	290	1.75	0.36	1.20	0.0
2V3/82	0.71	0.69	290	1.75	0.38	1.13	0.0
1aV $\frac{1}{2}$ 1	0.50	0.77	130	1.75	0.23	1.05	0.0
1aV $\frac{1}{2}$ 2	0.51	0.78	130	1.75	0.23	1.07	0.0

Overall for Tables
3.18 and 3.19

X = 1.22
S = 0.25

Table 3.19 Data on reinforced concrete rectangular beams failing in shear

Tests reported by Hernandez (76) on prestressed concrete I-beams
(point load tests)

(1) Member ID	(2) $\frac{M_{test}}{\mu_{uo}}$ (Eq. 3.13)	(3) $\frac{V_{test}}{\nu_{uo}}$ (Eq. 3.14)	(4) ρ_{vfy} (psi)	(5) a/d	(6) $\tan \alpha$ (Eq. 3.16)	(7) I	(8) Level of Prestress $\sigma/f'c$
G5	0.96	0.76	180	3.6	0.21	1.38	0.19
G6	0.82	0.71	140	3.6	0.20	1.23	0.20
G7	1.03	0.70	230	3.5	0.27	1.39	0.13
G10	0.89	0.60	230	3.0	0.31	1.20	0.24
G20	0.91	0.40	270	3.5	0.72	1.05	0.26
G28	0.99	0.72	120	2.8	0.24	1.37	0.14
G29	1.03	0.76	320	5.4	0.29	1.43	0.14
G34	1.11	0.70	330	2.93	0.35	1.45	0.15
					X =	1.31	
					S =	0.14	

Tests reported by MacGregor, Sozen and
Siess (110) on prestressed concrete I-beams (point load test)

BW1438	0.97	0.42	167	3.56	0.68	1.13	0.17
CW1437	0.95	0.37	208	3.56	0.87	1.07	0.19
CW1439	0.80	0.35	167	3.56	0.83	0.94	0.20
CW1447	0.88	0.42	138	3.55	0.63	1.04	0.24
CW1450	0.89	0.37	180	3.55	0.81	1.02	0.26
CW1451	0.67	0.45	99	3.63	0.41	0.90	0.27
CW1454	0.69	0.48	97	3.61	0.38	0.94	0.24
					X =	1.01	
					S =	0.08	
					Overall for Table 3.20	X =	1.17
						S =	0.19

Table 3.20 Data on prestressed concrete I-beams
failing in shear

Tests reported by Moayer and Regan (33) on prestressed concrete T-beam (Point load)

(1) Member ID	(2) $\frac{M}{M_{uo}}$ test (Eq. 3.13)	(3) $\frac{V}{V_{uo}}$ test (Eq. 3.14)	(4) $\rho v f_y$ (psi)	(5) a/d	(6) $\tan \alpha$ (Eq. 3.16)	(7) I	(8) Level of Prestress σ / f'_c
P4	1.21	0.55	155	3.45	0.52	1.42	0.07
P8	0.93	0.99	104	3.64	0.12	1.55	0.14
P13	1.11	0.98	104	3.51	0.14	1.68	0.05
P18	1.00	0.97	104	3.68	0.13	1.60	0.13
P24	1.11	0.54	155	3.51	0.49	1.33	0.05
P25	1.19	0.79	104	5.32	0.21	1.51	0.05
P26	1.07	0.56	155	3.68	0.41	1.32	0.12
P27	1.09	0.70	104	5.57	0.18	1.43	0.13
P28	1.00	0.59	155	3.64	0.36	1.28	0.13
P29	1.06	0.61	104	5.51	0.23	1.34	0.13
P49	0.73	0.50	155	3.61	0.37	0.98	0.16
P50	0.89	0.44	290	3.61	0.58	1.07	0.14
				X =		1.38	
				S =		0.20	

Table 3.21 Data on prestressed concrete T-beams failing in shear

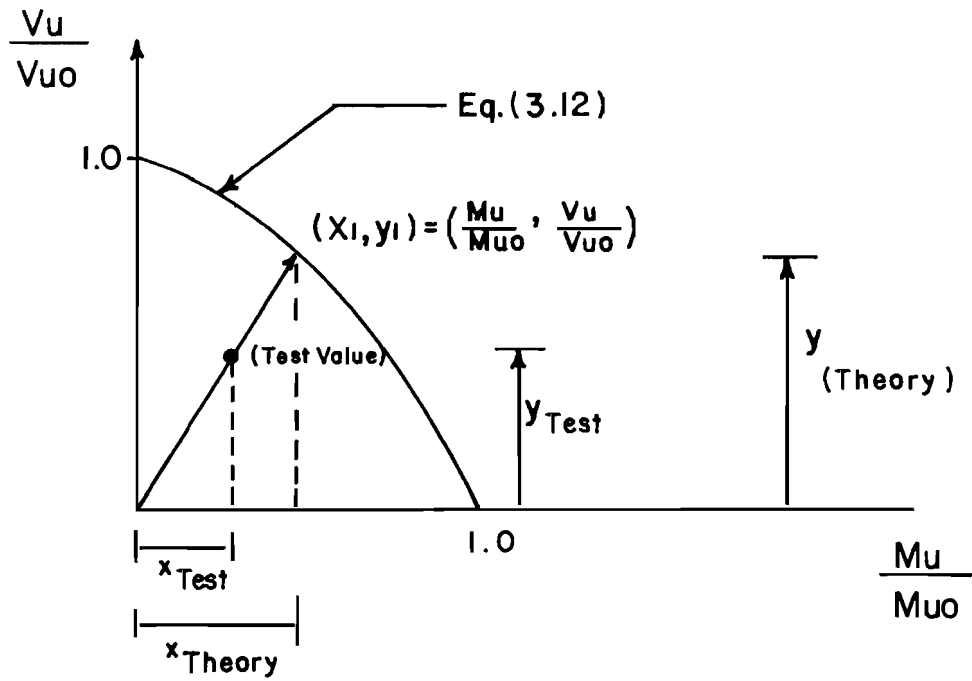


Fig. 3.36 Evaluation of the accuracy of the truss model predictions in the area of shear-bending by means of the dispersion index I

correctly detailed and premature failures due to crushing of the concrete in the web or in the concrete compression zone were prevented, the truss model adequately predicted the ultimate strength of those members.

The test data used in this section to evaluate the truss model are that of reinforced and prestressed concrete one-way members failing in shear where yielding of the transverse reinforcement was achieved at or previous to failure, unless otherwise indicated. Members where web crushing occurred at failure are examined in Sec. 3.6.

Tables 3.18 and 3.19 show test data for reinforced concrete rectangular one-way members failing in shear. In column (7) are given the values of the dispersion index I . Shown at the bottom of Table 3.19 are the values of the mean ($\bar{X} = 1.22$) and the standard deviation ($S = 0.25$) of the index I for all reinforced concrete beams reported in the data of Tables 3.18 and 3.19. As can be seen from the values of the index I , the truss model is conservative in virtually every case. The excessive conservatism seen in members C1-1, C1-2, C6-2, C6-3, C6-4, and D1-1 of Table 3.18 can be explained by observing the values of $\tan \alpha$ shown in column (6). The value of $\tan \alpha$ is the tangent of the angle of inclination at failure of the diagonal strut (see Eq. 3.64 of Report 248-2).

$$\tan \alpha = [S_y * z] / [V_{TEST} * s] \quad (3.16)$$

It is determined by the amount of web reinforcement and level of shear present in the member at failure. This corresponds to the angle of

inclination α that should be reached at failure provided that all the strength of the member is given by truss action, i.e. the member is in the Full Truss State. The values of $\tan\alpha$ for these specimens are all below 0.35 and are well outside the suggested limits that $0.5 \leq \tan\alpha \leq 2.0$. However, the maximum possible tangent of the angle of inclination of the failure crack as given by the a/d ratio (1.57) by setting $a = z \cot\alpha$ and $z = 0.9d$ is equal to 0.46. Therefore, the computed tangent α equal to 0.35 obtained from Eq. 3.16 which assumes that the member was in the full truss state, i.e. that all the strength was provided by truss action, was never reached. This means that the member at failure was in a transition state between its uncracked state and the full truss state. As explained in Sec. 2.5, in this transition state concrete in the web contributes to the shear capacity of the member. This additional contribution by the concrete would then account for the additional strength observed in those members. The additional concrete contribution to the shear carrying capacity in this transition state is evaluated in Sec. 3.8.

Tables 3.20 and 3.21 show test data for prestressed concrete beams with I and T cross sections failing in shear. The value of the mean of the dispersion index I is 1.17 for the case of members with I-shape cross section, with a standard deviation of 0.19. For the case of members with T-shaped cross section, the mean is 1.38 and the standard deviation is 0.20. This indicates that the truss model predicted values for the case of prestressed concrete members failing in shear are in

good agreement and in most cases conservative when compared with actual test values.

It is also apparent from the data examined that the truss model predictions once more become very conservative for members with an angle of inclination of the diagonal strut at failure outside the limits suggested in Report 248-2 ($0.5 \leq \tan \alpha \leq 2.0$). For members with an angle α inside the proposed limits the truss model predictions become much more accurate as can be seen from the test data of Ref. 110, beam G20 from Ref. 76, and beams P4 and P50 from Ref. 33.

Finally, the truss model is evaluated using test data from reinforced and prestressed continuous members failing in shear.

Table 3.22 shows the data for two-span continuous reinforced concrete members. The mean of the dispersion index I given in column (7) is 0.96 and the standard deviation 0.14. In general, it can be said that the truss model adequately predicts the strength of those members. The unconservative values predicted for members C3H1, C3H2, C2A1, and C2H1 are explained by the fact that neither the stirrup nor the longitudinal reinforcement had yielded at failure thus indicating a premature type failure due to crushing of the concrete in the web. In the case of specimens E2H1 and E2H2, failure was due to a combination of shear and bond splitting which would indicate poor detailing of the longitudinal tension steel, thus causing a premature failure of the members.

Table 3.23 shows data on continuous prestressed concrete members failing in shear where yielding of the transverse reinforcement was

Tests reported by Rodriguez, Bianchini, Viest, Kesler (146) on two-span continuous reinforced concrete beams (point load tests)

(1) Member ID	(2) Mtest Mu0(Eq. 3.15)	(3) Vtest Vu0(Eq. 3.14)	(4) ρvfy (psi)	(5) a/d	(6) tanα Eq. 3.16	(7) I	(8) Level of Prestress σ/f'c
C6A1	0.85	0.73	610	1.36	0.66	1.27	0.0
E6H1	0.77	0.54	1020	1.38	1.00	1.05	
E6H2	0.57	0.54	770	1.37	0.84	0.90	
C6H1	0.65	0.48	1050	1.33	1.17	0.90	
C6H2	0.60	0.56	750	1.37	0.81	0.94	
E6I2	0.73	0.50	1020	1.38	1.23	0.99	
C6I2	0.76	0.52	1040	1.36	1.23	1.02	
C3A2	0.92	0.65	310	2.74	0.51	1.26	0.0
E3H1	0.74	0.51	530	2.83	0.75	1.00	
E3H2	0.65	0.51	410	2.66	0.69	0.93	
C3H1	0.61	0.45	510	2.73	0.84	0.84	
C3H2	0.54	0.45	410	2.74	0.74	0.80	
E2A1	0.81	0.63	180	4.08	0.41	1.15	0.0
E2A2	0.70	0.57	180	4.08	0.46	1.03	
E2A3	0.71	0.59	190	4.10	0.43	1.04	
C2A1	0.58	0.46	190	4.08	0.58	0.84	
C2A2	0.69	0.57	190	4.04	0.47	1.00	
E2H1	0.54	0.42	410	3.99	0.84	0.77	
E2H2	0.45	0.44	270	4.20	0.61	0.72	
C2H1	0.63	0.41	420	4.16	0.84	6.83	
C2H2	0.57	0.48	270	3.98	0.59	0.85	
B2A1	0.68	0.59	140	4.08	0.42	1.02	0.0
B2H1	0.68	0.51	280	4.08	0.64	0.95	
B2H2	0.56	0.58	180	4.08	0.45	0.92	
				X =		0.96	
				S =		0.14	

Table 3.22 Data on two-span continuous reinforced concrete beams with rectangular cross section

Tests reported by Mattock and Kaar (111) on continuous prestressed concrete I-beams. (Point load tests)

(1) Member ID	(2) \overline{M}_{test} \overline{M}_{uo} (Eq. 3.13)	(3) \overline{V}_{test} \overline{V}_{uo} (Eq. 3.14)	(4) $\rho v f_y$ (psi)	(5) a/d	(6) $\tan \alpha$ (Eq. 3.16)	(7) I	(8) Level of Prestress $\sigma/f'c$
S7	1.12	1.20	282	2.0	0.21	1.89	0.15
S13	1.08	0.84	282	4.5	0.31	1.54	0.14
S10	0.94	1.29	188	2.0	0.17	1.83	0.15
S21	0.65	1.25	188	2.0	0.17	1.62	0.14
				X =		1.72	
				S =		0.17	

Table 3.23 Data on continuous prestressed concrete members with I-shape cross section failing in shear

achieved at failure. Unfortunately, the amount of data in this area is almost nonexistent and in the few available cases sometimes the information is incomplete. For the specimen shown in Table 3.23, the truss model predictions were very conservative as indicated by the mean of the dispersion index of 1.72 with a standard deviation of 0.17. This again is due to the very low values of $\tan\alpha$ of these specimens. All were far outside the suggested limits.

After a complete evaluation of the truss model ultimate load predictions in the area of bending and shear on reinforced and prestressed concrete members, it is apparent that the truss model adequately represents the strength of these members provided that yielding of the transverse reinforcement occurs at failure, and that premature failures due to crushing of the concrete in the web and poor detailing are avoided. This together with observation of the limits on $\tan\alpha$ proposed in Report 248-2 will yield very reasonable and safe results.

It was also observed that in those cases where the stirrups yielded and the value of the required angle of inclination of the diagonal strut at failure was way below the suggested lower limit of $\tan\alpha = 0.5$, the truss model predictions were very conservative. This indicates that in such cases the concrete in the web of the member provided a substantial contribution to the shear capacity of the member. This additional concrete contribution in the transition state between the uncracked state and the full truss state is examined in Sec. 3.8.

3.6 Evaluation of the Compression Strength of the Diagonal Strut

In Sec. 2.3 it was shown that the maximum shear stress v_{\max} is achieved when the angle of inclination of the diagonal compression strut is of 45 degrees, and is given by the relation

$$v_{\max} = f_d/2 \quad (3.17)$$

where f_d is the compression stress in the diagonal strut of the truss model. It was also suggested that by limiting the compression stress in the diagonal strut f_d to a value equal or less than a maximum allowable compression stress f_c failure due to crushing of the concrete in the diagonal strut would be avoided if the member was designed for an angle of inclination at failure between 26 and 64 degrees.

In this section, test results of beams which failed due to web crushing are examined in order to evaluate proposed limits for the maximum allowable compression stress, f_c , in the diagonal strut of the truss model.

Thürlimann (162) on the basis of test evidence and practical experience proposed that the allowable compression stress f_c should be taken as

$$f_c = f_d \max = 0.35f_c' + 696 \leq 2400 \text{ psi} \quad (3.18)$$

where f_c and f_c' are in terms of psi. Thürlimann states that the limit of 2400 psi, which corresponds to f_c' of about 4800 psi, is somewhat arbitrary. It was set at 4800 psi simply because that was the maximum range of f_c' in the tests considered in the evaluation of Eq. 3.18.

In this study a best fit curve of the form $k \sqrt{f'_c}$ to approximate Eq. 3.18 proposed by Thürlimann resulted in the relation

$$f_c = 34 \sqrt{f'_c} \quad (3.19)$$

Combining Eqs. 3.17 and 3.19 results in the maximum value for the shear stress v_{\max} allowed in order to avoid crushing of the diagonal compression strut of the truss model

$$v_{\max} < f_c/2 = 17 \sqrt{f'_c} \quad (3.20)$$

Equation 3.20 is applicable to the cases of shear, torsion, and combined shear and torsion.

In Tables 3.24 and 3.25, results of reinforced and prestressed concrete one-way flexural members subjected to shear and failing in a web crushing mode are shown. For comparison the value of the shear stress at failure v_{\max}

$$v_{\max}(V) = V_{\text{test}}/[bwz] \quad (3.21)$$

is plotted against the value of f'_c for each specimen of Tables 3.24 and 3.25 in Fig. 3.37. Also shown in Fig. 3.37 are the limiting values for the maximum shear stress of $17 \sqrt{f'_c}$ from Eq. 3.20 and

$$v_{\max} < 15 \sqrt{f'_c} \quad (3.22)$$

which is a more conservative value and is equivalent to a maximum allowable compression stress in the diagonal strut of $30 \sqrt{f'_c}$.

Tests reported by Robinson (151) on reinforced concrete rectangular beams

(1) Member ID	(2) F' _c ksi	(3) v(max) Eq. 3.21 ksi	(4) <u>(3)</u> v(Eq. 3.20)	(5) <u>(3)</u> v(Eq. 3.22)	(6) Level of Prestress σ/f' _c
NRS	2.16	0.89	1.13	1.28	0.0
NR10	3.44	1.66	1.66	1.89	
NT8-1	2.88	1.55	1.70	1.93	
NT8-2	2.94	1.55	1.68	1.91	
NT10	2.45	1.22	1.45	1.64	
			X = 1.52	X = 1.73	
			S = 0.24	S = 0.28	

Tests reported by Leonhardt and Walther
(101,102) on reinforced concrete T-beams

TA1	2.49	0.91	1.07	1.22	0.0
TA2	2.49	0.97	1.02	1.16	
TA3	2.31	0.74	0.90	1.03	
TA13	2.87	0.94	1.03	1.17	
TA14	2.87	0.91	1.00	1.13	
TA1	3.53	1.56	1.54	1.75	
			X = 1.09	X = 1.24	
			S = 0.23	S = 0.26	

Tests reported by Bennett and Balasooriya (39)
on reinforced concrete I-beams

2B6	6460	2.01	1.47	1.67	0.0
Overall for Table 3.24			X = 1.30	X = 1.48	
			S = 0.31	S = 0.45	

Table 3.24 Shear tests on reinforced concrete members
experiencing web crushing failure

Tests reported by MacGregor, Sozen and Siess (110) on prestressed concrete I-beams

(1) Member ID	(2) f'_c ksi	(3) v (max) Eq. 3.21 ksi	(4) $\frac{(3)}{v(\text{Eq}3.20)}$	(5) $\frac{(3)}{v(\text{Eq}3.22)}$	(6) Level of Prestress σ/f'_c
CW.13.28	4.33	1.12	1.00	1.13	0.14

Tests reported by Bennett and Balasooriya (39) on prestressed concrete I-beams

3A2	6.05	1.94	1.47	1.66	0.43
2A3	4.9	2.25	1.39	2.14	0.55
2B2	6.23	2.78	2.07	2.35	0.36
2B3	6.37	2.83	2.08	2.36	0.25
2B4	5.52	2.20	1.75	1.98	0.21
2B5	5.65	2.10	1.64	1.86	0.14
3C2	4.82	2.10	1.78	2.02	0.37
3C3	4.88	2.19	1.84	2.09	0.32
3C4	4.42	1.57	1.39	1.57	0.26
3C5	4.58	1.36	1.18	1.34	0.10
3B1	6.42	2.38	1.75	1.98	0.34
3D2	6.42	2.14	1.57	1.78	0.35
2F1	5.68	2.28	1.78	2.02	0.35
2F2	5.68	2.23	1.74	1.97	0.30
2F3	5.68	1.99	1.55	1.76	0.20
2F4	5.80	1.83	1.42	1.61	0.07

Overall for Table 3.24	X = 1.64	X = 1.36
	S = 0.29	S = 0.33

Table 3.25 Shear tests on prestressed concrete members experiencing web crushing

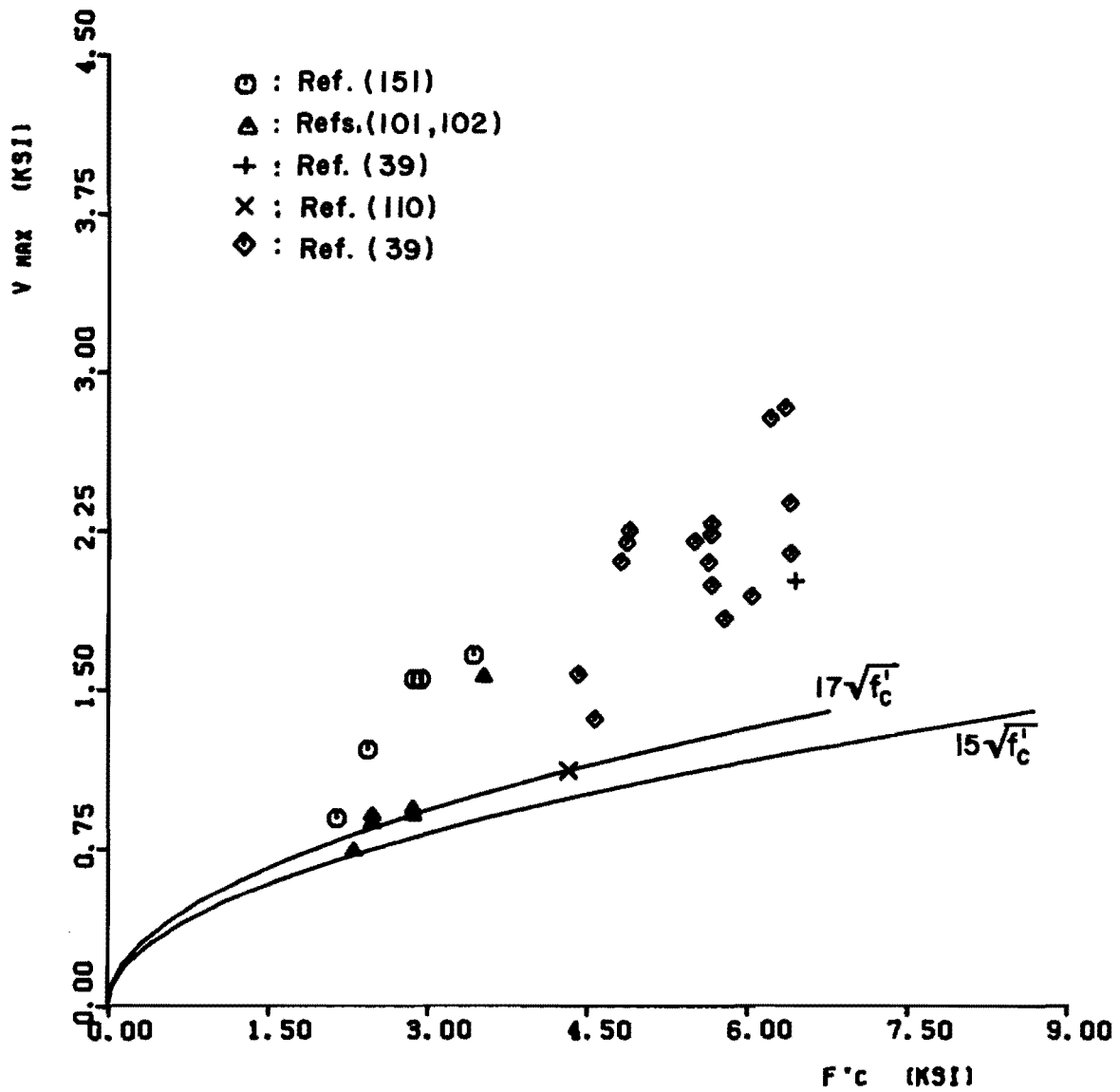


Fig. 3.37 Shear stress at failure vs specified compressive strength of the concrete f'_c for the case of reinforced and prestressed concrete beams failing due to web crushing

As can be seen from Fig. 3.37, the limiting value of $17\sqrt{f'_c}$ was not conservative for all cases. $15\sqrt{f'_c}$, however, yields conservative results in all cases.

Test results of reinforced and prestressed concrete members subjected to pure torsion which failed due to crushing of the web are presented in Table 3.26.

The values of the shear stress due to the torsional moment at failure

$$v_{\max}(T) = T_{\text{test}}/[2A_0b_e] \quad (3.23)$$

and f'_c for each of the specimens of Table 3.26 are plotted in Fig. 3.38 for comparison. Once again the limit $15\sqrt{f'_c}$ although extremely conservative for some cases, is a safe lower bound value in the case of members subjected to pure torsion and experiencing web crushing.

In the case of combined shear and torsion, the shear stresses are additive on one side of the member and oppose each other on the opposite side. However, since the direction of the applied torsional moment is not always known, it is suggested that the shear stress be evaluated as the sum of the shear stresses due to shear and torsion obtained from Eqs. 3.21 and 3.23. In Table 3.27 the test results of prestressed concrete members subjected to combined shear and torsion failing due to web crushing are presented.

For comparison the values of v_{\max} at failure and f'_c for each of the specimens of Table 3.27 are plotted in Fig. 3.39.

Tests reported by Hsu (82) on reinforced concrete rectangular beams

(1) Member ID	(2) f'c ksi	(3) v(max) Eq. 3.23 Ksi	(4) (3) v(Eq. 3.20)	(5) (3) v(Eq. 3.22)	(6) Level of Prestress $\sigma/f'c$
B6	4.18	2.00	1.82	2.06	0.0
M6	4.26	2.13	1.92	2.17	
I6	6.64	2.80	2.01	2.28	
J4	2.43	1.40	1.67	1.89	
G5	3.90	1.78	1.68	1.90	0.0
K4	4.15	3.47	3.15	3.58	
C3	3.90	0.97	0.92	1.04	
C4	3.94	1.28	1.20	1.36	
C5	3.95	1.55	1.45	1.64	
C6	4.00	2.23	2.10	2.38	
			X = 1.79	X = 2.03	
			S = 0.60	S = 0.69	

Tests reported by Wyss, Garland and Mattock (173)
on reinforced concrete I-(I) and rectangular (R) members

C6(I)	6.24	4.74	3.54	4.01	0.0
D5(R)	6.79	2.49	1.78	2.02	
D6(R)	6.89	2.25	1.60	1.81	
			X = 2.31	X = 2.61	
			S = 1.07	S = 1.21	

Tests reported by Wyss, Garland and Mattock (173)
on prestressed concrete I-beams

A5(I)	6.00	4.05	3.07	3.48	0.19
A6(I)	6.00	4.19	3.17	3.60	0.19
D6(I)	6.00	4.62	3.50	3.97	0.09
C6(I)	6.0	4.95	3.75	4.25	0.09
			X = 3.37	X = 3.83	
			S = 0.31	S = 0.35	
Overall for Table 3.26			X = 2.25	X = 2.56	
			S = 0.90	S = 1.02	

Table 3.26 Torsion tests on reinforced and prestressed concrete members experiencing web crushing failures

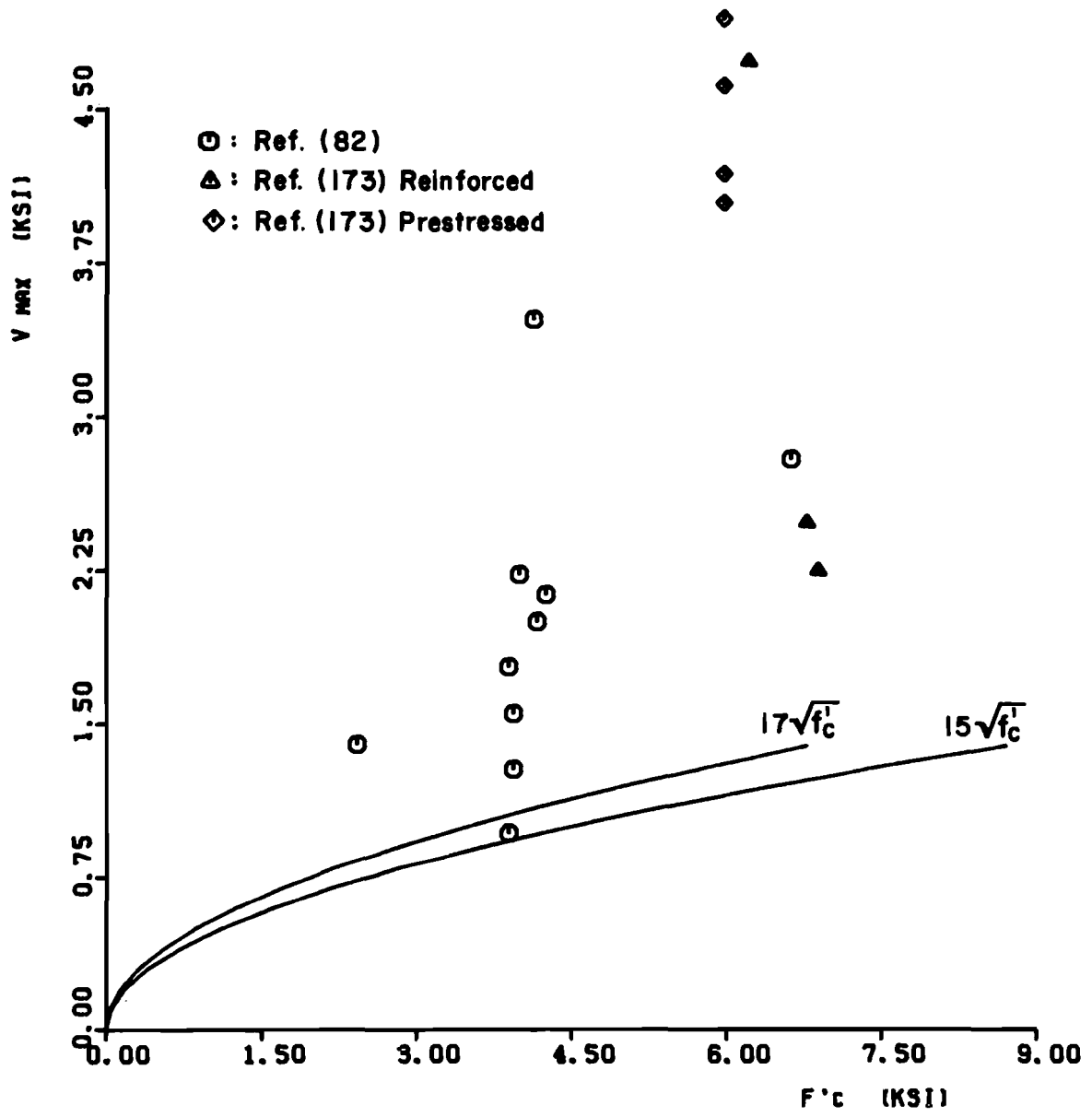


Fig. 3.38 Shear stress due to torsion at failure vs specified compressive strength of the concrete f'_c for the case of a reinforced and prestressed concrete beam failing due to web crushing

Tests reported by Henry and Zia (75) on prestressed concrete rectangular beams

(1) Member ID	(2) f'c ksi	(3) v (max) Eq. 3.21 ksi	(4) <u>(3)</u> v(Eq. 3.20)	(5) <u>(3)</u> v(Eq. 3.22)	(6) Level of Prestress $\sigma/f'c$
IV-4	5.90	2.14	1.63	1.85	0.13
IV-2-5	6.04	2.62	1.98	2.25	0.13
V-2-3	4.90	1.93	1.62	1.84	0.21
V-3-4	4.48	2.44	2.78	3.15	0.23
V-4-5	4.29	1.69	1.52	1.73	0.25
V-3-6	5.08	2.10	1.74	1.97	0.20
V-4-6	5.08	1.44	1.19	1.35	0.20
			X = 1.78	X = 2.02	
			S = 0.50	S = 0.57	

Tests reported by McMullen and Woodhead (113) on prestressed concrete rectangular beams

II-4	5.78	2.23	1.73	1.96	0.12
II-5	5.52	2.52	2.00	2.27	0.13
III-3	6.06	2.09	1.58	1.79	0.18
III-5	6.58	2.60	1.88	2.14	0.18
III-6	6.58	3.25	3.36	2.67	0.17
V-1	5.73	2.27	1.76	1.99	0.24
V-2	5.73	2.02	1.57	1.77	0.21
V-3	6.72	2.09	1.50	1.70	0.19
V-4	6.72	2.02	1.45	1.65	0.19
V-5	5.52	2.27	1.80	2.04	0.23
V-6	5.64	1.94	1.52	1.72	0.21
V-7	5.64	2.25	1.76	1.99	0.22
			X = 1.74	X = 1.97	
			S = 0.26	S = 0.29	
Overall for Table 3.27			X = 1.76	X = 1.99	
			S = 0.35	S = 0.40	

Table 3.27 Combined torsion and shear tests on prestressed concrete members experiencing web crushing

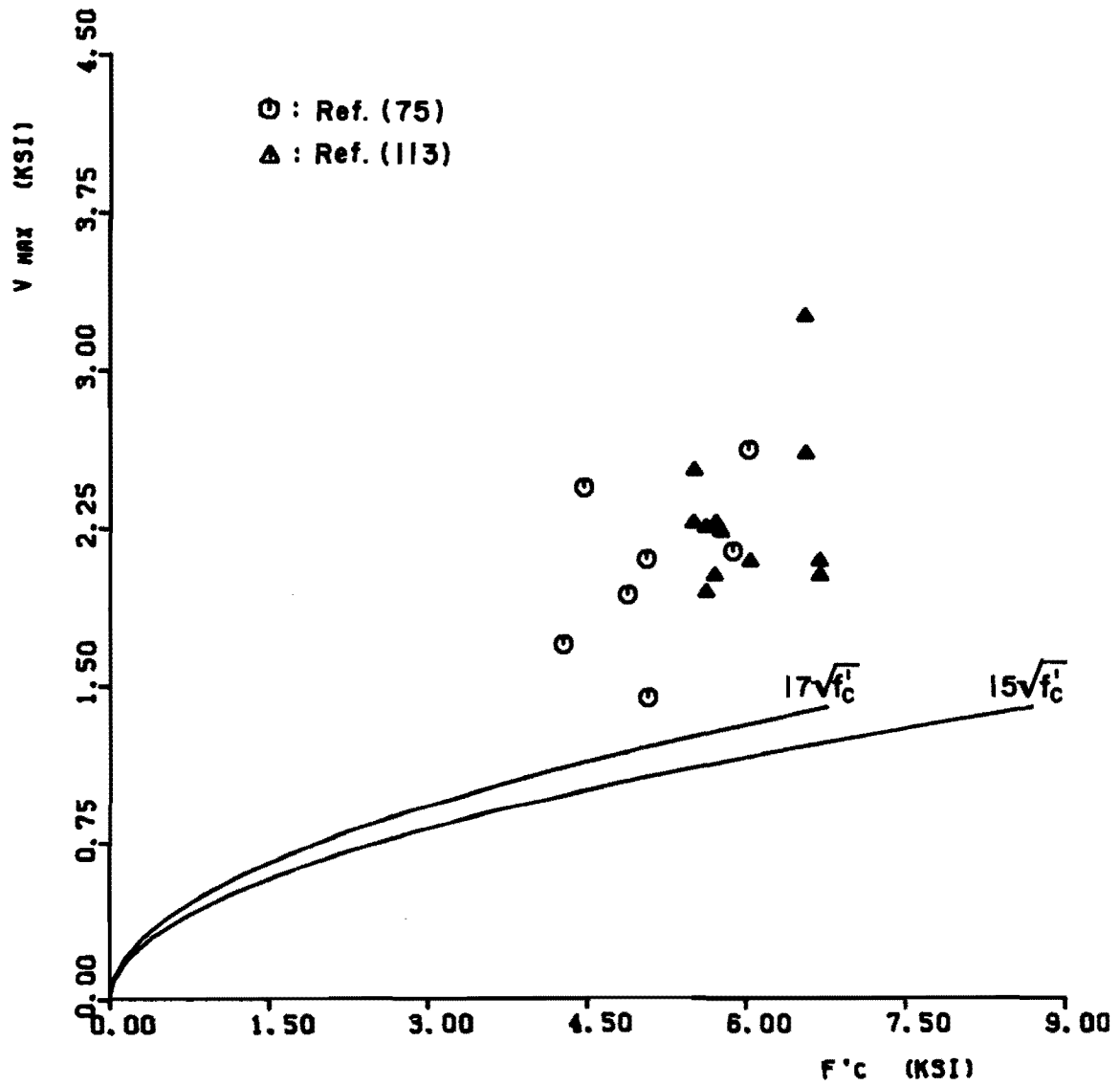


Fig. 3.39 Shear stress due to shear and torsion vs the maximum allowed shear stress for prestressed concrete members failing due to web crushing

As can be seen from Fig. 3.39, for the case of combined actions both limits (Eqs. 3.20 and 3.22) yield very conservative results. This also supports the assumption that evaluating the maximum applied shear stress when designing for the case of combined shear and torsion by summing the shear stresses due to shear and torsion obtained from Eqs. 3.21 and 3.23 would yield conservative results.

The fact that in Figs. 3.37, 3.38, and 3.39 the computed value of the shear stress at failure for each specimen larger than the possible limiting value $15\sqrt{f'_c}$ indicates that each specimen failed at a higher level of shear stress than that predicted by the web crushing criteria given in Eq. 3.22. Therefore, the requirement that f_d be limited to $30\sqrt{f'_c}$ appears to be very conservative. The lack of ductility in web crushing failures makes it highly desirable to be very conservative in this area.

In Fig. 3.40 the values of the shear stress at failure due to web crushing from shear and/or torsion, are compared with f'_c for each of the specimens of Tables 3.24, 3.25, 3.26 and 3.27. Also shown are the upper limits of $10\sqrt{f'_c}$ for shear and $12\sqrt{f'_c}$ for torsion as given in current AASHTO Specifications. The proposed new limit of $15\sqrt{f'_c}$ is plotted for comparison.

Figure 3.40 shows that the proposed limit of $15\sqrt{f'_c}$ is a conservative and realistic requirement and is somewhat less restrictive than the current upper limits in the AASHTO Standard Specifications (12,17).

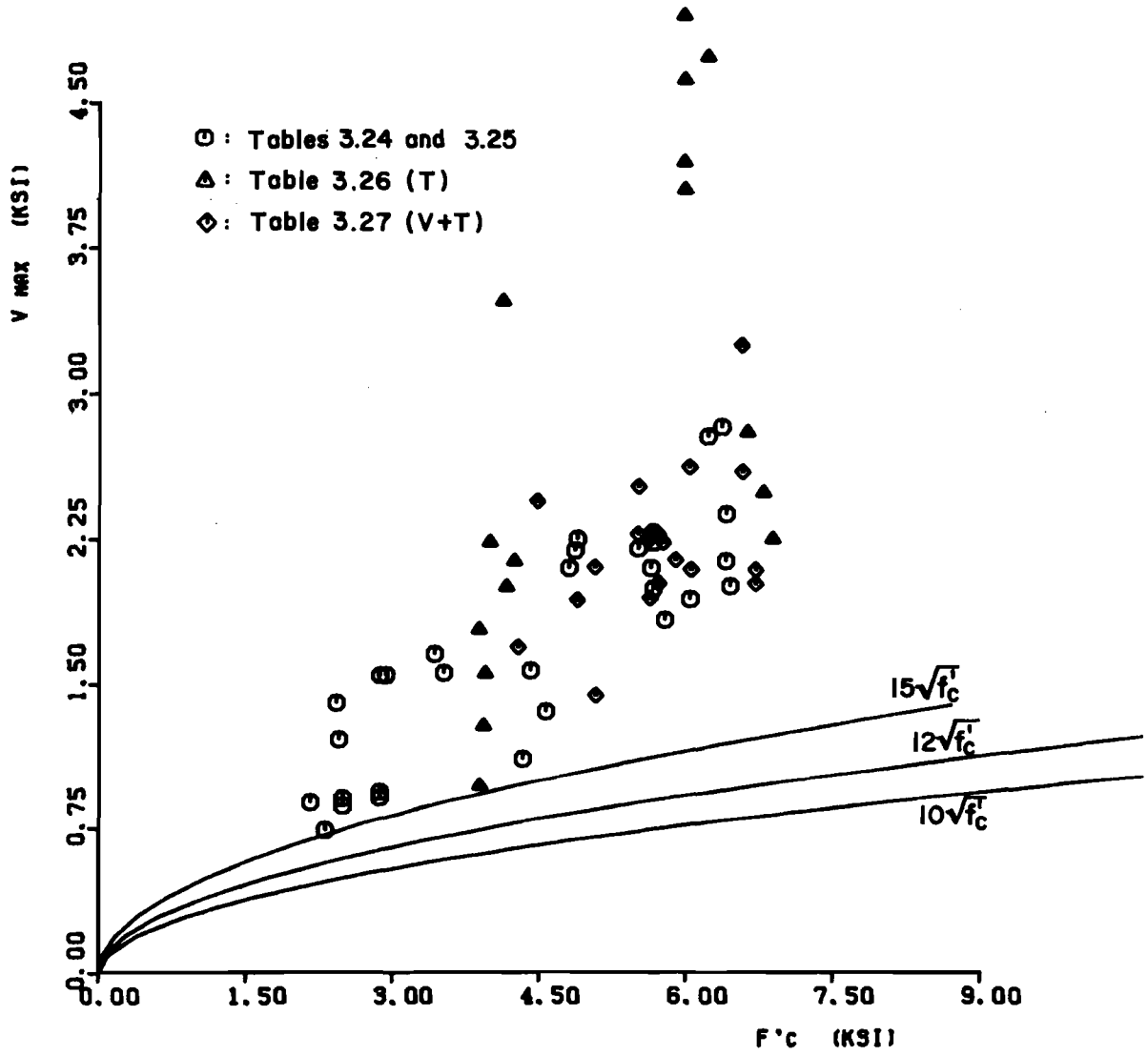


Fig. 3.40 Shear stress due to shear and/or torsion vs concrete compression strength f'_c for reinforced and prestressed concrete members failing due to web crushing

With regard to the proposed limit on the value of f_c as a function of f'_c the test results reviewed in this section indicate that the limit should be extended to include an f'_c of approximately 7000 psi. The new limit of 7000 psi is proposed due to the fact that it is the range covered by the available test data. Further information is required on very high strength concretes although the data trends look generally favorable.

3.7 Different Types of Failure

In this section those tests reported in references cited in Secs. 3.2, 3.3, and 3.4, which were excluded from tables and plots in those sections because both longitudinal and transverse reinforcement had not yielded at failure, are evaluated to ascertain the truss model accuracy in predicting the ultimate strength of such members. Theoretically, such members would not be covered by full truss behavior. Also in this section, several members in which the truss model predicted strength was not achieved because of poor detailing are examined.

3.7.1 Torsion. The test data shown in Tables 3.28 and 3.29 include pure torsion tests on reinforced and prestressed concrete beams of rectangular, inverted T and I cross section.

The test data shown in Table 3.28 include those beams in which only longitudinal reinforcement yielded at failure. The mean of the ratio of test to predicted torsional moment is 1.02 with the standard deviation 0.15. Table 3.29 includes data on beams in which only transverse reinforcement yielded prior to failure. The mean of the

Tests reported by Hsu (82) on reinforced concrete rectangular beams

(1) Member ID	(2) r	(3) T _{test} (k-in)	(4) T _u (Eq. 3.1) (k-in)	(5) α (Eq. 3.23) degrees	(6) λ (3) (4)	(7) v _{test} Eq. 3.23 ksi	(8) v(max) Eq. 3.22 ksi	(9) (7) (8)	(10) Level of Prestress $\sigma/f'c$
B5	1.0	497	619	43	0.80	1.77	0.97	1.82	0.0
B7		238	246	55	0.97	0.76	0.92	0.83	
D1		198	178	44	1.11	0.62	0.93	0.67	
D2		245	257	43	0.95	0.81	0.91	0.89	
D3		346	369	43	0.94	1.17	0.96	1.22	
D4		424	487	43	0.87	1.47	1.00	1.47	
J1		190	179	45	1.06	0.59	0.68	0.86	
C1		100	81	44	1.23	0.50	0.94	0.53	
C2		135	143	44	0.94	0.70	0.93	0.75	
					X = 0.99				
					S = 0.13				

Tests reported by McMullen and Rangan (114)
on reinforced concrete rectangular sections

B4	1.0	281	277	43	1.01	2.82	1.12	2.52	0.0
----	-----	-----	-----	----	------	------	------	------	-----

Tests reported by Mirza (116) on prestressed
concrete inverted T bent caps

TP55	0.10	960	746	38	1.82	2.71	1.07	2.54	0.06
------	------	-----	-----	----	------	------	------	------	------

Overall for Table 3.28

X = 1.02
S = 0.15

Table 3.28 Data on reinforced and prestressed concrete beams subjected to pure torsion where only the longitudinal reinforcement yielded prior to failure

Tests reported by Hsu (82) on reinforced concrete rectangular beams

(1) Member ID	(2) r	(3) Ttest k-in	(4) Tu (Eq. 3.1) K-in	(5) α (Eq. 3.23) degrees	(6) (3) (4)	(7) vtest Eq. 3.23 Ksi	(8) v(max) Eq. 3.22 Ksi	(9) (7) (8)	(10) Level of Prestress %/f'c
B10	1.0	304	362	23	0.84	1.09	0.93	1.17	0.0
M3		388	387	38	1.00	1.35	0.93	1.44	
M4		439	499	38	0.88	1.57	0.93	1.69	
M5		493	638	37	0.77	1.81	0.96	1.64	
J3		312	370	43	0.84	1.05	0.74	1.41	
G3		439	414	43	1.06	1.05	0.94	1.12	
					X = 0.90				
					S = 0.11				

Tests reported by McMullen and Rangan (114) on reinforced concrete rectangular beams

AlR	1.0	111	90	44	1.23	0.52	1.10	0.47	0.0
-----	-----	-----	----	----	------	------	------	------	-----

Tests reported by Mitchell and Collins (120) on prestressed concrete rectangular beams

P5	1.0	995	1098	24	0.91	1.35	1.13	0.66	0.30
----	-----	-----	------	----	------	------	------	------	------

Tests reported by Wyss, Garland and Mattock (173) on prestressed concrete I-beams

A4	0.29	430	569	26	0.76	3.64	1.16	3.13	0.19
B5	0.33	544	443	47	1.23	4.60	1.16	3.96	0.09

X = 1.0
S = 0.33
X = 0.95
S = 0.17

Overall for Table 3.29

Table 3.29 Data on reinforced and prestressed concrete beams under pure torsion with only yielding of the transverse reinforcement prior to failure

ratio of test to predicted torsional moment is 0.95 with a standard deviation of 0.17. From the test data in Tables 3.28 and 3.29 it appears that, in general for the case of pure torsion, the truss model yields reasonable results.

However, Hsu (82) in several cases (specimens B5, B10, M5, J3) reported test results which apparently show the truss predictions to be unconservative. But on close examination of these small beams with extremely heavy longitudinal and transverse reinforcement it was found that the calculated shear stresses due to torsion were far in excess of the web crushing limit proposed in Sec. 3.6. The calculated maximum shear stress due to torsion for those specimens is given in column (7) of Tables 3.28 and 3.29. Shown in column (8) of the same tables is the proposed limit value of the shear stress in order to preclude web crushing failures. In column (9) both values of the shear stress are compared. As can be seen, the shear stresses of specimens B5, B10, M5, and J3 as well as several others were far in excess of the limits set on the truss theory based on web crushing.

In specimen A4 from Ref. 173 the transverse reinforcement was not provided in the form of closed hoops. Instead, a single legged stirrup was placed in the web of the member. This poor detailing for torsion, together with a shear stress far in excess of the allowed value caused a premature failure.

These specimens should not be used in judging the overall accuracy of the truss model unless T_u is based on web crushing limits

from Sec. 3.6. If this is done, then all the values would be much greater than 1.

It appears that the lack of yielding of either one of the types of reinforcement increases the scatter in the accuracy of the basic truss model predictions. Such lack of yielding can be treated by improved truss model versions which are not as simple for design purposes (180,182).

This scatter is caused by the partial overreinforcement of the member, which induces at failure large tensile stresses in the other reinforcement together with excessive compression stresses in the diagonal strut of the truss model. These large stresses sometimes would lead to premature failures due to crushing of the concrete. These types of failure must be prevented in the truss model design approach.

3.7.2 Torsion-Bending. Shown in Table 3.30 are test data on reinforced and prestressed concrete beams of trapezoidal and rectangular solid and hollow cross sections subjected to combined torsion and bending. The test data from Ref. 86 in Table 3.30 belongs to beams where only the transverse reinforcement yielded at failure. Tests from Ref. 161 and specimen D1 from Ref. 33 belong to beams where only the longitudinal steel yielded prior to failure. In specimens D2 and D3 from Ref. 33, and specimen 1 from Ref. 70, neither yielding of the transverse or the longitudinal reinforcement was reported at failure.

Shown in column (5) of Table 3.30 are the values of the previously explained dispersion index I (see Fig. 3.5), which is used as a measure of the dispersion between test obtained values and truss model

Tests reported by Johnston and Zia (86) on prestressed concrete box beams

(1) Member ID	(2) r	(3) $\frac{M_{test}}{\mu_o}$ Eq. 3.15	(4) $\frac{T_{test}}{\tau_o}$ Eq. 3.1	(5) I	(6) v_{test} Eq. 3.23 ksi	(7) $v(\max)$ Eq. 3.22 ksi	(8) $\frac{(6)}{(7)}$	(8) Level of Prestress $\sigma/f'c$
H-0-3-2	0.5	0.06	0.88	0.85	0.74	0.96	0.77	0.13
H-0-3-3		0.25	0.93	0.80	0.79	0.96	0.82	
H-0-3-4		0.14	0.93	0.82	0.79	0.96	0.82	
H-0-6-2		0.07	0.95	0.88	0.57	0.96	0.59	
H-0-6-4		0.17	1.09	0.93	0.66	1.12	0.59	0.09
				X = 0.86				
				S = 0.05				

Tests reported by Taylor and Warwaruk (161) on prestressed concrete trapezoidal box beams

T1	0.36	0.68	0.86	0.96	0.50	0.95	0.53	0.12
T2	0.36	1.09	0.58	1.19	0.34	0.98	0.35	0.12
				X = 1.08				
				S = 0.16				

Tests reported by Gesund, Schuette, Buchanan and Gray (70) on reinforced concrete rectangular beams

1	0.62	0.40	0.94	0.97	1.22	1.06	1.15	0.0
---	------	------	------	------	------	------	------	-----

Tests reported by Pandit and Warwaruk (33) on reinforced concrete rectangular beams

D1	0.34	0.74	0.57	0.87	1.43	1.05	1.36	0.0
D2		0.42	0.94	0.80	2.36	1.07	2.20	
D3		0.23	0.90	0.65	2.25	0.98	2.30	

				X = 0.77				
				S = 0.11				
Overall for Table 3.30				X = 0.88	N = 11			
				S = 0.14				

Table 3.30 Data on reinforced and prestressed concrete members subjected to torsion bending

predictions, as given by the proper interaction equations, measured along radial lines from the origin. The mean of the dispersion index I for all the specimens shown in Table 3.30 is 0.88 and the standard deviation 0.14.

It seems that the truss model predictions become unconservative in the case of combined torsion-bending in the case of members where yielding of both reinforcements is not reached at failure. More so in the cases where yielding of the longitudinal reinforcement is not reached prior to failure. However, these apparent unconservative results again can be explained by the effect of partial overreinforcement discussed in the previous section. The large compression stresses induced by the partial overreinforcement eventually lead to failure due to crushing of the concrete in the web such as in the case of member D3 on Table 3.30. In these cases the value of T_u should be based on the web crushing limits suggested in Sec. 3.6. If this is done then the values obtained would be very conservative. Better agreement should be possible if the effective shell thickness is determined as suggested by Marti (182).

3.7.3 Torsion-Bending-Shear. Table 3.31 shows data on prestressed concrete beams of rectangular solid and box sections where only yielding of the transverse reinforcement was reported at failure. The dispersion index I shown in column (6) of Table 3.31 is once again used as a measure of the accuracy of the truss model predictions in the same manner previously explained in Sec. 3.4.

Tests reported by Mukherjee and Warwaruk (123) on prestressed concrete rectangular sections

(1) Member ID	(2) r	(3) M _{test} Mu _o Eq. 3.5	(4) T _{test} Mu _o Eq. 3.1	(5) V _{test} Vu _o Eq. 3.9	(6) I	(7) v _{test} (T,V) ksi	(8) v(max) Eq. 3.28 ksi	(9) (7) (8)	(10) Level of Prestress $\sigma/f'c$
V122	1.0	1.07	0.82	0.27	1.61	1.50	0.98	1.53	0.13
V202		1.52	0.88	0.31	2.09	1.73	1.06	1.63	0.26
V203		0.34	1.19	0.19	1.38	2.22	1.05	2.11	0.27
V204		0.20	1.23	0.11	1.34	2.27	1.13	2.01	0.25
V205		0.07	1.12	0.04	1.16	2.04	1.12	1.81	0.25
V223		0.56	1.28	0.19	1.63	2.22	1.14	1.94	0.23
V224		0.23	1.38	0.11	1.51	2.36	1.16	2.04	0.23
V225		0.07	1.23	0.05	1.27	2.07	1.10	1.88	0.25
				X =	1.50				
				S =	0.29				

Tests reported by Johnston and Zia (86) on prestressed concrete box sections

H-4-3-1	0.5	0.06	0.82	0.11	0.89	1.84	0.96	1.92	0.13
H-4-3-2		0.14	0.78	0.22	0.96	2.84	0.96	2.97	0.13
H-4-6-1		0.07	0.94	0.13	1.02	1.48	1.15	1.29	0.09
H-4-6-3		0.10	0.55	0.60	0.86	4.60	1.15	4.00	0.09
H-4-6-5		0.17	0.89	0.49	1.27	4.07	0.10	3.71	0.10
H-6-3-1		0.23	0.93	0.13	1.20	2.06	1.15	1.80	0.09
H-6-3-2		0.25	0.86	0.24	1.19	3.13	1.15	2.73	0.19
H-6-6-1		0.05	0.97	0.14	1.03	1.59	1.10	1.45	0.10
H-6-6-2		0.10	0.91	0.26	1.06	2.39	1.15	2.08	0.10
				X =	1.05				
				S =	0.14				
Overall for Table 3.31				X =	1.26				
				S =	0.31				

Table 3.31 Data on prestressed concrete beams under combined torsion-bending-shear experiencing only yielding of the transverse reinforcement at failure

For the data shown in Table 3.31 the mean of the dispersion index I is 1.26 and the standard deviation 0.31. In this case the truss model predictions seem to be overconservative. Very few specimens were under strength. The few which experienced lower values were well within normal scatter. There was considerably more scatter in the dispersion index. This indicates that the lack of yielding of both reinforcements introduced other factors that are not adequately represented by the truss model.

The test data shown in Table 3.32 are for prestressed rectangular beams experiencing only yielding of the longitudinal reinforcement at failure. The very conservative predictions obtained in these cases seem to confirm the assumption that members experiencing only yielding of the longitudinal reinforcement at failure might be in a transition state between the uncracked and the full truss state as far as shear stresses are concerned. This would introduce an additional concrete contribution to the ultimate shear capacity of the member. This would explain the conservative results given by the truss model in such cases.

3.7.4 Failures Due to Inadequate Detailing. During the course of this study it was made clear that adequate detailing is of utmost importance in the design approach using the truss analogy in the case of members subjected to shear, torsion-bending, or combined torsion-bending-shear.

In this section several cases of failure due to inadequate detailing are studied to highlight the importance of adequate detailing

Tests reported by Mukherjee and Warwaruk (123) on prestressed concrete rectangular sections

(1) Member ID	(2) r	(3) $\frac{M_{test}}{\mu_{uo}}$ (Eq. 3.5)	(4) $\frac{T_{test}}{\tau_{uo}}$ (Eq. 3.1)	(5) $\frac{V_{test}}{\nu_{uo}}$ (Eq. 3.9)	(6) I	(7) v_{test} (T, V) (ksi)	(8) v_{max} Eq. 3.22 (ksi)	(9) 7/8	(10) Level of Prestress σ/f'_c
V107	1.0	1.08	0.28	0.23	1.15	0.61	0.91	0.67	0.16
V127	1.0	1.56	0.42	0.32	1.84	0.84	1.02	0.82	0.12
V207		1.69	0.45	0.36	2.05	0.97	1.07	0.91	0.27
V227		1.99	0.66	0.50	2.86	1.32	1.07	1.24	0.26

X = 1.98
S = 0.70

Table 3.32 Data on prestressed concrete members subjected to torsion-bending-shear where only the longitudinal steel yielded at failure

in the design as well as to illustrate how the truss model can be useful to handle the special detailing cases.

Shown in Table 3.33 are data for prestressed concrete inverted T bent caps failing prematurely due to inadequate detailing. Specimens TP43, TP54, and TP63 from Ref. 116 were prestressed concrete inverted T bent caps subjected to pure torsion (see Fig. 3.41a). As reported in Ref. 116, failure of specimens TP43 and TP54 was due to a combination of punching action and bracket action in the bottom flange of the inverted T bent cap. In specimen TP63, failure was entirely due to punching action. Punching action failure of the flange occurred by punching of the concrete along a truncated pyramid around the concentrated load (see Fig. 3.41b). This phenomenon caused the separation of the pyramid from the bottom of the beam without any crushing of the concrete in the compression zone of the flange. The other contributor to the failure mechanism was produced by the flange acting as a short bracket to transmit the load to the web. This phenomenon was analyzed in Sec. 2.2.3 of this study. As previously explained, the truss model can be used to determine the necessary transverse reinforcement in the flange. Supplementary horizontal transverse reinforcement should be distributed as shear friction reinforcement to control cracking along the potential slip plane. If the crack faces are rough and irregular, any slip will be accompanied by a horizontal separation of the crack faces. At ultimate the horizontal crack separation will be sufficient to stress this reinforcement to its yield point.

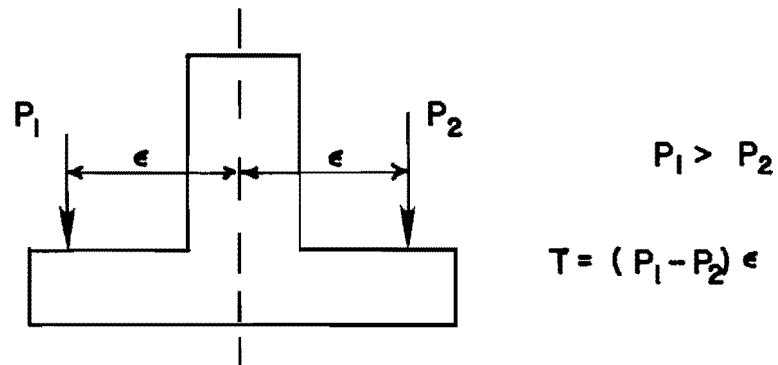
Tests reported by Mirza (116) on prestressed concrete inverted T beams

(1) Member ID	(2) r	(3) Ttest (k-in)	(4) Tu(Eq 3.1) (in-kip)	(5) $\frac{Ttest}{Tu}$	(6) Tan α Eq. 3.16	(7) Level of Prestress σ/f'_c
TP43	2.94	549	789	0.70	0.821	0.16
TP54	0.16	665	1019	0.65	0.568	0.11
TP63	2.94	648	1149	0.56	1.164	0.16

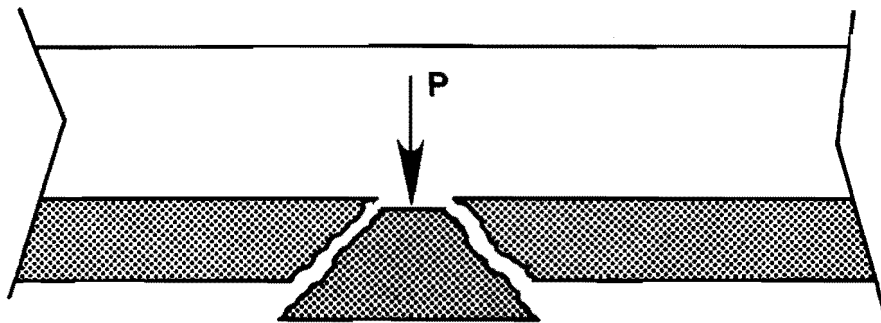
$$X = 0.64$$

$$S = 0.07$$

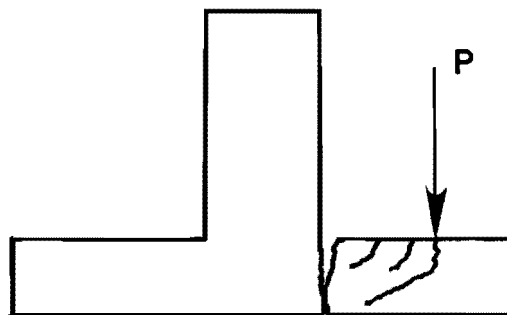
Table 3.33 Data on prestressed concrete inverted T bent caps failing prematurely due to improper detailing



(a) Typical cross section



(b) Punching failure (sideview)

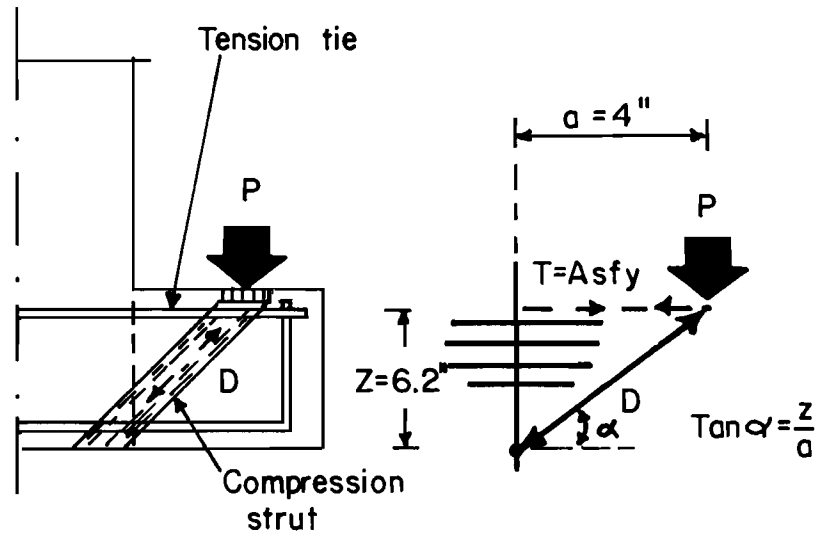


(c) Bracket action

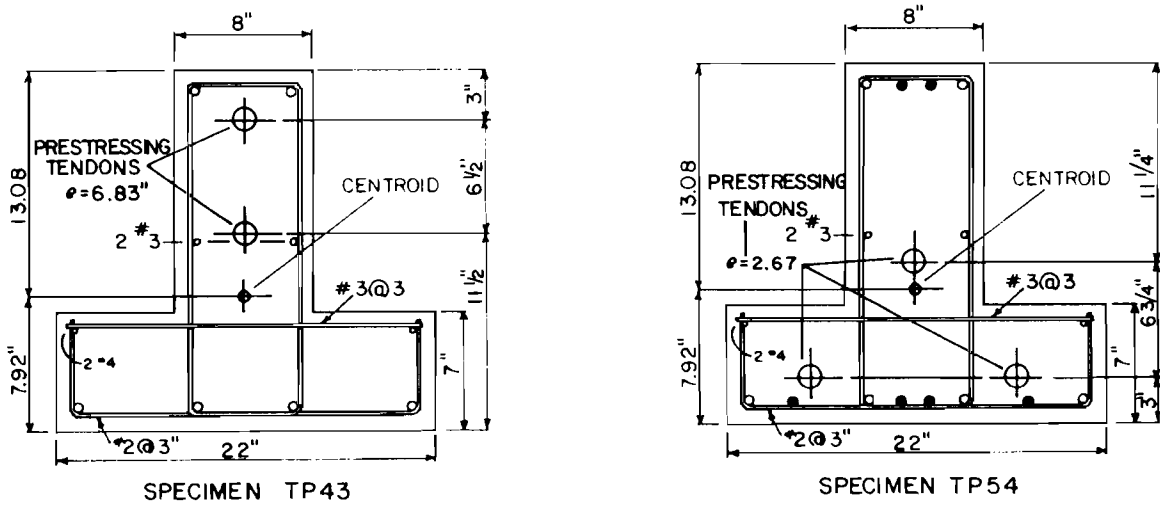
Fig. 3.41 Cross section and types of premature failures due to improper detailing occurring in specimens TP43, TP54, and TP63 (from Ref. 116)

Applying the previous discussion to Fig. 3.41c, the design of the web-flange section can be conducted using a simple truss analogy consisting of the upper transverse reinforcement in the bracket acting as a horizontal tie with concrete struts at an angle α acting as inclined compression members (see Fig. 3.42a).

The design details of this type of truss model have been discussed in Sec. 2.2.3. The ultimate load P acting on those two specimens was 78.4 kips in TP43 and 95 kips for TP54. The flange region of TP43 was analyzed using the truss model shown in Fig. 3.42 and assuming an effective width of flange as the base plate width, 6 in., plus $2\sqrt{3}$ times the truss model depth. This was found assuming $\alpha = 30^\circ$ for the transverse direction ($b_{eff} = 6 + (2\sqrt{3})(5.6) = 25.4$ in.). The truss model indicated that the effective tension steel A_s was 0.99 in.² since f_y was 70 ksi. This could develop a tension tie force of 69k. The transverse truss model shown in Fig. 3.42a indicated that the required tension force was 58k for TP43 and 68k for TP54. The area provided to act as a tension tie in the flange region of the member was 0.87 in.² Thus, if the transverse reinforcement was only 85% effective in TP43, failure would occur at the actual test load. Even if fully effective, the load limit in TP54 would be the test load. Since the outer end anchorage on the transverse #3 bars was a tack weld to #4 longitudinal bars, it is somewhat surprising that the flanges resisted load as well as they did. However, it is clear that the inadequate transverse reinforcement in the flange kept the full strength of the



(a) Truss analogy for the flange region together with well distributed horizontal shear reinforcement



(b) Details of specimens TP43 and TP54 (from Ref. 116)

Fig. 3.42 Truss model and reinforcement details of the web flange connection region of the inverted T-bent cap

girders from being developed. Thus, improper detailing was the basic cause of the premature failure.

The punching shear mechanism which was involved in the failure of these specimens constitutes a problem of major significance in the case of slab members (two-way shear action). The problem of shear in slabs (two-way members) is very different from the problem of shear in beams (one-way elements). It is necessary to recognize the difference between the behavior of beams and slabs. It has been found (28) that in the area where principal bending moments are significant the nominal ultimate two way or punching shear stress which can be developed in a slab is considerably greater than the one way shear strength in a beam. Because shear in slabs is a multidimensional problem, this increase is associated with factors not usually associated with the behavior of beams:

1. Distribution of moments.
2. Lack of symmetry.
3. Inadequacy of simple static analysis.
4. In-plane forces generated by restraints provided by the supports and by nonyielding portions of the slab.

Because of the complexity involved in the case of two-way members and the inclination in American design to develop equations or specifications suitable for codification, most research on the shear strength of slabs has been concerned with the generation of experimental data to support the current empirical design procedures used in the ACI Building Code (24) and the AASHTO Standard Specifications (12). Consideration of two-way shear is specifically excluded from this study.

The importance of good detailing is shown in the values of the ratio of torsional moment at failure to the predicted torsional capacity shown in Table 3.33. The mean of the ratio was 0.63 and the standard deviation 0.07. This clearly indicates the danger involved in the case of premature failures, i.e. failures where yielding of the steel reinforcement is not reached because of improper detailing of the member.

Table 3.34 shows data on reinforced concrete L-beams under combined torsion-bending-shear which failed prematurely due to inadequate detailing. Specimens 3LS-4 and 3LS-7 from Ref. 104 failed locally at the supporting diaphragms. Unfortunately in this case, no more information was available in regard to the actual causes of failure. Although beam 3LS-4 shows unconservative results, beam 3LS-7 seemed to yield reasonable results. However, without more information no further conclusions can be drawn from these two specimens.

Shown in Table 3.35 are data for specimen 0.5B from Ref. 50. This specimen was a prestressed concrete I-beam with web reinforcement and a composite slab cast on top. Beam 0.5B was about a one-half scale model of the Texas Standard Type B girder. This member was subjected to a uniformly distributed load. Specimen 0.50B was tested in a different phase of this research project. Details of all the specimens as well as the loading scheme are reported by Castrodale (50).

Figure 3.43 shows details of the cross section at the end regions of the member. Figures 3.44a and 3.44b illustrate the premature failure that took place during the testing of this specimen.

Tests reported by Liao and Ferguson (104) on reinforced concrete L-beams

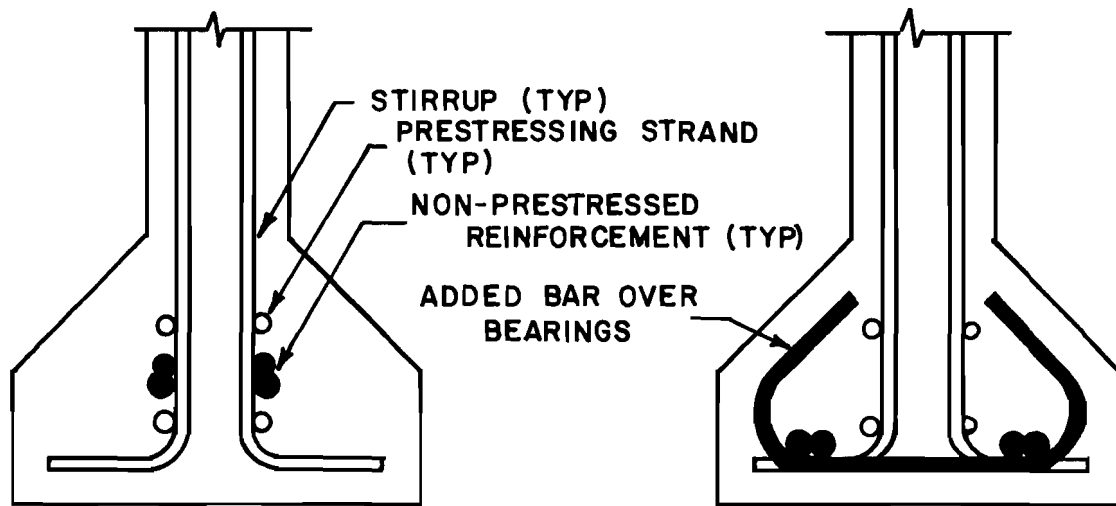
(1) Member ID	(2) r	(3) $\frac{T_{test}}{T_{uo}}$ (Eq. 3.5)	(4) $\frac{M_{test}}{M_{uo}}$ Eq. 3.5	(5) $\frac{V_{test}}{V_{uo}}$ Eq. 3.9	(6) I	(7) Level of Prestress σ/f'_c
3LS-4	1	0.62	0.30	0.17	0.80	0.0
3LS-7	1	0.91	0.26	0.14	1.06	0.0

Table 3.34 Data on reinforced concrete L-beams under combined torsion-bending-shear failing locally at the diaphragm region

Tests reported by Castrodale (50) on prestressed concrete I-beams

(1) Member ID	(2) Section from support C.L. (ft)	(3) $\frac{M_{test}}{M_{uo}}$ Eq. 3.13	(4) $\frac{V_{test}}{V_{uo}}$ Eq. 3.14	(5) I	(6) $\rho v f_y$ (psi)	(7) Level of Prestress σ/f'_c
050B	0.0	0.0	0.47	0.47	290	0.11
	1.367	1.20	0.38	0.49	290	
	2.73	0.35	0.29	0.51	290	
	4.10	0.46	0.26	0.58	170	
	5.467	0.53	0.14	0.56	170	
	Centerline	0.56	0.0	0.56	170	

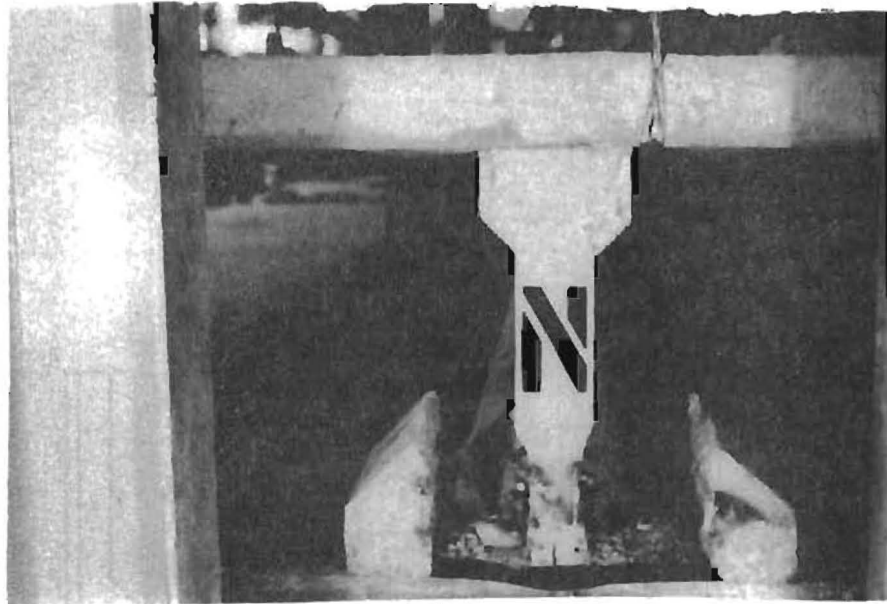
Table 3.35 Data on prestressed concrete I beam 0.50B (from Ref. 50)



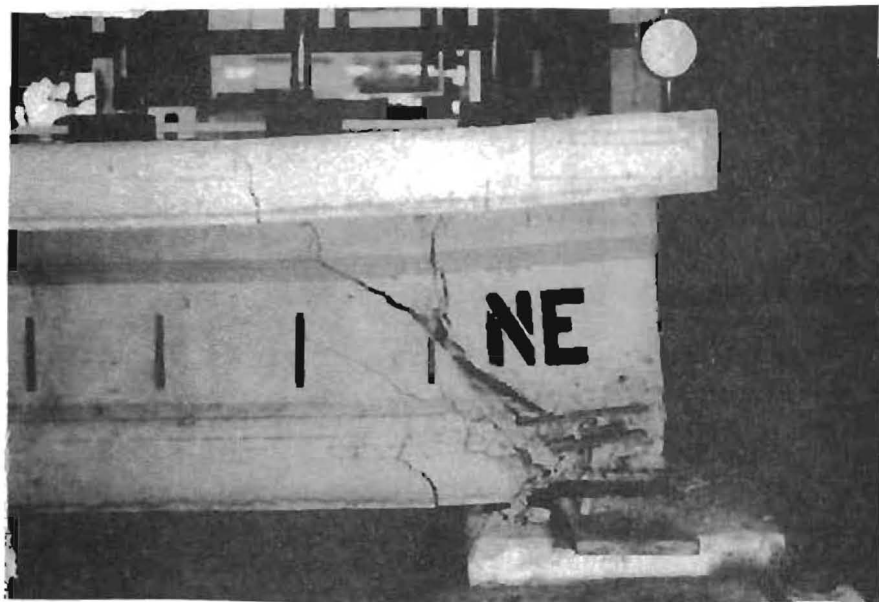
(a) Specimen 0.5B (also Specimens 0.5A and 0.4A)

(b) Revised cross section for Specimens 0.4B and 0.45

Fig. 3.43 Revision in reinforcement detailing at the end region due to premature failure of specimen 0.5B



(a)



(b)

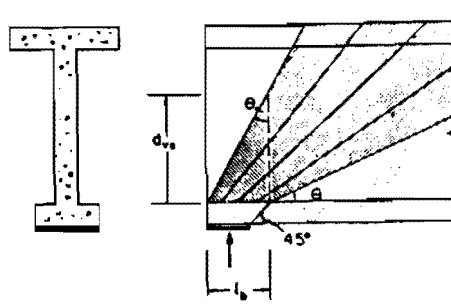
Fig. 3.44 Premature failure due to inadequate detailment of the end region of specimen 0.5B

As can be seen from Fig. 3.44a there was a complete separation of the bottom flange from the vertical web of the member at the bearing. The mechanisms involved in this premature failure due to improper detailing are examined with the aid of the truss model.

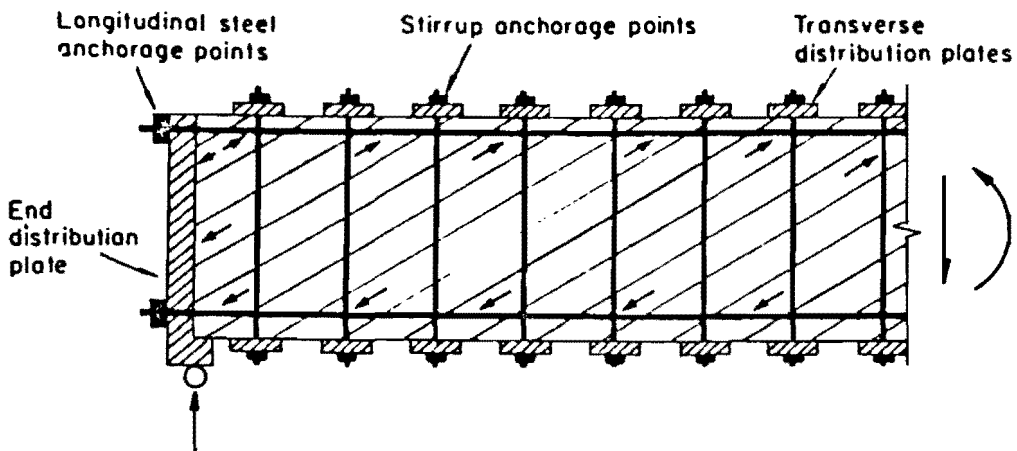
Figure 3.45a from Ref. 56 illustrates the fanning effect of the diagonal compression struts of the truss model at the end regions of the member. This fanning effect, previously explained in Sec. 2.2.2, results in high diagonal compression stresses which in the case of flange sections are directly transmitted through the vertical web of the member.

The concentration of diagonal compression stresses can be attenuated by adequately detailing the longitudinal steel reinforcement at the end regions of the member. As shown in Figs. 3.45b and 3.45c from Ref. 56, the attenuation of the diagonal compression stresses is achieved by distributing the horizontal component of the diagonal compression strut over the entire end region of the members by means of end distribution plates, as shown in Fig. 3.45b, or by the uniform distribution of the longitudinal reinforcement, as shown in Fig. 3.45c.

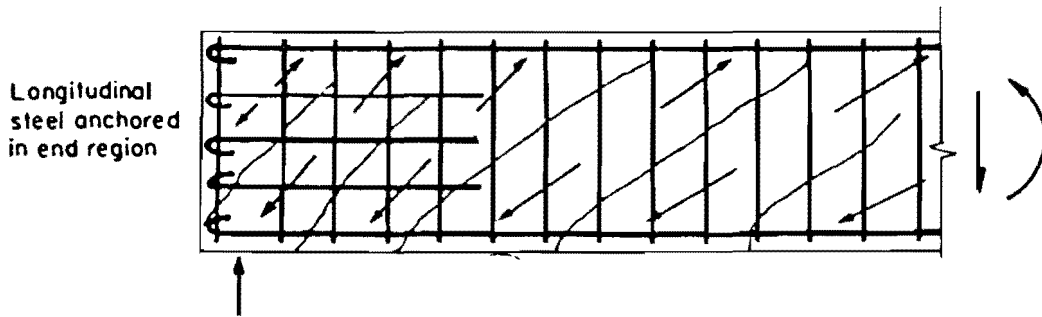
The large concentration of diagonal compression stresses induced by the improper detailing at the end regions of beam 0.50B was the major cause of the premature failure of this specimen. As can be seen from Fig. 3.43a, the concentration of all the longitudinal reinforcement at one particular location failed to adequately distribute the diagonal compression stresses and caused an excessive concentration of these over the bearing area, as shown in Fig. 3.45a.



(a) Fanning of diagonal compression at ends of beams



(b) Uniform distribution of the diagonal compression stresses by means of end distribution plates



(c) Uniformly distributed longitudinal steel at the ends of the member

Fig. 3.45 Distribution of the diagonal compression stresses at the end regions of simple supported beams where the reaction induces compression (from Ref. 56)

This large concentration of diagonal compression forces caused extreme deformation of the neoprene bearing pad. These deformations induced tensile splitting stresses between the web and the bottom flange. Closed stirrups at the end of the girder had been omitted. The lack of horizontal reinforcement across this failure plane allowed the crack to grow without control and finally caused separation of the bottom flange from the web as shown in Figs. 3.44a and 3.44b. In order to prevent this type of failure in subsequent specimens the detailing of the cross section at the end region was changed as shown in Fig. 3.43b. The longitudinal steel was more evenly distributed across the entire tension flange and additional reinforcement to hold the flanges and vertical web together was added over the bearing area. The revised design performed very satisfactorily.

The data shown in Table 3.35 are plotted in Fig. 3.46. The ratios of tested vs predicted values are plotted for different sections along the span of the member. Fig. 3.46 together with the values of the dispersion index I of Table 3.35 for different sections along the span-length of the member clearly illustrate the unconservative results caused by the premature failure of specimen 0.50B due to inadequate detailing.

The examples of premature failures due to improper detailing examined in this section help to illustrate the danger involved from poor detailing procedures. They also help to show how the truss model can be utilized to first spot the problematic regions and then to

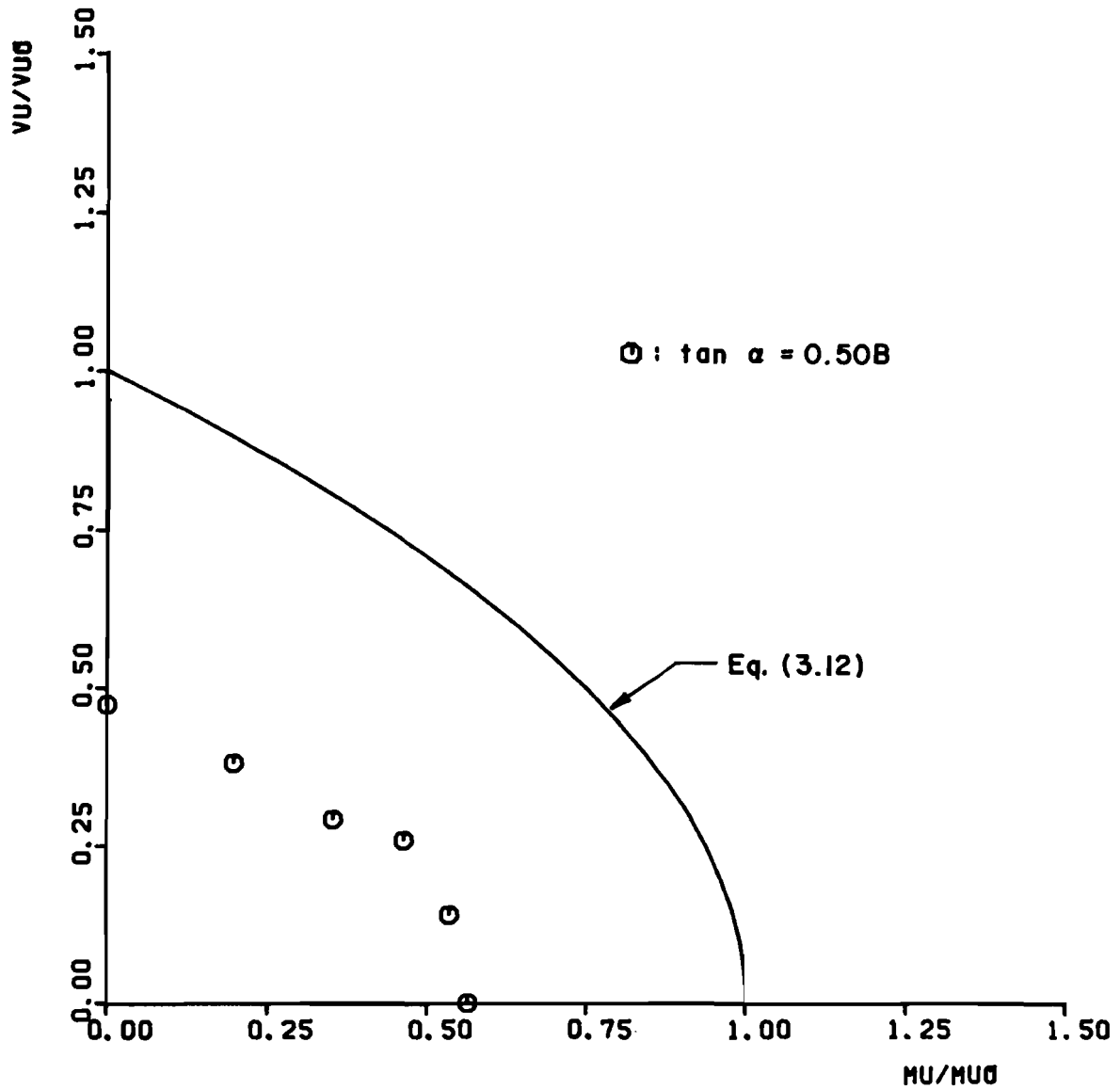


Fig. 3.46 Comparison between the ultimate load interaction predicted by the truss model and the ultimate test values at different sections along the span length for beam 0.50B

adequately detail the member so that its ultimate strength is fully attained.

3.8 Evaluation of the Additional Concrete Contribution in the Uncracked and Transition States

In Sec. 2.5 it was suggested that three well-defined failure states could be distinguished in the case of reinforced and prestressed concrete beams subjected to shear and/or torsion. The first is the uncracked state. This failure state is characterized by a shear failure when first inclined cracking of the web occurs. Then there is a transition state for the section at which failure might be in between the uncracked state and its ultimate full truss state. Failure occurs sometime after initial inclined cracking but before full development of the truss state.

In Sec. 2.5 it was also suggested that in the uncracked and transition states the concrete in the web contributes an additional shear resistance. In the uncracked state this concrete contribution is equal to the shear stress necessary to produce initial diagonal cracking in the web of the member, v_{cr} , and is taken equal to

$$v_{cr} = 2 \sqrt{f'_c} \quad (3.24)$$

where f'_c is the specified compressive strength of the concrete, psi.

It should be noted that the a/d or M/V_d effect is not included in the v_{cr} expression. The reason is that the a/d ratio influences the ultimate strength of the member, but it has no bear on the shear stress required to produce initial diagonal cracking.

As more diagonal cracks appear in the web, the member enters a transition state in which more cracking takes place and/or the previously existing cracks continue to grow and become wider. The shear carrying capacity of the concrete in the web relies heavily on mechanisms such as aggregate interlock and the tensile capacity of the concrete. Obviously, as the cracking becomes more extensive the contribution of such mechanisms should continuously diminish. Thus, in this transition state the concrete in the web should provide an additional continuously diminishing shear resistance.

Thürlimann (162) and the Swiss Code (156) suggest that the concrete contribution can be taken equal to the uncracked shear strength v_{cr} up to first diagonal cracking. It can then be assumed as continuously diminishing and finally becoming zero when the applied shear stress equals to 3 times the uncracked shear strength v_{cr} .

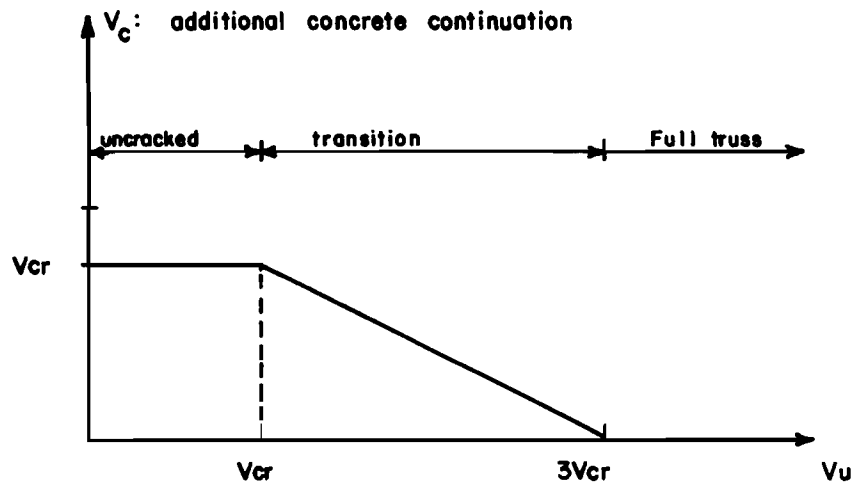


Fig. 3.47 Concrete contributions for the case of reinforced concrete members (from Refs. 156 and 162)

Figure 3.47 shows the proposed concrete contribution in the uncracked and transition states for the case of reinforced concrete members. Since only underreinforced sections are being considered and premature failures due to either crushing of the concrete or poor detailing are avoided, the presence of prestress will only influence the cracking load and will not influence the ultimate load of prestressed concrete members (162,165,166) in the full truss state.

Consider the case of a prestressed concrete member prior to cracking subjected to a bending moment and a shear force. The Mohr circle for an element at the neutral axis of the member is shown in Fig. 3.48.

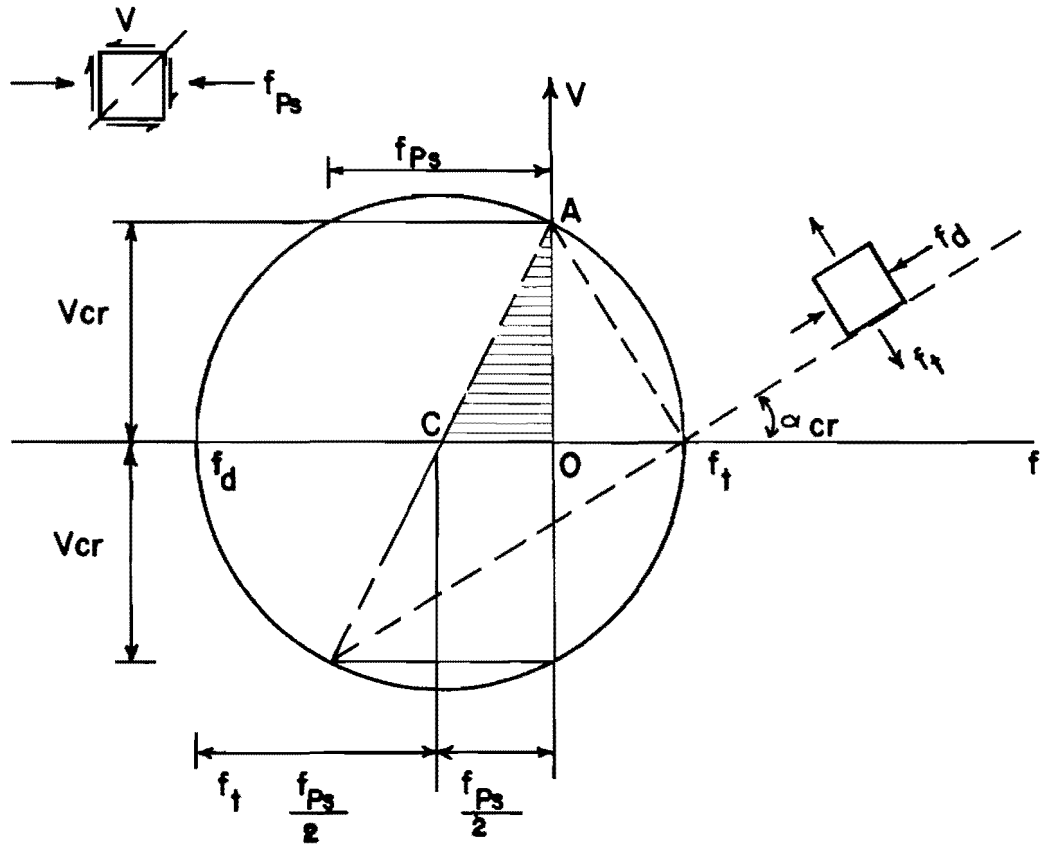
From Fig. 3.48, it becomes apparent that since the resulting principal tension stress is smaller than the applied shear stress the cracking load for the member is increased by a factor K due to the presence of prestressing where

$$K = [1 + (f_{ps}/f_t)]^{0.5} \quad (3.25)$$

The term f_{ps} is the compression stress at the neutral axis of the member due to the effective prestress force F_{se} and can be expressed as:

$$f_{ps} = F_{se}/A_c \quad (3.26)$$

where A_c is the gross area of the prestressed concrete member. The term f_t is the principal tensile stress required to produce diagonal cracking of the concrete member, and will be taken equal to v_{cr} from Eq. 3.24. Thus, in the case of prestressed concrete members the concrete



$$\begin{aligned} \bar{A}O &= [(\bar{c}A^2 - \bar{c}O)^2]^{0.5} = v_{cr} \\ v_{cr} &= [(f_t + \frac{f_{ps}}{2})^2 - (\frac{f_{ps}}{2})^2]^{0.5} \\ &= f_t \sqrt{1 + (f_{ps}/f_t)} \\ v_{cr} &= Kf_t \end{aligned}$$

Fig. 3.48 Effect of prestressing on the shear strength of an uncracked concrete member

contribution in the uncracked state is taken equal to $K \cdot v_{cr}$. By assuming continuously diminishing resistance function due to the K term, the Swiss Code (156) suggests that the concrete contribution in the transition state varies linearly between the uncracked shear strength of the prestressed concrete member, $K \cdot v_{cr}$ at the beginning of the transition state to a value of zero when the applied shear stress is equal to $(2 + K) \cdot v_{cr}$. However, while $K = \sqrt{1 + f_{ps}/f_t}$ the Swiss code imposes a strict limit of 1 on K in those regions of the member where the resulting extreme fiber tensile stress at ultimate exceeds twice the cracking shear stress v_{cr} . Figure 3.49 shows the additional concrete contribution for the case of prestressed concrete members.

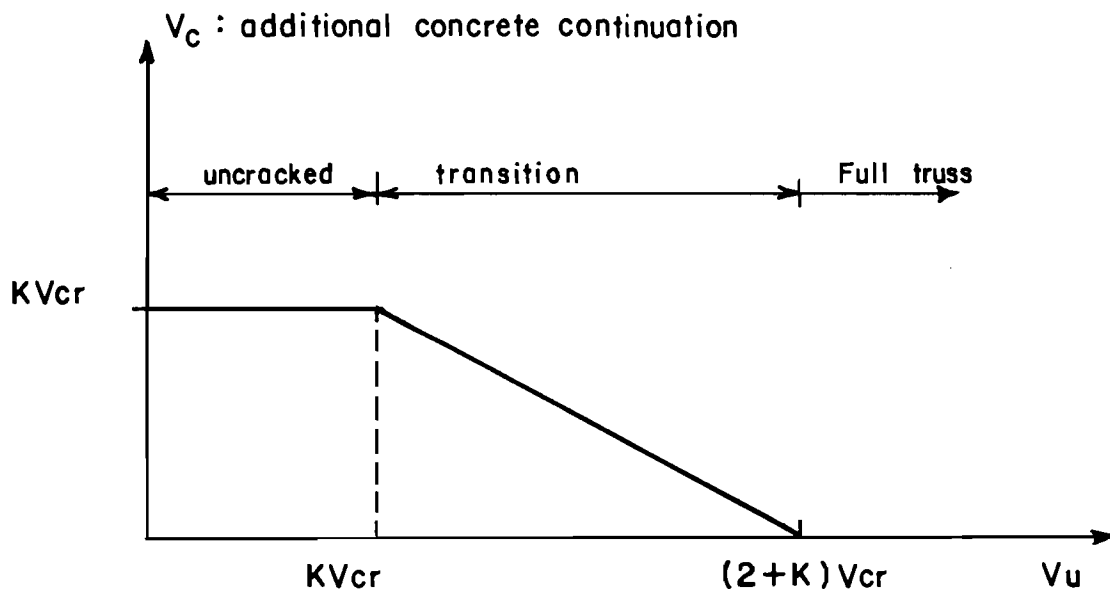


Fig. 3.49 Additional concrete contribution for the case of prestressed concrete members (156, 162)

Thürlimann (162) suggests that the value of K can be taken equal to 2. The study presented in this section strongly supports such a limit. Thus, it is recommended that for the case of prestressed concrete members K be evaluated using Eq. 3.25 but must not be taken greater than 2.

In this section this approach for quantifying the additional concrete contribution in the transition state, shown in Figs. 3.47 and 3.49 for reinforced and prestressed members, respectively, is evaluated using test data of reinforced and prestressed concrete members failing in shear and containing no or very small amounts of web reinforcement. The ratio of web reinforcement is defined as

$$\rho_v = A_v/[b_w*s] \quad (3.27)$$

Members with very light web reinforcement are those where the ratio of web reinforcement evaluated using Eq. 3.27 times the yield strength of the web reinforcement $\rho_v f_y$ is less than 100 psi.

Data from Ref. 99 for reinforced concrete beams with no or very light web reinforcement and subjected to bending and shear by means of concentrated loadings are presented in Tables 3.36, 3.37, 3.38, 3.39, and 3.40. The value of v_{cr} represents the shear stress required to produce initial diagonal cracking in the web of the member and is evaluated using Eq. 3.24. It should be noted that v_{cr} represents the shear stress required to produce initial diagonal cracking in the member. This stress is being evaluated using the ultimate test values of member with no or very light web reinforcement. This might seem an

Transition study				Reinforced (non-prestressed)			
(1) Author	(2) Member ID	(3) v _{test} Eq. 3.21 (ksi)	(4) v _{cr} (ksi)	(5) ρ _v f _y (psi)	(6) f' _c (ksi)	(7) a/d	(8) $\frac{v_{test}}{v_{cr}}$
Richart series 1911	291.1	0.18	0.08	0	1.69	2.4	2.25
	291.2	0.16	0.08				2.00
	291.3	0.19	0.08				2.38
	294.1	0.18	0.08				2.25
	294.2	0.14	0.08				5.75
	294.3	0.17	0.08				2.13
	293.4	0.19	0.09		2.35		2.38
Richart series 1917	16B20.1	0.22	0.14	0	4.77	4.8	1.57
	16B20.2	0.21					1.50
	16B1.1	0.22					1.57
	16B1.2	0.20					1.43
	16B2.1	0.19					1.36
	16B2.2	0.21					1.50
Richart and Jensen series 1931	1	0.48	0.14	0	4.76	1.52	3.43
	2	0.53	0.14				3.79
	3	0.50	0.13				3.85
	4	0.45	0.12				3.75
	5	0.35	0.09				3.89
	6	0.39	0.10				3.90
Moretto 1945	1N1	0.39	0.12	0	3.55	1.75	3.25
	1N2	0.49	0.12				4.08
	2N1	0.43	0.13				3.31
	2N2	0.50	0.14				3.57
Clark 1951	A0-1	0.18	0.11	0	3.13	2.34	1.64
	A0-2	0.22	0.12				1.83
	B0-1	0.25	0.12				2.08
	B0-2	0.19	0.12				1.58
	B0-3	0.26	0.12				2.17
	C0-3	0.34	0.12				2.83
	D0-1	0.45	0.12				3.75
	D0-3	0.45	0.12				3.75
				mean =	X =		2.6
				Standard deviation =	S =		0.95

Table 3.36 Test data on beams with no web reinforcement failing in shear (from Ref. 99)

Transition study				Reinforced (non-prestressed)			
(1) Author	(2) Member ID	(3) vutest Eq. 3.21 ksi	(4) vcr ksi	(5) ρvfy psi	(6) f'c ksi	(7) a/d	(8) vutest vcr
Laupa 1953	S2	0.17	0.12	0	3.9	4.5	1.42
	S3	0.21	0.14		4.69		1.50
	S4	0.22	0.13		4.47		1.69
	S-5	0.20	0.13		4.33		1.54
	S-11	0.13	0.09		2.14		1.44
	S-13	0.20	0.12		3.80		1.67
Moody 1953 series A	A1	0.20	0.13	0	4.4	3	1.54
	A2	0.23	0.13		4.5		1.77
	A3	0.26	0.13		4.5		2.00
	A4	0.24	0.14		4.57		1.71
	B1	0.19	0.11		3.07		1.73
	B2	0.20	0.11		3.13		1.82
	B3	0.19	0.11		2.79		1.73
	B4	0.19	0.10		2.43		1.90
	C1	0.07	0.06		0.92		1.17
	C2	0.08	0.06		0.88		1.33
Moody 1953 series B	C3	0.08	0.07		1.00		1.14
	C4	0.08	0.07		0.98		1.14
	1	0.23	0.15	0	5.32	3.41	1.53
	2	0.14	0.10		2.42		1.40
	3	0.21	0.12		3.735		1.75
	4	0.17	0.09		2.23		1.89
	5	0.21	0.13		4.45		1.62
	6	0.14	0.09		2.29		1.56
	7	0.20	0.13		4.48		1.54
	8	0.12	0.09		1.77		1.33
	9	0.21	0.15		5.97		1.40
	10	0.19	0.12		3.47		1.58
	11	0.24	0.15		5.53		1.60
	12	0.19	0.11		2.93		1.73
	13	0.22	0.15		5.48		1.47
	14	0.17	0.12		3.27		1.42
15	0.20	0.15		5.42		1.33	
16	0.15	0.09		2.37		1.67	
						X	1.56
						S	0.21

Table 3.37 Test data on beams with no web reinforcement failing in shear (from Ref. 99)

Transition study			Reinforced (non-prestressed)				
Author	Member ID	v_{utest} Eq. 3.21 (ksi)	v_{cr} (ksi)	$\rho_{vf} f_y$ (psi)	f'_c ksi	a/d	$\frac{v_{utest}}{v_{cr}}$
Moody series	24a	0.50	0.10	0	2.58	1.52	5.00
	24b	0.51	0.11		2.99		4.64
III	25a	0.45	0.12		3.53		3.75
	25b	0.49	0.10		2.50		4.9
1953	26a	0.71	0.11		3.14		6.45
	26b	0.67	0.11		2.99		6.09
	27a	0.59	0.11		3.10		5.36
	27b	0.60	0.12		3.32		5.05
	28a	0.51	0.12		3.38		4.25
	28b	0.58	0.12		3.25		4.83
	29a	0.76	0.11		3.15		6.00
29b	0.74	0.12		3.62		6.17	
X = mean =							5.20
S = st. dev. =							0.83

Table 3.38 Test data on beams with no web reinforcement failing in shear (from Ref. 99)

Transition study		failing in Shear			Reinforced (non-prestressed)		
(1) Author	(2) Member ID	(3) vutest Eq. 3.21 Ksi	(4) vcr ksi	(5) ρ _v f _y psi	(6) f' _c ksi	(7) a/d	(8) $\frac{vutest}{vcr}$
Krefeld	4A3	0.22	0.13	0.0	4.44	2.34	1.69
	5A3	0.35	0.13		4.33	2.34	2.69
	11A2	0.25	0.13		4.38	2.92	1.92
Thurston	12A2	0.28	0.13		4.36	3.85	2.15
(90)	18A1	0.21	0.11	0.0	2.80	2.90	1.91
	18B2	0.24			2.88	2.90	2.18
	18C2	0.25			3.28	2.90	2.27
	18D2	0.20			3.20	2.90	1.82
	13A2	0.16	0.11	0.0	2.89	2.87	1.45
	14A2	0.15			3.00	3.77	1.36
	15A2	0.15			2.92	2.87	1.36
	15B2	0.17			3.00	2.87	1.55
	16A2	0.18			3.22	3.81	1.64
	17A2	0.19			3.19	3.77	1.73
	18E2	0.27			2.87	2.87	2.45
	19A2	0.20			2.98	3.81	1.82
	20A2	0.23			3.05	3.85	2.09
	21A2	0.26			2.89	3.85	2.36
	3AAC	0.23	0.14	0.0	5.01	3.58	1.64
	4AAC	0.24	0.13		4.25	3.60	1.85
	5AAC	0.24	0.14		4.76	3.60	1.71
	6AAC	0.25	0.14		4.99	3.65	1.79
	3AC	0.22	0.14		4.62	4.77	1.57
	4AC	0.22	0.13		4.42	4.80	1.69
	5AC	0.23	0.14		4.76	4.83	1.64
6AC	0.25	0.14		4.95	4.87	1.79	
4CC	0.22	0.15		5.57	6.0	1.47	
5CC	0.24	0.15		5.43	6.0	1.60	
6CC	0.27	0.15		5.57	6.09	1.80	
5EC	0.22	0.15		5.43	7.24	1.47	
6EC	0.21	0.14		4.90	7.30	1.50	
					X	1.81	
					S	0.33	

Table 3.39 Test data on beams with no web reinforcement failing in shear (from Ref. 90)

Transition study			failing in Shear		Reinforced (non-prestressed)		
(1) Author	(2) Member ID	(3) vutest Eq. 3.21 Ksi	(4) vcr ksi	(5) ρvfy psi	(6) f'c ksi	(7) a/d	(8) $\frac{vutest}{vcr}$
	26-1	0.29	0.15	79	5.82	4.0	1.93
Krefeld	29a-1	0.22	0.15	53	5.63		1.47
&	29b-1	0.22	0.15	53	5.46		1.47
Thurston	213.5-1	0.21	0.15	35	5.64		1.40
(90)	29a-2	0.30	0.15	62	5.39		2.00
	29b-2	0.28	0.15	62	6.00		1.87
rectang.	29c-2	0.22	0.12	62	3.50		1.83
sections	29d-2	0.23	0.13	62	4.41		1.77
	29e-2	0.29	0.17	62	7.03		1.71
	29g-2	0.21	0.10	62	2.28		2.10
	213.5a-2	0.22	0.15	42	5.36		1.47
	218a-2	0.23	0.15	31	5.45		1.53
	29-3	0.25	0.14	40	4.97		1.79
	318-1	0.31	0.15	93	5.81		2.07
	321-1	0.23	0.15	79	5.62		1.53
	318-2	0.25	0.15	64	5.65		1.67
	321-2	0.23	0.15	55	5.51		1.53
	313.5-3	0.30	0.16	65	6.19		1.88
	318-3	0.24	0.16	48	6.24		1.50
	321-3	0.20	0.16	42	6.24		1.25
Palaskas	#2	0.16	0.14	0	4.75	4.14	1.14
Attigobe	A00	0.14	0.14	0	4.74	3.92	1.00
and	A25	0.19	0.14	32	4.72	3.97	1.36
Darwin	A25a	0.20	0.14	32	4.79	4.00	1.43
(134)	A50	0.25	0.12	74	3.81	3.96	2.08
T-beams	A50a	0.24	0.13	75	4.06	3.94	1.85
	A75	0.30	0.14	97	4.67	3.92	2.14
	B00	0.15	0.14	0	4.64	3.88	1.07
	B25	0.17	0.13	32	4.47	3.93	1.31
	B50	0.23	0.13	76	4.39	3.96	1.77
	C00	0.13	0.13	0	4.27	3.96	1.00
	C25	0.18		32	4.10	3.98	1.38
	C50	0.29		76	4.30	3.94	2.23
						X	1.62
						S	0.34

Table 3.40 Test data on reinforced concrete beams with no or very light web reinforcement failing in shear (from Refs. 90, 134)

incongruity. However, for members having no web reinforcement or very light amounts, the shear stress required to produce diagonal cracking generally corresponds to the shear stress required to produce failure in the member. The different a/d ratios of these members are also distinguished; "a" is the distance between the concentrated load and the centerline of the support, "d" is the distance between the centroid of the tensile reinforcement and the extreme compression fiber. This distinction is necessary since, as discussed in Report 248-2, the a/d ratio is of great significance in the ultimate load capacity in shear of reinforced concrete members. Small a/d ratios greatly increase the ultimate shear capacity of the member above the shear causing inclined cracking. However, the shear stress producing initial diagonal cracking remains almost the same regardless of the a/d ratio. Since in this section it is the shear capacity of the member prior to inclined cracking that is being evaluated, then it is necessary to identify the different a/d ratios used to test those members.

In Figs. 3.50, 3.51, 3.52, and 3.53 the suggested additional concrete contribution in the uncracked and transition states is evaluated using the data from Tables 3.36 and 3.39. This comparison for different values of the concrete compressive strength, f'_c , and different a/d ratios shows that the proposed concrete contribution is a safe lower bound. In these figures the effect of the a/d ratio becomes clear by showing that beams with small a/d ratios (1 to 2) consistently sustained large shear stresses at failure. This trend has been recognized in current American codes by introduction of the M/V_d term in v_c

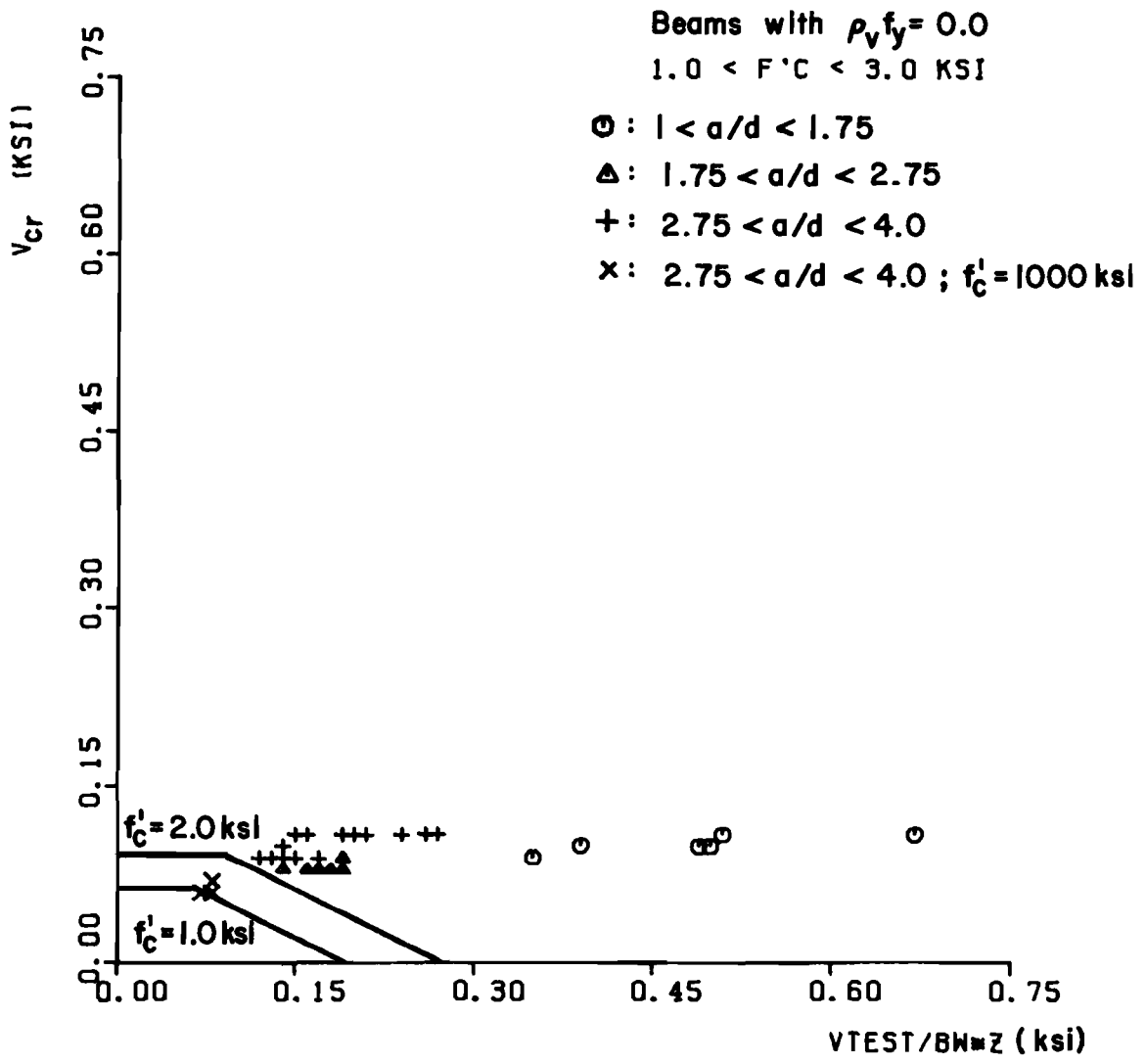


Fig. 3.50 Evaluation of the concrete contribution in the case of reinforced concrete beams

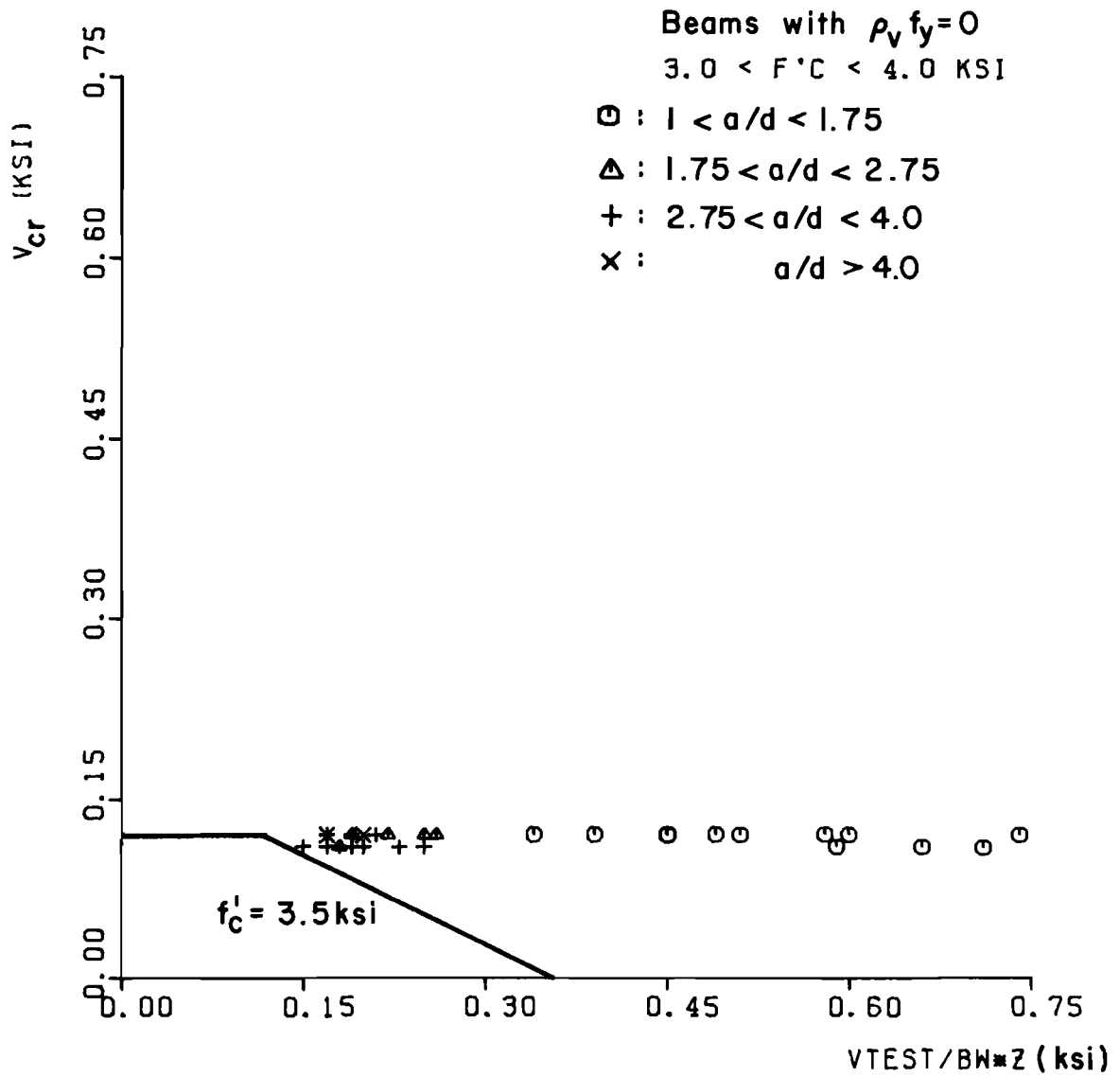


Fig. 3.51 Evaluation of the concrete contributions in reinforced concrete beams failing in shear

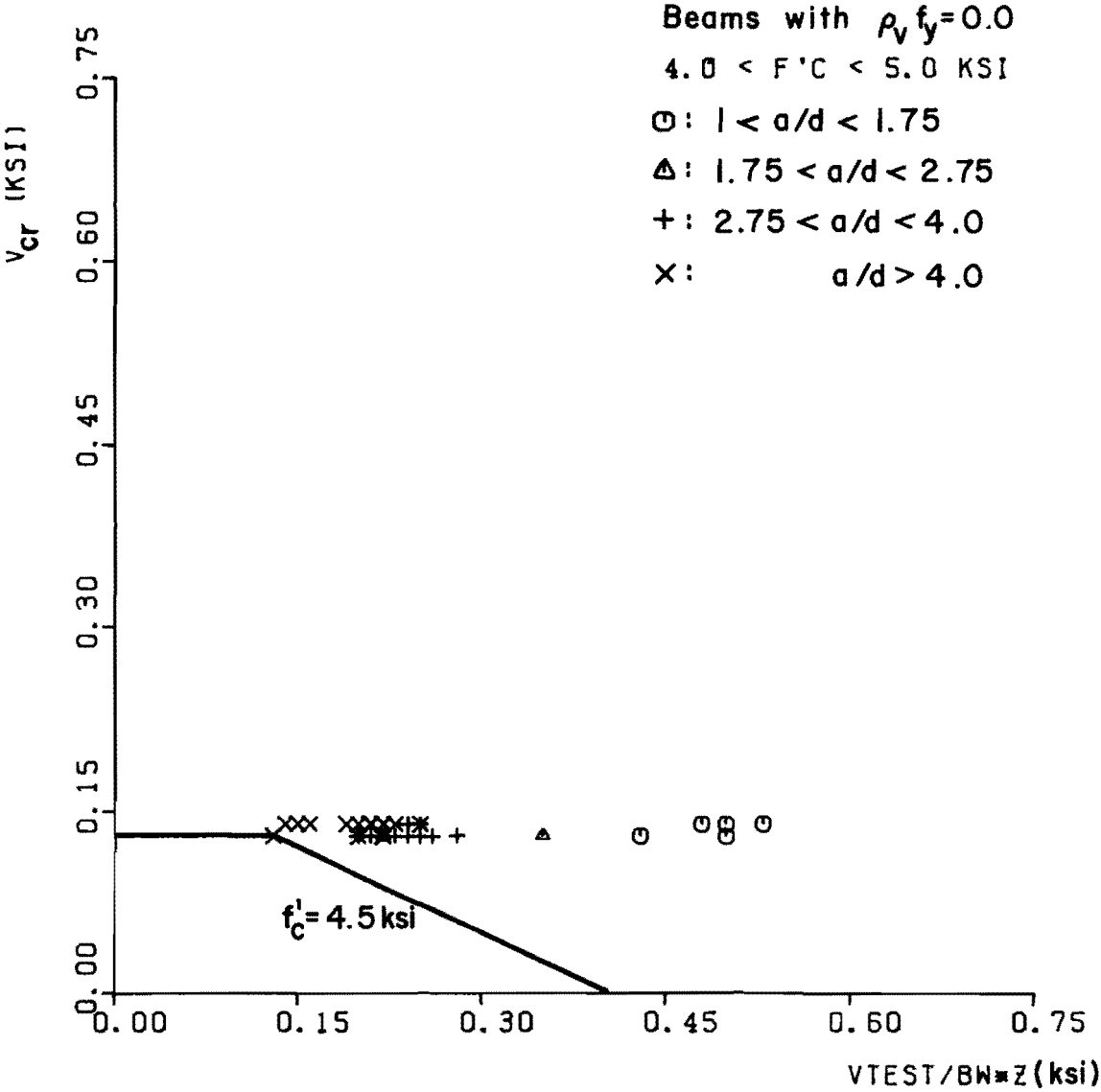


Fig. 3.52 Evaluation of the concrete contribution in reinforced concrete beams failing in shear

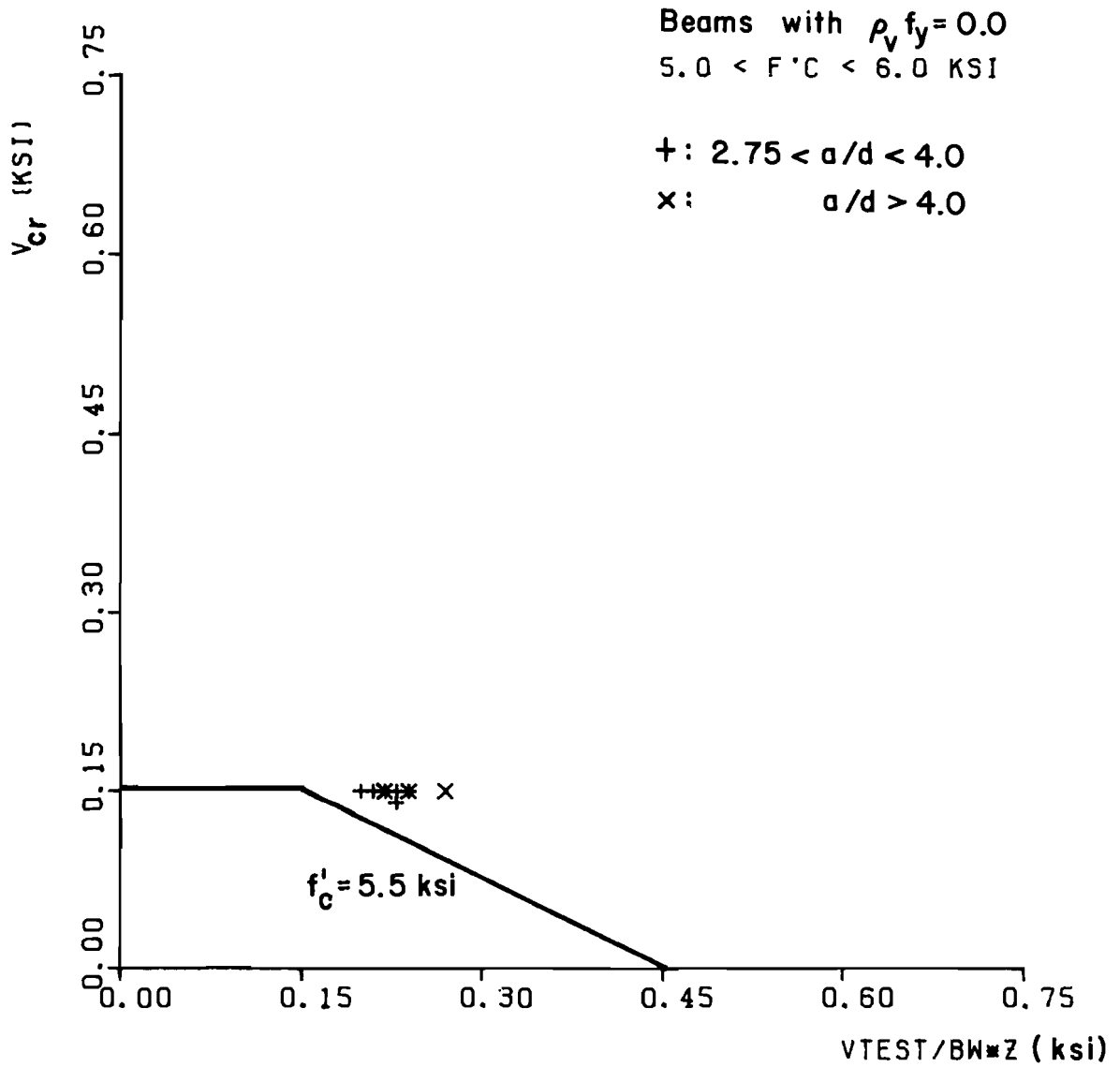


Fig. 3.53 Evaluation of the concrete contribution in reinforced concrete members failing in shear

expressions. However, the contribution at this term is relatively small for all except deep beams when shear reinforcement is pre-cut and the resulting complication in design has led many to question its usefulness (108).

The data shown in Table 3.40 for reinforced concrete beams failing in shear containing no or very light amounts of web reinforcement are plotted in Fig. 3.54. The beams shown in Table 3.40 were all tested using an a/d ratio larger than 3.5. Figure 3.54 shows a plot of the data for different values of the concrete compressive strength f'_c . Again, the proposed concrete contribution shows to be a safe lower bound. For these larger a/d ratios, the gross conservatism evident in some at the previous plots has vanished.

Tables 3.41 through 3.43 include test data (152) for 90 simply supported prestressed concrete beams. All beams, except four which were tested over a 7 ft. span, had 9 ft. spans and were subjected to bending and shear by means of concentrated loads. Only straight prestressed longitudinal reinforcement was used. The beams were either pretensioned or post-tensioned and grouted. The series included 43 rectangular beams (identified by the first letter A), 33 I-beams with 1.75 inch thick webs (letter C). The term K in Tables 3.41 through 3.43 is computed using Eq. 3.25 but in no case was taken greater than 2.0. The different a/d ratios, together with their respective f'_c were identified for each specimen.

Table 3.41 through 3.43 and Figs. 3.55 through 3.62 show a comparison between the test ultimate shear stresses from column (2) and

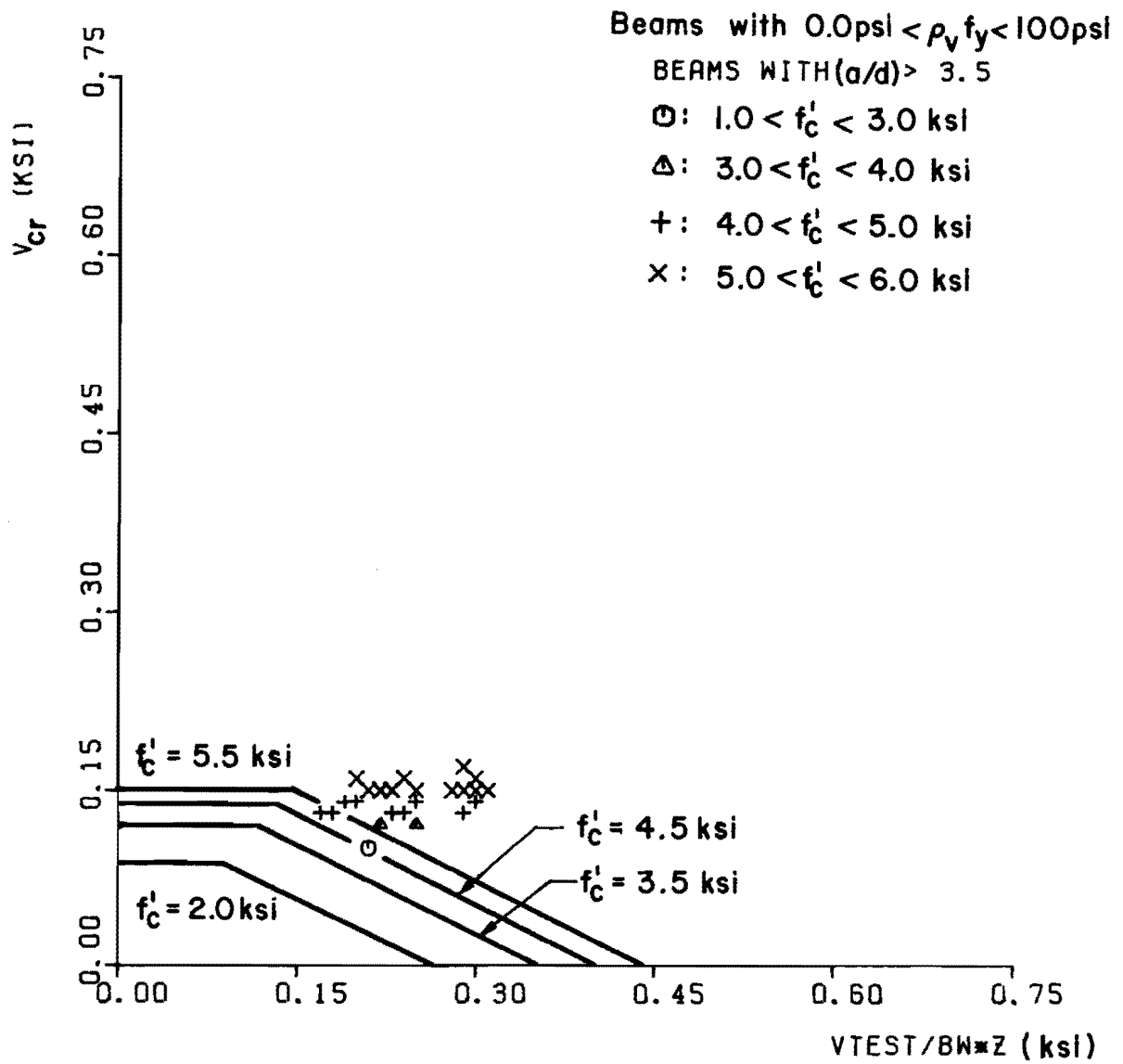


Fig. 3.54 Evaluation of the concrete contribution in the case of members with no or very light web reinforcement failing in shear

Transition study			Prestressed Data						
(1) Author	(2) Member ID	(3) vutest Eq. 3.21 (ksi)	(4) K Actual value	(5) K but <2	(6) Kvcr (ksi)	(7) ρvfy (psi)	(8) f'c (ksi)	(9) a/d	(10) $\frac{vutest}{Kvcr}$
Sozen	A.11.43	0.28	2.37	2.0	0.31	0	5.87	6.55	0.90
	A.11.51	0.15	2.15	2.0	0.22		2.96	6.40	0.68
	A.11.53	0.22	2.46	2.0	0.26		4.15	6.72	0.85
Zwoyer	A.11.96	0.21	2.82	2.0	0.21		2.77	6.42	1.00
Siess (152)	A.12.23	0.27	1.87	1.87	0.30	0	6.27	3.86	0.90
	A.12.31	0.29	2.14	2.0	0.28		4.73	4.17	1.04
	A.12.34	0.38	2.22	2.0	0.34		7.37	4.39	1.12
	A.12.36	0.22	1.96	1.96	0.25		4.18	3.92	0.88
	A.12.42	0.35	2.23	2.0	0.32		6.28	4.34	1.09
	A.12.46	0.32	2.42	2.0	0.26		4.36	4.39	1.23
	A.12.53	0.27	2.29		0.22		3.02	4.19	1.23
	A.12.56	0.29	2.37		0.26		4.36	4.19	1.12
	A.12.69	0.29	2.38		0.24		3.47	4.43	1.21
	A.12.73	0.32	2.55		0.23		3.35	4.27	1.39
	A.12.31	0.26	2.56		0.22		2.93	4.16	1.18
	A.14.39	0.33	2.00	2.00	0.23	0	3.44	2.87	1.43
	A.14.44	0.36	2.20		0.21		2.80	2.82	1.71
	A.14.55	0.41	2.28		0.24		3.66	2.81	1.71
	A.14.68	0.34	2.44		0.18		2.13	2.85	1.89
A.21.29	0.10	1.47	1.47	0.17	0	3.53	6.39	0.59	
A.21.39	0.12	1.65	1.65	0.17		2.66	6.03	0.71	
A.21.51	0.20	1.88	1.88	0.28		5.77	6.65	0.71	
A.22.20	0.17	1.47	1.47	0.19	0	4.20	4.26	0.89	
A.22.24	0.16	1.46	1.46	0.16		2.91	4.09	1.00	
A.22.27	0.16	1.51	1.51	0.17		3.35	4.30	0.94	
A.22.28	0.14	1.41	1.41	0.17		3.77	4.11	0.82	
A.22.31	0.18	1.70	1.70	0.20		3.37	4.47	0.90	
A.22.34	0.16	1.62	1.62	0.19		3.53	4.33	0.84	
A.22.36	0.17	1.65	1.65	0.21		3.94	4.31	0.81	
A.22.39	0.12	1.35	1.35	0.14		2.88	4.09	0.86	
A.22.40	0.31	1.89	1.89	0.28		5.44	4.39	1.11	
A.22.49	0.27	1.78	1.78	0.25		4.91	4.39	1.08	

Table 3.41 Data on prestressed concrete beams with no web reinforcement failing in shear (from Ref. 152)

Transition study			Prestressed Data						
(1) Author	(2) Member (ID)	(3) vutest Eq. 3.21 (ksi)	(4) K Act.	(5) K <2.0 val.	(6) Kvcr (ksi)	(7) ρvfy (psi)	(8) f'c (ksi)	(9) a/d	(10) vutest Kvcr
Sozen	A.32.19	0.12	1.0	1.0	0.14	0	4.81	3.99	0.86
	A.32.22	0.15	1.22	1.22	0.15		3.51	3.84	1.0
	A.32.27	0.13	1.10	1.10	0.13		3.62	3.93	1.00
	A.32.37	0.20	1.08	1.08	0.16		5.77	4.39	1.25
Zwayer	A.32.49	0.24	1.49	1.49	0.20		4.46	4.39	1.20
Siess (152)	B.11.20	0.26	1.99	1.99	0.27	0	4.65	5.29	0.96
	B.11.29	0.33	2.30	2.0	0.26		4.18	5.40	1.27
	B.11.40	0.40	2.66	2.0	0.26		4.22	5.40	1.54
	B.12.10	0.27	1.70	1.70	0.25	0	5.36	3.24	1.08
	B.12.12	0.29	1.77	1.77	0.23		4.38	3.23	1.26
	B.12.14	0.29	1.81	1.81	0.22		3.81	3.23	1.32
	B.12.19	0.30	1.88	1.88	0.20		2.94	3.25	1.50
	B.12.16	0.43	2.14	2.0	0.27		4.46	3.58	1.59
	B.12.29	0.49	2.26		0.27		4.40	3.69	1.81
	B.12.34	0.52	2.43		0.29		5.14	3.54	1.79
	B.12.35	0.42	2.39		0.23		3.24	3.60	1.83
	B.12.50	0.43	2.66		0.21		2.88	3.53	2.05
	B.12.61	0.46	2.82		0.22		3.06	3.64	2.09
	B.13.16	0.48	2.00	2.0	0.28	0	5.05	2.70	1.71
	B.13.26	0.55	2.24		0.28		4.73	2.79	1.96
	B.13.41	0.62	2.64		0.27		4.44	2.79	2.30
	B.21.26	0.24	1.76	1.76	0.23	0	4.32	5.19	1.04
	B.22.09	0.25	1.38	1.38	0.22	0	6.20	3.25	1.14
	B.22.23	0.35	1.65	1.65	0.24		5.16	3.59	1.46
	B.22.30	0.27	1.62	1.62	0.19		3.29	3.55	1.42
	B.22.41	0.31	1.77	1.77	0.19		2.75	3.59	1.63
	B.22.65	0.20	2.03	2.0	0.17		1.77	3.62	1.18
	B.22.68	0.36	2.15	2.0	0.22		3.00	3.64	1.64
	B.31.15	0.17	1.0	1.0	0.15	0	5.65	5.29	1.13

Table 3.42 Data on prestressed concrete beams with no web reinforcement failing in shear (from Ref. 152)

Transition Study						Prestressed Data			
(1) Author	(2) Member (ID)	(3) vutest Eq. 3.21 (ksi)	(4) K Actual value	(5) K	(6) Kvcr	(7) ρ_{vfy} (psi)	(8) f'_c (ksi)	(9) a/d	(10) $\frac{vutest}{Kvcr}$
	B.32.11	0.20	1.0	1.0	0.14	0	5.00	3.46	1.43
	B.32.19	0.19			0.14		4.58	3.53	1.36
Sozen	B.32.31	0.14			0.10		2.62	3.53	1.40
	B.32.34	0.18			0.10		2.62	3.53	1.40
	B.32.41	0.29			0.10		2.36	3.56	1.80
Zwoyer	B.32.54	0.27			0.10		2.57	3.47	2.70
Siess	C.12.09	0.49	1.74	1.74	0.27		6.22	3.26	1.81
	C.12.18	0.61	2.09	2.0	0.26		4.38	3.72	2.35
	C.12.19	0.70	2.13	2.0	0.31		5.89	3.56	2.26
(152)	C.12.32	0.51	2.61		0.17		1.88	3.65	3.00
	C.12.33	0.76	2.67		0.29		5.39	3.57	2.62
	C.12.40	0.41	2.28		0.22		2.89	3.72	1.86
	C.12.44	0.44	2.28		0.25		3.99	3.79	2.76
	C.12.50	0.57	2.76		0.22		3.10	3.60	2.59
	C.12.57	0.81	2.99		0.22		3.10	3.63	2.62
	C.22.29	0.28	1.59	1.59	0.15	0	2.27	3.46	1.87
	C.22.31	0.37	1.71	1.71	0.21		3.65	3.31	1.76
	C.22.36	0.33	1.88	1.88	0.23		3.60	3.52	1.43
	C.22.39	0.23	2.03	2.0	0.13		1.03	3.54	1.77
	C.22.40	0.59	2.48	2.0	0.27		4.54	3.65	2.19
	C.22.46	0.41	2.02	2.0	0.23		3.44	3.56	1.78
	C.22.62	0.35	1.91	1.91	0.19		2.51	4.00	1.84
	C.22.73	0.44	2.43	2.0	0.20		2.46	3.63	2.20
	C.32.11	0.30	1.0	1.0	0.17	0	6.87	3.25	1.76
	C.32.22	0.33			0.13		2.92	3.60	2.54
	C.32.37	0.29			0.12		3.63	3.60	2.42
	C.33.42	0.25			0.10		2.61	3.56	2.50
	C.32.50	0.31			0.11		2.82	3.37	2.82
	C.32.80	0.34			0.11		3.25	3.60	3.09

* Specimens A.12.48, A.12.60, A.22.26, A.32.08, A.32.11, A.32.17, V.11.07, V.12.07, V.13.07 failed in flexure

Combined of Tables 3.41, 3.42 and 3.43 X = 1.55
S = 0.63

Table 3.43 Data on prestressed concrete beams with no web reinforcement failing in shear (from Ref. 152)

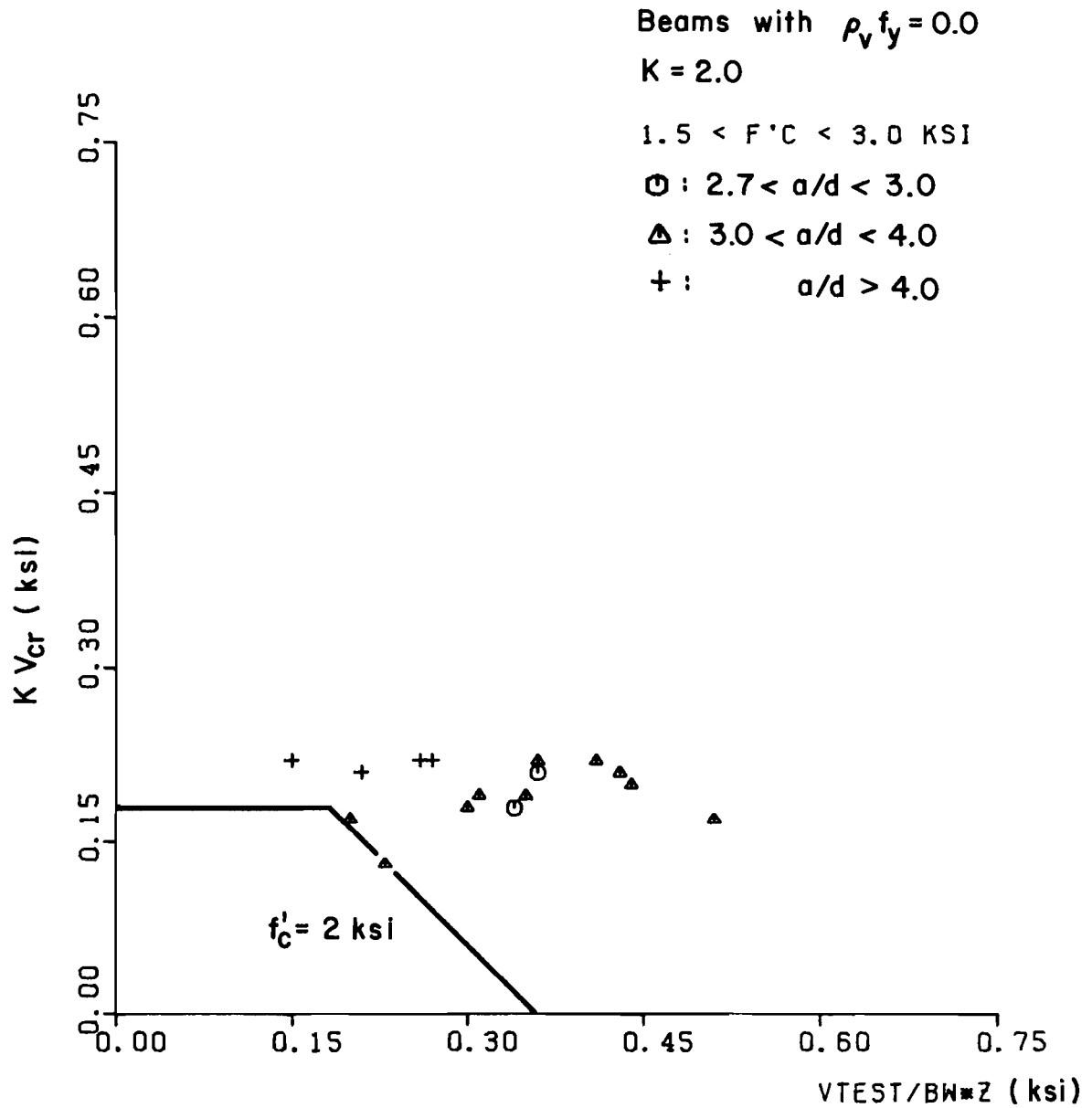


Fig. 3.55 Evaluation of the concrete contribution in prestressed concrete members failing in shear with $K = 2.0$

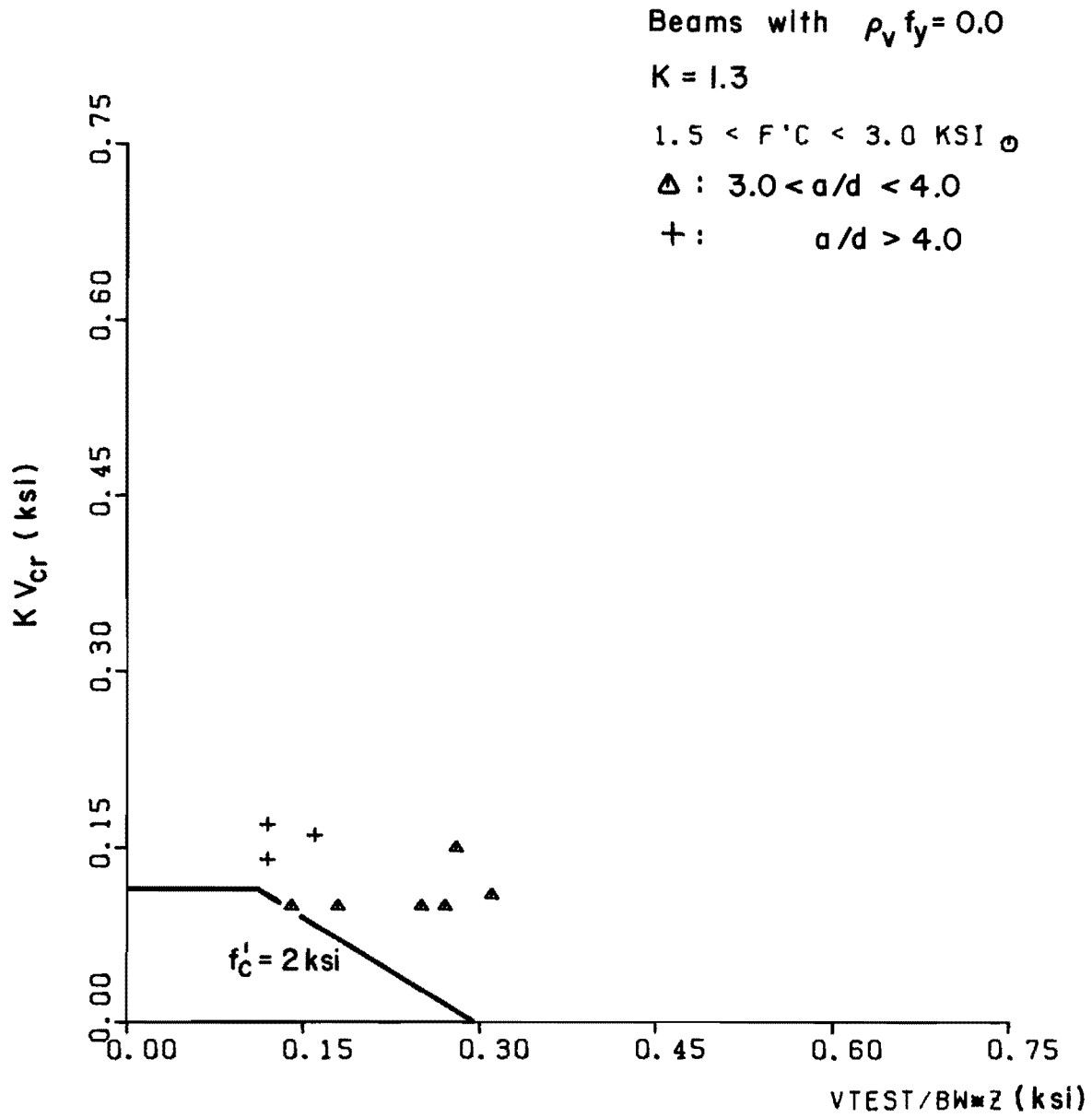


Fig. 3.56 Evaluation of the concrete contribution in prestressed concrete members failing in shear with $K = 1.3$

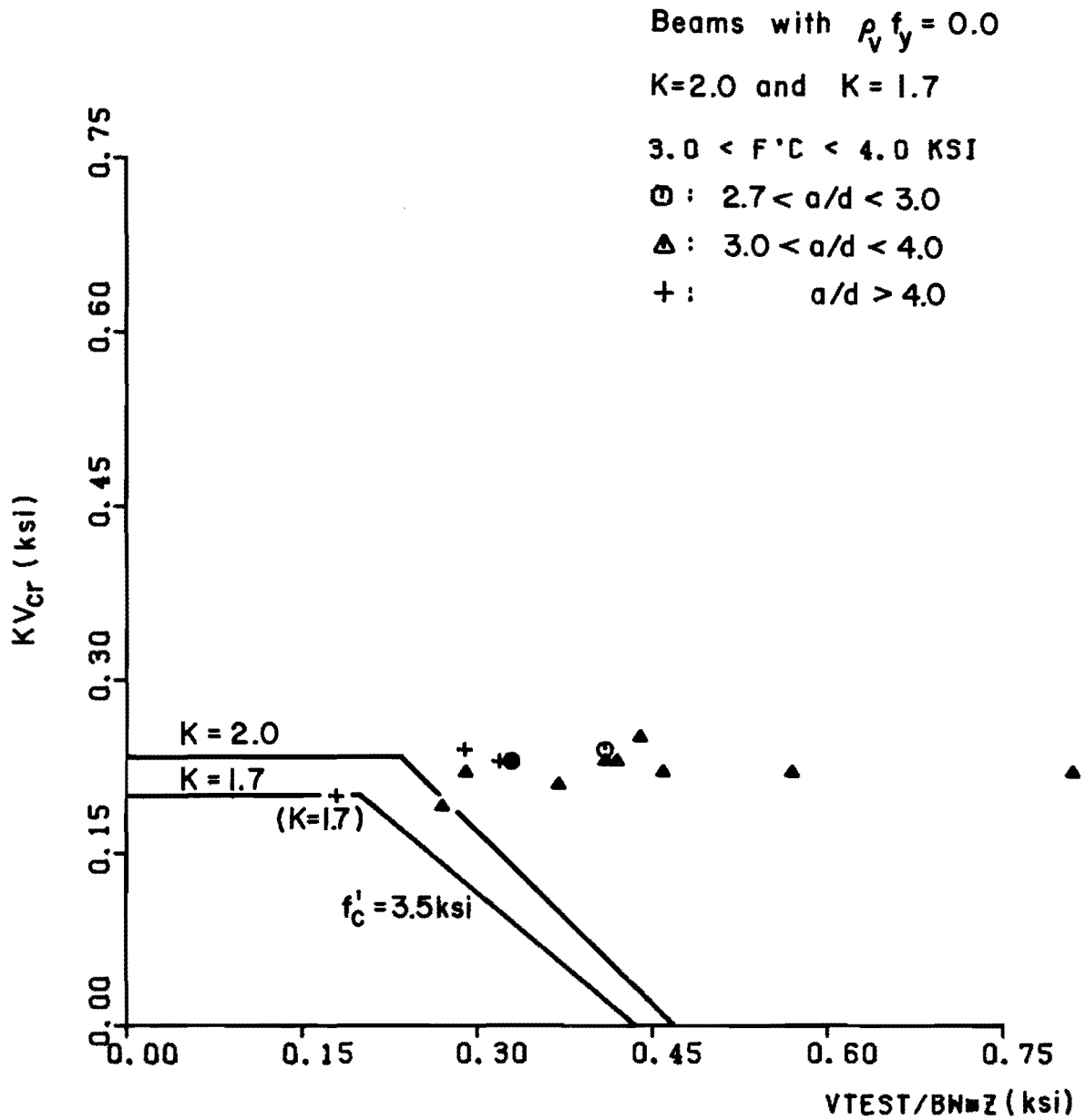


Fig. 3.57 Evaluation of the concrete contribution in prestressed concrete beams failing in shear with values of $K = 2.0$ and $K = 1.7$

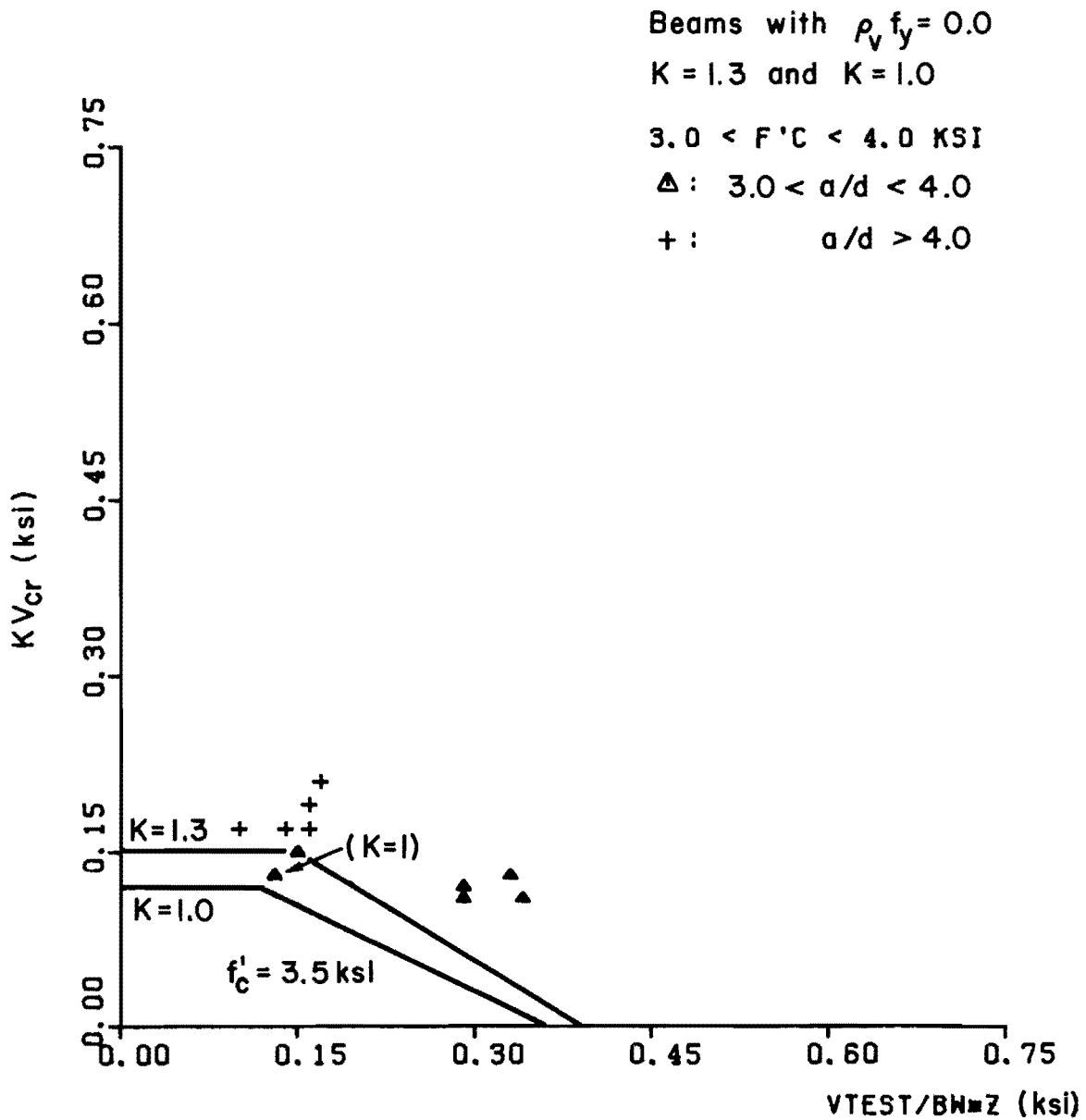


Fig. 3.58 Evaluation of the concrete contribution in prestressed concrete beams failing in shear with values of $K = 1.3$ and $K = 1.0$

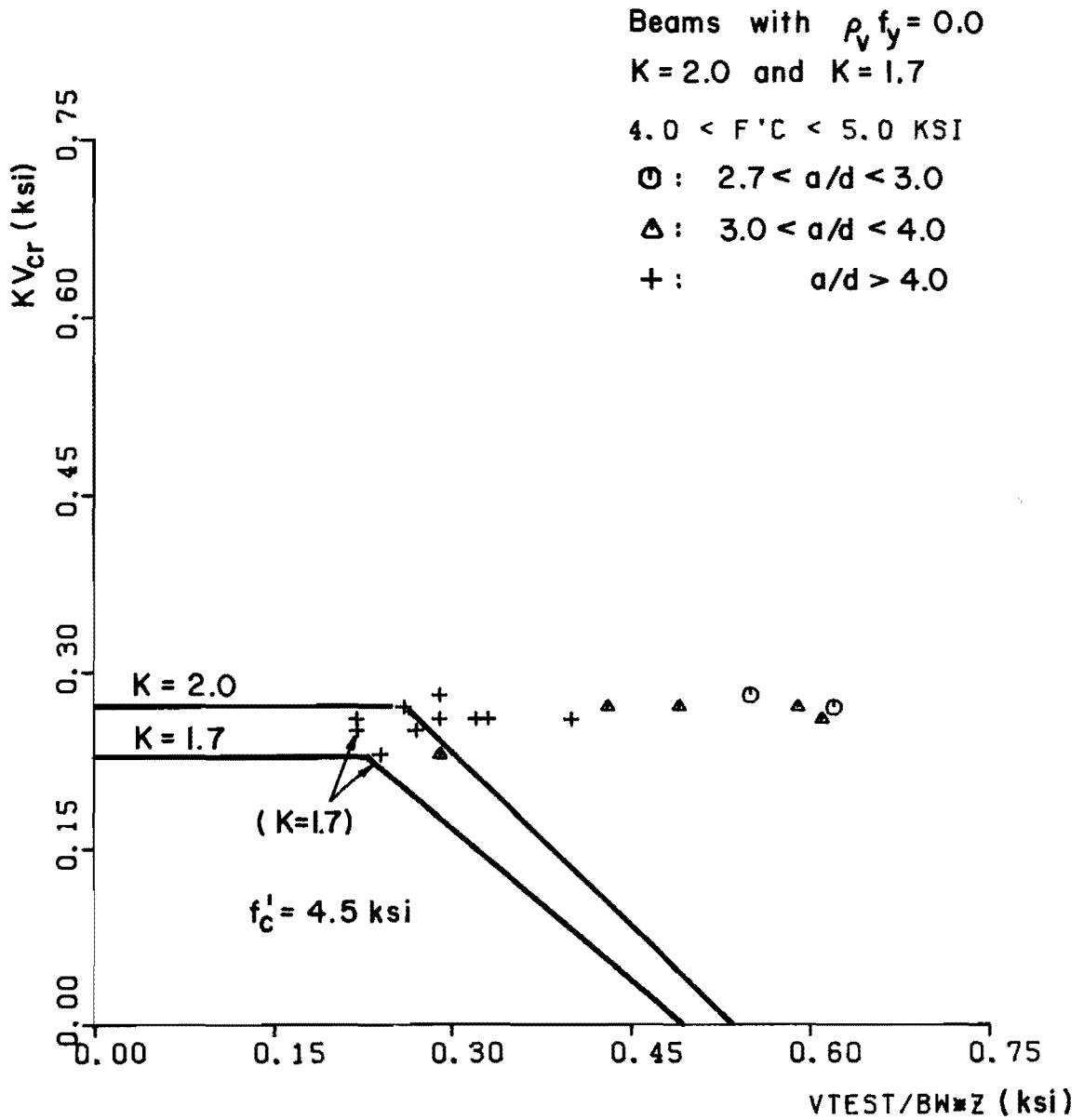


Fig. 3.59 Evaluation of the concrete contribution in prestressed concrete beams failing in shear with values of $K = 2.0$ and $K = 1.7$

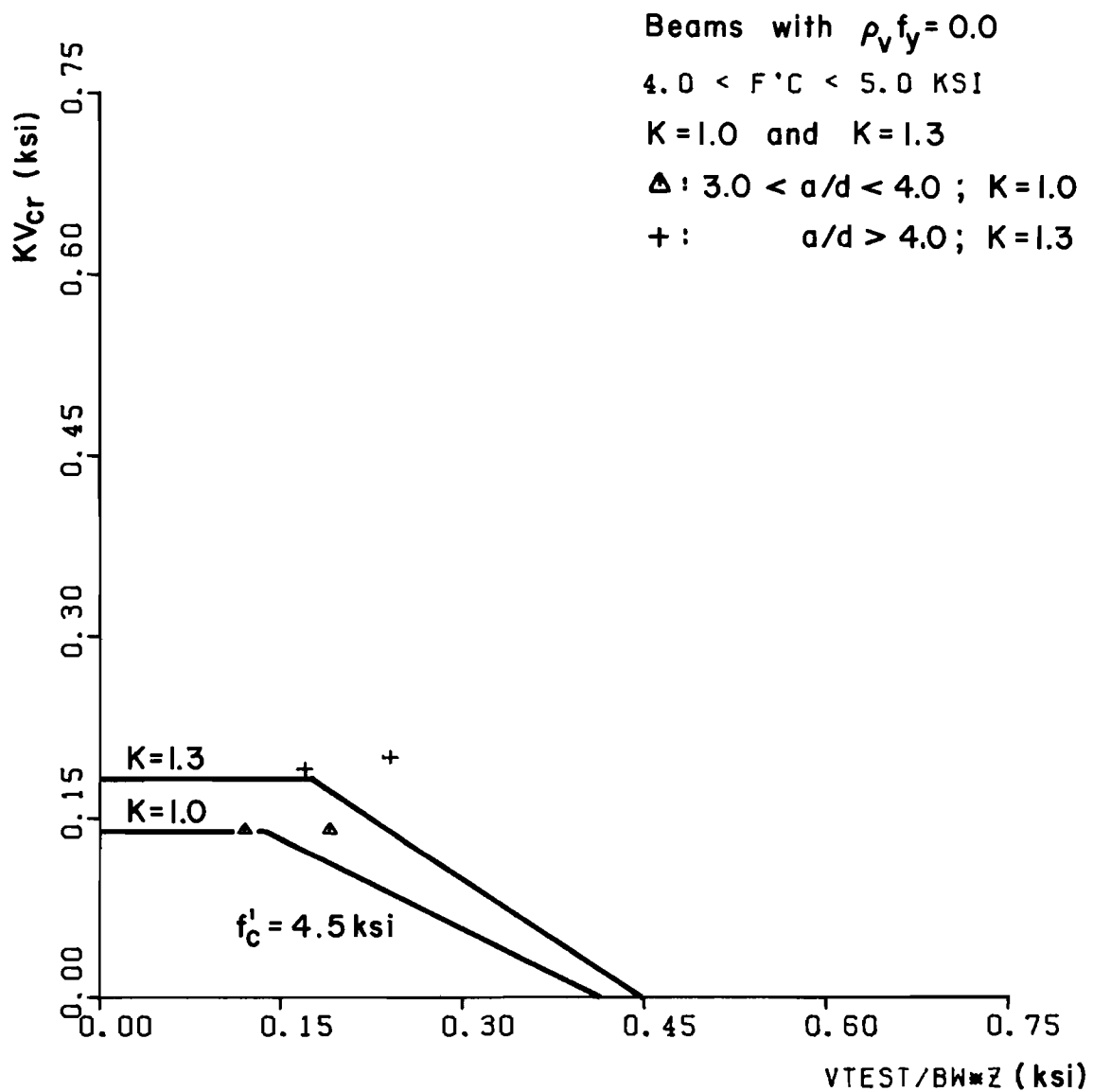


Fig. 3.60 Evaluation of the concrete contribution in prestressed concrete beams failing in shear with values of $K = 1.3$ and $K = 1.0$

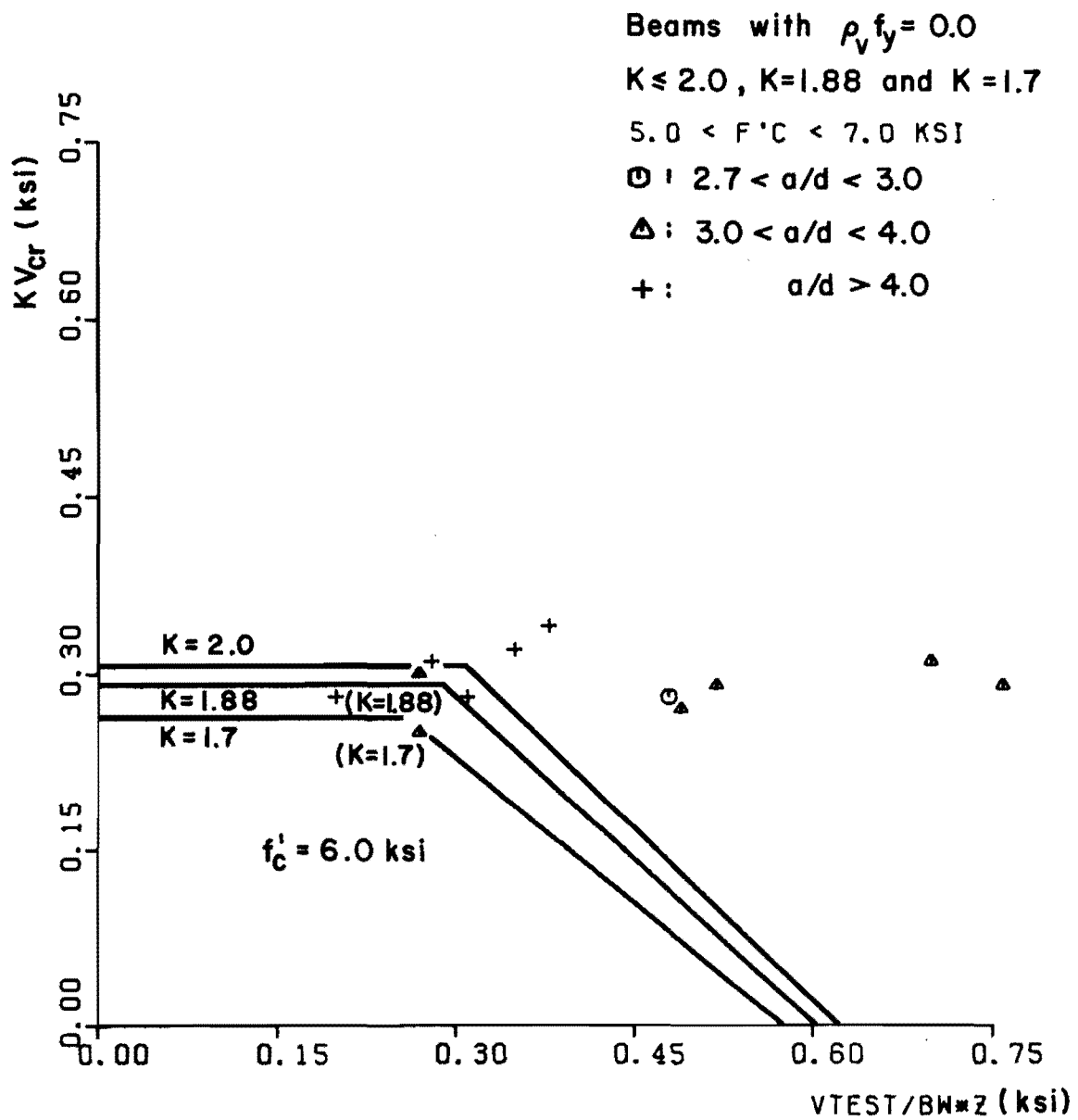


Fig. 3.61 Evaluation of the concrete contribution in prestressed concrete beams failing in shear with values of $K = 2.0$, $K = 1.88$ and $K = 1.7$

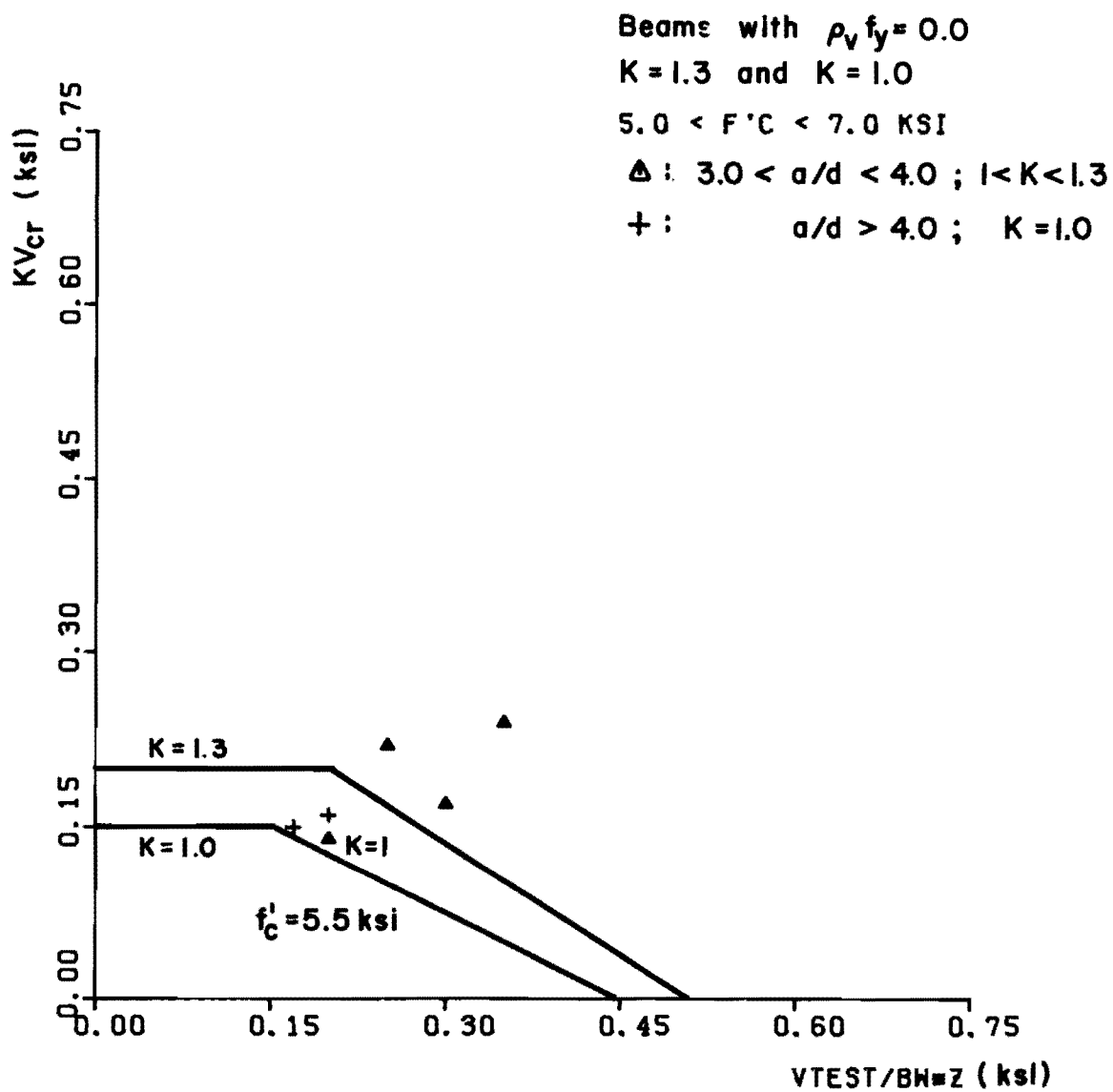


Fig. 3.62 Evaluation of the concrete contribution in prestressed concrete beams failing in shear with values of $K = 1.3$ and $K = 1.0$

the proposed concrete contribution in the uncracked and transition range from column (5) for different concrete compressive strengths f'_c different a/d ratios and different values of K. The proposed concrete contribution is also shown to be a safe lower bound for the case of prestressed concrete members subjected to bending and shear. Those figures which include several values of K indicate that the nature of the proposed correction based on the Mohr circle analysis seems quite reasonable in the lower capacity beams.

In the case of torsion in reinforced and prestressed concrete, rectangular members the shear stress due to torsion v_t in a member without web reinforcement can be evaluated using elastic theory (St. Venant's [154]) or plastic theory (Nadai's "Sand heap analogy" [154]). In either case, the shear stress due to torsion is computed using a similar relationship.

$$v_t = \psi_t * T / [x^2 y] \quad (3.28)$$

where T = torsional moment at the section; y, x = overall dimensions of the rectangular sections, $x < y$; and ψ_t = a stress factor function of y/x , which in the case of the elastic solution can be obtained from Fig. 3.63, and in the case of the plastic solution is given by

$$\psi_t = 2 / [1 - (x / (3y))] \quad (3.29)$$

where $\psi_t = 3$ when $x/y = 1$, and is equal to 2 when $x/y = 0$.

Concrete is not ductile enough in tension to allow a perfect plastic distribution of shear stresses. Therefore, the ultimate

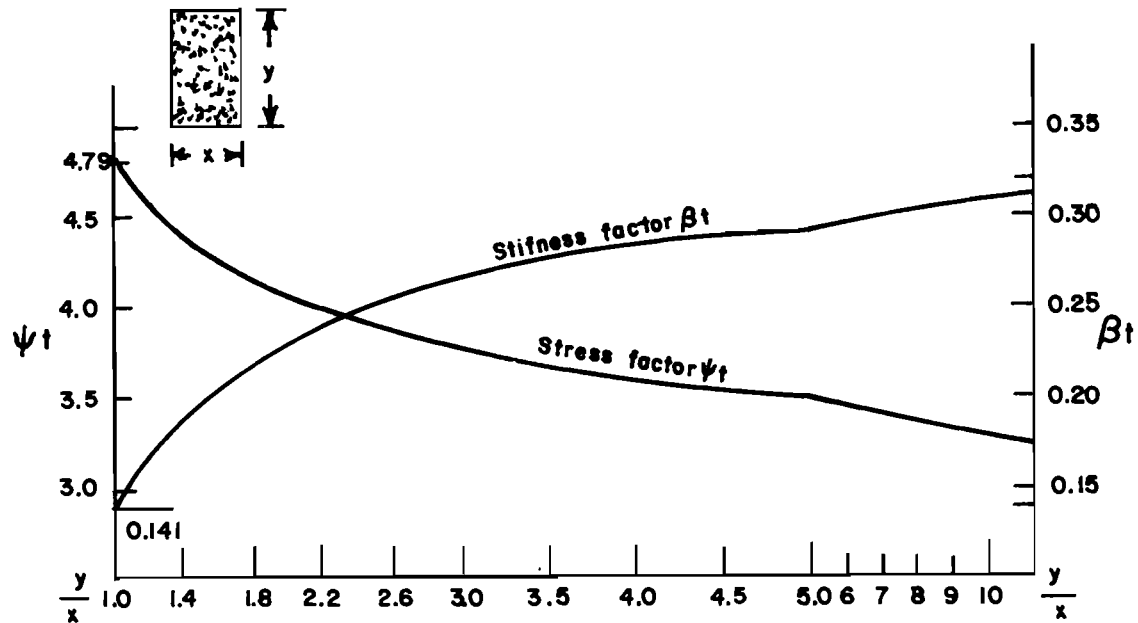


Fig. 3.63 Stiffness and strength factor for rectangular section subjected to torsion (from Ref. 135)

torsional strength of a plain concrete section will be between the values predicted by the plastic and elastic theories. In light of this fact, The ACI Committee 438 (34) proposed that the ultimate shear stress induced by torsion in plain concrete be evaluated as

$$v_T = 3T_u/[x^2y] \quad (3.30)$$

where $x < y$. The value of 3 for ψ_t is a minimum for the elastic theory and a maximum for the plastic theory (see Fig. 3.63 and Eq. 3.29). In

the case of I, L, and T-sections, i.e. sections formed of several rectangles, the following approximation is made

$$v_T = 3T_u / \Sigma [x^2 y] \quad (3.31)$$

where $x < y$ for each rectangle making up the cross section.

Numerous tests (169,135) indicate that for plain concrete sections the value of v_T when computed using Eqs. 3.30 and 3.31 is between $4\sqrt{f'_c}$ and $7\sqrt{f'_c}$. This value will also depend on the size of the specimen. ACI Committee 438 (34) proposed a value for the level of shear stress reached in reinforced concrete beams when diagonal tension cracks due to torsion are about to develop by suggesting the value of $6\sqrt{f'_c}$ (psi) be used for the evaluation of the diagonal cracking load.

For the case of combined bending and torsion in members with no web reinforcement it has been found (Mattock [33]) that the torsional resistance of a cracked section is approximately 1/2 of the ultimate torsional strength of the uncracked section, provided a certain amount of bending is present. Thus, the nominal torsional shear stress carried by the concrete in its uncracked state is assumed by ACI 318-77 (24) to be 40% of the cracking stress of $6\sqrt{f'_c}$.

$$v_T = 0.4(6)\sqrt{f'_c} = 2.4\sqrt{f'_c} \text{ (psi)} \quad (3.32)$$

For the case of combined shear and torsion Ersoy and Ferguson (33), based on the study of a large amount of test results on reinforced concrete beams with no web reinforcement, suggested that the shear stresses v_T and v_y which formed an approximate lower bound for the

plotted experimental points (33) were found to be respectively

$$v_V = 2.68 \sqrt{f'_c} \text{ (psi)} \quad (3.33)$$

and

$$v_T = 4.8 \sqrt{f'_c} \text{ (psi)} \quad (3.34)$$

ACI 318-77 (24) suggests that the nominal shear stress be taken as $2\sqrt{f'_c}$ for the case of shear, and $2.4\sqrt{f'_c}$ for the case of torsion. This relatively small difference between the shear and torsion values seems to be an unnecessary complication for combined actions since minimum web reinforcement should always be present in combined actions states.

In light of the previous discussion it is suggested that the concrete contribution in the uncracked and transition states for reinforced beams subjected to torsion and/or shear be taken the same as shown in Fig. 3.47 with the value of v_{cr} assumed as $2\sqrt{f'_c}$.

Shown in Table 3.44 are data from reinforced concrete rectangular beams with no web reinforcement subjected to pure torsion. Fig. 3.64 shows an evaluation of the proposed concrete contribution. As can be seen from this plot, the proposed concrete contribution for the case of members under pure torsion constitutes a safe lower bound.

In the case of prestressed concrete members subjected to torsion, the concrete contribution shown in Fig. 3.49 is evaluated using the test data shown in Table 3.45. The data in Table 3.45 are plotted for comparison in Figs. 3.65 through 3.67. As can be seen from these plots, the proposed concrete contribution in the uncracked and transition states for the case of prestressed concrete members

Transition study			Reinforced concrete Pure Torsion		
(1) Author	(2) Member ID	(3) v_{ttest} Eq. 3.31 Ksi	(4) v_{cr} Ksi	(5) f'_c Ksi	(6) $\frac{v_{ttest}}{v_{cr}}$ $\frac{(3)}{(4)}$
Hsu (88)	A1	0.32	0.13	4060	2.46
	A2	0.34		4080	2.62
	A3	0.31		4000	2.38
	A4	0.30		4120	2.31
	A5	0.32		4230	2.46
	A6	0.32		4160	2.46
	A7	0.41		3920	3.15
	A8	0.43		4290	3.31
	A9	0.43		4470	3.31
	A10	0.36	0.12	3860	3.0
					X = 2.75
					S = 0.40

Table 3.44 Data on reinforced concrete rectangular beams with no web reinforcement under pure torsion

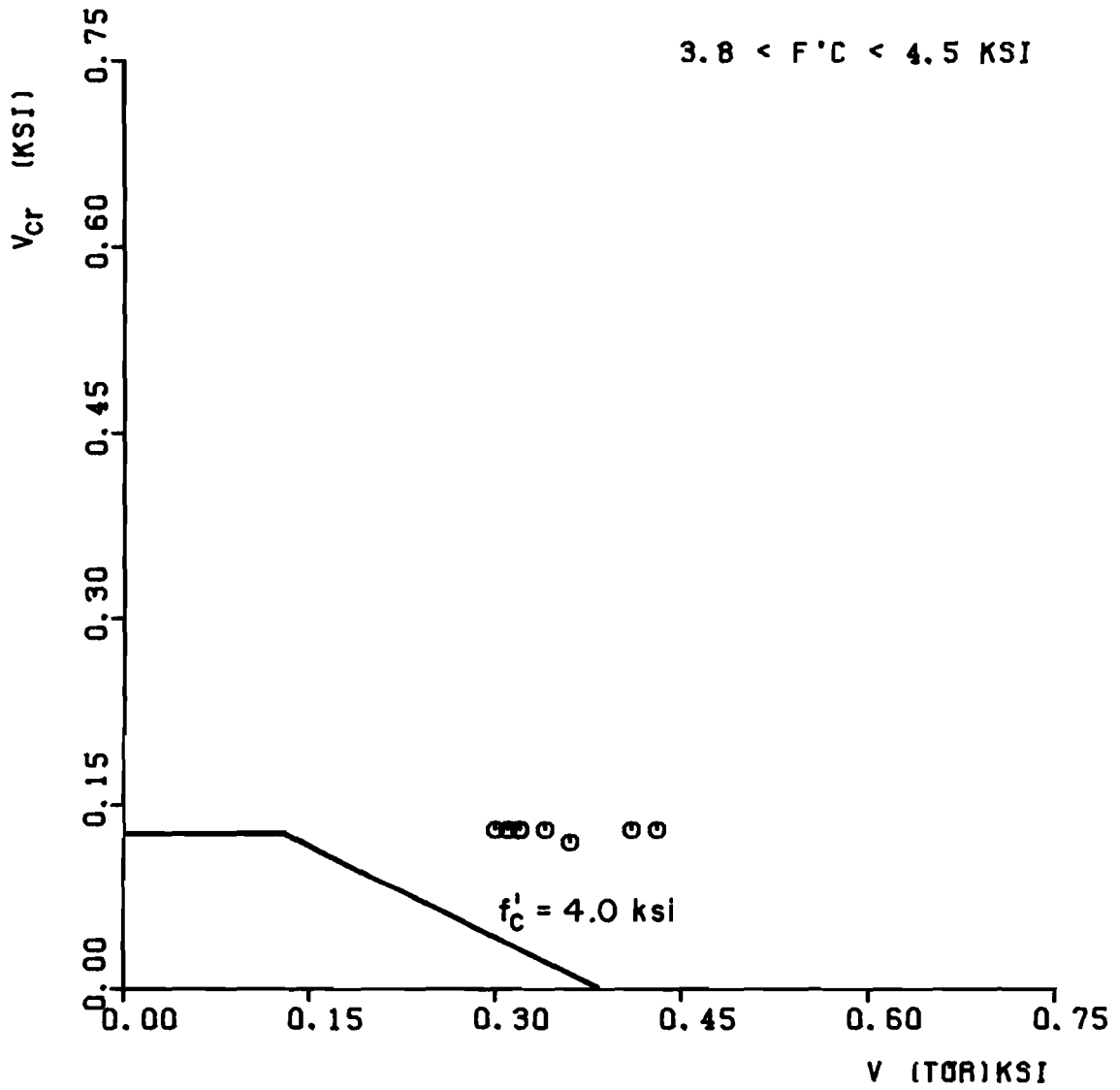


Fig. 3.64 Evaluation of the concrete contribution in reinforced concrete rectangular members under pure torsion

(1) Author	(2) Member ID	(3) vutest Eq. 3.31 ksi	(4) K Actual	(5) K with limit ≤ 2	(6) f'c ksi	(7) K(5) vcr ksi	(8) $\frac{vutest}{K v_{cr}}$	(3) (7)
Rectangular beams series								
Zia (176)	OR1	0.69	2.58	2.0	8.05	0.36	1.92	
	OR2	0.73	2.58		8.05	0.36	2.03	
	OR3	0.73	2.56		8.20	0.36	2.03	
	2R1	0.75	2.58		8.50	0.37	2.03	
	2R2	0.80	2.58		8.54		2.16	
	2R3	0.77	2.58		8.54		2.08	
	2.5R1	0.71	2.54		8.54		1.92	
	2.5R2	0.74	2.54		8.54		2.00	
	2.5R3	0.67	2.54		8.54		1.81	
	T-beams series							
	0.25T1	0.83	2.68	2.0	6.59	0.32	2.59	
	0.25T2	0.85	2.68		6.59	0.32	2.66	
	2.25T1	0.57	2.60		6.79	0.33	1.73	
	2.25T2	0.54	2.60		6.79		1.64	
	2.75T1	0.55	2.58		6.79		1.67	
	2.75T2	0.54	2.57		3.88		1.64	
I-Beam series								
	0.75I1	0.86	2.76	2.0	4.75	0.28	3.07	
	0.75I2	0.85	2.76		4.75	0.28	3.04	
	3I1	0.84	2.73		5.27	0.29	2.90	
	3I2	0.94	2.73		5.27	0.29	3.24	
	3.5I1	1.00	2.57		6.21	0.32	3.13	
	3.5I2	0.99	2.57		6.21	0.32	3.09	
	Mean	X =					2.30	
	Standard deviation	S =					0.57	

Table 3.45 Data on prestressed concrete rectangular, T, and I-beams with no web reinforcement subjected to pure torsion (from Ref. 176)

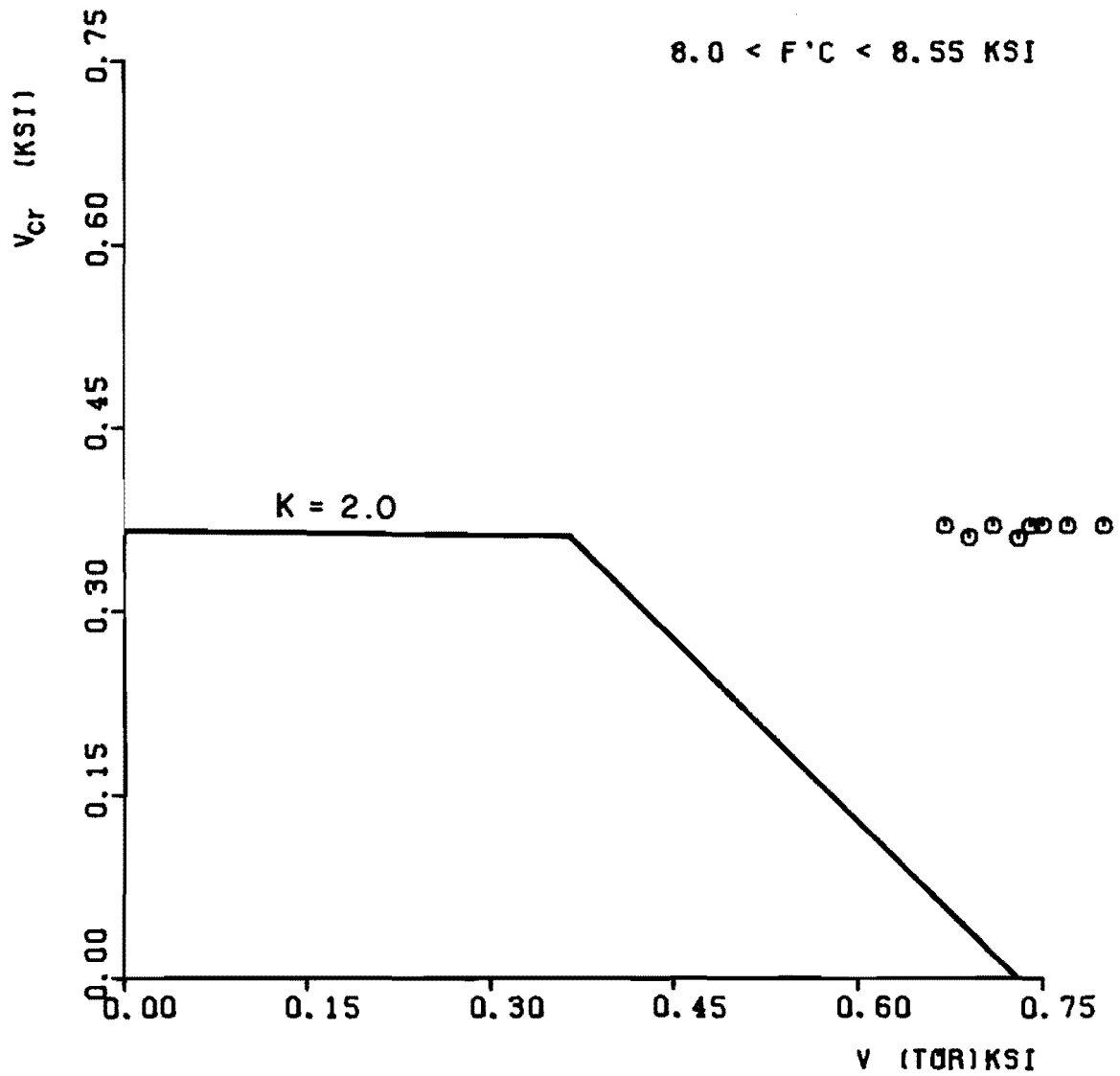


Fig. 3.65 Evaluation of the concrete contribution in prestressed concrete rectangular members subjected to torsion with $K = 2.0$

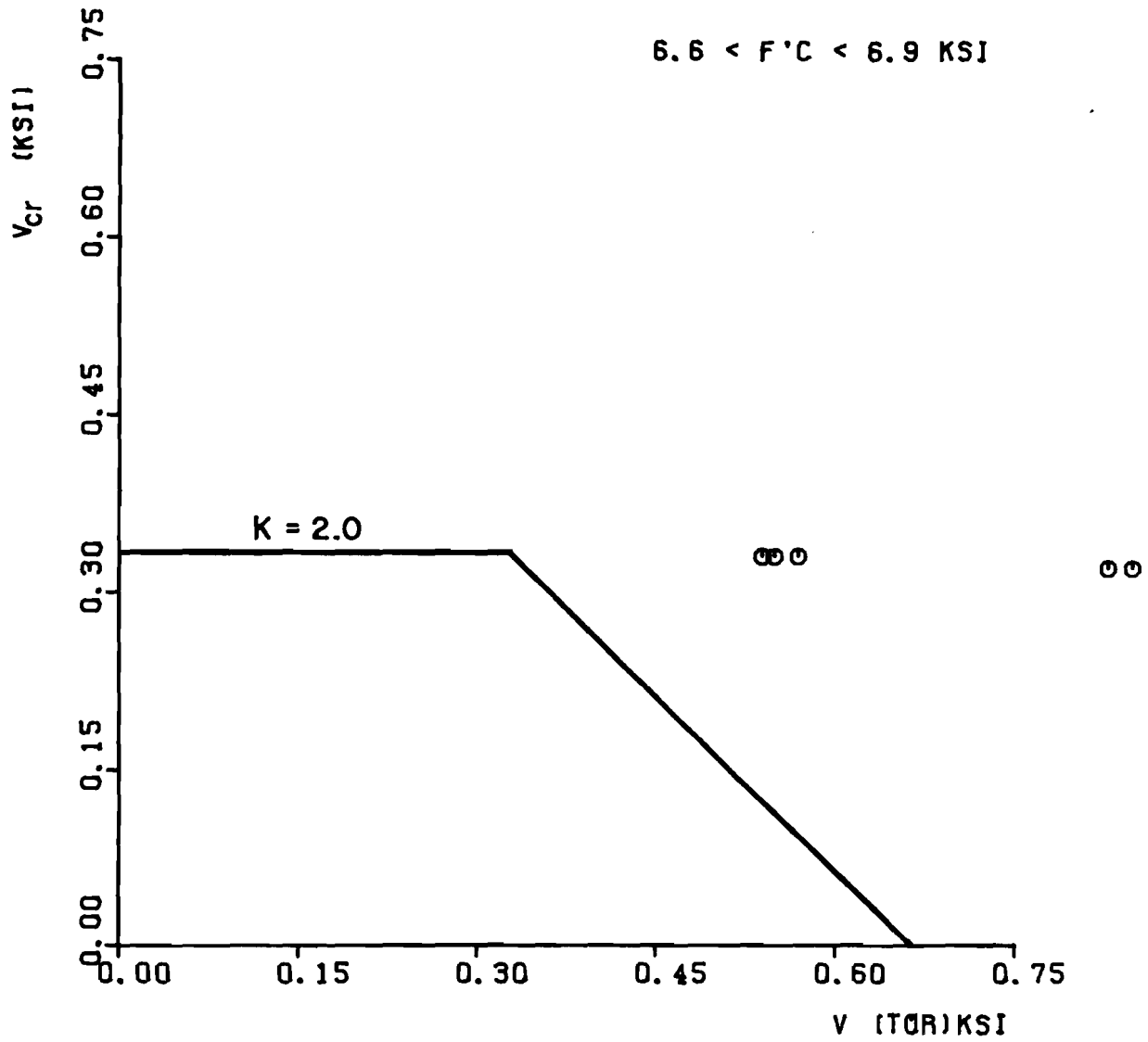


Fig. 3.66 Evaluation of the concrete contribution in prestressed concrete T-beams subjected to torsion with $K = 2.0$

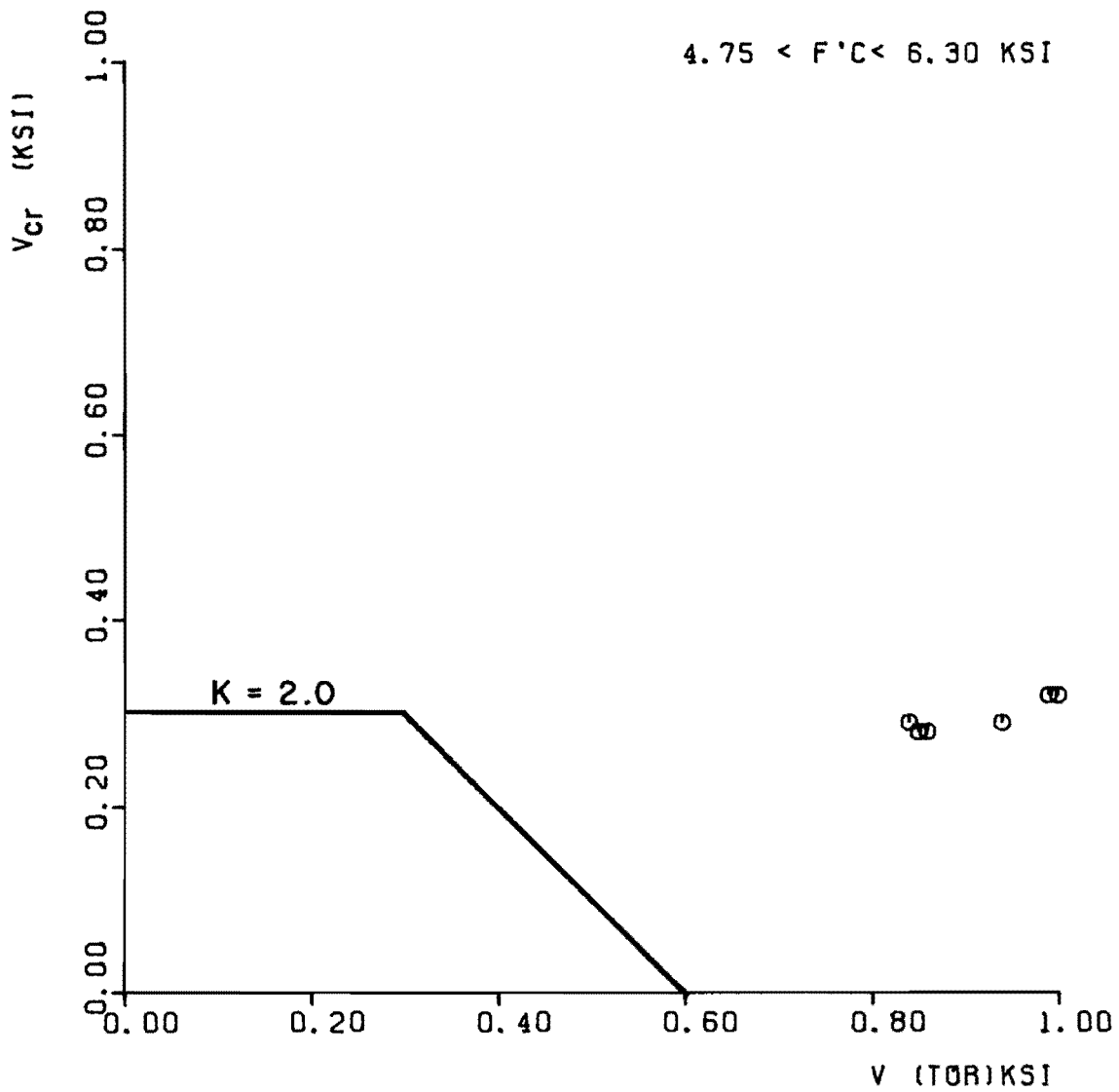


Fig. 3.67 Evaluation of the concrete contribution in prestressed concrete I-beams subjected to torsion with $K = 2.0$

constitutes an extremely safe lower bound in the case of members subjected to torsion.

As a result of the evaluation of the proposed concrete contribution in the uncracked and transition states in reinforced and prestressed concrete beams subjected to shear and/or torsion, it can be concluded that the proposed values constitute good lower estimates of the contribution in uncracked and transition states in those members. Based on the test data studied, if a larger concrete contribution was allowed it would yield unconservative results, as can be seen from Figs. 3.52, 3.57, 3.60, and 3.61.

3.9 Comparison between ACI/AASHTO and Truss Model Predicted Values with Test Results

In this section the ACI/AASHTO and Truss Model predicted values are compared using the test results examined in Secs. 3.2, 3.3, 3.4, 3.5, and 3.7. The comparison between the two methods is carried out in the areas of torsion, torsion-bending, and torsion-bending-shear only for reinforced concrete members since the current ACI (24) and AASHTO (12) design recommendations do not include provisions for the case of torsion in prestressed concrete members acting alone or combined with bending and/or shear. However, both design approaches are compared in the area of bending and shear for both prestressed and reinforced concrete members failing in shear.

The current ACI and AASHTO design procedures have been examined in Report 248-2. The ACI/AASHTO predicted ultimate strengths are evaluated in accordance with the guidelines given in Refs. 24 and 12.

3.9.1 Torsion. In the case of pure torsion the ACI/AASHTO ultimate strength is evaluated in accordance with the guidelines given in Refs. 24 and 12 discussed in Sec. 2.4 of Report 248-2.

Shown in Tables 3.46 through 3.50 are data on reinforced concrete rectangular, L, and I-beams subjected to pure torsion previously examined in Sec. 3.2. Specimens B6, M6, I6, J4, G5, K4, C3, C4, C5, and C6 from Ref. 82 and D5, D6, and C6 from Ref. 173 failed in a web crushing mode and have already been used in Sec. 3.6 to compare the proposed upper limit for the diagonal compression stress with the current ACI/AASHTO upper limits to prevent web crushing, and thus are not included in this section. Figure 3.68 shows a comparison between the ACI/AASHTO and Truss Model predicted ultimate strength using the data from Tables 3.46 through 3.50. As can be seen from Fig. 3.68, the Truss Model predictions are in generally better agreement with the test results and show significantly less scatter than the ACI/AASHTO predicted values.

3.9.2 Torsion-Bending. In the case of combined torsion-bending the ACI/AASHTO ultimate strength is evaluated following the requirements given in Refs. 24 and 12. The comparison between the ACI/AASHTO and Truss Model approaches in the case of combined actions has to be conducted in a different manner than the one followed in the case of single actions (pure torsion). Since the ACI/AASHTO design procedures do not consider the interaction between bending and torsion directly in the design, both ultimate predicted strengths (pure torsion and pure bending) are computed separately.

Tests reported by Hsu (82) on reinforced concrete rectangular beams

(1) Member Id	(2) r	(3) $\frac{T_{test}}{T_{ACI/AASHTO}}$	(4) $\frac{T_{test}}{T_u(Eq.3.1)}$	(5) $\alpha(Eq.3.2)$ degrees
B1	1.0	0.99	1.13	45
B2		1.02	1.04	44
B3		1.01	0.94	43
B4		0.97	0.89	43
B5		0.93	0.80	43
B7	1.0	0.74	0.97	55
B8		0.77	0.78	76
B9		1.37	1.06	34
B10		1.53	0.84	23
D1		1.01	1.11	44
D2		0.96	0.95	43
D3		1.02	0.94	43
D4		0.96	0.87	43
M1		1.28	1.21	39
M2		1.35	1.15	39
M3		1.27	1.00	38
M4		1.14	0.88	38
M5		1.04	0.77	37
I2	1.0	1.09	1.17	45
I3		1.12	1.09	43
I4		1.14	1.09	44
I5		1.11	1.04	44
J1		1.06	1.06	45
J2		1.05	0.97	45
J3		0.96	0.84	43
G1		0.60	1.15	45
G2		1.02	1.19	44
G3		1.01	1.06	43

Table 3.46 Data on reinforced concrete beams with web reinforcement subjected to pure torsion

Tests reported by Hsu (82) on reinforced concrete rectangular beams

(1) Member ID	(2) r	(3) $\frac{T_{test}}{T_{ACI/AASHTO}}$	(4) $\frac{T_{test}}{T_u}$ Eq. 3.1	(5) α (Eq.3.2) degrees
G4	1.0	1.12	1.07	43
G6		0.99	1.09	45
G7		1.01	1.06	44
G8		1.27	1.08	44
N1		1.06	0.94	49
N1a		1.05	0.93	49
N2		1.12	0.93	49
N2a		1.02	0.85	49
N3		1.06	0.84	49
N4		1.28	0.70	50
K1		1.06	1.35	44
K2		1.12	1.25	44
K3		1.38	1.15	43
C1		1.04	1.23	44
C2		1.00	0.94	44
Overall for Tables 3.45 and 3.46	X S	1.07 0.17	1.01 0.15	N = 43

* Specimens B6, M6, I6, I4, G5, K4, C3, C4, C5, C6 are compared in Table 3.56.

Table 3.47 Data on reinforced concrete beams with web reinforcement subjected to pure torsion

Tests reported by McMullen and Rangan (114)
on reinforced concrete rectangular beams

(1) Member ID	(2) r	(3) $\frac{T_{test}}{T_{ACI/AASHTO}}$	(4) $\frac{T_{test}}{T_u}$ Eq 3.1	(5) α (Eq 3.2) degrees
A1	1.0	1.04	1.29	44
A1R		1.02	1.23	44
A2		1.28	1.21	44
A3		1.25	1.08	43
A4		1.23	0.98	43
B1R		1.80	1.35	44
B2		2.30	1.24	44
B3		2.32	1.12	44
B4		2.40	1.01	43
	X	1.63	1.17	N = 9
	S	0.58	0.13	

Tests reported by Liao and Ferguson (104) on
reinforced concrete rectangular beams

PT4	1.0	2.65	0.91	9
PT5		2.12	0.83	16
	X	2.39	0.87	N = 2
	S	0.37	0.06	

Tests reported by Wyss, Garland and Mattock (173)
on reinforced concrete rectangular beams

D2	1.0	.86	0.80	42
D3		1.0	0.87	45
D4		1.11	0.96	43
	X	0.99	0.88	N = 3
	S	0.13	0.08	
Overall X for Table 3.38		1.60	1.06	N = 14
	S	0.63	0.18	

Table 3.48 Data on reinforced concrete rectangular beams
with web reinforcement subjected to pure
torsion

Tests reported by Liao and Ferguson (104) on reinforced concrete L-beams

(1) Member ID	(2) r	(3) <u>Ttest</u> T _{ACI/AASHTO}	(4) <u>Ttest</u> T _u (Eq. 3.1)	(5) σ (Eq. 3.2) degrees
PT1	1.0	1.42	0.92	9
PT2		1.66	0.96	16
PT7		1.08	1.11	31
PT8		1.61	1.03	16
	X	1.44	1.01	N = 4
	S	0.26	0.08	

Tests reported by Rajagopalan and Ferguson (140) on reinforced concrete L-beams

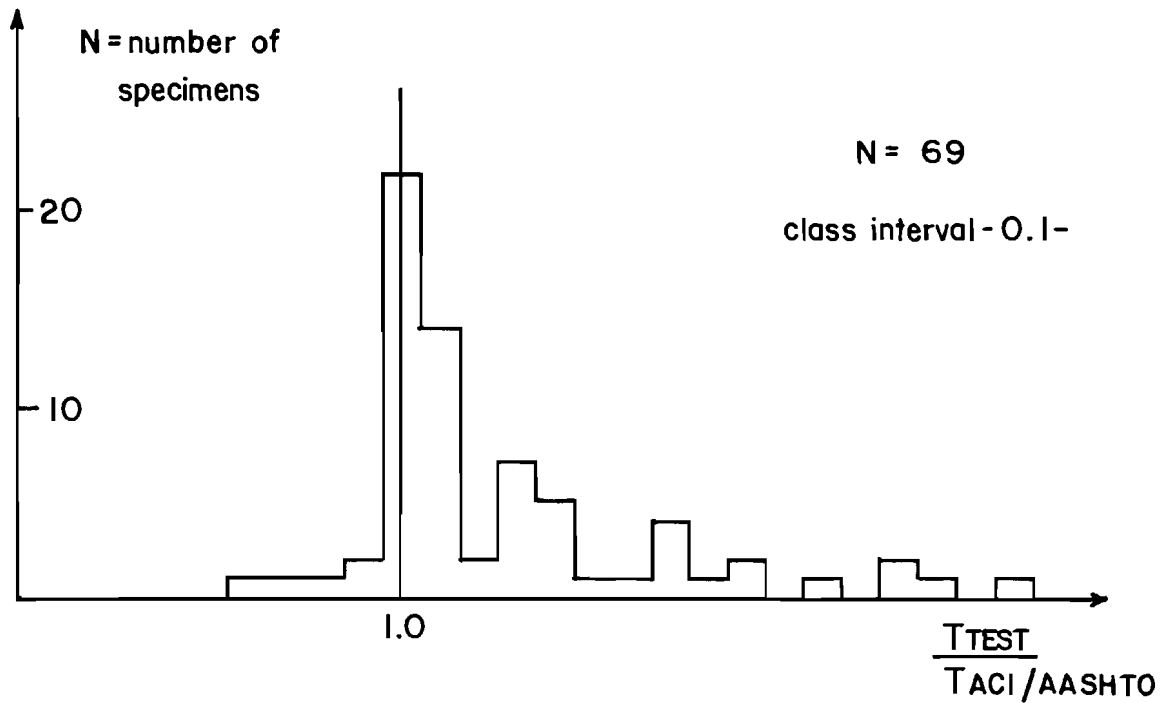
R7	1.0	1.68	1.21	18
R8		1.86	1.38	12
R17		1.68	1.18	24
R19		1.95	1.35	17
	X	1.79	1.28	N = 4
	S	0.14	0.10	
Overall for Table 3.49	X	1.62	1.14	N = 8
	S	0.27	0.17	

Table 3.49 Data on reinforced concrete L-beams with web reinforcement subjected to pure torsion

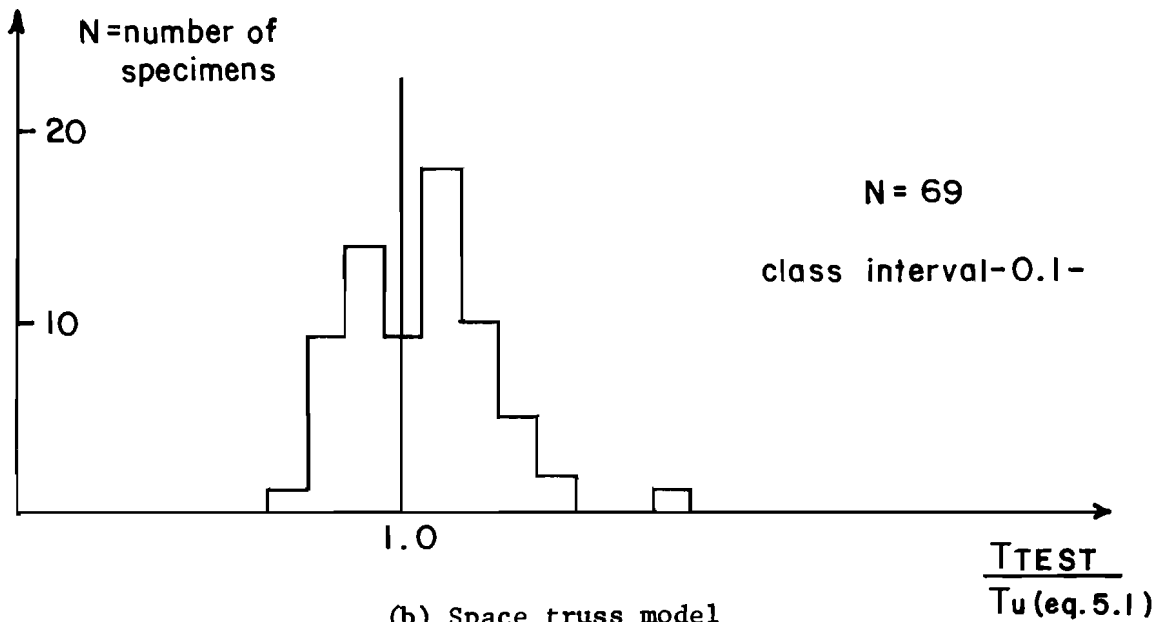
Tests reported by Wyss, Garland and Mattock (173) on reinforced concrete I-beams

(1) Member ID	(2) r	(3) $\frac{T_{test}}{T(ACI/AASHTO)}$	(4) $\frac{T_{test}}{T_u}$ (Eq. 3.1)	(5) α (Eq. 3.2) Degrees
C2	1.0	1.44	1.69	42
C3		1.35	1.43	45
C4		1.42	1.27	44
C5		1.73	0.95	45
	X	1.49	1.34	
	S	0.17	0.31	N = 4

Table 3.50 Data on reinforced concrete I-beams with web reinforcement subjected to pure torsion



(a) ACI/AASHTO



(b) Space truss model

Fig. 3.68 Comparison between the ACI/AASHTO and space truss model predictions with test results of reinforced concrete beams under pure torsion

The design procedure suggested in the ACI Building Code (24) and AASHTO Specifications (12) requires that in the case of combined actions the torsion reinforcement, both longitudinal and transverse, where required shall be provided in addition to the reinforcement required to resist flexure, shear and axial forces. Therefore, when computing the flexural capacity of the member, the area of longitudinal reinforcement required for torsion assumed uniformly distributed over the cross section should not be considered as part of the reinforcement resisting the applied flexural moment. However, if this approach is followed in computing the flexural capacity of the member according to ACI/AASHTO (24,12), in the case of members subjected to combined torsion and bending unreasonable results can be obtained in some cases. For example, in the cases of members 2, 4, 6, and 8 from Ref.70 in Table 3.51, it was found that the area of longitudinal reinforcement required for torsion was larger than the total area of longitudinal reinforcement provided in those members. This means that the flexural capacity of the member was zero. This is not true, since those members in fact were able to carry a bending moment at failure in excess of 50% of its pure flexural strength. This points out the lack of rationale in the evaluation of the amount of longitudinal reinforcement required for torsion in the current ACI/AASHTO procedures. Since in the cases where the amount of transverse reinforcement provided to resist torsion is important, the amount of longitudinal steel required for torsion is a function of the amount of transverse reinforcement provided for torsion, but does not consider directly the actual level of applied torque.

Tests reported by Gesund, Schuetter, Buchanan, and Gray [76]
on reinforced concrete rectangular beams.

(1)	(2)	(3)	(4)	(5)	(6)
Member ID	r	I (space truss)	$\frac{M_{TEST}}{M_{ACI/AASHTO}}$	$\frac{T_{TEST}}{T_{ACI/AASHTO}}$	Mode of failure (ACI/AASHTO)
1	0.7	0.97	0.43	1.20	T
2	0.7	0.94	0.55	0.82	T
3	0.7	0.81	0.66	0.90	T
4	0.7	0.90	0.73	0.55	M
5	0.7	1.04	0.80	0.77	M
6	0.7	1.01	0.92	0.47	M
7	0.7	0.93	0.93	0.64	M
8	0.7	0.98	0.94	0.35	M
9	0.7	1.18	0.42	1.04	T
10	0.7	1.03	0.62	0.80	T
11	0.7	0.98	0.48	0.75	T
12	0.7	1.03	0.75	0.60	M
	\bar{x}	0.98	0.69	0.74	N=12
	s	0.09	0.19	0.24	

Table 3.51 Data on reinforced concrete rectangular beams
with web reinforcement subjected to combined
bending torsion

In view of the previous discussion, it was decided to use the pure flexural capacity (when $T_u = 0$) and the pure torsional capacity (when $M_u = 0$) of the section for the purpose of the comparative study carried out in this section.

The ratios of the bending moment at failure to the predicted pure flexural capacity according to ACI/AASHTO (24,12) and the torsional moment at failure to the predicted pure torsional capacity are shown in columns (4) and (5) of Tables 3.51 and 3.52.

Shown in Tables 3.51 and 3.52 are data on reinforced concrete rectangular beams subjected to combined torsion-bending. The ratios of columns (4) and (5) are compared and the largest one indicates the predicted mode of failure under current ACI/AASHTO approaches. In column (7) this dominant mode of failure is identified for each specimen. "T" means that torsion controlled; "M" indicates that flexure controlled.

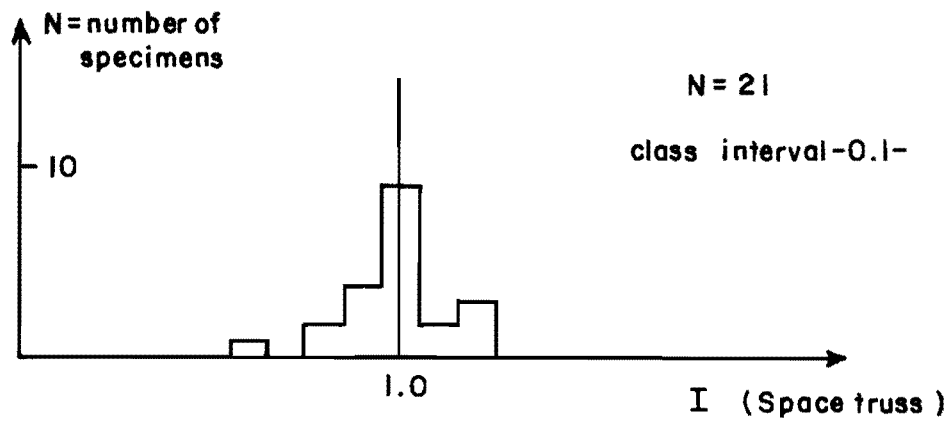
Next, the largest value of column (4) and (5) for each specimen is compared with the previously explained accuracy index "I" of the Truss Model.

Figure 3.69 shows a comparison between the ACI/AASHTO and Truss Model predictions using the data from Tables 3.51 and 3.52. As can be seen from Fig. 3.69 the truss model shows a better agreement with test results in both flexure and torsion type failures. This is understandable, since the truss model considers the interactions between torsion bending, thus reflecting it in the ultimate predicted values.

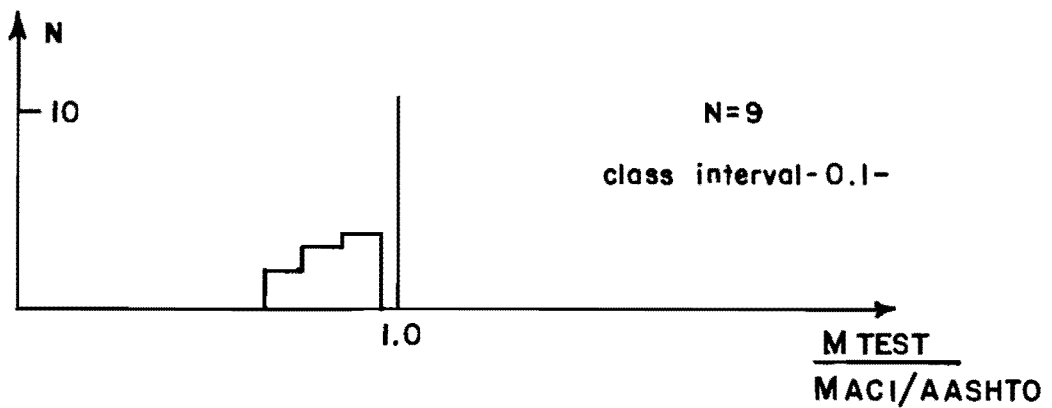
Tests reported by Pandit and Warwaruk [33]
on reinforced concrete rectangular beams.

(1)	(2)	(3)	(4)	(5)	(6)
Member ID	r	I (space truss)	$\frac{M_{TEST}}{M_{ACI}/}$ AASHTO	$\frac{T_{TEST}}{T_{ACI}/}$ AASHTO	Mode of failure
B2	0.5	1.13	0.81	0.74	M
B3	0.5	1.03	0.45	0.88	T
C1	0.5	1.14	0.89	0.64	M
C2	0.5	1.04	0.62	0.87	T
D1	0.34	0.87	0.74	0.82	T
D2	0.34	0.80	0.45	1.34	T
D3	0.34	0.65	0.23	1.32	T
E1	1.0	1.23	0.80	0.63	M
E2	1.0	1.16	0.45	0.83	T
	\bar{x}	1.01	0.60	0.90	N=9
	s	0.19	0.22	0.26	

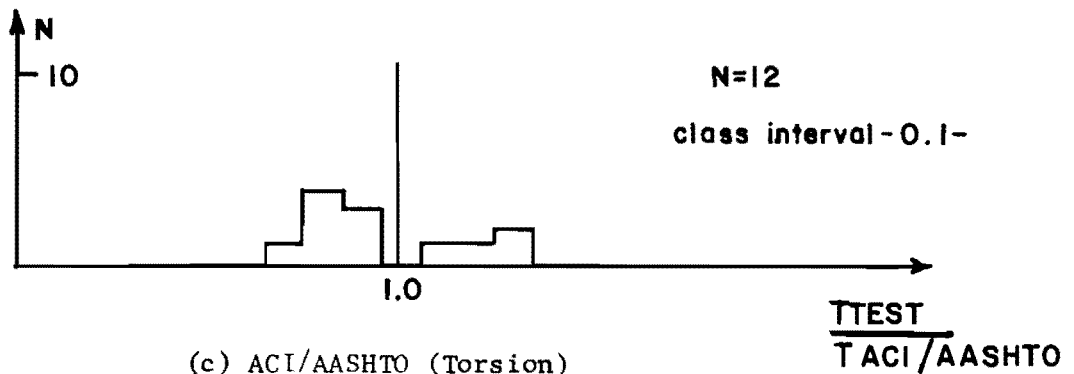
Table 3.52 Data on reinforced concrete rectangular beams
with web reinforcement subjected to combined
bending torsion



(a) Space truss model



(b) ACI/AASHTO (Flexure)



(c) ACI/AASHTO (Torsion)

Fig. 3.69 Comparison between the ACI/AASHTO and space truss model predictions with test results of reinforced concrete beams under combined torsion bending

3.9.3 Torsion-Bending-Shear. In the case of combined torsion-bending-shear the ACI/AASHTO ultimate predicted values are evaluated in accordance with the requirements given in Refs. 24 and 12 and previously discussed in Report 248-2.

Since the current ACI/AASHTO design recommendations do not directly consider the interaction between torsion and bending the comparison has to be carried out as in the case of combined torsion-bending. However, since the ACI/AASHTO design procedures do consider the interaction between torsion and shear, in this case the value of the torsional moment computed to evaluate the ratio of column (5) of Tables 3.53 and 3.54 do reflect the level of shear force present at ultimate in the member.

Shown in Tables 3.53 and 3.54 are data on reinforced concrete rectangular and L-beams subjected to combined torsion-bending-shear. Once more the dominant mode of failure for each specimen given in column (7) is selected by choosing the largest of the two ratios given in columns (4) and (5) for each specimen.

Figure 3.70 shows a comparison between the Space Truss and the ACI/AASHTO predicted values with the data from Tables 3.53 and 3.54. As can be seen from Fig. 3.70 the Truss Model is as good as the current ACI/AASHTO procedures for the case of failures controlled by flexure. In the case of failures controlled by torsion (Fig. 3.70c), the Truss Model predicted values (see Fig. 3.70a) show a much better agreement with test results greatly reducing the scatter between the predicted and observed ultimate values.

Tests reported by Collins, Walsh, Archer, and Hall [33] on rectangular solid beams (R)						
(1)	(2)	(3)	(4)	(5)	(6)	(7)
Member ID	r	I (space truss)	$\frac{M_{TEST}}{M_{ACI/AASHTO}}$	$\frac{T_{TEST}}{T_{ACI/AASHTO}}$	V_{TEST} (k)	Mode of failure
RE2(R)	1.0	1.05	0.22	0.82	0.9	T-S
RE3(R)	1.0	1.09	0.31	0.80	1.3	T-S
RE4(R)	1.0	1.24	0.60	0.74	2.4	T-S
RE5(R)	1.0	1.30	0.76	0.65	3.1	M
RE4*(R)	1.0	1.25	0.94	0.38	3.8	M
RU1(R)	0.26	0.75	0.21	0.88	0.3	T-S
RU3A*(R)	0.26	0.73	0.21	0.88	0.3	T-S
RU5(R)	0.26	1.11	0.84	0.92	7.1	T-S
RU5A(R)	0.26	1.16	0.88	0.81	7.6	M
RU6(R)	0.26	1.19	0.95	0.73	8.0	M
	\bar{x}	1.09	0.59	0.76		N=10
	s	0.20	0.32	0.16		
Tests reported by Liao and Ferguson [104] on reinforced concrete L-sections.						
3LS-6(L)	1.0	1.20	0.24	2.6	1.74	T-S
3LS-8(L)	1.0	1.07	0.23	2.31	1.63	T-S
3LS-3(L)	1.0	1.18	0.60	1.76	4.06	T-S
1.5LS-1(L)	1.0	1.10	0.32	1.88	4.78	T-S
3LS-2(L)	1.0	1.30	0.43	2.29	3.06	T-S
1.5LS-2(L)	1.0	1.20	0.24	2.41	3.53	T-S
	\bar{x}	1.18	0.34	2.21		N=6
	s	0.08	0.15	0.32		
Total	\bar{x}	1.12	0.50	1.30		N=16
Table 3.53	s	0.17	0.29	0.76		

Table 3.53 Data on reinforced concrete rectangular and L-beams with web reinforcement subjected to combined torsion-bending-shear

Tests reported by Osburn, Mayoglou, and Mattock [133] on rectangular (R) and L-beams (L)						
(1)	(2)	(3)	(4)	(5)	(6)	(7)
Member ID	r	I (space truss)	$\frac{M_{TEST}}{M_{ACI/}}$ AASHTO	$\frac{T_{TEST}}{T_{ACI/}}$ AASHTO	V_{TEST} (k)	Mode of failure
A1(R)	0.15	1.31	1.17	0.96	13.2	M
A2(R)	0.15	1.27	1.07	0.93	14.2	M
A3(R)	0.15	1.19	1.10	0.92	15.6	M
A4(R)	0.15	1.03	1.07	0.88	17.2	M
A5(R)	0.15	0.91	1.06	0.99	20.2	M
B1(R)	0.15	1.24	1.09	1.20	8.72	T-S
B2(R)	0.15	1.15	1.05	1.16	9.1	T-S
B3(R)	0.15	1.15	1.09	1.18	10.4	T-S
B4(R)	0.15	1.07	0.98	1.11	11.2	T-S
B5(R)	0.15	1.04	1.06	1.09	12.8	T-S
C1(R)	0.10	1.14	1.10	0.93	10.0	M
C2(R)	0.12	0.94	0.95	0.80	10.55	M
C3(R)	0.13	1.03	1.04	0.87	13.4	M
C4(R)	0.10	0.94	1.00	0.94	16.1	M
D1(L)	0.10	1.26	1.10	1.00	10.8	M
D2(L)	0.12	1.12	1.00	0.94	12.3	M
D3(L)	0.13	0.92	0.96	0.90	13.4	M
D4(L)	0.10	0.93	0.87	0.90	15.9	T-S
E1(L)	0.10	1.24	1.09	0.99	10.7	M
E2(L)	0.12	1.02	0.93	0.85	11.4	M
E3(L)	0.13	1.00	0.93	0.85	12.97	M
E4(L)	0.10	0.80	0.76	0.77	13.9	T-S
	\bar{x}	1.08	1.02	0.96	N=22	
	s	0.14	0.09	0.12		

Table 3.54 Data on reinforced concrete rectangular and L-beams with web reinforcement subjected to combined torsion-bending-shear

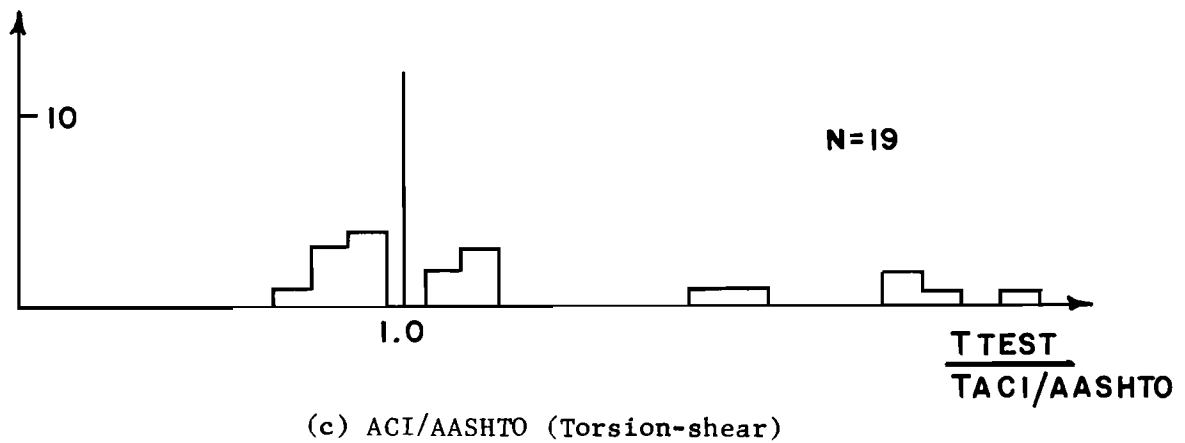
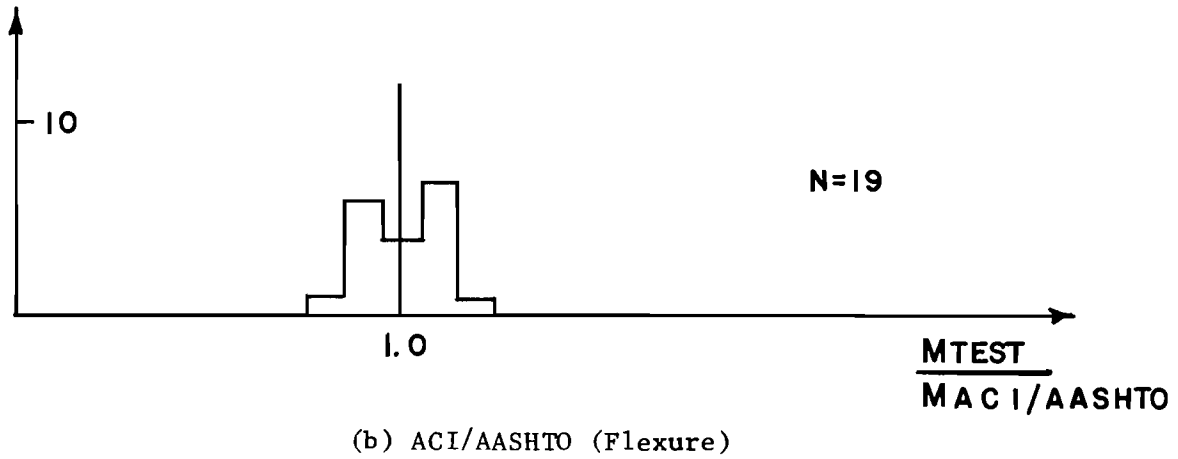
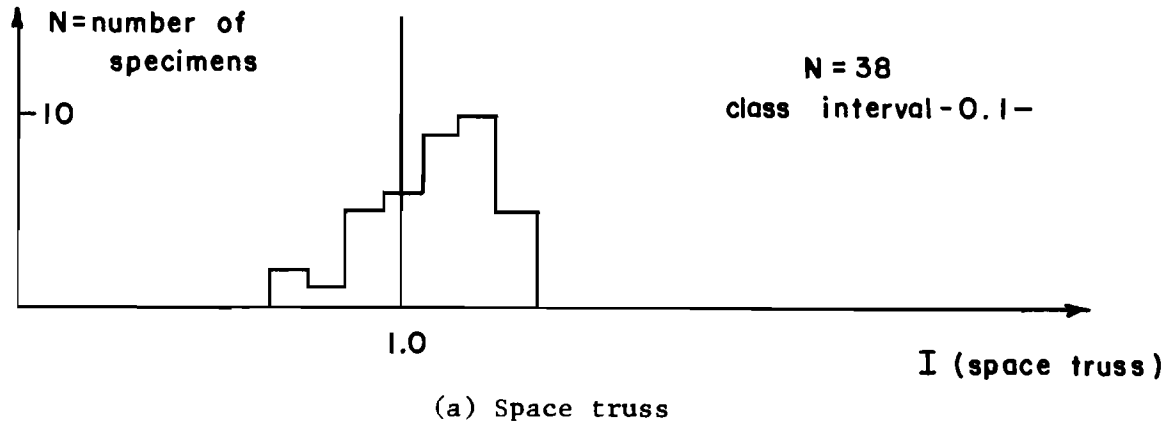


Fig. 3.70 Comparison between the space truss and the ACI/AASHTO prediction with test results of reinforced concrete beams under torsion-bending-shear

3.9.4 Bending and Shear. In this section the data examined in Sec. 3.5 on reinforced and prestressed concrete beams with web reinforcement failing in shear are utilized to compare the Truss Model predictions and the ACI/AASHTO ultimate expected values.

The ACI/AASHTO predicted ultimate strength is evaluated in accordance with the requirements given in Refs. 24 and 12, and previously discussed in Report 248-2.

In computing the concrete contribution in the case of AASHTO/ACI predicted values, the formula $1.9\sqrt{f'_c} + 2500 \rho_w V_d/M$ is used; where ρ_w is a ratio of longitudinal reinforcement defined as $A_s/[b_w d]$, A_s being the area of longitudinal tension reinforcement, V and M are the ultimate test values, and "d" is the distance between the extreme compression fiber and the centroid of the longitudinal tension reinforcement.

Shown in Tables 3.55 through 3.57 are data from simply supported reinforced concrete rectangular beams failing in shear. Given in column (5) of Tables 3.55 through 3.57 is the ratio of the test value to the ACI/AASHTO predicted value. In column (4) the dispersion index "I" of the Truss Model, previously explained in Sec. 3.5, is given.

In Fig. 3.71 the values of columns (4) and (5) from Tables 3.55 through 3.57 are shown to compare the truss model predictions and the ACI/AASHTO expected ultimate load values with data from reinforced concrete beams failing in shear. As can be seen from Fig. 3.71, the Truss Model predictions, although conservative, show much better agreement with the actual test values. They significantly reduce the scatter of the test to predicted shear ratio.

Tests reported by Schaeffer (153) on reinforced concrete rectangular beams

Member ID	$\rho_v f_y$ psi	$\tan \alpha$ Eq. 3.16	I space truss	$\frac{V_{test}}{V_{ACI/AASHTO}}$	Level of Prestress $\sigma/f'c$
RL-0.50	310	0.52	1.02	1.31	0.0
RL-1.25	800	0.49	0.96	1.34	
RH-0.50	400	0.49	1.16	1.36	
		X	1.05	1.34	N = 3
		S	0.10	0.03	

Tests reported by O. Moretto (99) on reinforced concrete rectangular beams

1V $\frac{1}{4}$ 1	150	0.24	1.14	1.76	0.0
1V $\frac{1}{4}$ 2		0.24	1.14	1.81	
2V $\frac{1}{4}$ 1		0.20	1.33	2.00	
2V $\frac{1}{4}$ 2		0.20	1.33	1.98	
1V $\frac{3}{8}$ 1	290	0.38	1.15	1.58	
1V $\frac{3}{8}$ 2		0.36	1.21	1.60	
2V $\frac{3}{8}$ 1		0.36	1.20	1.54	
2V $\frac{3}{8}$ 2		0.38	1.13	1.49	
1aV $\frac{1}{4}$ 1	130	0.23	1.05	1.83	
1aV $\frac{1}{4}$ 2		0.23	1.07	1.86	
		X	1.18	1.75	N = 10
		S	0.10	0.18	
All values in Table 3.55	in	X	1.15	1.65	N = 13
		S	0.11	0.24	

Table 3.55 Data on simply supported reinforced concrete rectangular beams failing in shear

Tests reported by A.P. Clark (53) on reinforced concrete rectangular beams

(1) Member ID	(2) $\rho v f_y$ psi	(3) $\tan \alpha$ Eq. 3.16	(4) I space truss	(5) $\frac{V_{test}}{\sqrt{ACI/AASHTO}}$	(6) Level of Prestress σ/f'_c
B1-1	180	0.30	1.23	1.58	0.0
B1-2		0.34	1.14	1.41	
B1-3		0.30	1.25	1.60	
B1-4		0.32	1.17	1.50	
B1-5		0.36	1.06	1.32	
B2-1	350	0.58	1.13	1.10	
B2-2		0.54	1.19	1.16	
B2-3		0.52	1.24	1.21	
C1-1	170	0.29	1.50	1.63	
C1-2		0.25	1.70	1.84	
C1-3		0.33	1.34	1.45	
C1-4		0.28	1.56	1.64	
C3-1		0.36	1.21	1.43	
C3-2		0.40	1.09	1.29	
C3-3		0.43	1.02	1.20	
C2-1	330	0.56	1.33	1.12	
C2-2		0.53	1.39	1.17	
C2-4		0.56	1.33	1.10	
C4-1	170	0.27	1.27	1.75	
C4-2		0.19	1.73	2.11	
C6-3		0.18	1.78	2.18	
C6-4		0.19	1.75	2.09	
D1-1	220	0.35	1.55	1.51	
D1-3		0.41	1.32	1.29	
D3-1	440	0.55	1.24	1.19	
D2-1	290	0.49	1.37	1.20	
D2-2		0.46	1.47	1.27	

Table 3.56 Data on simply supported reinforced concrete rectangular beams failing in shear

Tests reported by A.P. Clark (53) on reinforced concrete rectangular beams (continuation)

(1) Member ID	(2) $\rho v f_y$ psi	(3) $\tan \alpha$ Eq. 3.16	(4) I space truss	(5) $\frac{V_{test}}{V_{ACI/AASHTO}}$	(6) Level of Prestress σ / f'_c
D4-1	590	0.92	1.25	0.95	0.0
D1-5	170	0.38	1.10	1.34	
D1-7		0.36	1.13	1.38	
D1-8		0.35	1.19	0.45	
E1-2	260	0.47	1.30	1.28	
D2-6	220	0.51	1.14	1.12	
D2-7		0.56	1.04	1.03	
D2-8		0.51	1.13	1.15	
D4-1	180	0.41	1.19	1.31	
D4-2		0.45	1.09	1.21	
D4-3		0.42	1.16	1.32	
D5-1	130	0.36	1.10	1.32	
D5-2		0.34	1.17	1.40	
D5-3		0.34	1.17	1.40	
A1-1	180	0.41	1.06	1.25	
A1-2		0.43	0.99	1.18	
A1-3		0.41	1.06	1.25	
A1-4		0.41	1.06	1.25	
3.56 and 3.57 combined		X	1.26	1.38	
		S	0.20	0.28	N = 45

Table 3.57 Data on simply supported reinforced concrete rectangular beams

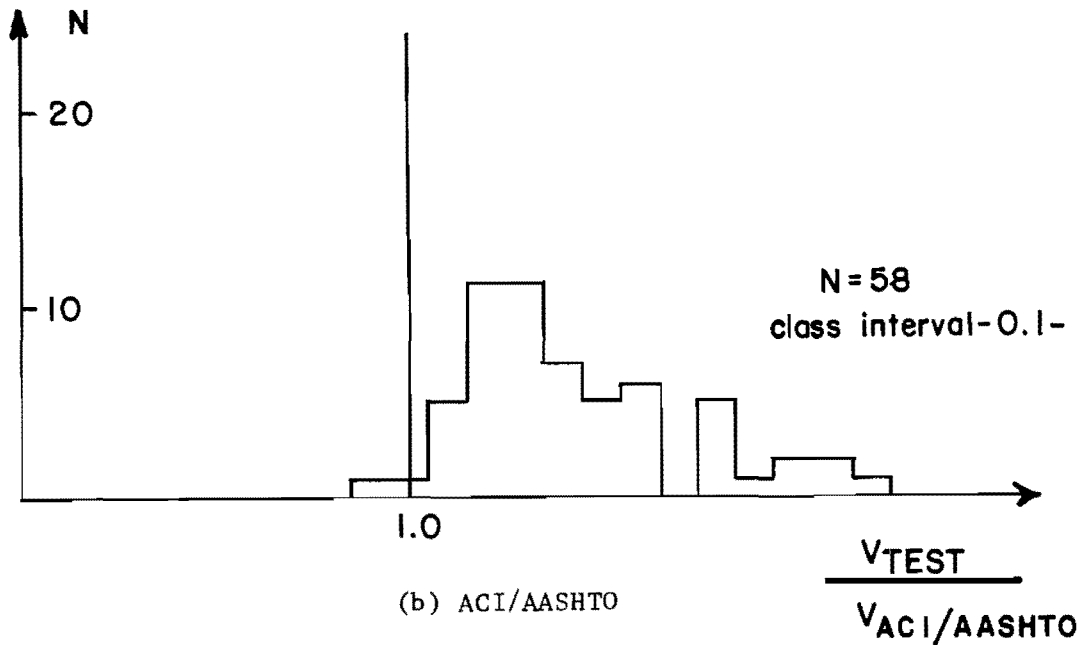
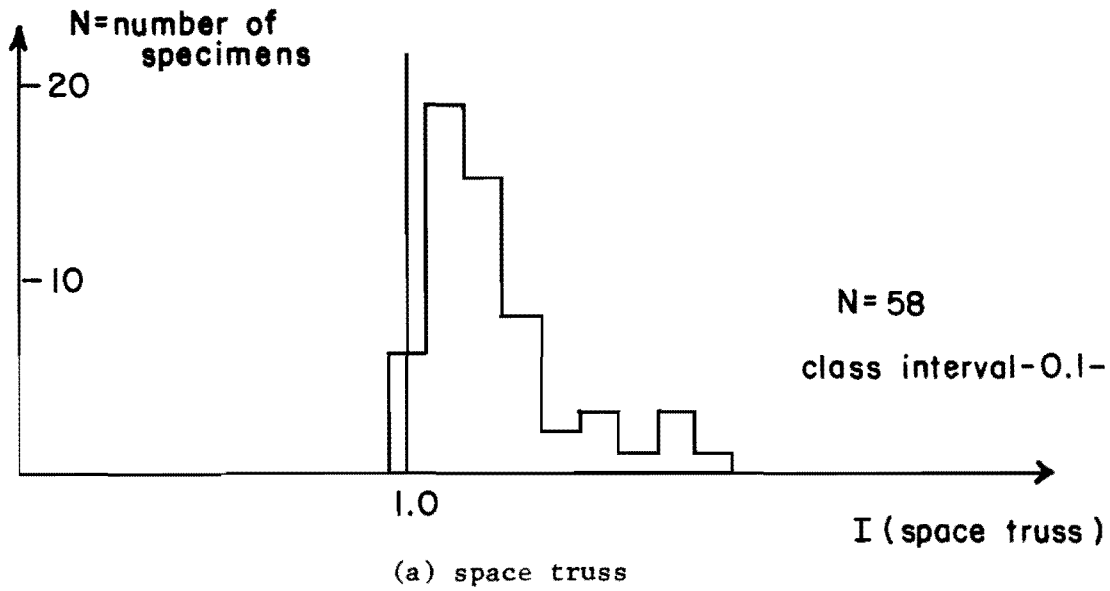


Fig. 3.71 Comparison between the ACI/AASHTO and space truss model predictions with test results of reinforced concrete beams where shear failures were observed

Shown in Tables 3.58 and 3.59 are data on simply supported prestressed concrete T, and I beams failing in shear. Figure 3.72 shows a comparison between the Space Truss Model and the ACI/AASHTO predictions with test data given in Tables 3.58 and 3.59. Again, the Truss Model predictions show considerably less scatter than the ACI/AASHTO values. However, in this case the Truss Model yields very conservative results.

The test data from Ref. 110 are shown in Table 3.60. Although it was reported that all the specimens shown in Table 3.60 had failed in shear, when the ratio V_{test} to $V_{\text{ACI/AASHTO}}$ was evaluated, the ACI/AASHTO predictions were found to be very unconservative. In order to clarify this point the maximum shear value corresponding to the ultimate flexural capacity of the section was evaluated in accordance with the guidelines given in Refs. 24 and 12 for each specimen. Column (6) of Table 3.60 shows the values of ratio of the test shear to the maximum possible value of shear as limited by the flexural capacity of the section. As can be seen in all cases, except specimens CW1451 and CW1454, flexure would control the maximum shear that could be carried by the section, thus indicating flexure type failures at relatively high shear levels.

Nevertheless, by comparing the values of the mean (X) and the standard deviation (S) of the index "I" given in column (4) with the corresponding values of the ratio for column (6) in Table 3.60, it can be seen that even in the case of flexure failure the Truss Model compares rather well with the ACI/AASHTO procedures.

Tests reported by Moayer and Regan (33)
on prestressed concrete T-Beams

(1) Member ID	(2) ρvfy psi	(3) $\tan \alpha$ Eq. 3.16	(4) Ispace truss	(5) $\frac{V_{test}}{V_{ACI/AASHTO}}$	(6) Level of Prestress $\sigma / f'c$
P4	155	0.52	1.42	1.05	0.07
P8	104	0.12	1.55	1.60	0.14
P13	104	0.14	1.68	1.65	0.05
P18	104	0.13	1.60	1.50	0.13
P24	155	0.49	1.33	1.03	0.05
P25	104	0.21	1.51	1.45	0.05
P26	155	0.41	1.32	1.04	0.12
P27	104	0.18	1.43	1.37	0.13
P28	155	0.36	1.28	1.15	0.13
P29	104	0.23	1.34	1.40	0.13
P49	155	0.37	0.98	1.15	0.16
		X	1.38	1.28	N = 2
		S	0.20	0.24	

Tests reported by Castrodale (50) on prestressed
concrete I-beams under distributed loadings

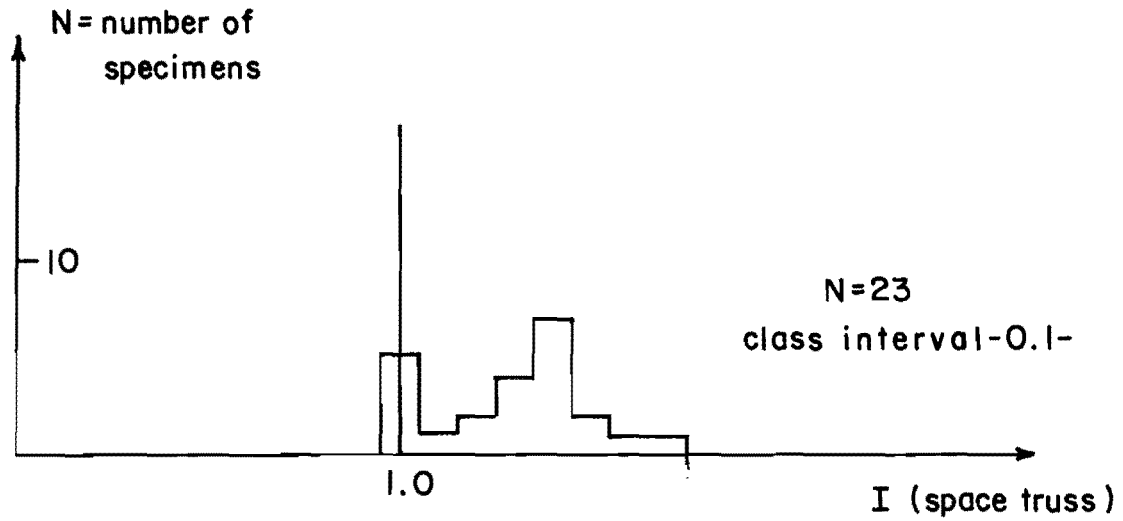
0.40A	180	0.17	1.04	1.84	0.10
0.40B	180	0.17		2.00	0.13
0.45	220	0.19		2.00	0.12
		X	1.04	1.95	N = 3
		S	0.0	0.09	
Overall for Table 3.58		X	1.31	1.41	N = 15
		S	0.23	0.35	

Table 3.58 Data on simply supported prestressed concrete
T and I beams failing in shear

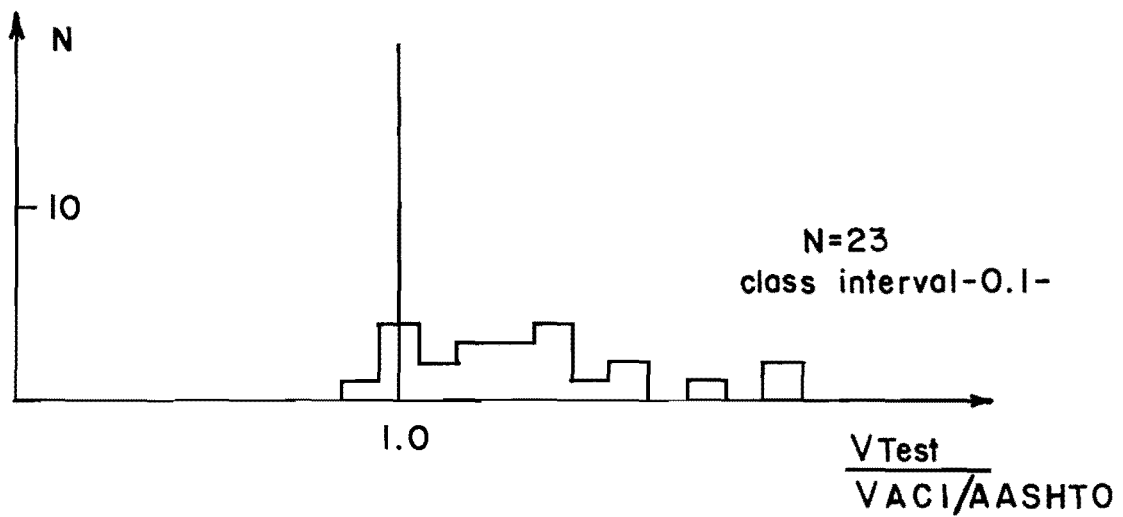
Tests reported by Hernandez (76) on prestressed concrete I-beams

(1) Member ID	(2) $\rho_v f_y$ psi	(3) $\tan \alpha$ Eq. 3.16	(4) I_{space} truss	(5) $\frac{V_{test}}{V(ACI/AASHTO)}$	(6) Level of Prestress σ/f'_c
C5	180	0.21	1.38	1.34	0.19
G6	140	0.20	1.23	1.21	0.20
G7	230	0.27	1.39	1.28	0.13
G10	230	0.31	1.20	1.20	0.24
G20	270	0.72	1.05	0.94	0.26
G28	120	0.24	1.37	1.30	0.14
G29	320	0.29	1.43	1.38	0.14
G34	330	0.35	1.45	1.16	0.15
		X	1.31	1.23	
		S	0.14	0.14	
					N = 8

Table 3.59 Data on simply supported prestressed concrete beams failing in shear



(a) Space truss



(b) ACI/AASHTO

Fig. 3.72 Comparison between the space truss model and the ACI/AASHTO predictions with test results of prestressed concrete beams failing in shear

Tests reported by MacGregor, Sozen and Siess (110) on prestressed concrete I-beams

(1) Member ID	(2) $\rho_{vf} f_y$ psi	(3) tan α Eq. 3.16	(4) I space truss	(5) $\frac{V_{test}}{V_{ACI/AASHTO}}$ (shear)	(6) $\frac{V_{test}}{V_{ACI/AASHTO}}$ (flexure)	(7) Level of Prestress σ / f'_c
BW1438	167	0.68	1.13	0.75	1.05	0.17
CW1437	208	0.87	1.07	0.89	1.02	0.19
CW1439	167	0.83	0.94	0.76	0.87	0.20
CW1447	138	0.63	1.04	0.92	0.99	0.24
CW1450	180	0.81	1.02	0.91	1.02	0.26
CW1451	99	0.41	0.90	0.91	0.91	0.27
CW1454	97	0.38	0.94	1.00	0.99	0.24
		X	1.01	0.88	0.98	
		S	0.08	0.09	0.06	N = 7

Table 3.60 Data on prestressed concrete I-beams
(from Ref. 110)

Tables 3.61 and 3.62 show data for reinforced and prestressed concrete continuous beams failing in shear. Figure 3.73 shows a comparison between the ACI/AASHTO and Space Truss Model predictions with test data from Tables 3.61 and 3.62 on continuous beams failing in shear. It is apparent that the Truss Model tends to yield reasonable predicted values; however, it is slightly more unconservative than the current ACI/AASHTO design procedures. The shaded portion of the space truss values in Fig. 3.73 are specimens in which $\tan\alpha$ falls significantly outside the space truss limits, these should not be considered in judging the accuracy of the design procedure.

After comparing both procedures with test results it can be concluded that:

1. In the cases of pure torsion, combined torsion-bending and torsion-bending-shear the Truss Model yields conservative results and is in better agreement with observed test values than the current ACI/AASHTO procedures.
2. In the case of bending and shear the Truss Model again is in better agreement with test results than the current ACI/AASHTO procedures. However, it seems to yield more conservative predictions than in the case of combined actions.

Tests reported by Rodriguez, Bianchini, Viest and Kesler (146)
on two-span continuous reinforced concrete beams

(1) Member ID	(2) $\rho v f_y$ psi	(3) $\tan \alpha$ Eq. 3.16	(4) I space truss	(5) $\frac{V_{test}}{V_{ACI/AASHTO}}$	(6) Level of Prestress σ/f'_c
C6A1	670	0.66	1.27	1.33	0.0
E6H1	1020	1.00	1.05	1.45	
E6H2	770	0.84	0.90	1.27	
C6H1	1050	1.17	0.90	1.27	
C6H2	750	0.81	0.94	1.32	
E6I2	1020	1.23	0.99	1.20	
C6I2	1040	1.23	1.02	1.30	
C3A2	310	0.51	1.26	1.21	
E3H1	530	0.75	1.00	0.98	
E3H2	410	0.69	0.93	0.95	
C3H1	510	0.84	0.84	0.98	
C3H2	410	0.74	0.80	0.90	
E2A1	180	0.41	1.15	1.25	
E2A2	180	0.46	1.03	1.17	
E2A3	190	0.43	1.04	1.26	
C2A1	190	0.58	0.84	0.92	
C2A2	190	0.47	1.00	1.13	
E2H1	410	0.84	0.77	0.81	
E2H2	270	0.61	0.72	1.00	
C2H1	420	0.84	0.83	0.83	
C2H2	270	0.59	0.85	1.03	
B2A1	140	0.42	1.02	1.11	
B2H1	280	0.64	0.95	0.98	
B2H2	180	0.45	0.92	1.19	
		X	0.96	1.12	
		S	0.14	0.18	

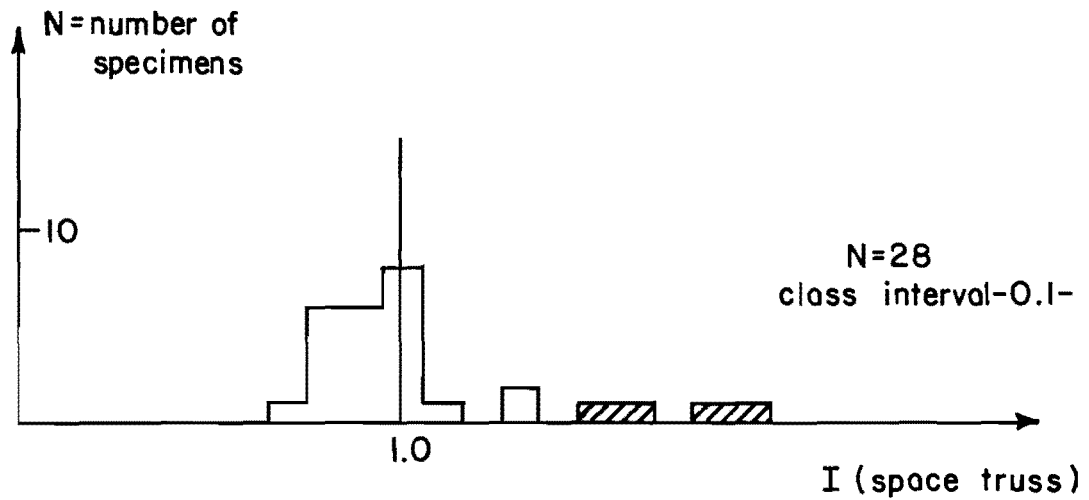
N = 24

Table 3.61 Data on two-span continuous reinforced concrete
beams failing in shear

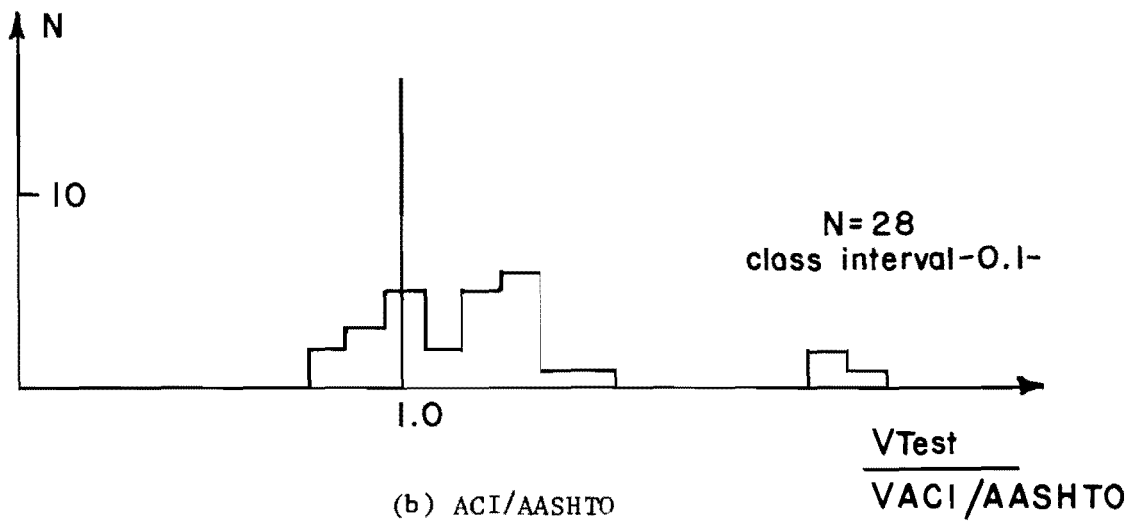
Tests reported by Mattock and Kaar (111) on semi-continuous prestressed concrete I-beams.

(1) Member ID	(2) $\rho v f_y$ psi	(3) $\tan \alpha$ Eq. 3.16	(4) I space truss	(5) $\frac{V_{test}}{V(ACI/AASHTO)}$	(6) Level of prestress σ/f'_c
S7	282	0.21	1.89	2.07	0.15
S13	282	0.31	1.54	1.53	0.14
S10	188	0.17	1.83	2.18	0.15
S21	188	0.17	1.62	2.08	0.14
		X =	1.72	1.97	
		S =	0.17	0.29	N = 4

Table 3.62 Data on semicontinuous prestressed concrete I beams failing in shear



(a) Space truss



(b) ACI/AASHTO

Fig. 3.73 Comparison between the space truss model and the ACI/AASHTO predictions with test results of continuous reinforced and prestressed concrete beams failing in shear

CHAPTER 4

CONCLUSIONS

4.1 Summary

In this report a complete evaluation of the truss model in the areas of shear, torsion, and shear and torsion, has been conducted by careful comparison with several hundred experimental results.

A comparison of the variable angle truss model predicted ultimate values with test results of reinforced and prestressed concrete one-way flexural members where failure produced yielding of the longitudinal and web reinforcement was carried out. This comparative study showed that the truss model predicted ultimate strength is in very good agreement with observed ultimate values of members where yielding of the reinforcement at failure was reported.

In Sec. 3.2 it was pointed out that the basic truss model used herein does not include the effects of warping torsion. This type of torsion becomes significant in the case of open-ended members formed by three or more walls, where the torsional warping of the cross section is restrained. In these cases, the basic truss model tends to underestimate the torsional capacity of those members. More advanced truss models have been proposed for cases where warping torsion is important.

It was also shown that the truss model interaction equations very adequately represent the ultimate load interaction of reinforced

and prestressed one-way flexural members subjected to torsion-bending, and torsion-bending-shear.

In Sec. 3.6 an upper limit for the compression stress in the diagonal strut was proposed based on a study of data from reinforced and prestressed concrete beams under torsion, shear and combined torsion-shear failing due to crushing of the web. A very conservative expression was proposed which still liberalizes current maximum shear stress allowables.

In Sec. 3.7 failures due to poor detailing were examined in order to illustrate the importance of adequate detailing in the Truss Model approach and at the same time to show how the Truss Model can help the designer to adequately detail reinforced concrete members. Further examples will be provided in a later report.

The value of the concrete contribution in the uncracked and transition state was investigated in Sec. 3.8 using data of beams with no or very light web reinforcement. The concrete contribution was shown to be important but to be able to be conservatively predicted by a relatively simple transition zone expression.

Finally, in Sec. 3.9 an extensive comparison between the ACI/AASHTO and Truss Model ratios of predicted ultimate strengths to test results was conducted. It showed that the truss model is more accurate and that it significantly reduced scatter compared to current procedures. It certainly has the potential to provide a uniform framework for considering combined actions.

4.2 Recommendations

With the general interaction behavior and expected failure capacities confirmed by test results, the general procedures derived from the truss model are translated in Report 248-4F into design recommendations and draft AASHTO requirements. A review of some of the current design procedures available in other codes is also given in Report 248-4F. In that report, the design procedures based on the truss model are applied through a series of design examples. A parallel design using the current AASHTO design procedures, wherever available, is conducted and a comparison of the results of the two design procedures is presented.

This page replaces an intentionally blank page in the original.

-- CTR Library Digitization Team

REFERENCES

1. American Association of State Highway Officials, Standard Specifications for Highway Bridges, American Association of State Highway Officials, 1935.
2. American Association of State Highway Officials, Standard Specifications for Highway Bridges, American Association of State Highway Officials, 1941.
3. American Association of State Highway Officials, Standard Specifications for Highway Bridges, American Association of State Highway Officials, 1944.
4. American Association of State Highway Officials, Standard Specifications for Highway Bridges, American Association of State Highway Officials, 1949.
5. American Association of State Highway Officials, Standard Specifications for Highway Bridges, American Association of State Highway Officials, 1953.
6. American Association of State Highway Officials, Standard Specifications for Highway Bridges, American Association of State Highway Officials, 1957.
7. American Association of State Highway Officials, Standard Specifications for Highway Bridges, American Association of State Highway Officials, 1961.
8. American Association of State Highway Officials, Standard Specifications for Highway Bridges, American Association of State Highway Officials, 1965.
9. American Association of State Highway Officials, Standard Specifications for Highway Bridges, American Association of State Highway Officials, 1969.

10. American Association of State Highway Officials, Standard Specifications for Highway Bridges, American Association of State Highway Officials, 1973.
11. American Association of State Highway and Transportation Officials, Interim Specifications Bridges, American Association of State Highway and Transportation Officials, 1974.
12. American Association of State Highway and Transportation Officials, Standard Specification for Highway Bridges, American Association of State Highway and Transportation Officials, 1977.
13. American Association of State Highway and Transportation Officials, Interim Specifications, Bridges, American Association of State Highway and Transportation Officials, 1978.
14. American Association of State Highway and Transportation Officials, Interim Specifications, Bridges, American Association of State Highway and Transportation Officials, 1979.
15. American Association of State Highway and Transportation Officials, Interim Specifications, Bridges, American Association of State Highway and Transportation Officials, 1980.
16. American Association of State Highway and Transportation Officials, Interim Specifications, Bridges, American Association of State Highway and Transportation Officials, 1981.
17. American Association of State Highway and Transportation Officials, Interim Specifications, Bridges, American Association of State Highway and Transportation Officials, 1982.
18. American Concrete Institute, ``Standard Building Regulations for the Use of Reinforced Concrete,`` ACI Standard Specification No.23, Vol. 16, February 1920, pp. 283-322.
19. American Concrete Institute, Building Code Requirements for Reinforced Concrete (ACI 318-51), ACI Journal, April 1951.
20. American Concrete Institute, Building Code Requirements for Reinforced Concrete (ACI 318-56), ACI Journal, May 1956.
21. American Concrete Institute, Building Code Requirements for

- Reinforced Concrete (ACI 318-63), American Concrete Institute, 1963.
22. American Concrete Institute, Commentary on Building Code Requirements for Reinforced Concrete (ACI 318-63), American Concrete Institute, 1965.
 23. American Concrete Institute, Building Code Requirements for Reinforced Concrete (ACI 318-71), American Concrete Institute, 1971.
 24. American Concrete Institute, Building Code Requirements for Reinforced Concrete (ACI 318-77), American Concrete Institute, 1977.
 25. American Concrete Institute, ``Tentative Recommendations for Prestressed Concrete (ACI 323),'' ACI Journal, Vol. 29, No. 7, Jan. 1958, pp. 545-578.
 26. ACI-ASCE Committee 326, ``Shear and Diagonal Tension,'' ACI Journal, Vol. 59, Jan., Feb. 1962, pp. 3-30, 277-333.
 27. ACI-ASME Committee 359, Code for Concrete Reactor Vessels and Containments (ACI 359-74), ASME Boiler and Pressure Vessel Code, Section III, Div. 2, American Society of Mechanical Engineers, 1975.
 28. ACI-ASCE Committee 426, ``The Shear Strength of Reinforced Concrete Members,'' Journal of the Structural Division, ASCE, Vol. 99, No. St6, June 1973, pp. 1091-1187.
 29. ACI-ASCE Committee 426, Suggested Revisions to Shear Provisions for Building Codes, American Concrete Institute, Detroit, 1977, pp. 99.
 30. American Concrete Institute, Analysis of Structural Systems for Torsion, Publication SP-35, Detroit, 1973, .
 31. ACI Committee 438, Torsion in Concrete, American Concrete Institute Bibliography, Detroit, 1978, .
 32. American Concrete Institute, Shear in Reinforced Concrete, ACI Publication SP-42, Detroit, 1974, .
 33. American Concrete Institute, Torsion of Structural Concrete, Publication SP-18, Detroit, 1974, .
 34. ACI Committee 438, ``Tentative Recommendations for the Design of Reinforced Concrete Members to Resist Torsion,'' Journal of

- the American Concrete Institute, Vol. 66, No. 1, Jan. 1969, pp. 1-7.
35. American Concrete Institute, Analysis of Structural Systems for Torsion, Publication SP-35, Detroit, 1973, .
 36. ACI Committee 408, ``Suggested Development, Splice and Standard Hook Provisions for Deformed Bars in Tension,`` Concrete International, July 1979, pp. 44-46.
 37. Badawy, H.E.I., McMullen, A.E., and Jordaan, I.J., ``Experimental Investigation of the Collapse of Reinforced Concrete Curved Beams,`` Magazine of Concrete Research, June 1977, pp. 59-69.
 38. Behera, V., Reinforced Concrete Beams, with Stirrups, Under Combined Torsion, PhD dissertation, The University of Texas at Austin, January 1969.
 39. Bennett, E.W., and Balasooriya, B.M.A., ``Shear Strength of Prestressed Beams with Thin Webs Failing in Inclined Compression,`` ACI Journal, Vol. 68, No. 3, March 1971, pp. 204-212.
 40. Benneth, E.W., Abdul-Ahad, H.Y., and Neville, A.M., ``Shear Strength of Reinforced and Prestressed Concrete Beams Subjected to Moving Loads,`` Journal of the Prestressed Concrete Institute, Vol. 17, No. 6, Nov./Dec. 1972, pp. 58-69.
 41. Birton, T.G., and Kirk, D.W., ``Concrete T-Beams Subject to Combined Loading,`` Journal of the Structural Division, ASCE, Vol. 99, No. St4, April 1973, pp. 687-700.
 42. Bishara, A., ``Prestressed Concrete Beams Under Combined Torsion, Bending and Shear,`` ACI Journal, Vol. 66, No. 7, July 1969, pp. 525-539.
 43. Bresler, B., and MacGregor, J.G., ``Review of Concrete Beams Failing in Shear,`` Journal of the Structural Division, ASCE, Vol. 93, No. ST1, February 1967, pp. 343-372.
 44. Brecht, H.E., Hanson, J.M., and Hulsbos, C.L., ``Ultimate Shear Tests of Full-Sized Prestressed Concrete Beams,`` Report 223.28, Fritz Engineering Laboratory, December 1965.
 45. Campbell, T.I., and de V. Batchelor, B., ``Effective Width of Girder Web Containing Prestressing Ducts,`` Journal of the Structural Division, ASCE, Vol. 107, No. St5, May 1981, pp. 733-744.

46. Campbell, T.I., Chitnuyanondh, L., and Batchelor, B. de V., ``Rigid-plastic Theory vs. Truss Analogy Method for Calculating the Shear Strength of Reinforced Concrete Beams,'' Magazine of Concrete Research, Vol. 32, No. 110, March 1980, pp. 39-44.
47. Campbell, T.I., Batchelor, B. de V., and Chitnuyanoudh, I., ``Web Crushing in Prestressed Concrete Girders with Ducts in the Webs,'' PCI Journal, Vol. 24, No. 5, September, October. 1979, pp. 70-88.
48. Caflish, R., Krauss, R., and Thürlimann, B., ``Biege- und Schubversuche an Teilweise Vorgespannten Betonbalken, Serie C.,' ' Bericht 6504-3, Institut für Baustatik, ETH Zurich, February, 1971.
49. Canadian Standards Association, ``Canadian Code Draft- Clause 11 Shear and Torsion'', Draft #9, unpublished.
50. Castrodale, R.W., ``A Comparison of Design for Shear in Prestressed Concrete Bridge Girders'', Thesis, University of Texas at Austin, unpublished.
51. Christophe, P., Le Béton Arme et ses Applications, Librairie Polytechnique, 1902, 2nd edition.
52. Chana, P.S., ``Some Aspects of Modelling the Behavior of Reinforced Concrete Under Shear Loading,' ' Technical Report 543, Cement and Concrete Association, July 1981.
53. Clark, A.P., ``Diagonal Tension in Reinforced Concrete Beams,' ' ACI Journal, Vol. 48, No. 2, October 1951, pp. 145-156.
54. Clarke, J.L., Taylor, H.P.J., ``Web Crushing-A Review of Research,' ' Technical Report, Cement and Concrete Association, August 1975.
55. Comité Euro-International du Béton, ``Shear, Torsion, and Punching,' ' Bulletin D'Information, , 1982, Number 146
56. Collins, M.P., and Mitchell, D., ``Shear and Torsion Design of Prestressed and Non-Prestressed Concrete Beams,' ' PCI Journal, Vol. 25, No. 5, September, October 1980, pp. 32-100.
57. Collins, M.P., ``Towards a Rational Theory for RC Members in Shear,' ' Journal of the Structural Division, ASCE, , Vol. 104, No. ST4, April 1978, pp. 649-666.
58. Collins, M.P., ``Investigating the Stress-Strain Characteristics of Diagonally Cracked Concrete,' ' IABSE Colloquium on

- Plasticity in Reinforced Concrete, May 1979, pp. 27-34, Copenhagen.
59. Collins, M.P., ``Reinforced Concrete Members in Torsion and Shear,`` IABSE Colloquium on Plasticity in Reinforced Concrete, May 1979, pp. 119-130, Copenhagen.
 60. Cowan, H.J., ``Torsion in Reinforced and Prestressed Concrete Beams,`` The Journal Institute of Engineers, September 1956, pp. 235-239.
 61. Cooper, M.J., and Martin, L.H., ``Prestressed Concrete Beams with No Stirrups in Torsion, Bending, and Shear, Proceedings,`` Institute of Civil Engineers, Part 2, June 1977, pp. 455-468.
 62. Comite Euro-International du Beton, CEB-FIP Model Code for Concrete Structures, International System of Unified Standard Codes of Practice for Structures, Paris, , Vol. II, 1978.
 63. Degenkolb, H.J. ``Concrete Box Girder Bridges,`` American Concrete Institute Monograph No.10,.
 64. Debaiky, S.Y., and Elniema, E.I., ``Behavior and Strength of Reinforced Concrete Haunched Beams in Shear,`` Journal of the American Concrete Institute, Vol. 79, No. 3, May/June 1982, pp. 184-194.
 65. Fenwick, R.C., The Shear Strength of Reinforced Concrete Beams, PhD dissertation, The University of Canterbury, Christchurch, New Zealand, 1966.
 66. Final Report of the Joint Committee on Concrete and Reinforced Concrete, ``Joint Committee on Concrete and Reinforced Concrete,`` ASTM, Vol. 17, 1917, pp. 202-262, Discussion, pages 263-292
 67. FIP, FIP Recommendations on Practical Design of Reinforced and Prestressed Concrete Structures, CEB/FIP, 1982, pp. 32-41, Model Code (MC-78).
 68. Fisher, G.P., and Zia, P., ``Review of Code Requirements for Torsion Design,`` ACI Journal, Vol. 61, No. 1, Jan. 1964, pp. 1-44.
 69. Gausel, E., ``Ultimate Strength of Prestressed I-Beams Under Combined Torsion, Bending, and Shear,`` Journal of the American Concrete Institute, Vol. 67, No. 9, September 1970, pp. 675-679.

70. Gesund, H., Schuete, F.J., Buchanan, G.R., and Gray, G.A., ``Ultimate Strength in Combined Bending and Torsion of Concrete Beams Containing both Longitudinal and Transverse Reinforcement,`` ACI Journal, Vol. 611, No. 12, December 1964, pp. 1509-1522.
71. Grob, J., ``Ultimate Strength of Beams with Thin Walled Open Cross-Sections,`` Bericht 56, Institut fur Baustatik und Konstruktion ETHZ, 1970, Birkhauser Verlag Basel und Stuttgart.
72. Grob, J., and Thürlimann, B., Ultimate Strength and Design of Reinforced Concrete Beams Under Bending and Shear, IABSE, Zurich, 1976, pp. 15, Publication No.36 II.
73. Hanson, J.M., Ultimate Shear Strength of Prestressed Concrete Beams With No Web Reinforcement, PhD dissertation, Lehigh University, 1964.
74. Henley, H.G., ``Report of the Committee on Laws and Ordinances,`` National Association of Cement Users, Vol. 4, 1908, pp. 233-239.
75. Henry, R.L., and Zia, P., ``Behavior of Rectangular Prestressed Concrete Beams Under Combined Torsion Bending and Shear,`` Report, University of North Carolina State, University at Raleigh, April 1971.
76. Hernandez, G., Strength of Prestressed Concrete Beams With Web Reinforcement, PhD dissertation, University of Illinois, Urbana., May 1958.
77. Hicks, A.B., ``The Influence of Shear Span and Concrete Strength Upon the Shear Resistance of a Pretensioned Concrete Beam,`` Magazine of Concrete Research, November 1958, pp. 115-121, University of London, Imperial College of Science and Technology.
78. Hognestad, E., ``What Do We Know About Diagonal Tension and Web Reinforcement In Concrete?,`` Circular Series 64, University of Illinois Engineering Experiment Station, March 1952.
79. Hsu, T.C., and Kemp, E.L., ``Background and Practical Application of Tentative Design Criteria for Torsion,`` Journal of the American Concrete Institute, Vol. 66, No. 1, January 1969, pp. 12-23.
80. Hsu, T.C., ``Torsion of Structural Concrete-Plain Concrete Rectangular Sections,`` Bulletin D134, Portland Cement Association, September 1968.

81. Hsu, T.C., ``Torsion of Structural Concrete, A Summary of Pure Torsion,' ' Bulletin D133, Portland Cement Association, 1968.
82. Hsu, T.C., ``Torsion of Structural Concrete—Behavior of Reinforced Concrete Rectangular Members,' ' Bulletin D135, Portland Cement Association, 1968.
83. Humphrey, R., ``Torsional Properties of Prestressed Concrete,' ' The Structural Engineer, Vol. 35, 1957, pp. 213-224.
84. CEB/FIP, International Recommendations for the Design and Construction of Concrete Structures, Cement and Concrete Association, Paris, 1970, pp. 80, English edition, . London 1971.
85. Jirsa, J.O., Baumgartner, J.L., and Mogbo, N.C., ``Torsional Strength and Behavior of Spandrel Beams,' ' Journal of the American Concrete Institute, Vol. 66, No. 11, November 1969, pp. 926-932.
86. Johnston, D.W., and Zia, P., ``Prestressed Box Beams Under Combined Loading,' ' Journal of the Structural Division, ASCE, No. St7, July 1975, pp. 1313-1331.
87. Kemp, E.L., Sozen, M.A., and Siess, C.P., ``Torsion in Reinforced Concrete,' ' Structural Research Series 226, University of Illinois Urbana, September 1961.
88. Kirk, D.W., and McIntosh, D.G., ``Concrete L-Beams Subjected to Combined Torsional Loads,' ' Journal of the Structural Division, ASCE, No. ST1, January 1975, pp. 269-282.
89. Kirk, D.W., and Loveland, N.C., ``Unsymmetrically Reinforced T-Beams Subject to Combined Bending And Torsion,' ' ACI Journal, Vol. 69, No. 8, August 1972, pp. 492-499.
90. Krefeld, W.J., and Thurston, C.W., ``Studies of the Shear and Diagonal Tension Strength of Simply Supported Reinforced Concrete Beams,' ' Tech. report, Columbia University in the City of New York, June 1963.
91. Krpan, P., and Collins, M.P., ``Predicting Torsional Response of Thin-Walled Open RC Members,' ' Journal of the Structural Division, ASCE, Vol. 107, No. St6, June 1981, pp. 1107-1128.
92. Krpan, P., and Collins, M.P., ``Testing Thin-Walled Open RC Structures in Torsion,' ' Journal of the Structural Division, ASCE, Vol. 107, No. ST6, June 1981, pp. 1129-1140.
93. Lampert, P., and Thürlimann, B., ``Ultimate Strength and Design

- of Reinforced Concrete Beams in Torsion and Bending,' IABSE, No. 31-I, October 1971, pp. 107-131, Publication. Zurich.
94. Lampert, P., and Collins, M.P., ``Torsion, Bending, and Confusion - An Attempt to Establish the Facts,' Journal of the American Concrete Institute, August 1972, pp. 500-504.
 95. Lampert, P., and Thürlimann, B., ``Torsionsversuche an Stahlbetonbalken,' Bericht 6506-2, Institut für Banstatik ETH, June 1968.
 96. Lampert, P., and Thürlimann, B., ``Torsions-Biege-Versuche an Stahlbetonbalken,' Bericht 6506-3, Institut für Banstatik ETH, January 1969, Zurich.
 97. Lampert, P., Postcracking Stiffness of Reinforced Concrete Beams in Torsion and Bending, American Concrete Institute, Detroit, SP-35-12, 1973.
 98. Laupa, A., The Shear Strength of Reinforced Concrete Beams, PhD dissertation, The University of Illinois, Urbana, September 1953, Thesis.
 99. Laupa, A., Siess, C.P., and Newmark, N.M., ``Strength in Shear of Reinforced Concrete Beams,' Bulletin 428, University of Illinois Engineering Experiment Station, March 1955, Volume 52.
 100. Leonhardt, F., ``Shear and Torsion in Prestressed Concrete,' FIP Symposium, 1970, pp. 137-155, Session IV, Prague.
 101. Leonhardt, F., and Walther, R., ``Tests on T-Beams Under Severe Shear Load Conditions,' Bulletin 152, Deutscher Ausschuss für Stahlbeton, 1962, Berlin.
 102. Leonhardt, F., and Walther, R., ``Shear Tests on T-Beam with Varying Shear Reinforcement,' Bulletin 156, Deutscher Ausschuss für Stahlbeton, 1962, Berlin.
 103. Lessig, N.N., ``Determination of Load Bearing Capacity of Reinforced Concrete Elements with Rectangular Cross Section Subject to Flexure with Torsion,' Foreign Literature Study 371, Concrete and Reinforced Concrete Institution, 1959, Translated from Russian, PGA Research and Development Lab., Skokie, Ill.
 104. Liao, H.M., and Ferguson, P.M., ``Combined Torsion in Reinforced Concrete L-Beams with Stirrups,' ACI Journal, Vol. 66, No. 12, December 1969, pp. 986-993.

105. Losberg, A., ``Influence of Prestressed Reinforcement on Shear Capacity of Beams in Plastic Design Preliminary Report from a Current Research Project,' ' Technical Report, Chalmers Tekniska Hogskola, March 1980.
106. MacGregor, J.G., Siess, C.P., and Sozen, M.A., ``Behavior of Prestressed Concrete Beams Under Simulated Moving Loads,' ' ACI Journal, Vol. 63, No. 8, August 1966, pp. 835-842.
107. MacGregor, J.G., Sozen, M.A., and Siess, C.P., ``Strength of Prestressed Concrete Beams with Web Reinforcement,' ' ACI Journal, Vol. 62, No. 12, December 1965, pp. 1503-1520.
108. MacGregor, J.G., and Gergely, P., ``Suggested Revisions to ACI Building Code Clauses Dealing with Shear in Beams,' ' ACI Journal, Vol. 74, No. 10, October 1977, pp. 493-500.
109. MacGregor, J.G., Sozen, M.A., and Siess, C.P., ``Effect of Draped Reinforcement on Behavior of Prestressed Concrete Beams,' ' ACI Journal, Vol. 32, No. 6, 1960, pp. 649-677.
110. MacGregor, J.G., Sozen, M.A., and Siess, G.P., ``Strength and Behavior of Prestressed Concrete Beams with Web Reinforcement,' ' Report, University of Illinois, Urbana, August 1960.
111. Mattock, A.H., and Kaar, P.H., ``Precast-Prestressed Concrete Bridges, 4. Shear Tests of Continuous Girders,' ' Bulletin D134, Portland Cement Association, January 1961, pp. 146.
112. Mattock, Alan H., ``Diagonal Tension Cracking in Concrete Beams with Axial Forces,' ' Journal of the Structural Division, ASCE, Vol. 95, No. ST9, September 1969, pp. 1887-1900.
113. McMullen, A.E., and Woodhead, H.R., ``Experimental Study of Prestressed Concrete Under Combined Torsion, Bending, and Shear,' ' Journal of the Prestressed Concrete Institute, Vol. 18, No. 5, Sept./October 1973, pp. 85-100.
114. McMullen, A.E., and Rangan, B.V., ``Pure Torsion in Rectangular Sections - A Re-Examination,' ' ACI Journal, Vol. 75, No. 10, October 1978, pp. 511-519.
115. Mirza, S.A., ``Stirruped Beams of Various Shapes Under Combined Torsion, Shear and Flexure,' ' Master's thesis, The University of Texas at Austin, August 1968, M.S. Thesis.
116. Mirza, S.A., Concrete Inverted T-Beams in Combined Torsion, Shear, and Flexure, PhD dissertation, University of Texas at Austin, May 1974, Dissertation.

117. Mistic, J., and Warwaruk, J., ``Strength of Prestressed Solid and Hollow Beams Subjected Simultaneously to Torsion, Shear and Bending,' ' ACI Publication, No. SP-55, —, pp. 515-546, Detroit.
118. Mitchell, D., and Collins, M.P., ``Detailing for Torsion,' ' ACI, No. 9, September 1976, pp. 506-511.
119. Mitchell, D., and Collins, M.P., ``Diagonal Compression Field Theory - A Rational Model for Structural Concrete in Pure Torsion,' ' ACI, Vol. 71, No. 8, August 1974, pp. 396-408.
120. Mitchell, D., and Collins, M.P., ``Influence of Prestressing on Torsional Response of Concrete Beams,' ' Journal of the Prestressed Concrete Institute, May/June 1978, pp. 54-73.
121. Moretto, O., ``An Investigation of the Strength of Welded Stirrups in Reinforced Concrete Beams,' ' Journal of the American Concrete Institute, Vol. 48, No. 2, October 1951, pp. 145-156.
122. Morsch, E., ``Die Schubfestigkeit des Betons,' ' Beton und Eisen, Vol. 1, No. 5, October 1902, pp. 11-12, Berlin.
123. Mukherjee, P.R., and Warwaruk, J., ``Torsion, Bending, and Shear in Prestressed Concrete,' ' Journal of the Structural Division ASCE, No. ST4, April 1971, pp. 1963-1079.
124. Muller, P., ``Failure Mechanisms for Reinforced Concrete Beams in Torsion and Bending,' ' Bericht 65, Insitut fur Baustatik und Konstrucktion ETH, September 1976, Zurich.
125. Murashkin, G.V., ``The Effect of Prestress on Ultimate and Cracking Strengths of Reinforced Concrete Beams Subject to Torsion and Bending,' ' Tech. report 10, Beton i Zhelezobeton, October 1965, PCA Foreign Literature Study No. 474, PCA Research and Development Lab., Shokie, Illinois.
126. National Association of Cement Users, NACU Standard No.4, Standard Building Regulations for Reinforced Concrete, 1910, Volume 66, pages 349-361.
127. Nielsen, M.P. and Braestrup, N.W., ``Plastic Shear Strength of Reinforced Concrete Beams,' ' Tech. report 3, Bygningsstatistiske Meddelelser, 1975, volume 46.
128. Nielsen, M.P., Braestrup, N.W., and Bach, F., Rational Analysis of Shear in Reinforced Concrete Beams, IABSE, 1978.
129. Nielsen, M.P., Braestrup, M.W., Jensen, B.C., and Bach, F.,

- Concrete Plasticity, Dansk Selskab for Bygningsstatistik, SP , 1978, October.
130. Nylander, H., ``Vridning och Vridningsinspanning vid Belongkonstruktioner,`` Bulletin 3, Statens Committee fur Byggnadsforskning, 1945, Stockholm, Sweden.
 131. Ojha, S.K., ``Deformations of Reinforced Concrete Rectangular Beams Under Combined Torsion, Bending, and Shear,`` ACI, Vol. 71, No. 8, August 1974, pp. 383-391.
 132. Okamura, H., and Ferghaly, S., ``Shear Design of Reinforced Concrete Beams for Static and Moving Loads,`` ASCE, No. 287, July 1979, pp. 127-136.
 133. Osburn, D.L., Mayoglow, B., and Mattock, A.H., ``Strength of Reinforced Concrete Beams with Web Reinforcement in Combined Torsion, Shear, and Bending,`` ACI, Vol. 66, No. 1, January 1969, pp. 31-41.
 134. Palaskas, M.N., Attiogbe, E.K., and Darwin, D., ``Shear Strength of Lightly Reinforced T-Beams ,`` Journal of the American Concrete Institute, Vol. 78, No. 6, Nov./Dec. 1981, pp. 447-455.
 135. Park, R., and Paulay, T., Reinforced Concrete Structures, John Wiley and Sons, New York, London, Sidney, Toronto, 1976, A Wiley Interscience Publication.
 136. Prakash Rao, D.S., ``Design of Webs and Web-Flange Connections in Concrete Beams Under Combined Bending and Shear,`` ACI, Vol. 79, No. 1, Jan./Feb. 1982, pp. 28-35.
 137. Progress Report of the Joint Committee on Concrete and Reinforced Concrete, ``ASTM,`` volume 9, pages 226-262.
 138. Progress Report of the Joint Committee, Tentative Specifications for Concrete and Reinforced Concrete, ``ASTM,`` year 1921, vol.21, pages 212-283.
 139. Rabhat, G.B., and Collins, M.P., ``A Variable Angle Space Truss Model for Structural Concrete Members Subjected To Complex Loading,`` ACIA Publication, No. SP-55, , pp. 547-588, Douglas MacHenry International Symposium on Concrete and Concrete Structures, Detroit.
 140. Rajagopalan, K.S., and Ferguson, P.M., ``Distributed Loads Creating Combined Torsion, Bending and Shear on L-Beams With Stirrups,`` ACI, January 1972, pp. 46-54.

141. Rajagopalan, K.S., and Ferguson, P.M., ``Exploratory Shear Tests Emphasizing Percentage of Longitudinal Steel,'' ACI, Vol. 65, August 1968, pp. 634-638.
142. Rangan, B.V., ``Shear Strength of Partially and Fully Prestressed Concrete Beams,'' Univiv Report R-180, University of New South Wales, February 1979.
143. Rangan, B.V., and Hall, A.S., ``Studies on Prestressed Concrete I-Beams in Combined Torsion, Bending, and Shear,'' Unicev Report R-161, University of New South Wales, October 1976.
144. Rangan, B.V., and Hall, A.S., ``Studies on Prestressed Concrete Hollow Beams in Combined Torsion and Bending,'' Unicev Report R-174, University of New South Wales, February 1978.
145. Rangan, B.V., and Hall, A.S., ``Proposed Modifications to the Torsion Rules in the SAA Concrete Codes,'' Unicev Report R-196, University of New South Wales, July 1980.
146. Rodriguez, J.J., Bianchini, A.C., Viest, I.M., and Kesler, C.E., ``Shear strength of Two-span Continuous Reinforced Concrete Beams,'' ACI Journal, Vol. 30, No. 10, April 1959, pp. 1089-1131.
147. Regan, P.E., ``Shear Tests of Rectangular Reinforced Concrete Beams,'' Tech. report, Polytechnic of Central London, May 1980.
148. Regan, P.E., ``Recommendations on Shear and Torsion: A Comparison of ACI and CEB Approaches,'' ACI, No. SP-59, 1979, pp. 159-175, Bulletin 113, Detroit.
149. Richart, F.E., ``An Investigation of Web Stresses in Reinforced Concrete Beams,'' Bulletin 166, University of Illinois, Urbana, June 1927.
150. Ritter, W., "Die Bauweise Hennebique," Schweizerische Bauzeitung, Vol. 33, No. 5, pp. 41-3; No. 6, pp. 49-52; No. 7, pp. 59, 61; February 1899, Zürich.
151. Robinson, J.R., ``Essais a L'Effort Tranchant des Poutres a Ame Mince en Beton Arme,'' Annales des Ponts et Chaussees, Vol. 132, Mar./Apr. 1961, pp. 225-255, Paris.
152. Sozen, M.A., Zwoyer, E.M. and Siess, C.P., ``Investigation of Prestressed Concrete for Highway bridges, Part 1. Strength in Shear of beams without web reinforcement,'' University of Illinois, Vol. 56, No. 62, April 1959, pp. 62-69.

153. Schaeffer, T.C., ``Verification of a Refined Truss Model for Shear Design in Reinforced And Prestressed Concrete Members,`` Master's thesis, University of Texas at Austin, August 1981, Thesis.
154. Seely, F.B., and Smith, J.O., Advanced Mechanics of Materials, Wiley and Sons, Inc.
155. Sewell, J.S., ``A Neglected Point in the Theory of Concrete-Steel,`` Engineering News, Vol. 49, No. 5, January 1903, pp. 112-113, New York.
156. SIA, ``Supplement to Structural Design Code SIA 162 (1968),`` Directive RL 34, Zurich, 1976.
157. Smith, K.N., and Vantsiotis, A.S., ``Deep Beam Test Results Compared with Present Building Code Models,`` ACI, Vol. 79, No. 4, July/August 1982, pp. 280-287.
158. Smith, K.N., and Vantsiotis, A.S., ``Shear Strength of Deep Beams ,`` ACI, Vol. 79, No. 3, May/June 1982, pp. 201-213.
159. Swamy,N., ``The Behavior and Ultimate Strength of Prestressed Concrete Hollow Beams Under Combined Bending and Torsion,`` Magazine of Concrete Research, Vol. 14, No. 40, 1962, pp. 13-24.
160. Talbot, A.N., ``Tests of Reinforced Concrete Beams:Resistance to Web Stresses, Series of 1907 and 1908,`` Bulletin 29, University of Illinois Engineering Experiment Station, January 1909, pages 85.
161. Taylor, G., and Warwaruk, J., ``Combined Bending, Torsion and Shear of Prestressed Concrete Box Girders,`` ACI, Vol. 78, No. 5, Sept./Oct 1981, pp. 335-340.
162. Thürlimann, B., ``Lecture Notes from Structural Seminar``, University of Texas at Austin.
163. Thürlimann, B., ``Plastic Analysis of Reinforced Concrete Beams,`` Bericht 86, Institut für Baustatik und Konstruktion ETH, November 1978, Zurich , pages 90.
164. Thürlimann, B., ``Plastic Analysis of Reinforced Concrete Beams,`` Introductory Report, IABSE Colloquium, 1979, Copenhagen, pages 20.
165. Thürlimann, B., ``Shear Strength of Reinforced and Prestressed Concrete Beams CEB Approach,`` Tech. report, ACI Symposium 1976, February 1977, Revised Copy, pages 33.

166. Thürlimann, B., ``Torsional Strength of Reinforced and Prestressed Concrete Beams-CEB Approach,' ' Bulletin 113, ACI Publication SP-59, 1979, Detroit.
167. Victor, J.D., and Aravindan, P.K., ``Prestressed and Reinforced Concrete T-Beams Under Combined Bending and Torsion,' ' ACI, Vol. 75, No. 10, October 1978, pp. 526-532.
168. Walsh, P.F., Collins, M.P., and Archer, F.E., ``The Flexure-Torsion and Shear-Torsion Interaction Behavior of Rectangular Reinforced Concrete Beams,' ' Civil Engineering Transactions, October 1967, pp. 313-319, Australia.
169. Walsh, P.F., Collins, M.P., and Archer, F.E., and Hall, A.S., ``Experiments on the Strength of Concrete beams in Combined Flexure and Torsion,' ' UNICIV, No. R-15, February 1966, pp. 59, University of New South Wales, Australia.
170. Werner, M.P., and Dilger, W.H., ``Shear Design of Prestressed Concrete Stepped Beams,' ' Journal of the Prestressed Concrete Institute, Vol. 18, No. 4, July/August 1973, pp. 37-49.
171. Withey, M.O., ``Tests of Plain and Reinforced Concrete, Series of 1906,' ' Bulletin of the University of Wisconsin, Engineering Series, Vol. 4, No. 1, November 1907, pp. 1-66.
172. Withey, M.O., ``Tests of Plain and Reinforced Concrete, Series of 1907,' ' Bulletin of the University of Wisconsin, Engineering Series, Vol. 4, No. 2, February 1908, pp. 71-136.
173. Wyss, A.N., Garland, J.B., and Mattock, A.H., ``A Study of the Behavior of I-Section Prestressed Concrete Girders Subject to Torsion,' ' Structures and Mechanics Report SM69-1, March 1969, University of Washington.
174. Zia, P., McGee, W.D., ``Torsion Design of Prestressed Concrete,' ' Journal of the Prestressed Concrete Institute, Vol. 19, No. 2, March/April 1974, pp. 46-65.
175. Zia, P., ``What Do We Know About Torsion in Concrete Members?,' ' Journal of the Structural Division, ASCE, Vol. 96, No. St 6, June 1970, pp. 1185-1199.
176. Zia, P., ``Torsional Strength of Prestressed Concrete Members,' ' ACI, Vol. 57, 1961, pp. 1337-1359.
177. Ramirez, Julio A., "Reevaluation of AASHTO Design Procedures for Shear and Torsion in Reinforced and Prestressed Concrete Beams," Unpublished Ph.D. dissertation, The University of Texas at Austin, December 1983.

178. Ramirez, J. A., and Breen, J. E., "Experimental Verification of Design Procedures for Shear and Torsion in Reinforced and Prestressed Concrete," Research Report 248-3, Center for Transportation Research, The University of Texas at Austin, December 1983.
179. Ramirez, J. A., and Breen, J. E., "Proposed Design Procedures for Shear and Torsion in Reinforced and Prestressed Concrete," Research Report 248-4F, Center for Transportation Research, The University of Texas at Austin, December 1983.
180. Müller, P., "Plastische Berechnung von Stahlbetonscheiben und-balken," Bericht 83, Institut für Baustatik und Konstruktion, ETH Zürich, 1978.
181. Müller, P., "Plastic Analysis of Torsion and Shear in Reinforced Concrete," IABSE Colloquium on Plasticity in Reinforced Concrete," Copenhagen, 1979, Final Report, IABSE V. 29, Zürich, 1979, pp. 103-110.
182. Marti, P., "Strength and Deformations of Reinforced Concrete Member under Torsion and Combined Actions," CEB Bulletin No. 146, "Shear, Torsion, and Punching," January 1982.
183. Marti, P., "The Use of Truss Models in Detailing," Paper preprint for the Annual Convention of the American Concrete Institute, Phoenix, Arizona, March 1984.
184. Marti, P., "Basic Tools of Reinforced Concrete Beam Design," ACI Journal, Vol. 81, 1984, in press.